Spokesperson: Neville W. Reay
Department of Physics
Ohio State University
Columbus, Ohio 43210
614-422-7436
FTS (8) 940-7436

A PROPOSAL TO MEASURE CHARM AND R DECAYS VIA HADRONIC PRODUCTION IN A HYBRID EMULSION SPECTROMETER

N. Ushida
Aichi University of Education, Kariya, Japan

M. Johnson
Fermi National Accelerator Laboratory, Batavia, Illinois

G. Fujioka, H. Fukushima, C. Yokoyama
Physics Department, Kobe University, Kobe, Japan

Y. Homma, Y. Tsuzuki
Faculty of Liberal Arts, Kobe University, Kobe, Japan

S. Y. Bahk, C. O. Kim, J. N. Park, J. S. Song
Korea University, Seoul, Korea

H. Fuchi, K. Hoshino, K. Niu, K. Niwa, H. Shibuya, Y. Yanagisawa
Department of Physics, Nagoya University, Nagoya, Japan

J. Kalen, S. Kuramata, N. W. Reay,
K. Reibel, R. A. Sidwell, N. R. Stanton
Department of Physics, Ohio State University, Columbus, Ohio

K. Moriyama, H. Shibata
Faculty of Sciences, Okayama University, Okayama, Japan

T. Hara, O. Kusumoto, Y. Noguchi, M. Teranaka
Osaka City University, Osaka, Japan

J.-Y. Harnois, C. D. J. Hebert, J.Hebert, B. McLeod
Department of Physics, University of Ottawa, Ottawa, Ontario, Canada

H. Okabe, J. Yokota
Science Education Institute of Osaka Prefecture, Osaka, Japan

S. Tasaka
Institute for Cosmic Ray Research, University of Tokyo, Tanashi, Tokyo, Japan

T. S. Yoon
Department of Physics, University of Toronto, Toronto, Ontario, Canada

R. Heisterberg
Department of Physics, Virginia Tech, Blacksburg, Virginia

J. Kimura, Y. Maeda
Yokohama National University, Yokohama, Japan

May 1, 1980

Table of Contents

A. Summary of the Experiment

We propose an experiment which employs a hybrid emulsion spectrometer to measure lifetimes and decay properties for B mesons and charmed particles produced by interactions of high energy pions. Use of a high-momentum pion beam should maximize the B production cross-section at presently available energies; emulsion is the highest resolution detector for observing short lifetimes, and the electronic detection system is needed to select interesting events, locate them within the emulsion and provide information about decay products. A variation of this technique has proven successful in measuring the lifetimes of neutrino-produced charmed particles (Fermilab Experiment 531). We believe that the experience therein gained will permit us to switch to hadronic production, where there are more B and charmed particles to be found, and also more problems. Subject to development of a new form of solid-state detector, in a four month run with modest beam we should be able to obtain more than 1000 charmed particle decays, and based on a 100 nbn cross-section, about 30 B decays. There is also hope of seeing a small number of tau-lepton decays.

Developing the new detector will require one to two years, thus actual running of the experiment could not take place before 1983. Though yields in the proposal are quoted for 400 GeV operation, based on the threshhold behavior for ψ production we estimate that the signal for B production would be improved a factor of four if the experiment were run at Tevatron energies.

B. Physics Motivation

We wish simultaneously to search for B-meson decays and to make a high statistics measurement of charm decays.

The latter measurement provides an acceptable and secure motivation for the experiment. A ±10% knowledge of lifetimes permits conversion of

branching ratios into absolute partial decay rates without loss of precision. A current experiment[1] shows hints of two neutral lifetimes and possibly the existence of weakly decaying neutral charmed baryons. Definitive studies of the above plus the possibility of observing sequential $F \to \tau \to$ other lepton decays creates interest in a high statistics charm measurement. Observation of visible decay lengths also provides a relatively background-free sample of charmed particles for studying production dynamics. Provided trigger rates are acceptable, we may request a second run with geometry expanded to include particle identification.

However, the discovery of the upsilon family of resonances, and particularly the broad γ''', is considered to be strong evidence for the existence of b quarks, hence B mesons and baryons.

This experiment will have three nanobarn sensitivity for detecting B mesons, provided lifetimes are between 3×10^{-15} and 3×10^{-12} seconds. Should B mesons exist at this level, their sequential $B \to$ charm $\to$ strange decays should be topologically quite striking and relatively background free. In terms of the Kobayashi-Maskawa[2] six quark model, measurement of the B meson lifetimes and relative branching ratios into charm would permit determination of the extended Cabbibo angles θ_2 and θ_3 (where θ_1 is the usual Cabbibo angle θ_c). As all angles and CP violating phases are expected to be small, we can approximate

$$\sin \theta_i \equiv s_i$$

$$\cos \theta_1 = \cos \theta_2 = \cos \theta_3 = 1$$

If we also assume the ratio,

$$\frac{(B \to \text{charm} + X)}{(B \to \text{no charm})} \approx \left| \frac{S_3 + S_2 e^{i\delta}}{S_1 S_3} \right|^2 >> 1 \quad ,$$

Then,

$$\tau_B \approx \left(\frac{M_c}{M_B} \right)^5 \frac{1}{\left| S_3 + S_2 e^{i\delta} \right|^2} \tau_{\text{charm}} \quad .$$

The θ_i are given in terms of quark mass ratios by many of the higher symmetry models which predict proton decay,[3] and charm lifetimes are 10^{-13} to 10^{-12} seconds;[1]

$$\tau_B \approx \left(\frac{1.9\ \text{GeV}}{5.3\ \text{GeV}}\right)^5 (10 - 100)\ (10^{-13} \text{ to } 10^{-12} \text{ seconds})$$

$$\tau_B \approx 5 \times 10^{-15} \text{ to } 5 \times 10^{-13} \text{ seconds}$$

Should B lifetimes lie in this measurable range, the Higgs particle would have to be heavier than the B, else τ_B would be considerably shorter.

However, it may be that the b quark (and perhaps the tau lepton) are not members of doublets. In this case, theoretical predictions have even more freedom, and information obtained on B-meson decays could prove to be even more exciting.

C. Description of the Experiment

1. Design Motivation

The apparatus is a hybrid emulsion spectrometer similar in concept but technically more demanding than the one used successfully in experiment 531, and it will be operated in a π^- beam rather than in a neutrino beam. The sensitivity of the experiment is ultimately limited by the volume of emulsion (50ℓ) and the maximum tolerable track density ($700/mm^2$) to a total of 7×10^7 interactions. It is feasible to search for $1 - 2 \times 10^4$ of these events in the emulsion, so it is important a) to find efficient selection criteria and b) to eliminate unnecessary losses of good events due to spectrometer acceptance and reconstruction and scanning inefficiencies.

The configuration and mounting of the emulsion is determined by the following considerations: 1) The thickness along the beam direction should be as small as possible to reduce secondary interactions, but not so small

that edge effect losses are serious. 2) The exposure area (beam spot size) must be large enough so that the maximum exposure density does not occur in less than one beam pulse, since moving the emulsion more often than this is not practical. 3) Unnecessary exposure of emulsion outside the beam due to beam halo should be minimized. 4) Precise alignment of emulsion relative to the spectrometer must be performed. These considerations lead to a design in which many small modules $\sim(10\text{cm})^2$ x (2 - 3cm thick) are sequentially exposed at the rate of one every 1 - 2 hours. Each small module is mounted on a precision movable stage which allows exposure of a different $(7\text{mm})^2$ area to every beam pulse.

The design of the electronic spectrometer is motivated by the following requirements: 1) Finding events in the emulsion quickly and efficiently-- This is probably best done by following a tagged beam track. Since the average separation of beam tracks in the emulsion will be only $\sim 40\mu$. unambiguous tagging requires position resolutions $\sim \pm 20\ \mu$. 2) Large acceptance for beauty (B) and charm (C) decay products; 3) Good reconstruction efficiency for high-multiplicity, sharply-collimated events typical of hadronic interactions at 375 GeV; 4) Minimum decay path for π's and K's-- Since we will depend on a single-μ trigger, the apparatus must be kept short. 5) Ability to detect secondary vertices-- The relatively long lifetime of the $D^{\pm}(10.3\ ^{+10.5}_{-\ 4.1} \times 10^{-13}\ \text{sec})$[1] makes feasible the efficient selection of a highly enriched $D^{\pm}$ sample (and some D^{o}, $F^{\pm}$, and Λ_c as well) by successfully resolving production and decay vertices with the electronic spectrometer. Excellent position resolution in the detector downstream of the emulsion therefore becomes very desirable. 6) Successful kinematic reconstruction of B and C events, implying satisfactory momentum resolution for charged particles and the ability to detect neutrals.

2. Solid State Detectors

It is very difficult to satisfy the above design criteria with existing technology. Drift chambers, for example, fall short of the position resolution required for beam tagging and decay vertex resolution by factors of ~7. Even worse, they can achieve track pair resolution no better than about 2mm, so that tracks more closely spaced than this are lost. Since projected angles between tracks of $\lesssim$ 1mrad occur with appreciable probability in hadron interactions at 375 GeV, it is impossible to place drift chambers close to the emulsion target without incurring unacceptable reconstruction losses. (Yet, high resolution detectors close to the emulsion target are essential if the apparatus is to be kept short.)

We have therefore produced a spectrometer design which relies heavily on a new technology, that of position-sensitive silicon detectors[4], and have begun a program of prototyping and testing. More details are provided in Appendix I. Briefly, these proposed devices are thin silicon semiconductor detectors on which are deposited many narrow parallel metal strips with a center-to-center spacing of 40μ (Figure 1). These strips are to be read out individually over a limited area corresponding to the region of highest track density, and will be read out in groups using the charge-interpolation technique[5] with taps every 5 to 10 strips in regions where the average track density is lower. In designing the spectrometer we have assumed that we will succeed in producing detectors with the following characteristics: (1) active area up to 8cm diameter; (2) thickness 0.4mm; (3) position resolution $\pm$ 20μ; (4) track pair resolution 40μ; (5) successful operation in magnetic fields $\lesssim$ 1.0T. There is at present no reason to believe that any of these requirements are unreasonable.

3. Discussion of Apparatus

A schematic elevation view of the experiment is shown in Figure 2. Note that the total length of the apparatus between the emulsion target and the upstream side of the calorimeter is less than 1.5m. The major components are the beam and beam detectors, emulsion target, vertex detector, charged particle spectrometer, γ detector, neutral hadron detector, muon identifier, and trigger counters.

a. Beam and beam detectors. Because of the expected rapid increase of B cross section with energy, a π^- beam of the highest available momentum (~375 GeV) is essential. The momentum bite can be large, and an intensity ~2×10^4/pulse is satisfactory. The optimum spot size at the emulsion is 0.7cm square. Because the emulsion target is much larger than this and will be shifted by one spot size after each beam pulse, it is very important that the integrated halo for several centimeters around the beam is a small fraction of the total intensity to avoid increasing the level of background tracks in the emulsion.

To keep the emulsion exposure density uniform, a beam plug with an out-to-in response time of 0.1 second which can be actuated by a preset beam counter must be incorporated well upstream in the beam line.

The transverse coordinates of beam tracks at the emulsion will be determined to $\pm 20\mu$ by three small silicon detectors (called SS triplet in Figure 2) of the type shown in Figure 1-a, located immediately upstream of the emulsion. It is also desirable to determine beam track slopes to better than ± 0.02mrad for use in surveying the rest of the apparatus. A second set of three silicon detectors is therefore located 2.0m further upstream.

b. Emulsion. Nuclear emulsion is a suitable detector to observe short-lived particles with lifetime of 3×10^{-15} to 3×10^{-12} seconds. One can handle enough emulsion to get relatively rare events, but the limitation of using it is in analyzing large numbers of events under the microscope.

Recently a microscope with TV monitor and computer-controlled, digitized stage has been developed at Nagoya University and has turned out to be very powerful in analyzing E531 neutrino events.

In this experiment we will use as much emulsion as possible and as high a track density as tolerable to get good sensitivity to small cross sections. The total amount of emulsion we can handle is about 50ℓ, and is limited primarily by cost. Maximum tolerable intensity is a slightly subjective number but is around $(6 \pm 2) \times 10^4/cm^2$. We can get more than 7×10^7 interactions using 50ℓ of emulsion and 2×10^4/pulse beam intensity. To reduce the secondary phenomena, e.g., γ-ray conversion and secondary interactions, the thinner the emulsion module along the beam direction the better. But we have to reduce edge effects especially for the pellicles. The compromised depth is 2 - 3cm. The track density at the downstream end of modules is then 1.5 times as much as at the upstream end. We can get some information about maximum tolerable intensity from NA-19 at CERN, in which Nagoya people are involved.

Although the area of each emulsion module is about 10cm x 10cm, the size of beam spot is around 7mm x 7mm, and therefore we must have some movable stage to expose uniformly over the whole area.

The accuracy of track detectors is so high that we have to be careful in mounting the emulsion module. A schematic drawing of the stage is shown in Figure 3. It is driven by computer-controlled pulse motors and the position of the stage is monitored by moiré image encoders (1μm accuracy) or

by laser diffraction encoders (0.1μm accuracy). In this way we can know the relative position of events in the module. We also need to know the relative position of the module and the counter systems with an accuracy of 10μm. For this purpose we will expose two low-beam density regions (1cm x 1cm). The total number of tracks in each of these regions will be about 100. Since beam tracks may easily be found in these low-density regions, translations transverse to and rotations about the beam line may be removed on a module by module basis. This will permit much greater precision for event searches in regions of high track density.

The events located by the spectrometer will be found by two methods. One is to follow the incident beam; another is conventional volume scanning. We will tag the incident beam which produced interesting events. We can follow all the tracks seen in one field of view. In this case we do not need very good accuracy. If the vertex predictions are sufficiently good, we can also use the conventional volume scan technique. The volume is estimated to be about $0.1mm^3$, which is about two orders of magnitude smaller than in E531, implying that the event finding speed is 100 times faster than before, exclusive of set-up time.

After events are found, each will be analyzed using a microscope with a simplified computer-guided, digitized stage. In this fashion we can fully analyze 5000 events a year, and inspect several times this many.

c. Vertex detector. The vertex detector consists of 15 silicon detectors arranged in 5 triplets mounted on 2.5cm centers. Each triplet measures 3 projections rotated 60° from each other (x,u,v). With the proposed ±20μ resolution the direction of stiff tracks can be measured to ±0.2mrad in each projection. Each detector (Figure 1-b) has an active area of 8cm diameter and is only 0.4mm thick to reduce multiple scattering. In the

central 1.4cm band of each detector every strip is read out separately to maintain 40μ track-pair resolution in the region of high track density. On either side of this central band the charge interpolation technique is used, with pulse height information from taps every 5 to 10 strips being read out, thus preserving the spatial resolution but relaxing the track-pair resolution.

We have studied the track-pair resolution requirements by use of a tape of measured 360 GeV π^-p events from a 30" bubble-chamber exposure. The real tracks were augmented by gammas from Monte Carlo π^o's which were allowed to convert with appropriate probability in a simulated 3cm emulsion target. The results of this study are summarized in Figure 4 and Table 1.

Table 1. Chamber parameters

Location	Z (cm)	Approx. Θ (mrad)	Track pair resolution (microns)	Track pair resolution Δx' (mrad)	Fraction of tracks blocked
Center of vertex detectors	~10	0 - 50	40μ	0.4	<9%
		50 - 150	200μ	2.0	<8%
		>150	400μ	4.0	<8%
Downstream silicon detectors	~80	0 - 50	400μ	0.50	<10%
Downstream drift chambers	~80	>50	2000μ	2.5mrad	<10%

The integral distribution in laboratory production angle Θ for all charged tracks in this sample is shown in Figure 4-a. Approximately half the tracks have Θ < 50mrad and 25% have Θ < 12mrad. Since the mean multiplicity of

charged hadrons and converted electrons is ~14, the effects of track masking can be appreciable. In Figure 4-b we plot the fraction of tracks produced at Θ which are masked in a given projection (x, e.g.) for various assumed slope resolutions $\Delta x'$. If, for example, the detector can resolve two tracks if their projected slopes differ by more than 0.4 mrad, the fraction of masked tracks is < 9% at all Θ. This condition obtains in the middle of the vertex detector (z = 10cm) where the pair resolution Δx is 40μ, giving $\Delta x' = 0.4$mrad. For $\Theta \geq$ 50mrad (> 150mrad) a $\Delta x'$ of 2.0mrad (4.0mrad) is sufficient to keep the masking below 10%. The outer regions of the silicon detectors therefore use the charge interpolation method. Similar considerations are used in designing the detectors downstream of the magnet (next section).

It should be noted that because the silicon detectors are thin it will be necessary to operate them at low temperature (-100°C) to obtain satisfactory signal/noise. The whole vertex detector must therefore be cryogenic.

The signal from each tap, or from each strip in the central region of the vertex detector, will require a low-noise amplifier and analogue readout. There are a total of 13,000 such lines in the beam, vertex and spectrometer arrays of silicon devices. We plan to store the analogue information in charge-coupled devices (CCD's) and digitize this data serially during readout.

d. Charged particle spectrometer. In order to achieve maximum aperture and minimum depth we have designed the spectrometer around the small iron magnet shown in Figures 1 (layout), and 5 (B-field).

This magnet has a pole-piece depth of only 35cm and allows a vertical aperture from the target of ±240mrad with a maximum vertical gap of 26cm.

The horizontal aperture is twice as large. By having the pole pieces open vertically outward (thereby deliberately creating a non-uniform field) a transverse kick of 0.20 GeV/c is obtained with a maximum field of 2.1T.[6]

The directions of charged particles downstream of the magnet are measured by silicon detectors at small angles and by drift chambers similar to those used in E531 at larger angles. The silicon detectors are of the type shown in Figure 1-c, with active areas of 8cm diameter and charge-interpolation readout with taps every 10 strips. There are 3 pairs of xuv triplets located at approximately 75, 85 and 110cm from the target. Stiff tracks with production angles $\theta \lesssim 50$mr pass through the first two pairs, while those with $\theta \lesssim 40$mrad pass through all three. If we use the rule of thumb that most B-meson and charm-decay tracks have $p_T \lesssim 1$ GeV/c, these silicon detectors measure momenta of most tracks having $p \gtrsim 20$ GeV. For tracks with $\theta \gtrsim 50$mr, which are on the average softer and more widely separated, a system of 12 drift chambers (4 pairs of xuv triplets)measure the directions with spatial resolution $\pm 150\mu$ and a lever arm of 30cm. As can be seen from the momentum resolution graphs in Figure 6, with this multi-element system momenta $p \lesssim 3$ GeV/c are measured to $\pm 1.5\%$, while most tracks at 50 GeV/c are still measured to $\pm 6\%$.

It is clear that to use the excellent resolution of silicon detectors to full advantage we must build stable mounting hardware and monitor the alignment carefully. Our experience with the much larger apparatus in E531 should be most useful here. In that experiment drift-chamber positions were found to be stable to $\pm 25\mu$ over times ~1 week, and absolute survey discrepancies between the drift chambers and emulsion fiducial sheet were $\sim \pm 50\mu$. In addition, we can record stiff beam tracks passing through the central regions of all the high-resolution devices, a very powerful survey tool which we did not have in E531.

e. Gamma detector. For electron/photon detection we have designed a segmented electromagnetic shower calorimeter consisting of alternate layers of 1 radiation length of lead and extruded aluminum proportional ionization chambers (EPIC). A similar device has been tested satisfactorily for use in E531. The overall dimensions of the detector are 1m x 1m with a total thickness of 14 radiation lengths of lead. Each EPIC chamber is constructed of aluminum extrusions with individual tube cross sections of 1cm x 1cm. The pulse heights from each tube will be read out from both ends using a charge-division technique to give both x and y position information from each chamber. The spatial resolution attainable with this technique is typically 1% of the wire length or ~1cm along the direction of the wire for a 1m chamber. To reduce the number of ADC channels required the pulse heights from groups of 32 tubes will be stored in a parallel input CCD and serially shifted into an ADC for digitization.

With one radiation length of lead sampling thickness, similar devices[7] using multi-wire proportional chambers operated at 1 atmosphere of pressure have achieved an energy resolution $\Delta E/E=0.30/\sqrt{E}$. This is about a factor of two worse than the resolution obtained with a lead-scintillator calorimeter. We expect to operate the gamma EPIC chambers at a pressure of ~10 atmospheres and estimate an improved energy resolution of $0.20/\sqrt{E}$.

Assuming a spatial resolution of ~2.0cm for showers, Monte Carlo studies using 350 GeV π^-p events from a 30" bubble chamber exposure indicate an overall efficiency of ~70% for resolving multiple showers in the γ-detector. Masking of one shower by another is worst in the central core for angles less than 50mrad. Here the efficiency drops to ≈40%. We are investigating the feasibility of using silicon detectors with lead converters to cover this central 50mrad with better position resolution.

Additional details and discussion of the spatial and energy resolution can be found in Appendix II.

f. Hadron calorimeter. The primary function of the hadron calorimeter is to measure the position and energy of neutral hadrons (K^o, Λ^o, and n). The position resolution that can be achieved is $\lesssim$ 25mm, or ~20mrad at 1.3m.[8] This angular resolution is well matched (in terms of contributions to the overall mass resolution) by an energy resolution of $\sim 1/\sqrt{E}$ for the range of energies of interest (5-25 GeV).

The major difficulty in finding neutral hadrons lies in separating them from the charged hadron background. We have estimated the detection efficiency by plotting the positions of charged hadrons at the front face of the calorimeter. A successful identification is assumed if no other hits lie with ±40mrad (±5cm) in the x projection. The resulting efficiency is shown in Figure 7 as a function of polar angle θ. Superimposed on this curve is the kaon angular distribution expected from $B \to \psi K^o\pi$. The net efficiency, including corrections due to loss of events with $p_{K^o} < 5$ GeV, and a finite absorber thickness ($1 - e^{-2} \simeq .84$) is 25%.

The proposed detector is shown in Figure 2. It consists of alternate layers of iron plates and extruded MWPC (EPIC chambers) with 2.54cm wire spacing operated at atmospheric pressure. We are using EPIC chambers of this kind in the second run of E531 and have tested sample chambers in the M5 beam line. The iron plates, which can be made from the E531 calorimeter steel with a minimum of cutting, have dimensions 1.2m high x 1.5m wide x 5cm thick for the first six plates, 2.4m x 3.0m x 10cm for the next two, and 2.4m x 3.0m x 20cm for the last 3 plates. EPIC chambers covering ±240 mrad from the target are inserted after each of the plates, and are read out from both ends using the charge division technique to give coupled two-dimensional information on the hit positions as is done in the gamma

detector. A total of 1,728 amplifiers is required. The analogue data will be stored in CCD's and digitized serially during readout.

g. Muon detector. The muon detector has two functions: to reduce the hadron flux sufficiently to give a manageable trigger rate, and to determine from the reconstructed event whether a given track which has traversed the detector is indeed a muon. The first objective is most simply accomplished by requiring enough range of iron. Using simulated decays of measured tracks from a 360 GeV bubble chamber exposure we found that 2.5m of iron (including that in the calorimeter) will give fewer than 20 triggers/10^3 interactions from upstream decays and punch through, while accepting muons above 3.5 GeV/c.

To meet the second objective it is essential to track the muon candidate from the emulsion through the spectrometer, hadron calorimeter, and absorber with frequent sampling of position and ionization in the iron to look for evidence of hadronic interaction. It is also very desirable to make a second momentum measurement after several interaction lengths of iron to be sure that no large energy loss has occurred, and that the correct candidate has been tracked through the region of heavy hadron showers.

The frequent sampling is performed in the EPIC chambers of the calorimeter. The second momentum measurement is performed with a square iron toroid (similar to those used in E613) 1.0m deep and 2.5m on a side. Assuming low carbon steel (1010 or equivalent), a current of 1000 Amp and 100 turns, one obtains reasonable saturation and a radial variation of magnetic field from 2.0 T near the center to 1.7 T at the outer rim. On either side of this toroid are 2 triplets of EPIC chambers instrumented for drift-chamber readout using surplus electronics from E531. This system will have a resolution

$$\frac{\delta p}{p} = \left[(.21)^2 + (.01p)^2 \right]^{\frac{1}{2}} , \quad (p \text{ in GeV/c})$$

where the first term is the multiple scattering contribution and the second results from the ±0.5mm resolution of the chambers.

Downstream of the toroid are three identical modules, each consisting of 0.4m of steel followed by two crossed bands of EPIC chambers with 5cm wire spacing, with each tube read out from both ends to give charge-division information. The final two modules serve to further constrain muon candidates above 3.5 GeV/c.

h. Trigger counters. As non-zero data from all events will be stored in a fast buffer memory during each spill, we are studying a variety of triggers, many of which require fast processing before recording on magnetic tape.

Though several techniques appear promising, we will present here only the simplest muon trigger, which should be sufficient to lower recorded events to a level of 20/pulse. This trigger will require non-halo beam to interact in the emulsion, giving rise to a downstream muon of more than 3.5 GeV.

The following sketch qualitatively indicates counter locations:

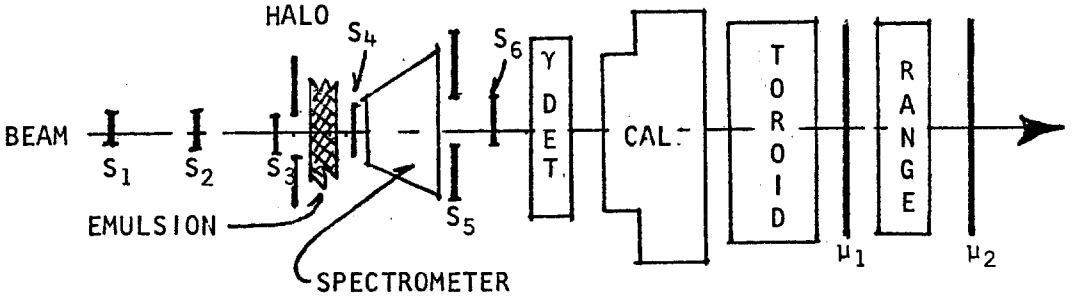

The trigger will consist of

$$\text{Trigger} = (\text{Beam}) \cdot (\text{Interaction}) \cdot (\text{Muon})$$

with components as listed below:

$$\text{Beam} = S_1 \cdot S_2 \cdot S_3 \cdot \overline{\text{Halo}}$$

$$\text{Interaction} = (S_4 \geq 4 \text{ in pulse height}) \cdot (S_5 \geq 2 \text{ pulse height})$$

(S_5 will have a small hole for non-interacting beam)

$$(\text{Muon}) = \mu_1 \cdot \mu_2$$

(The muon counters may have to be shielded against slow neutrons.)

D. Event Rates and Acceptances

In the standard model the B meson is expected to have a substantial branching ratio (B.R.) to muons either from direct decay:

(a) $B \to \mu$ + anything

or through the cascade

(b) $B \to D$ + anything
$\quad\quad\quad\hookrightarrow \mu$ + anything

In the first case, the muons are stiff and have a large transverse momentum ($p_T \sim 1$ GeV/c), while in the second case they are soft and have $p_T \sim 0.3 - 0.4$. We have therefore considered two methods of analysis of events; the first a tag of B decays with a stiff muon, the second a tag of events passing less stringent cuts on the muon, but having a reconstructed secondary vertex. The second analysis will also yield a large sample of charm decays.

Tagging interesting decays with muons requires that we can extract a signal out of the background of soft muons coming from π decays upstream of (as well as in) the calorimeter. We have generated muon spectra from pion decays (using 360 GeV/c π^- bubble-chamber data) and from $B \to \mu$ via Monte Carlo simulation of processes (a) and (b) above. The decay distance allowed is 120cm. We assume the B's are centrally produced with

$$\frac{d\sigma^3}{dx \ \ dp_\perp^2} = c(1 - x)^N e^{-ap_\perp}$$

In figures 8 and 9 we compare the p and p_T distributions for muons from these three sources, where we have taken N = 2 and a = 1 in the expression above in generating the B mesons. We have also calculated the muon spectrum for the process $K \to \mu\nu$ (not shown). The muon background is listed in Table II for several values of p and p_T.

Table II. Muon background per 360 GeV/c π^- interaction.

Off-line selection	p_μ GeV/c	p_T GeV/C	$\pi \to \mu$	$K \to \mu$
a	> 6	> 0.6	3×10^{-4}	0.5×10^{-4} (+ secondary vertex)
b	> 3.5	> 0.25	4×10^{-3}	4×10^{-4}

We have assumed 1/3 $K^{\pm}$/interactions, and a 63% B.R. to $\mu\nu$.

In addition to the decays of primary pions and kaons, one also has muons produced by decays of secondary and tertiary pions produced in the hadron absorber. This latter background is comparable to that listed in Table I but can largely be eliminated by comparing momenta of muons as measured in the spectrometer and in the toroid and by requiring that the muon point to the interaction vertex.

The yield of events is given by

$$\text{Yield} = (\text{No. interactions}) \times (\text{electronic live time}) \times (\text{scanning efficiency}) \times \left(\frac{\sigma B}{\sigma_{abs}}\right) \times \text{B.R.} \left(\frac{B \to \mu}{B \to \text{all}}\right) \times (\mu \text{ detection efficiency}).$$

A similar expression may be used for the charm yield.

We take the number of interactions to be 7×10^7, the electronic live time to be 80%, and the scanning efficiency to be 50% (the efficiency in E531 is 53%). σ_{abs} = 8.7mb/nucleon for pions in emulsion.

We calculate B yields based on a total cross section of 100 nb/nucleon.

This estimate is motivated in part by Figure 10 where we compare the πp inclusive cross sections for the bound quark states ϕ, ψ, Υ to the unbound states K, charm.[c] The bound states differ in cross section by 8 decades, yet they lie on a straight line. If we assume that the unbound states also lie on a straight line with a slope determined by the K and charm cross sections, we get a B cross section of approximately 200 nb/nucleon. Published theoretical estimates range from 8nb to ~1μb.[10] The Goliath result from CERN, if correct, would imply a cross section of several hundred nanobarns.

In the free quark model the b quark decays directly to muons (plus hadrons) with a B.R. ≈ 16%. Non-leptonic enhancements will reduce this ratio, especially for the B^+ which decays non-exotically, so we take the average B.R. for B^+ and B^0 to be 10%. For process (b) above, given equal numbers of D^{*o} and $D^{*\pm}$ in the debris of B decays one gets a D^+/D^0 ratio ≈2. Using 20% and 2% for the respective B.R. yields a net rate of 8%. The total B.R. of $B \to \mu$ is thus 18%.

For charm production we take σ = 20μb and an average semi-leptonic B.R. to muons of 10%.

For selection a, (p_μ > 6 GeV/c, p_T > 0.6) we have 1.5×10^4 events to examine and a yield of 19 B decays from process (a) and 5 from process (b), with a charm yield of 1300 events (650 pairs). The relevant muon acceptances are 60% for (a), and 20% for (b).

In addition to this straight forward cut on the prompt muon, which works well for muons from B decay, but loses 80% of the charm decays, we would select events where a muon is tagged as coming from a secondary vertex downstream of the primary interaction. To predict the success of this procedure we have computed the ratio $\delta z/\hat{z}$ for 5 $D^\pm$ events found so far in E531. Here, δz is the estimated error in the z (beam direction) coordinate of each event, based on the actual momenta and angles of the observed decay tracks, and $\hat{z} = c\beta\gamma\tau$ is the expected decay length for a lifetime $\tau = 10 \times 10^{-13}$ sec. For these 5 events, having

respective $D^{\pm}$ momenta of 9.8, 10.1, 16, 17, and 120 GeV/c, the corresponding ratios $\delta z/z$ are .22, .17, .14, .15, and .10, so that primary and secondary vertices are separated by 5 - 10 standard deviations. It should be noted that $\delta z/\hat{z}$ improves with D momentum because δz is dominated by multiple scattering in the emulsion for secondaries below ~8 GeV/c.

We estimate the efficiency of reconstructing three-prong secondary vertices (with a visible energy of greater than 10 GeV/c) could be as high as 80%. The background is primarily from nuclear interactions of pions. = 8 π's/interaction x (4% absorption length) x (40%, p > 10 GeV) x (70%, $\geq$ 3 prongs). We estimate the muon background to be $\leq 2 \times 10^{-3}$ from the secondaries.

For selection b, (p_μ > 3 GeV/c, p_T > 0.25 for muon from secondary vertex), we have a yield of 960 charm decays and 5 B decays for 8×10^3 events examined. (This yield is corrected for double counting in selection a.)

To summarize, we have

	B Yield $B \to D^* \mu\nu$	B Yield $B \to D4\pi$ $\hookrightarrow K^* \mu\nu$	Charm Yield	Background events to be scanned
Selection a $p_\mu > 6$, $p_T > 0.6$	19	5	1300	1.5×10^4
Selection b ($p_\mu > 3.5$, $p_T > 0.25$ secondary vertex)	--	5	960	8×10^3

E. Cost Estimates

		Total (in thousands)
	Items in parentheses already exist.	
1.	Fermilab:	
a.	20' x 30' of floor space, with provision for an upstream set of beam drift chambers. Utilities such as 30KW of 110 and 208V, water for magnet	----------
b.	Up to 200KW of electrical power delivered for magnets	----------
c.	1 toroid, estimate 50 tons @ $600/ton for cutting and machining, and $5000 for the coils	$ 35K
d.	Extra muon steel (could be taken from existing E-531 iron) assume cost to be 100 tons @ $300/ton	($ 30K)
e.	Calorimeter steel (could be made from E-531 calorimeter by cutting only 3 of 16 existing 2" plates). Assume cost to be $500/ton	($ 25K)
f.	Small conventional magnet, estimated at $1.00/lb for machined steel and $3.00/lb for copper, with a 30% cost overrun included	30K
g.	Prep electronics, mostly already in inventory	($ 90K)
h.	Rigging, 16 days @ $500/day	$ 8K
i.	250 hours of computer time, @ $400/hour	$ 100K
j.	Space in the village as provided for E531	----------
k.	Prototyping solid state detectors	$ 50K
	Existing Costs	($ 145K)
	New Costs	$ 223K
	Total Costs	$ 368K

2. Experimenters

a. Scintillation Counters		
i. Tubes, bases, power supplies, voltage dividers		($ 100K)
ii. Scintillation material		($ 20K) $ 15K
	Subtotal	($ 120K) $ 15K
b. Solid state detectors		
i. Prototyping, (30K is already committed).		($ 30K) $ 30K
ii. Hardware (including cryostats and stands) for 33 detectors, @ 2K/detector		$ 66K
iii. Electronics, 13000 wires @ $25/wire		$ 325K
	Subtotal	($ 30K) $ 421K
c. Drift chambers		
i. 12 chambers @ $2K/chamber (includes stands)		$ 24K
ii. Existing multiple hit/wire readout system for 250 wires		($ 25K)
	Subtotal	($ 25K) $ 24K
d. Gamma chambers		
i. Lead		$ 4K
ii. Stand		$ 2K
iii. Extruded tube chambers: 14 planes @ $400/plane		$ 6K
iv. Electronic readout of both ends of 1400 wires, @ $6.00/channel		$ 17K
	Subtotal	$ 29K

e. Calorimeter (exclusive of iron)

i.	Stand	$ 2K
ii.	Hardware for 108 chambers, @ $150/chamber	$ 16K
iii.	Electronics - 864 lines read out both ends, @ $6/channel	$ 10K
	Subtotal	$ 28K

f. Muon detector (exclusive of scintillator counters, toroid and range steel)

i.	Extruded tube drift chambers, 84 units @ $100/unit	$ 8K
ii.	Multiple hit/wire drift chamber readout system; 672 lines @ $100/line (mostly existing)	($ 59K) $ 8K
iii.	Tube chamber hardware, 66 units @ $100/unit	$ 7K
iv.	Electronic readout of both ends of 792 wires, @ $6/channel	$ 10K
	Subtotal	($ 59K) $ 33K

g. Emulsion related costs

i.	Precision front-end stand and emulsion movement mechanism	$ 50K
ii.	Misc. hardware (for punching, etc.)	$ 50K
iii.	Emulsion: 50 liters (@ $7K/liter by the end of 1982, current cost is $5K/liter)	$ 350K
iv.	Pouring laboratory (being constructed for E531 at Fermilab)	($ 80K)
v.	Developing laboratory (exists at Ottawa)	($ 100K)
vi.	Developing costs (chemicals, etc. @ 10% of cost of emulsion)	$ 35K
vii.	Emulsion scanning laboratories at Ottawa and in Japan	($ 825K)
	Subtotal	($1005K) $ 485K

h.	Computer (General Automation SPC 16/85)	($ 120K)
i.	1000 hours of AMDAHL 470 computer time at $500/hour	$ 500K
j.	Misc. fast electronics	($ 30K) $ 10K
k.	Operating costs, 12 months @ $5K/month	$ 60K
	Existing	($1389K)
	New	$1605K
	Total*	$2994K

*This total is within 30% of that estimated for the second run of E531. Based on experience gained in E531, we expect cost overruns to be less than 30%.

F. Time scale for the Experiment

We believe that with the good rate of progress on our existing E531 experiment, we have the capability of instituting a developmental program for solid state detectors. This program has already begun, with the placing of purchase orders for the prototype strip detectors from the Silicon Solid State Group at LBL. A testing cryostat is being designed and constructed by a student at Ohio State University. However, we believe this testing program will take two years and will require at least two prototypes before construction of the final detectors. It is important that such a program have clear goals generated by a pending experiment. Therefore, we propose the following schedule.

Summer, 1981	Complete testing of first prototypes.
Winter, 1982	Complete testing of final prototypes and commence full-scale construction.

Winter, 1983	Complete construction and commence installation.
Summer, 1983	Complete installation, have 1 month run to debug hardware.
Fall, 1983	Commence data run* of roughly 2-3 months.
Summer, 1984	First results of analysis appear.
Winter, 1986	Complete analysis.

*Note that emulsion data runs are necessarily short, well suited to the period of construction at Fermilab. Of course, the B-yield for the experiment would benefit a factor of 4 from pion beams available during Tevatron operation should it be available.

References

1. E531 preprints, N. Ushida, et al., "Measurement of the D^o Lifetime," and "Measurement of the D^+, F^+, and Λ_c^+ Charmed Particle Lifetimes," manuscript in preparation (1980).
2. M. Kobayashi and K. Maskawa, Prog. Theor. Phys. 49 652 (1973).
3. See, e.g., John Ellis, "Status of Gauge Theories," CERN preprint Th-2701 (1979); J. A. Harvey, P. Ramond, and D. B. Reiss, "CP Violation and Mass Relations in SO(10)," Cal Tech preprint 68-758 (1979); S. Nandi and K. Tanaka, Ohio State University preprint COO-1545-270 (to appear in Phys. Lett. B, May 1980).
4. J. E. Lamport, et al., Nucl. Instr. and Meth. 134 71 (1976).
5. V. Radeka and R. A. Boie, Proceedings of 1979 Nuclear Science Symposium (to be published in IEEE Trans. Nuc. Sci.).
6. We wish to thank Stan Snowdon of Fermilab for aiding in magnet design and computing typical field profiles for this magnet.
7. S. L. Stone, et al., Nucl. Instr. and Meth. 151 387 (1978).
8. A. Babaev, et al., Nucl. Instr. and Meth. 160 427 (1979).
9. Cross sections are plotted for data as close to 375 GeV/c as possible. The ϕ point is at 150 GeV/c from K. J. Anderson, et al., Phys. Rev. Lett. 37, 799 (1976). The ψ comes from a fit of the form $\sigma = 350\ e^{-9\sqrt{\tau}}$, where $\tau = m/\sqrt{s}$, to existing data listed in the review talk by J. Pilcher, Proc. Int. Symposium on Lepton and Photon Interactions, 185 (1979). The Υ point is also an extrapolation to 375 GeV from the data presented by W. Kienzle, op. cit., 161 (1979). The kaon point, quoted as 4 times the K_s^o cross section, is from N. W. Biswas, preprint "Inclusive Production of π^o, K_s^o, Λ^o, and $\bar{\Lambda}_o$ in 100, 200 and 360 GeV/c π^-p Interations," Fermilab No. 37870 (1980) and Notre Dame preprint 80-0068. The charm cross section is from J. Sandweiss, et al., Phys. Rev. Lett 44 1104 (1980).

10. B. L. Combridge, Nucl. Phys. B151 429 (1979); H. Fritzsch, Phys. Lett. 86B 164 (1979).

Figure Captions

1. Layout of position-sensitive silicon detectors. (a) Beam detector wafer; (b) Vertex detector wafer; (c) Downstream detector wafer.
2. Elevation view of the hadron hybrid spectrometer.
3. Emulsion module and movable mounting stage.
4. (a) Integral distribution in laboratory production angle Θ for charged hadrons and converted electrons from 360 GeV/c $\pi^- p$ events.
   (b) Fraction of tracks masked in the x projection vs. Θ for various resolutions in projected slope $\Delta x'$, for the above events.
5. Pole-piece geometry and calculated magnetic field for the spectrometer magnet shown in Figure 2.
6. Charged particle momentum resolution for tracks passing through the downstream drift chamber (solid curve) and through the downstream silicon detectors (dashed and dotted curves).
7. Neutral hadron detection efficiency. Fraction of hadron showers separated by more than 5cm in the x projection vs. production angle Θ (solid curve); angular distribution of K^o from $B \to \psi K^o \pi$ decay (dotted curve).
8. Momentum distributions of muons from π decay in ordinary hadronic events (dotted curve), from $B \to D \to \mu$ cascades (dashed curve), and from $B \to D^* \mu \nu$ (solid curve).
9. Transverse momentum distributions for muon from the three sources listed above.
10. Experimental cross sections for ϕ, ψ, and T production, and for K and D production from pions of ~350 GeV.

POSITION-SENSITIVE SILICON DETECTOR
(ACTUAL SIZE)

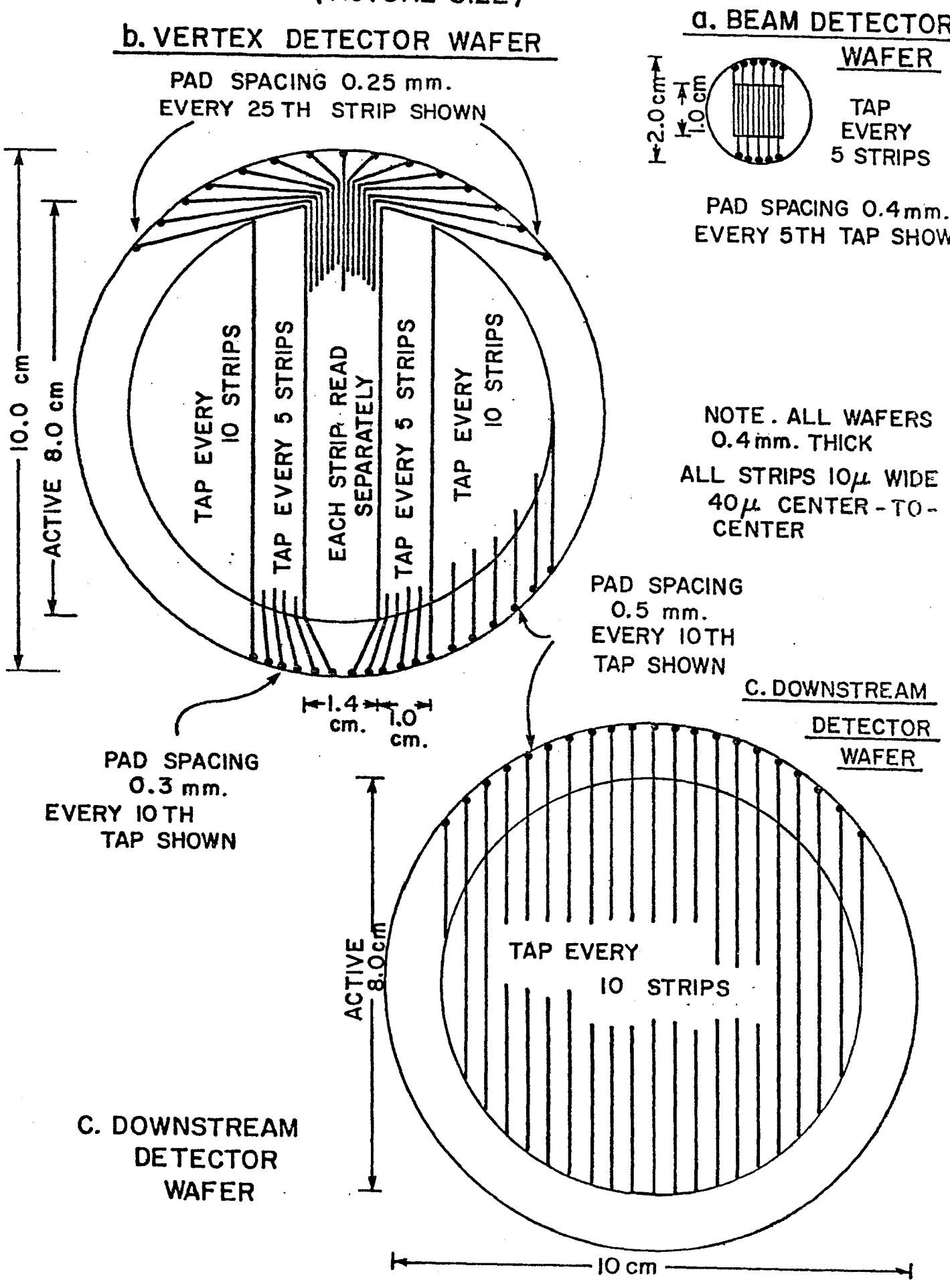

Figure 1

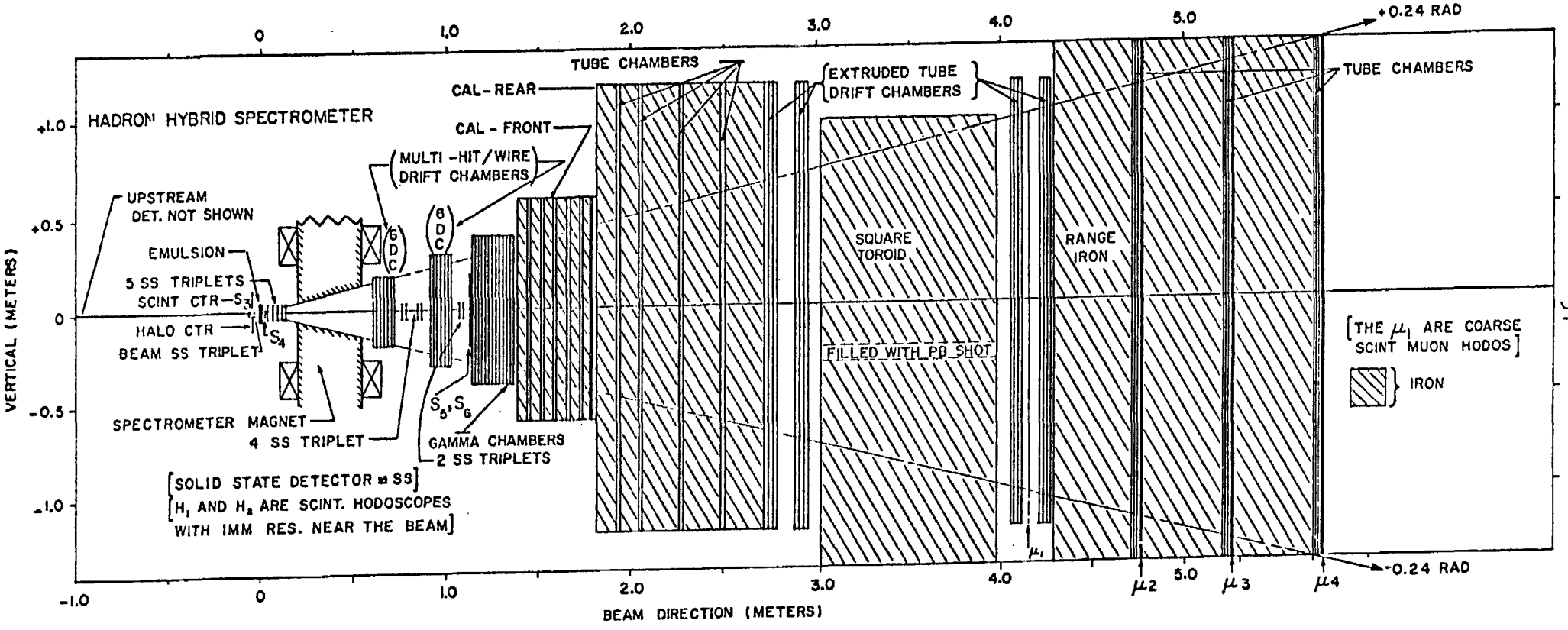
HADRON HYBRID SPECTROMETER
UPSTREAM DET. NOT SHOWN
EMULSION
5 SS TRIPLETS
SCINT CTR—S3
HALO CTR
BEAM SS TRIPLET
S4
SPECTROMETER MAGNET
4 SS TRIPLET
6 DC
6 DC
MULTI-HIT/WIRE DRIFT CHAMBERS
CAL-FRONT
CAL-REAR
TUBE CHAMBERS
S5, S6
GAMMA CHAMBERS
2 SS TRIPLETS
[SOLID STATE DETECTOR ≡ SS]
[H1 AND H2 ARE SCINT. HODOSCOPES WITH IMM RES. NEAR THE BEAM]
EXTRUDED TUBE DRIFT CHAMBERS
SQUARE TOROID
FILLED WITH Pb SHOT
RANGE IRON
μ1
μ2
μ3
μ4
+0.24 RAD
-0.24 RAD
TUBE CHAMBERS
[THE μ1 ARE COARSE SCINT MUON HODOS]
IRON
VERTICAL (METERS)
BEAM DIRECTION (METERS)
-1.0
-0.5
0
+0.5
+1.0
1.0
2.0
3.0
4.0
5.0

Figure 2

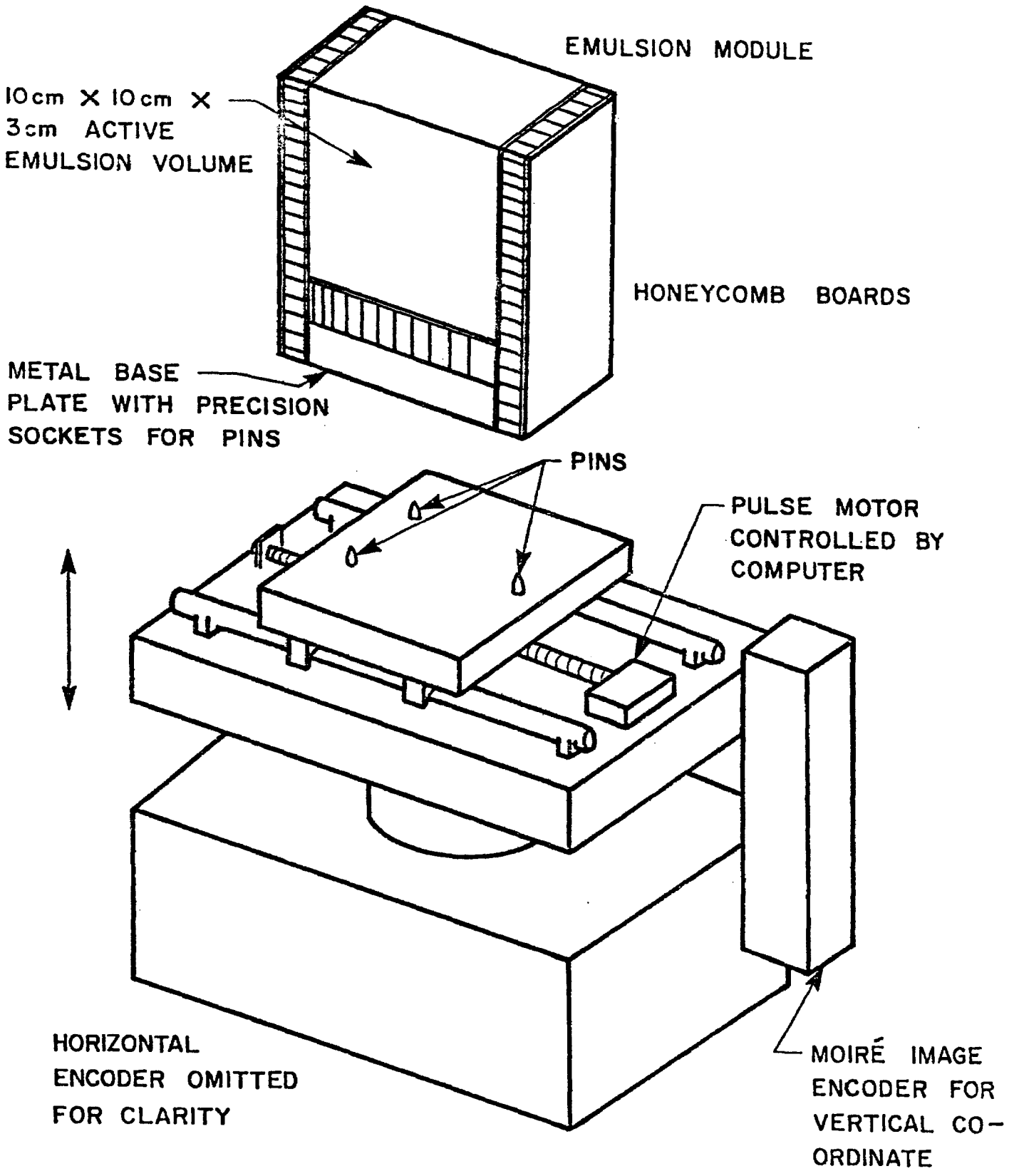

SCHEMATIC DRAWING OF EMULSION STAND

Figure 3

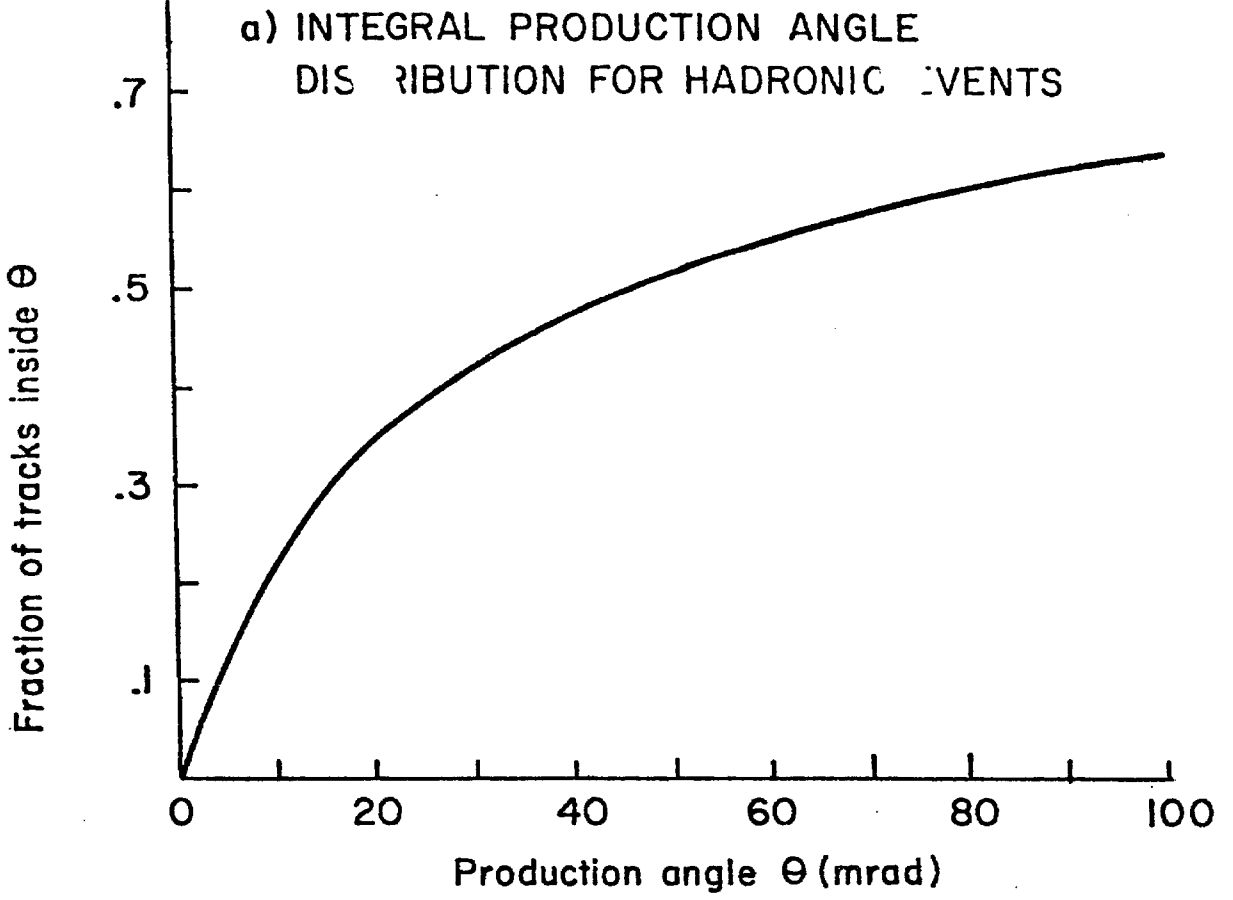
a) INTEGRAL PRODUCTION ANGLE
DIS RIBUTION FOR HADRONIC :VENTS
Fraction of tracks inside θ
.7
.5
.3
.1
0
20
40
60
80
100
Production angle θ (mrad)

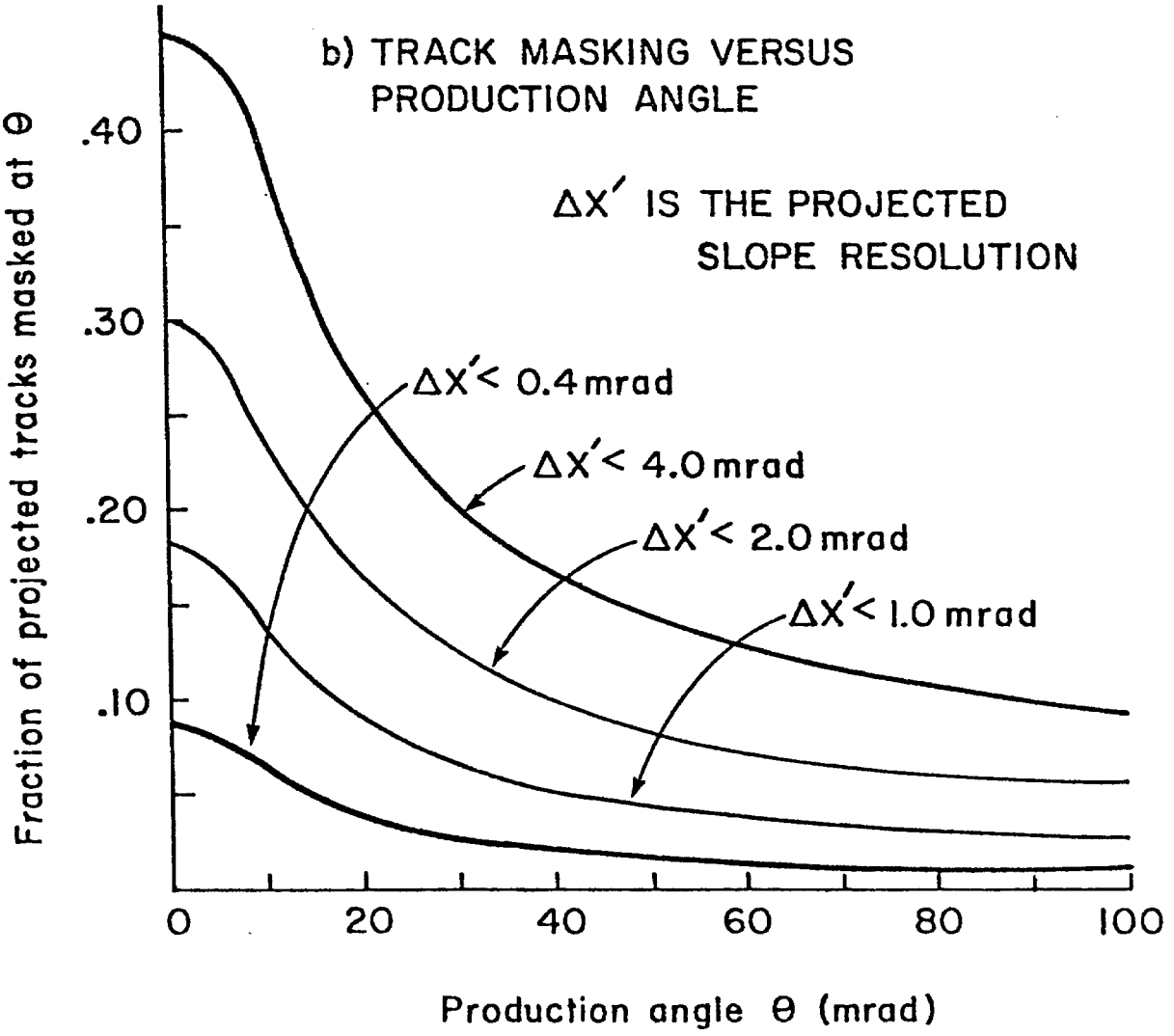
b) TRACK MASKING VERSUS
PRODUCTION ANGLE
ΔX′ IS THE PROJECTED
SLOPE RESOLUTION
Fraction of projected tracks masked at θ
.40
.30
.20
.10
ΔX′< 0.4 mrad
ΔX′< 4.0 mrad
ΔX′< 2.0 mrad
ΔX′< 1.0 mrad
0
20
40
60
80
100
Production angle θ (mrad)

Figure 4

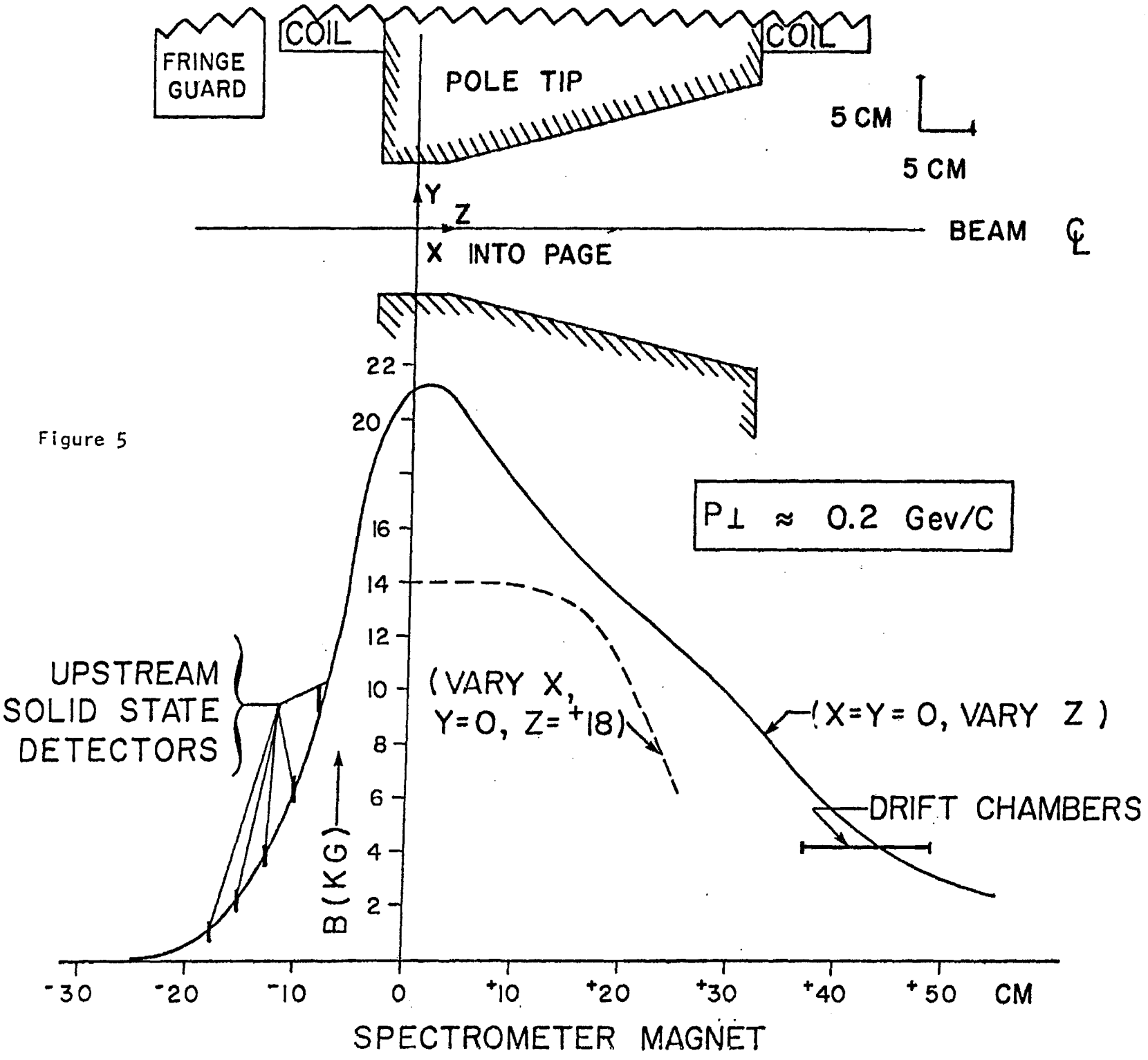
FRINGE GUARD
COIL
COIL
POLE TIP
5 CM
5 CM
Y
Z
X INTO PAGE
BEAM
22
20
16
14
12
10
8
6
4
2
B(KG)
P⊥ ≈ 0.2 Gev/C
UPSTREAM SOLID STATE DETECTORS
(VARY X, Y=0, Z=+18)
(X=Y=0, VARY Z)
DRIFT CHAMBERS
-30
-20
-10
0
+10
+20
+30
+40
+50
CM
SPECTROMETER MAGNET

Figure 5

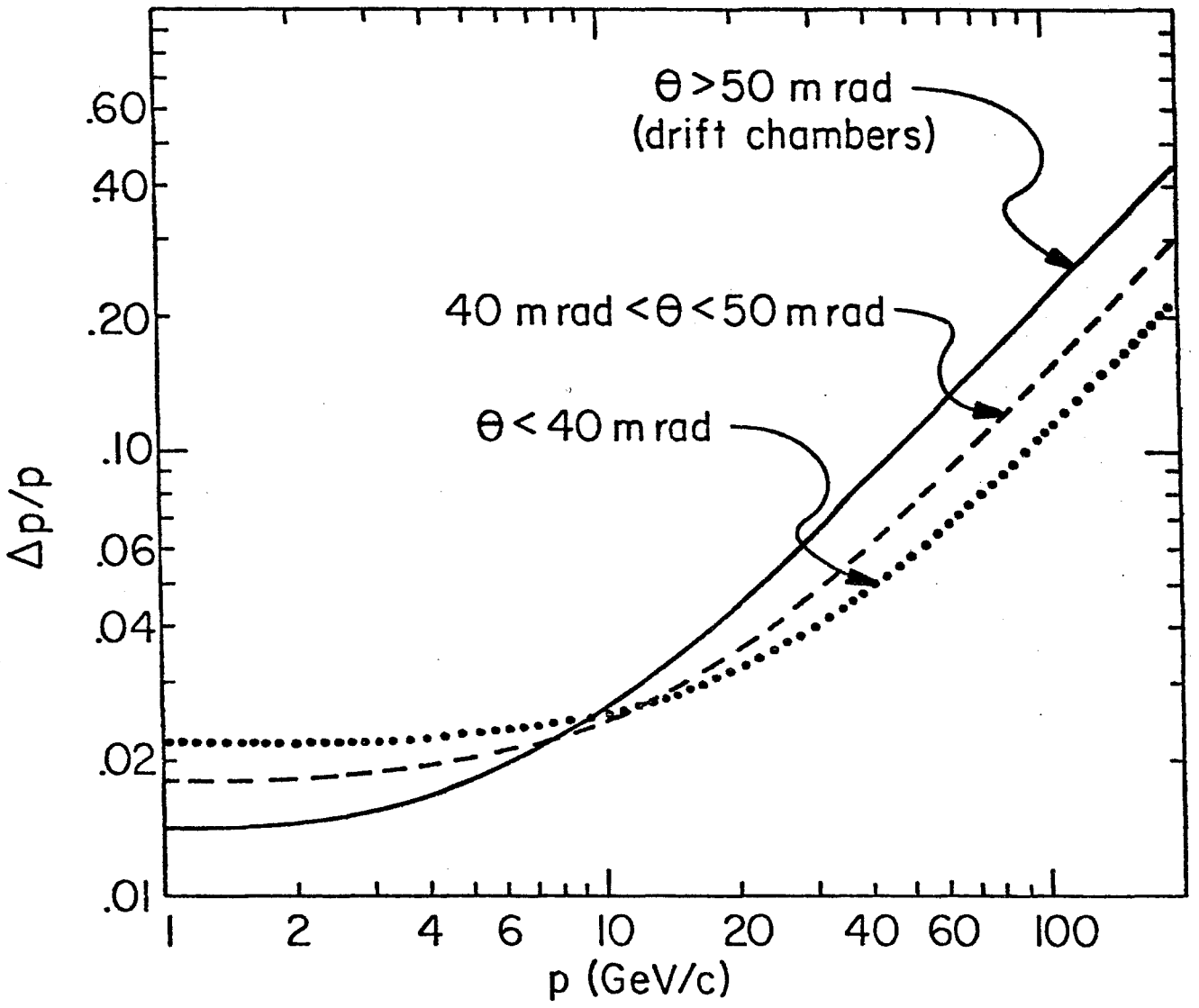
θ >50 m rad
(drift chambers)
40 m rad <θ <50 m rad
θ <40 m rad
Δp/p
.60
.40
.20
.10
.06
.04
.02
.01
1
2
4
6
10
20
40
60
100
p (GeV/c)

Figure 6

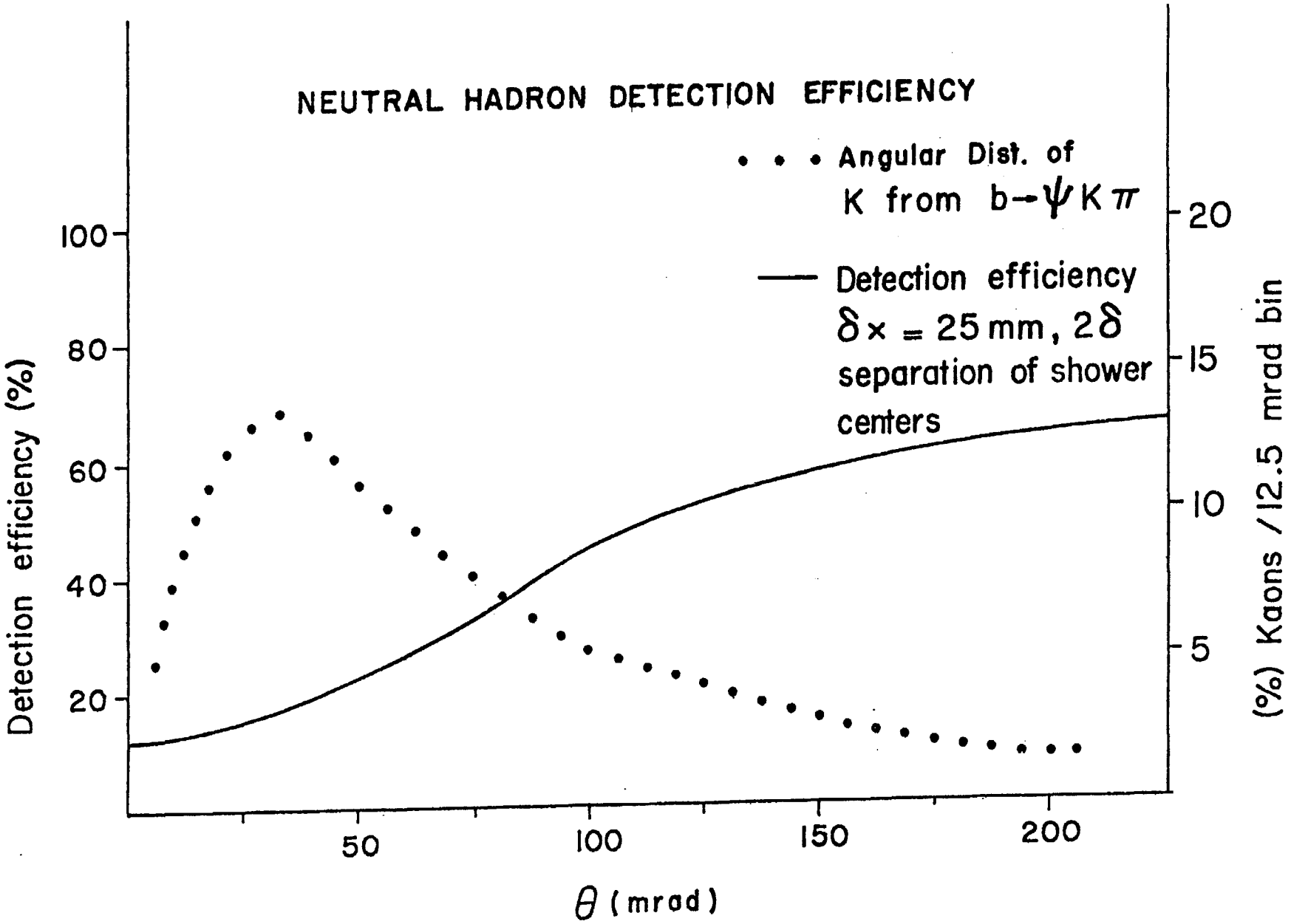
NEUTRAL HADRON DETECTION EFFICIENCY
• • • Angular Dist. of K from b→ψKπ
—— Detection efficiency δx = 25 mm, 2δ separation of shower centers
Detection efficiency (%)
100
80
60
40
20
50
100
150
200
θ (mrad)
20
15
10
5
(%) Kaons / 12.5 mrad bin

Figure 7

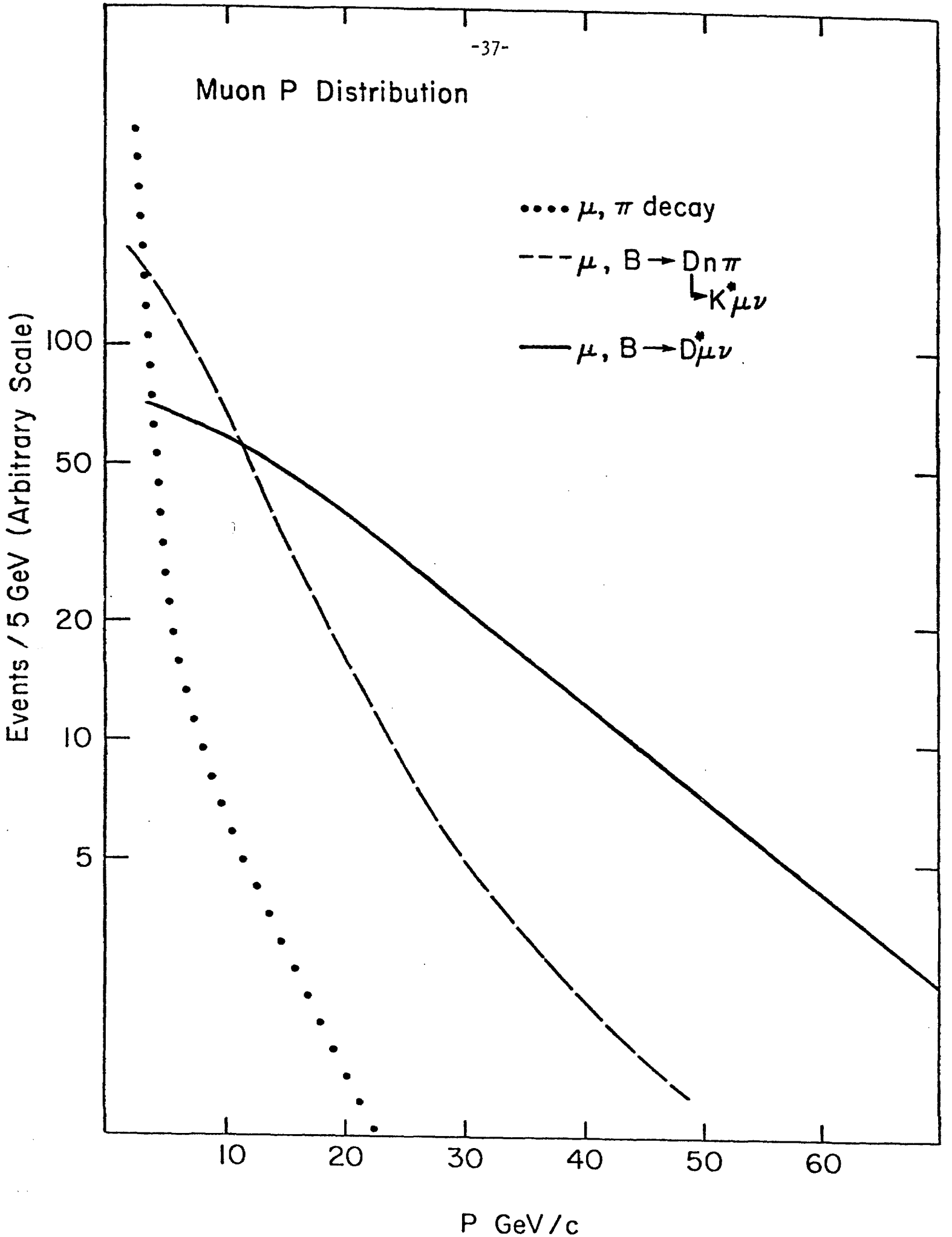
Muon P Distribution
•••• μ, π decay
– – – μ, B → Dnπ
↳ K*μν
—— μ, B → D*μν
Events / 5 GeV (Arbitrary Scale)
100
50
20
10
5
10
20
30
40
50
60
P GeV/c

Figure 8

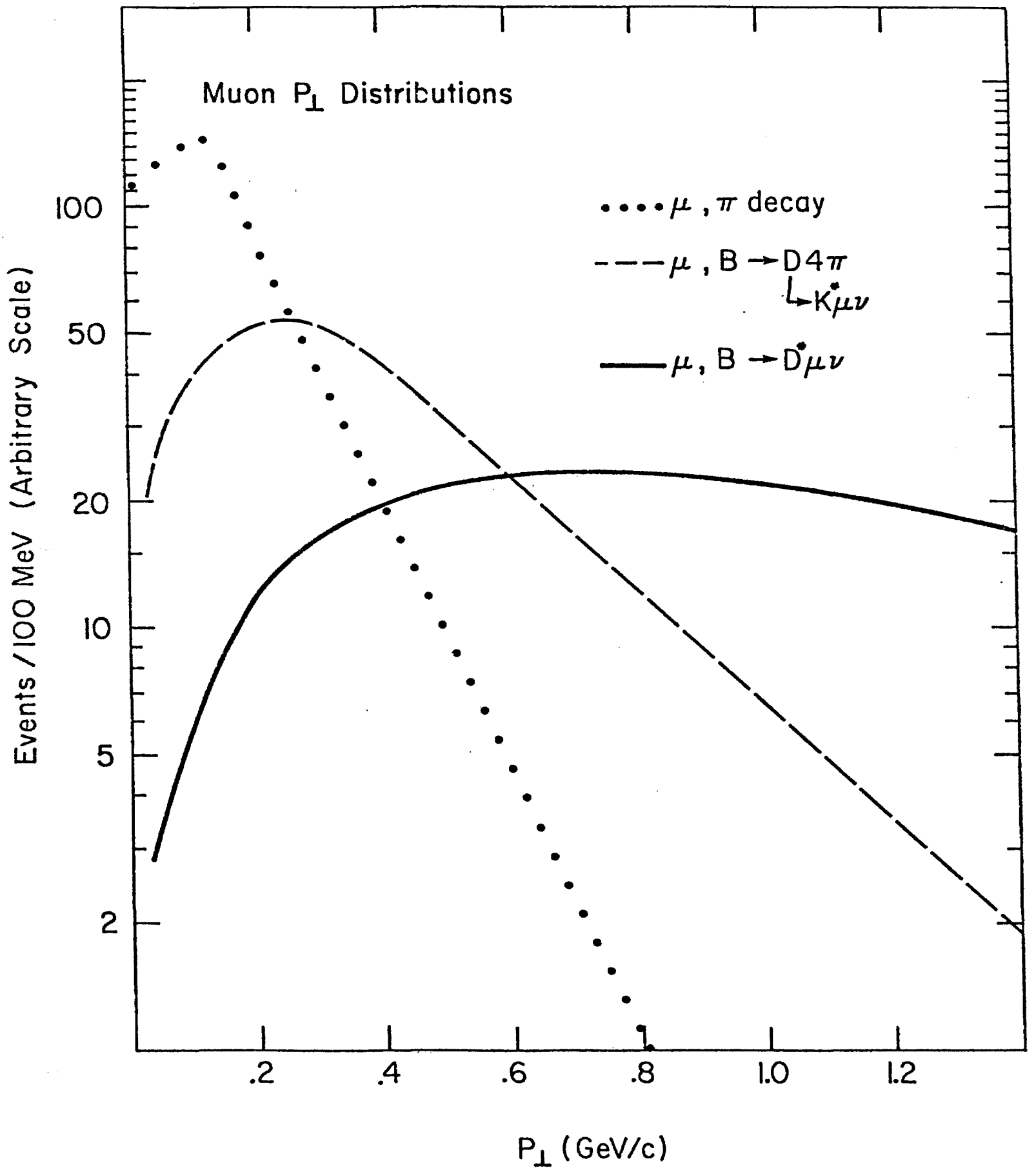
Muon $P_\perp$ Distributions
μ, π decay
μ, B → D4π
L→K$\mu\nu$
μ, B → D$\mu\nu$
Events / 100 MeV (Arbitrary Scale)
100
50
20
10
5
2
.2
.4
.6
.8
1.0
1.2
$P_\perp$ (GeV/c)

Figure 9

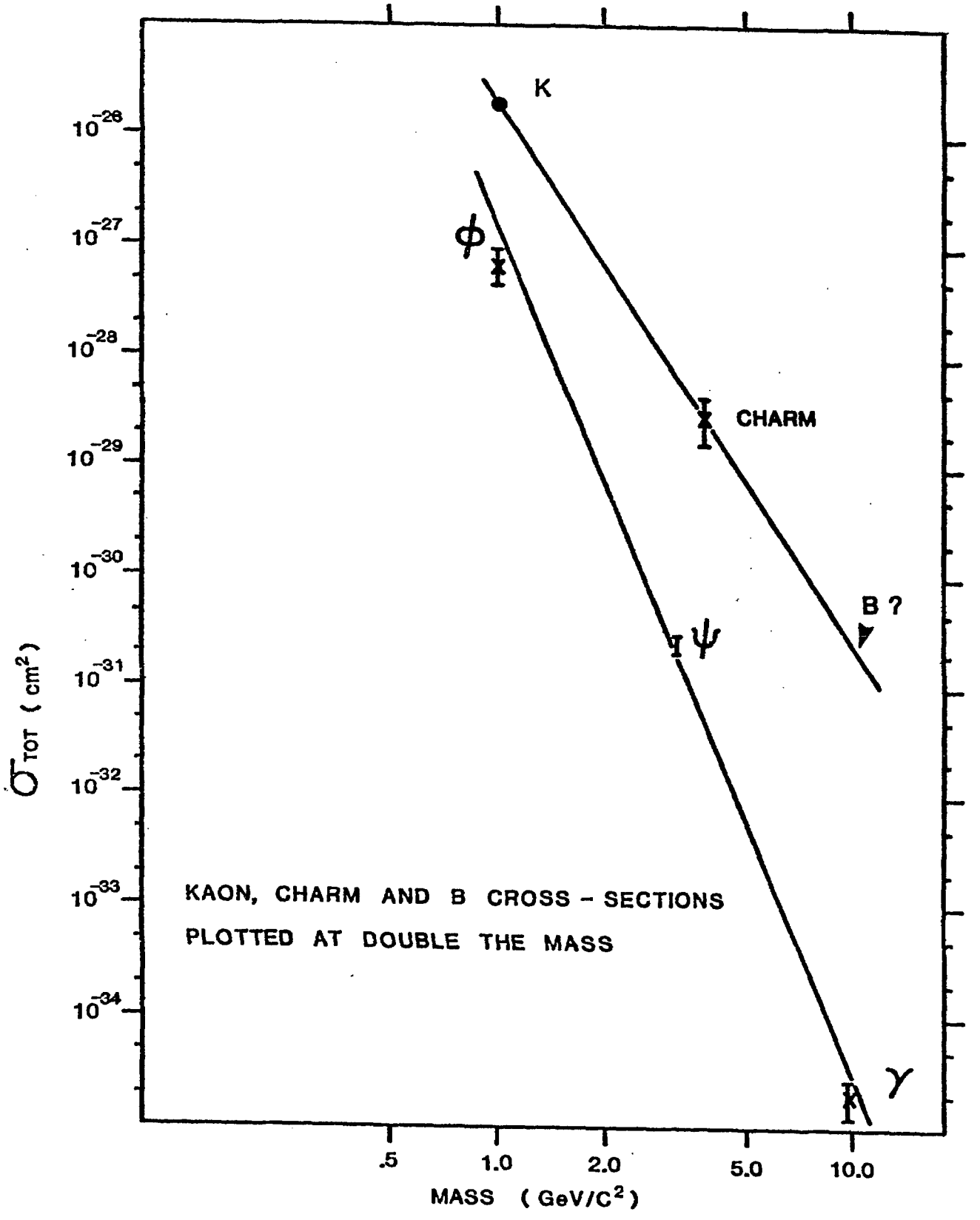
K
φ
CHARM
B ?
ψ
γ
KAON, CHARM AND B CROSS - SECTIONS
PLOTTED AT DOUBLE THE MASS
10^{-26}
10^{-27}
10^{-28}
10^{-29}
10^{-30}
10^{-31}
10^{-32}
10^{-33}
10^{-34}
σ_{TOT} (cm^2)
.5
1.0
2.0
5.0
10.0
MASS (GeV/C^2)

Figure 10

Appendix I

Prototyping of Position-Sensitive Semiconductor Detectors

Though developing solid state detectors will require an extended program, we believe it may be informative to delineate our first steps.

The semiconductor group of the research services division of Lawrence Berkeley Laboratory has agreed to construct six prototype devices according to the specifications shown in Figure I-1 (page 43). These prototypes are designed to test both of the readout techniques to be used in this experiment. Each is made from a wafer of high-resistivity P-type silicon 2cm in diameter and 0.4mm thick. The central active area, 1cm x 1cm square, is given an N-type layer on one side by a standard phosphorous diffusion technique, and the inactive outer portion is covered with an oxide layer. On the other side of the wafer, a pattern of 250 gold strips 0.01mm wide with 0.04mm center-to-center spacing will be laid down over a similar pattern of P-type boron implants covering this active area. These gold strips are fanned out over the inactive region so that at the rim the connection pads have a spacing of 0.25mm. Each detector will then be mounted on a ceramic ring holder to which external connections can be attached. Since every strip is brought out, these prototypes may be used to test both the individual-strip and the charge-division readout techniques with complete flexibility to choose the number of strips between taps.

In order for the charge-interpolation method to succeed it is important to stabilize the impedance between strips. This will be done by protecting the layer between strips with an oxide layer. At present, neither how well the surface under the oxide "pinches off", (i.e., how the impedance between strips varies with applied voltage), nor what noise levels and impedance values can be achieved is known. A preliminary series of tests will therefore be performed on some laboratory samples with 0.5mm spacing which are easier

to produce. If these tests are satisfactory, the six prototypes will then be constructed according to plan.

Ohio State University has committed $7K to this first stage of testing, which should take 2-3 months, and another $18K to the building of the six prototypes, which will take approximately six months more. Because detector noise may be a problem, Ohio State is constructing a cryostat with an internal heating system which will permit controlled stabilization of devices between ambient and liquid nitrogen temperatures.

Even in the initial test setup we must be prepared to detect (with good pulse-height accuracy) signals of a few femtocoulombs from over 100 lines. Thus, the detecting electronics and the test setup must be quite sophisticated. Initially, we propose to borrow about 100 channels of the liquid argon ADC systems designed by Tom Droege. This is one full CAMAC crate and will cover about 4mm of the first prototype. These have a one femtocoulomb least count and a four thousand count dynamic range. Since they are CAMAC modules, it will be easy to connect them to a small computer. This setup should allow understanding many of the properties of the detector such as charge collection efficiency and charge collection time. To make solid state detectors truly effective, we must have even lower noise amplifiers (0.2 femtocoulombs random noise), and 5% pulse height capability for more than ten thousand lines. Developing these amplifiers and a low cost CCD parallel in-series out analogue storage system with fast ADC conversion presents an electronic engineering task which must be pursued simultaneously with hardware development.

Of course, the bottom lines are detection efficiency, single-track spatial resolution and multitrack separation capability. Since these detectors will have state-of-the-art capability, many tests will have to be performed with a stack of at least three identical detectors in a high-momentum test beam.

Though for our proposed usage radiation damage will not be a problem, such may not always be the case for all applications. If solid state devices were to be used as vertex detectors in a colliding beam apparatus, radiation during injection could be severe. Therefore, we will also study the effect of radiation damage for our prototype devices.

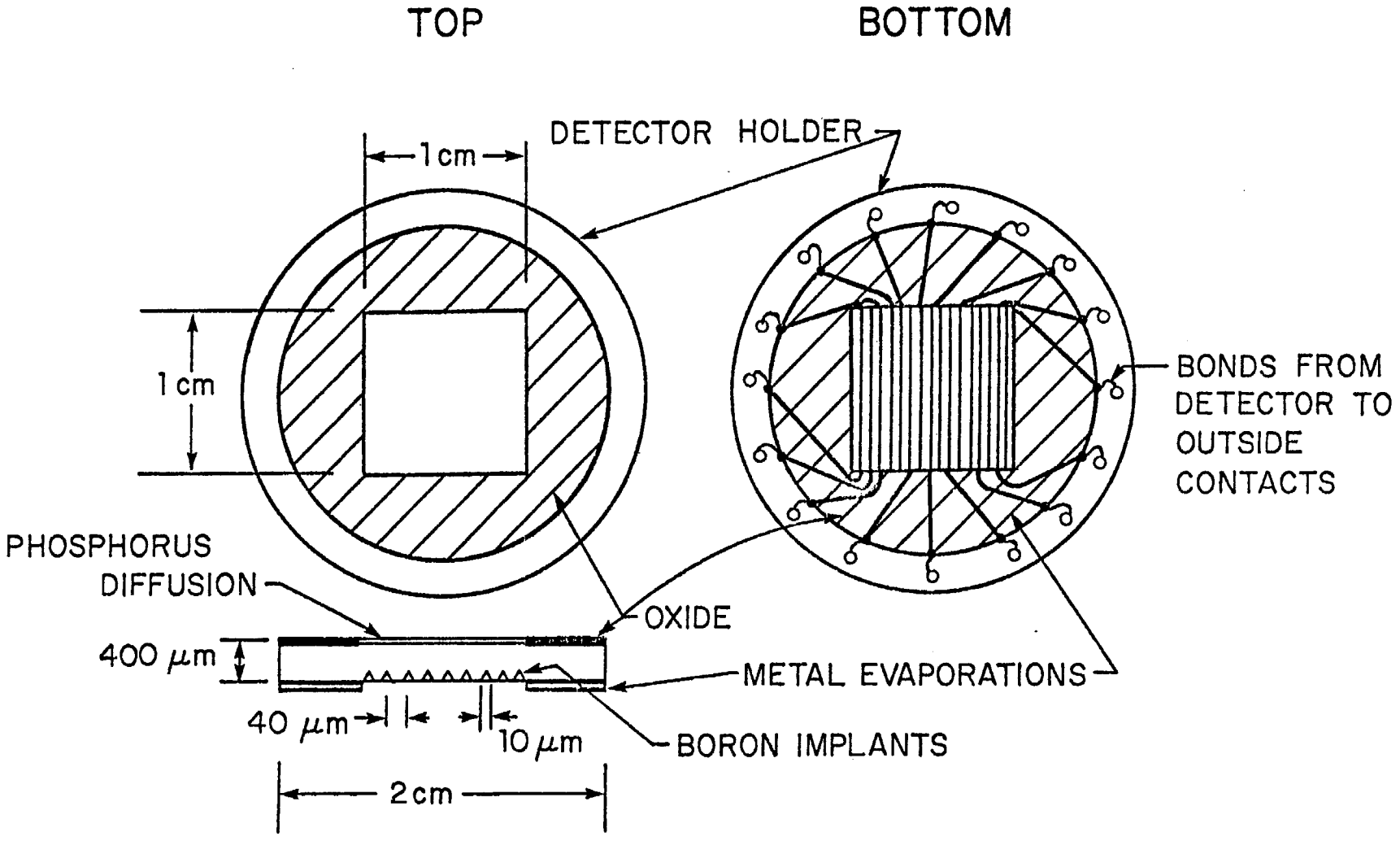
TOP
BOTTOM
DETECTOR HOLDER
1 cm
1 cm
BONDS FROM DETECTOR TO OUTSIDE CONTACTS
PHOSPHORUS DIFFUSION
OXIDE
400 μm
METAL EVAPORATIONS
40 μm
10 μm
BORON IMPLANTS
2 cm
CROSS SECTION OF DETECTOR

Figure 1-1

Appendix II

Event Reconstruction

This appendix is still in preparation, but will be available within two weeks.

Appendix II

Event Reconstruction

We have examined the performance of the spectrometer for several classes of monte-carlo generated decays. Some of the results of these studies have been described in the body of this proposal. In generating events we have assumed central production of pairs of beauty or charmed particles as in Section D above.

The mass resolution and acceptance for "typical" decays of $B \to D\pi^{\pm}\pi^{\mp}\pi^{\pm}\pi^{0}$ and $D \to K^{\pm}\pi^{\mp}\pi^{\pm}\pi^{0}$ are shown in Figure II-1 (a) and (b). A decay is considered to be within the acceptance of the spectrometer if all secondary products including γ's from π^{0} decay lie inside of a cone with half angle $\theta \leq 240$mr. The integrated acceptance for B is 66% and for charm 61%, and is $\geq$ 90% for $X_F \geq 0$. For most events the mass resolution is less than .02m.

In addition to the events completely contained in the spectrometer, we can expect to recover events with one or more charged tracks with $\theta_{LAB} > 240$mr. These tracks, which are slow ($p_{av} \simeq 1$ GeV/c), can be analyzed by measuring ionization and multiple scattering in the emulsion. The expected net resolution is $\sim$ 90 MeV and 210 MeV respectively for charmed and beauty decays in this category, and the acceptance rises to 80% of all decays.

The acceptance shown in Figure II-1 does not include any estimate of the "pattern recognition" losses such as masking of charged or neutral particles by nearby tracks. These masking losses are $\sim$ 5% for charged tracks, 20-30% for γ's from π^{0} decay, and $\geq$ 50% for all neutral hadrons.

An additional loss comes from secondary interactions and gamma conversions in the emulsion target. These secondary vertices can however be analyzed in the same manner as the charm decays with a similar high efficiency. Depending on decay topology one thus expects $\geq \frac{1}{2}$ of all non-leptonic decays to be fully

constrained. For comparison, the fraction of fully constrained events in E531 is 38%.

The final question we shall consider is what fraction of charmed decays is uniquely identified as to species (D^0, Λ_c, $D^{\pm}$, $F^{\pm}$, etc.) in the absence of any charged hadron identification. We find with E531 decays that when we ignore time-of-flight and ionization information, 60% of all events (whether constrained or not) are ambiguous - $\frac{1}{2}$ of mesons, $\sim$ 3/4 of baryons. By use of resonant production (D^*, F^*, Σ^*) we expect a reduction of ambiguities to the level of $\leq$ 40%.

In the table below we list Δm (mass difference between the charm ground state and first excited state), mass resolution, and acceptance (including the pattern recognition losses described above) for some of the anticipated resonance decay modes.

Resonance	Δm (MeV)	Mass Resolution (MeV)	Acceptance for π, γ
$D^{*+} \rightarrow D^0 \pi^+$	145	2	.90
$\rightarrow D^+ \pi^0$	140	3	.35
$\rightarrow D^+ \gamma$	140	20	.60
$F^* \rightarrow F\gamma$	80	15	.60
$\Sigma_c \rightarrow \Lambda_c \pi^{\pm}$	165	3.5	.90

In order for this technique to be useful for tagging of species the background in plots of Δm must be low, < 20%. For $D^0 \pi^+$, $\Lambda_c \pi^{\pm}$ and $D^+ \pi^0$, where the resolution is $\sim$ 3 MeV, this level of background can probably be achieved. Assuming that resonance production is half of total charm production we then have 35% of D^0 and $\sim$ 40% of D^+ and Λ_c^+ ambiguous. It is not clear whether plotting Δm is useful in identifying F^s.

Some charged particle identification is possible even with the very short distances available in the proposed spectrometer. A time-of flight system with

80 p sec resolution would separate π/p to 4 GeV/c (in E531 we obtain 120 ps with scintillators 1.7 in. long). Ionization in the emulsion is useful to distinguish π/k to 0.8 GeV/c and K/p to 1.5 GeV/c. Finally, we observe that pulse height will be recorded in the 33 silicon detectors for all secondaries with $\theta_{LAB} < 40mr$ and tagging of particle type using the relativistic rise of dE/dx may be possible.

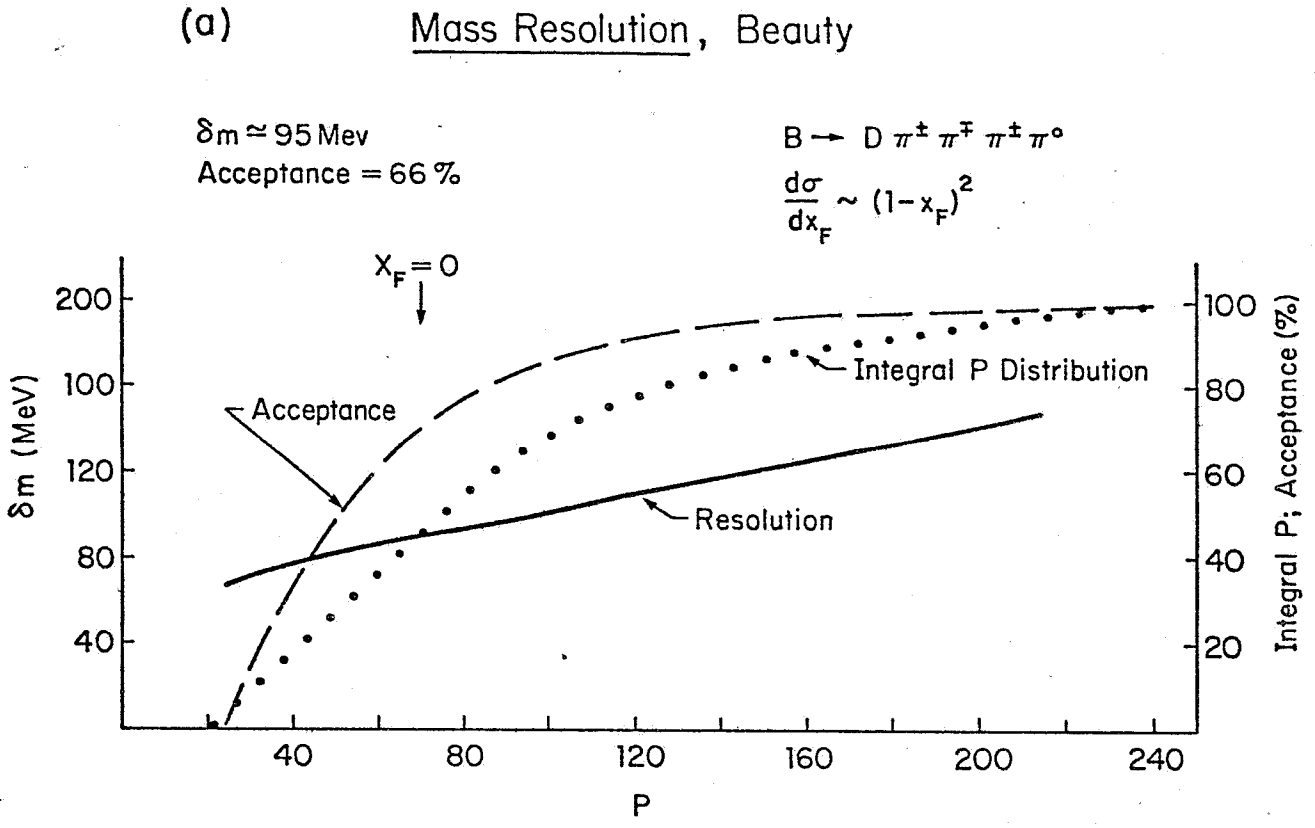
(a) Mass Resolution, Beauty
δm ≃ 95 Mev
Acceptance = 66 %
B → D π± π∓ π± π°
dσ/dx_F ~ (1−x_F)²
X_F = 0
Acceptance
Integral P Distribution
Resolution
δm (MeV)
Integral P; Acceptance (%)
P
200
100
120
80
40
100
80
60
40
20
40
80
120
160
200
240

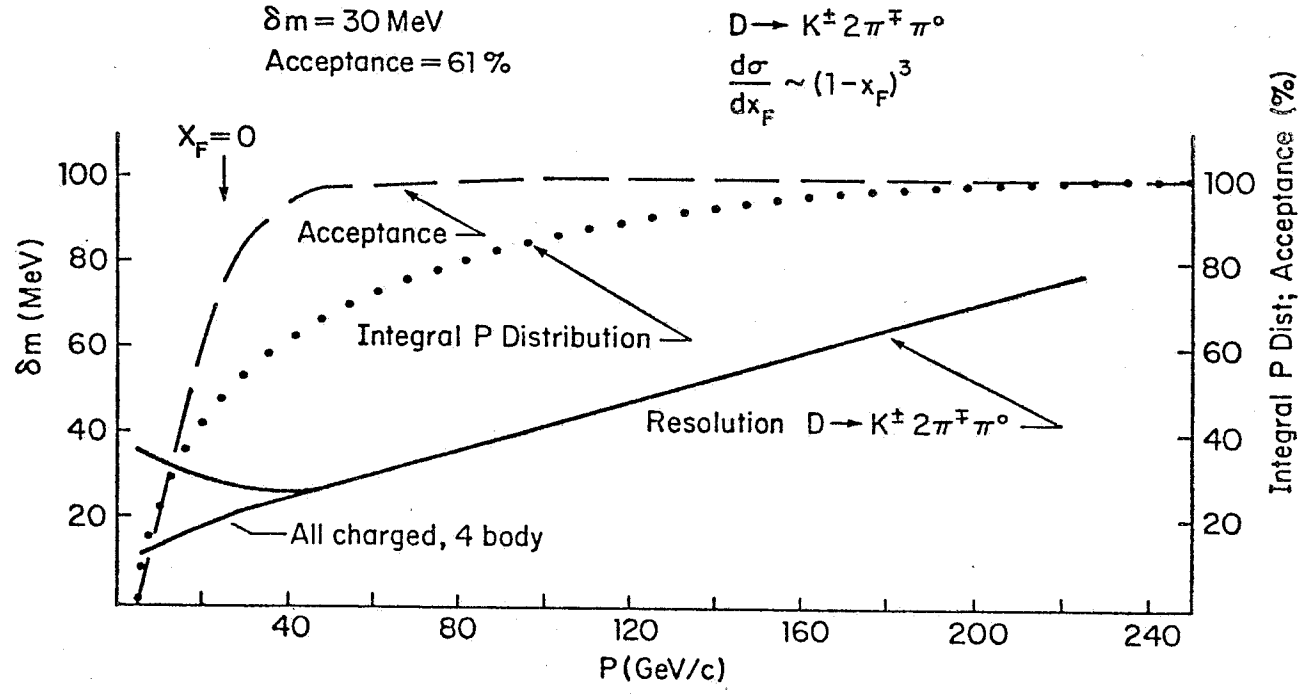
(b) Mass Resolution, Charm
δm = 30 MeV
Acceptance = 61 %
D → K± 2π∓ π°
dσ/dx_F ~ (1−x_F)³
X_F = 0
Acceptance
Integral P Distribution
Resolution D → K± 2π∓ π°
All charged, 4 body
δm (MeV)
Integral P Dist; Acceptance (%)
P (GeV/c)
100
80
60
40
20
100
80
60
40
20
40
80
120
160
200
240

FIGURE II-1

Figure I-6.

Stripe Hit Correlations

Matrix of correlated hits, first plane (1-4)→, second plane ↓ with last detector also hit.

DATA

3 MeV Source

a)

58	10	0	3
18	56	11	0
5	22	69	20
0	0	6	42

220	Diagonal
87	1 Off Diag.
8	> 1 Off
315	

30 MeV Linac

b)

80	2	4	0
15	86	9	3
3	13	174	9
6	4	22	116

456	Diagonal
70	1 Off Diag.
20	> 1 Off
546	

MONTE CARLO

c)

48	9	0	0
14	54	12	1
3	26	54	19
0	7	26	42

198	Diagonal
106	1 Off Diag.
11	> 1 Off
315	

d)

94	0	0	0
20	149	0	0
0	26	149	0
0	0	17	91

483	Diagonal
63	1 Off Diag.
0	> 1 Off
546	

Appendix II

Possible Beam Lines

At least three beam lines (M2, M6W, PC) appear to be compatible with our requirements for both present and Tevatron energies.

We require a beam at or near maximum machine energy which has 2-6 x 10^4/second intensity on a spot size 3 mm x 3 mm, and an integrated halo in a square 10 cm x 20 cm centered on the beam which is at most 7% of the beam intensity. (Note that for a 20-second Tevatron spill we would require roughly 1/2 x 10^6/pulse.)

The remainder of this section will be devoted to a discussion of measurements on the M6 charged beam (provided by P. Garbincius) and on the PC neutron beam (provided by M. Johnson). It is our feeling that the M2 hyperon channel also would be suitable, but we were unable to obtain applicable measurements.

For a 2 x 10^6 positive M6 beam at 100 GeV (2/3π, 1/3P) a spot 6 mm in width and 5 mm high was obtained for the ten percent beam density points. Ninety-eight percent of the beam was contained in a spot of 9 mm x 8 mm.

Halo was determined by three sets of three halo counters, each set mounted in a cloverleaf fashion with a 6 mm x 6 mm hole in the center. The sets of antis were mounted at the second focus and upstream and downstream of the hydrogen target.

The ratio of halo/beam summed over all three sets was 0.075, completely consistent with the fraction of beam overlapping the antis. Spot size and halo did not appear to be a strong function of the momentum setting for the beam, so additional collimation placed at the first focus and along the parallel section should be able to reduce them down to our requirements.

A neutron beam is being commissioned in Proton Center for E-630. They have obtained 0.3 x 10^6 neutrons per pulse in a spot sized 1 mm x 7 mm. The ratio of halo/beam = .04 for halo outside 2 mm x 9 mm. This beam may be converted to a diffracted proton beam of suitable intensity by targetting the main beam at a

small angle into a new curved channel. An additional set of three 10-ft. benders placed downstream of the hyperon magnet would be run with polarity opposite to that magnet, partially correcting for momentum dispersion. K. Stanfield and P. Garbincius believe that a diffracted proton beam could be constructed with a suitable spot size and a halo/beam ratio at least as low as that measured for the neutron beam.

In summary, we believe that our beam requirements are quite minimal and could be satisfied by several existing and proposed Tevatron beam lines with minimal additional cost to Fermilab. Furthermore, our experiment uses less than 15 meters of floor space and could be designed to move in and out of the beam in a day of rigging.

Appendix III

Spectrometer Magnet

Our compact geometry imposes definite constraints on the spectrometer magnet. To get the largest possible field integral we use a tapered vertical magnet gap which opens from 14 cm to 28 cm over a distance of 40 cm. To reduce interference of the coils (and their attendant fringe fields) with the silicon detectors and their amplifiers and connector boards, we propose to put two coils around the sides of an H-frame magnet rather than around the pole-tips as is usually done. A total of 500 kiloamp turns will produce a maximum field of 1.7 Tesla and a transverse momentum kick of 0.2 GeV/c. We are studying the feasibility of using Fe-Co pole tips (saturating at 1.5 times higher field) to increase this kick to 0.3 GeV/c.

Although we can accomplish these goals with conventional coils, fig. III-1 shows the improved geometry possible with superconducting coils. The dimensions of the two cryogenic cans containing such coils are 0.4 m ID by 0.6 m OD by 0.3 m high. The coils are circular and take up their own Lorentz forces by tension, permitting a simple support structure design. If one adds the saving in electric power, the superconducting option looks very attractive. The OU group of our collaboration has sufficient technical expertise and manpower to design the coil, cryostat and magnet but would need the cooperation of Fermilab to provide it with superconducting cable, transformer iron and other materials. Since this magnet requires only about 500 liters of liquid Helium per week it could be kept cold using Dewars; however, a refrigeration system, if one were available, might be a useful alternative.

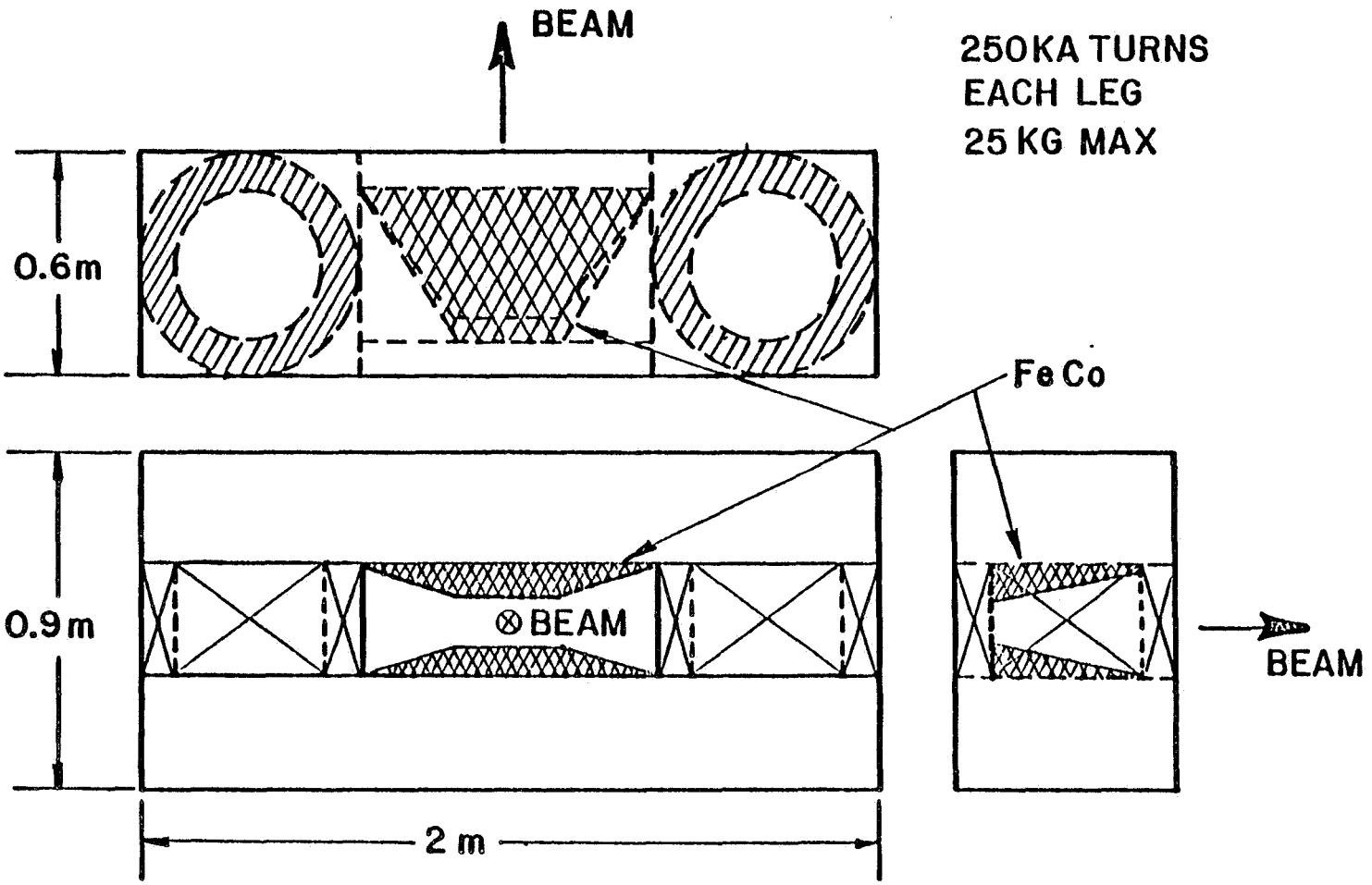

Figure III-1. Spectrometer magnet, drawn for superconducting coils.

Appendix IV

Calculation of Muon Background

The muon background from charged pion and K decay was calculated from ISR production data [18] at center of mass energies of 31 and 53 GeV. Special care was taken in parametrizing this data to be sure the behavior at high transverse momentum P_T was correctly described, since event selection depends at least in part on high-p_T muons. Comparison of the model with data at rapidity y=0 are shown for pions and K's in figs. IV-1a and IV-1b. The model also works well for nonzero y out to very near the edge of phase space.

Laboratory cross sections $d^2\sigma/dpdp_T$ were then calculated with this parametrization on a grid of p, p_T. In each bin of this grid the fraction of pion or K decays per meter is then $m/(c\tau p)$, where τ is the lifetime of the decaying particle of mass m. In each bin of p,p_T of interest a number of monte carlo decays ($\pi \rightarrow \mu\nu$, $K \rightarrow \mu\nu$) were generated proportional to the number of parent decays in the bin. The resulting integral muon spectra are plotted vs. p_T in figs. 9 , 10 for several cuts on lab momentum p. Note that the contributions from pion and K decay are comparable for $p_T > 1.2$ GeV/c.

An independent check on this calculation was provided by a tape [12] of 360 GeV π^-p bubble-chamber events. Charged tracks from these real events were assumed to be pions, and monte carlo decays were generated. The muon yield from this approach agrees with the above calculation to better than 10%.

For the background estimates in Section D; it is necessary to know the number of muons from <u>secondary</u> interactions in the emulsion passing the muon p, p_T cuts. The lab momentum spectrum of pions from 800 GeV interactions is known from the production model described above. It was assumed that this model is also approximately correct for interacting pions down to 10 GeV/c, and the

muon background program was run for "beams" with selected momenta between 10 and 800 GeV/c, corresponding to the interacting secondaries. The yield of muons passing the cuts for each such bin of secondary momentum was then weighted by the momentum spectrum of pions from 800 GeV interactions. The largest contribution to muons passing the cuts was from secondaries of order 100 GeV/c, which make about 6 charged prongs per interaction. We thus estimate that limiting charm decay vertex candidates to < 7 prongs will eliminate 40% of this interaction background.

The probability of a muon from a secondary interaction passing the p, P_T and prong cuts was found to be 0.13 times that of a muon from the primary vertex. This number must be multiplied by the probability of a secondary interaction. We assume 9 charged prongs plus 2 long-lived neutral hadrons per 800 GeV interaction, and use the pion mean free path [17] of 50 cm and an effective path in emulsion of 0.75 cm to obtain 0.165 secondary interactions per event.

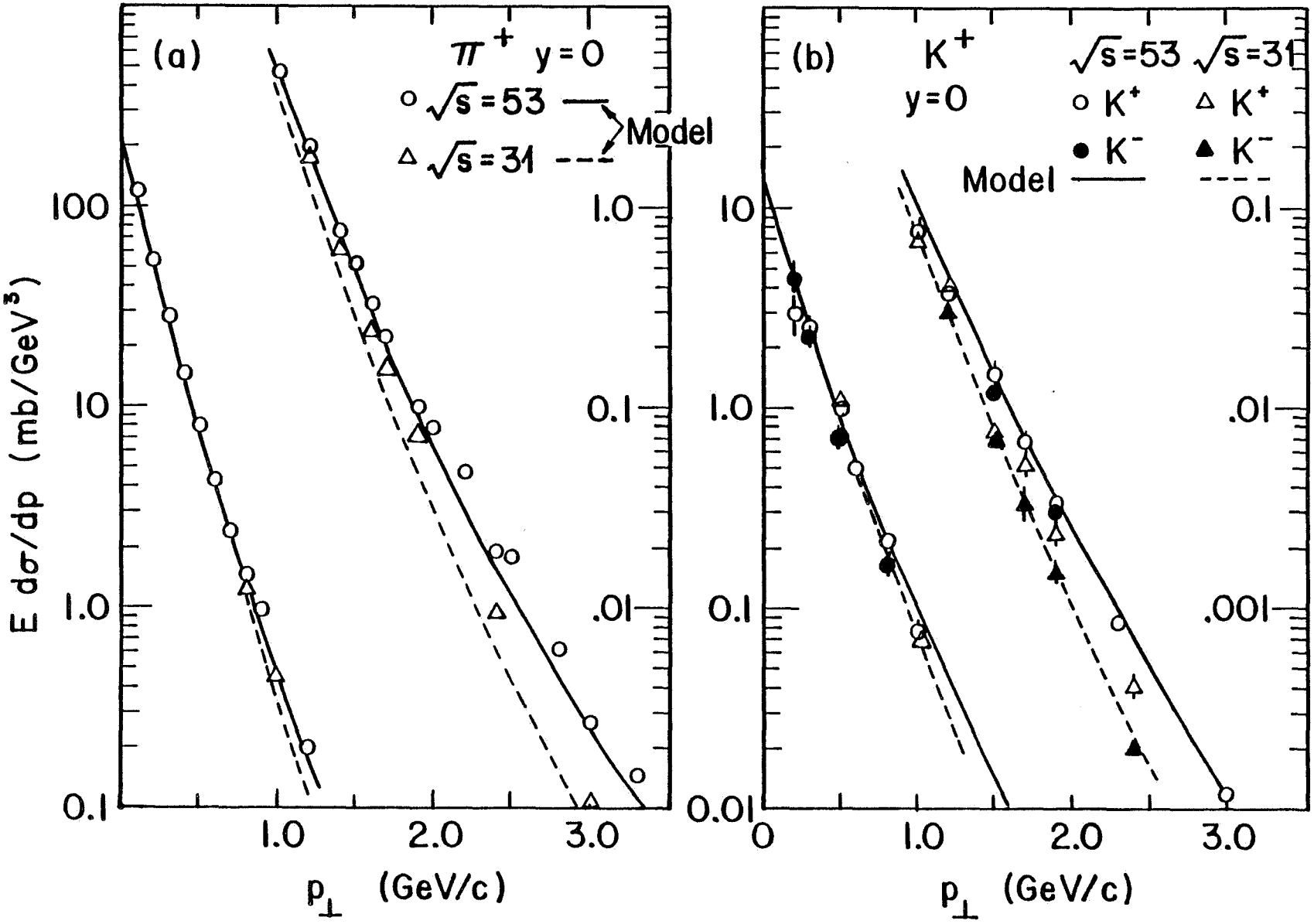
(a)
π⁺ y=0
○ √s=53
△ √s=31
Model
E dσ/dp (mb/GeV³)
100
10
1.0
0.1
1.0
.01
1.0
2.0
3.0
p⊥ (GeV/c)
(b)
K⁺
y=0
√s=53 √s=31
○ K⁺ △ K⁺
● K⁻ ▲ K⁻
Model
10
1.0
0.1
0.1
.01
.001
0.01
0
1.0
2.0
3.0
p⊥ (GeV/c)

Figure IV-1.

REFERENCES

1. N.Ushida et al., Phys.Rev.Lett. 45, 1049(1980); N.Ushida et al., Phys.Rev. Lett. 45, 1053(1980).
2. S.M.Errede, Ohio State University Ph.D. Thesis(in preparation).
3. M.J.Gutzwiller, Ohio State University Ph.D. Thesis(1981).
4. D.Andrews et al., Phys.Rev.Lett. 45, 219(1980); G.Finocchiaro et al., Phys. Rev.Lett. 45, 222(1980).
5. M.Kobayashi and K.Maskawa, Prog.Theor.Phys. 49, 652(1973).
6. See, e.g., John Ellis, "Status of Gauge Theories," CERN preprint Th-2701(1979); S.K.Nandi and K.Tanaka, Phys.Lett. 92B, 107(1980); J.A.Harvey, P.Ramond and D.B.Reiss, Phys.Lett. 92B, 309(1980).
7. H.Tye, "B Decays in the Weinberg-Salam Model," Cornell preprint CBX-81-9(1981).
8. E.H.Thorndike, "First Results on Bare b Physics," Proceedings of XX International Conference on High Energy Physics, Madison Wisconsin(1980), P.705; CLEO collaboration, "Charged and Neutral Kaon Production at the Upsilon 4s," CLNS 81-483(1981). It should be noted, however, that the large kaon signal at the upsilon 4S is not unambiguous evidence for dominant B→ charm(B.Gittelman, private communication), so that this upper limit on B lifetime is not rigorous until this important experimental question is settled.
9. V.Radeka and R.A.Boie, IEEE Trans.Nucl.Sci.27, 351(1980).
10. See, e.g., review by J.N.Marx in "Proceedings of Summer Institute on Particle Physics," SLAC Report No.239(1981), p.215.
11. S.L.Stone, et al., Nucl.Inst.and Meth. 151, 387(1978); See also Ref.14 .
12. We wish to thank J.Whitmore of Michigan State for providing us a tape of 360 GeV π^-p events from the 30-Inch bubble chamber. For 800 GeV design studies, these events were given an appropriate Lorentz boost, and were augmented by extra tracks generated by Monte Carlo to give the correct average multiplicity. Neutral pions(and their decay gammas) with the same p, p_t distribution as charged tracks were also generated by Monte Carlo for each bubble chamber event.
13. The EGS calculations were performed with lead rather than tungsten because lead parameters were "hard wired" into the program. Tungsten radiators will give even less shower spread than lead.
14. See, e.g., review by H.A.Gordon and S.D.Smith in "Proceedings of Summer Institute on Particle Physics," SLAC Report No.239(1981), p.241.
15. T.A.Gabriel and W.Schmidt, Nucl.Instr. and Meth. 134, 271(1978).
16. A.Zichichi, in talk presented at Physics in Collision Conference, Blacksburg, Va.(May, 1981).
17. The measured interaction mean free path for 200 GeV protons in emulsion is 35.5 ± 0.8 cm (J.Hebert, private communication). The MFP for high energy pions will be larger by a factor of about 1.5.
18. B.Alper et al., Nucl.Phys. B100, 237(1975)
19. J.Kirkby, "Review of e^+e^- Reactions in the Energy Range 3 to 9 GeV," in Proceedings of the International Symposium on Lepton and Photon Interactions, Fermilab(1979) p.107.
20. H.Winzeler, Nucl.Phys.69, 661(1965).

References continued

21. S.R.Amendolia et al., "A Multielectrode Silicon Detector for High Energy Physics Experiments," PISA 80-2(1980); Nucl.Inst. and Meth. 176, 457(1980).

22. E.H.M.Heijne et al., "A Silicon Surface Barrier Microstrip Detector Designed for High Energy Physics," CERN/EF/BEAM 80-6(1980); Nucl.Instr. and Meth. 178, 331(1980).

23. J.B.A.England et al., "Capacitative Charge Division Read-Out with a Silicon Strip Detector," CERN-EP/80-218(1980).

Appendix II

Event Reconstruction

We have examined the performance of the spectrometer for several classes of monte-carlo generated decays. Some of the results of these studies have been described in the body of this proposal. In generating events we have assumed central production of pairs of beauty or charmed particles as in Section D above.

The mass resolution and acceptance for "typical" decays of $B \to D\pi^{\pm}\pi^{\mp}\pi^{\pm}\pi^{0}$ and $D \to K^{\pm}\pi^{\mp}\pi^{\pm}\pi^{0}$ are shown in Figure II-1 (a) and (b). A decay is considered to be within the acceptance of the spectrometer if all secondary products including γ's from π^{0} decay lie inside of a cone with half angle $\theta \leq 240$mr. The integrated acceptance for B is 66% and for charm 61%, and is $\geq$ 90% for $X_F \geq 0$. For most events the mass resolution is less than .02m.

In addition to the events completely contained in the spectrometer, we can expect to recover events with one or more charged tracks with $\theta_{LAB} > 240$mr. These tracks, which are slow ($p_{av} \simeq 1$ GeV/c), can be analyzed by measuring ionization and multiple scattering in the emulsion. The expected net resolution is $\sim$ 90 MeV and 210 MeV respectively for charmed and beauty decays in this category, and the acceptance rises to 80% of all decays.

The acceptance shown in Figure II-1 does not include any estimate of the "pattern recognition" losses such as masking of charged or neutral particles by nearby tracks. These masking losses are $\sim$ 5% for charged tracks, 20-30% for γ's from π^{0} decay, and $\geq$ 50% for all neutral hadrons.

An additional loss comes from secondary interactions and gamma conversions in the emulsion target. These secondary vertices can however be analyzed in the same manner as the charm decays with a similar high efficiency. Depending on decay topology one thus expects $\geq \frac{1}{2}$ of all non-leptonic decays to be fully

constrained. For comparison, the fraction of fully constrained events in E531 is 38%.

The final question we shall consider is what fraction of charmed decays is uniquely identified as to species (D^0, Λ_c, $D^{\pm}$, $F^{\pm}$, etc.) in the absence of any charged hadron identification. We find with E531 decays that when we ignore time-of-flight and ionization information, 60% of all events (whether constrained or not) are ambiguous - $\frac{1}{2}$ of mesons, $\sim$ 3/4 of baryons. By use of resonant production (D^*, F^*, Σ^*) we expect a reduction of ambiguities to the level of $\leq$ 40%.

In the table below we list Δm (mass difference between the charm ground state and first excited state), mass resolution, and acceptance (including the pattern recognition losses described above) for some of the anticipated resonance decay modes.

Resonance	Δm (MeV)	Mass Resolution (MeV)	Acceptance for π, γ
$D^{*+} \rightarrow D^0 \pi^+$	145	2	.90
$\rightarrow D^+ \pi^0$	140	3	.35
$\rightarrow D^+ \gamma$	140	20	.60
$F^* \rightarrow F\gamma$	80	15	.60
$\Sigma_c \rightarrow \Lambda_c \pi^{\pm}$	165	3.5	.90

In order for this technique to be useful for tagging of species the background in plots of Δm must be low, < 20%. For $D^0 \pi^+$, $\Lambda_c \pi^{\pm}$ and $D^+ \pi^0$, where the resolution is $\sim$ 3 MeV, this level of background can probably be achieved. Assuming that resonance production is half of total charm production we then have 35% of D^0 and $\sim$ 40% of D^+ and Λ_c^+ ambiguous. It is not clear whether plotting Δm is useful in identifying F^s.

Some charged particle identification is possible even with the very short distances available in the proposed spectrometer. A time-of flight system with

80 p sec resolution would separate π/p to 4 GeV/c (in E531 we obtain 120 ps with scintillators 1.7 in. long). Ionization in the emulsion is useful to distinguish π/k to 0.8 GeV/c and K/p to 1.5 GeV/c. Finally, we observe that pulse height will be recorded in the 33 silicon detectors for all secondaries with $\theta_{LAB} < 40mr$ and tagging of particle type using the relativistic rise of dE/dx may be possible.

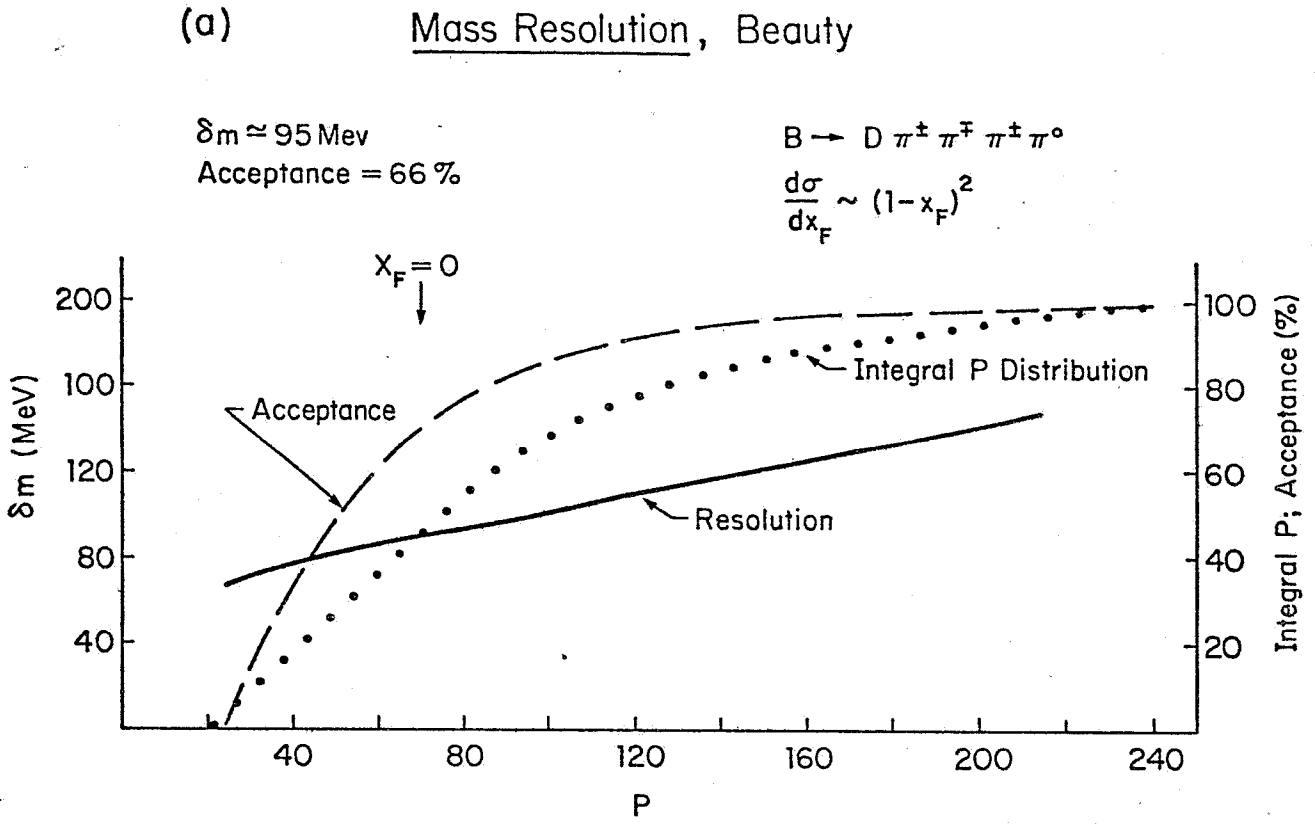
(a) Mass Resolution, Beauty
δm ≃ 95 Mev
Acceptance = 66 %
B → D π± π∓ π± π°
dσ/dx_F ~ (1−x_F)²
X_F = 0
Acceptance
Integral P Distribution
Resolution
δm (MeV)
Integral P; Acceptance (%)
P
200
100
120
80
40
100
80
60
40
20
40
80
120
160
200
240

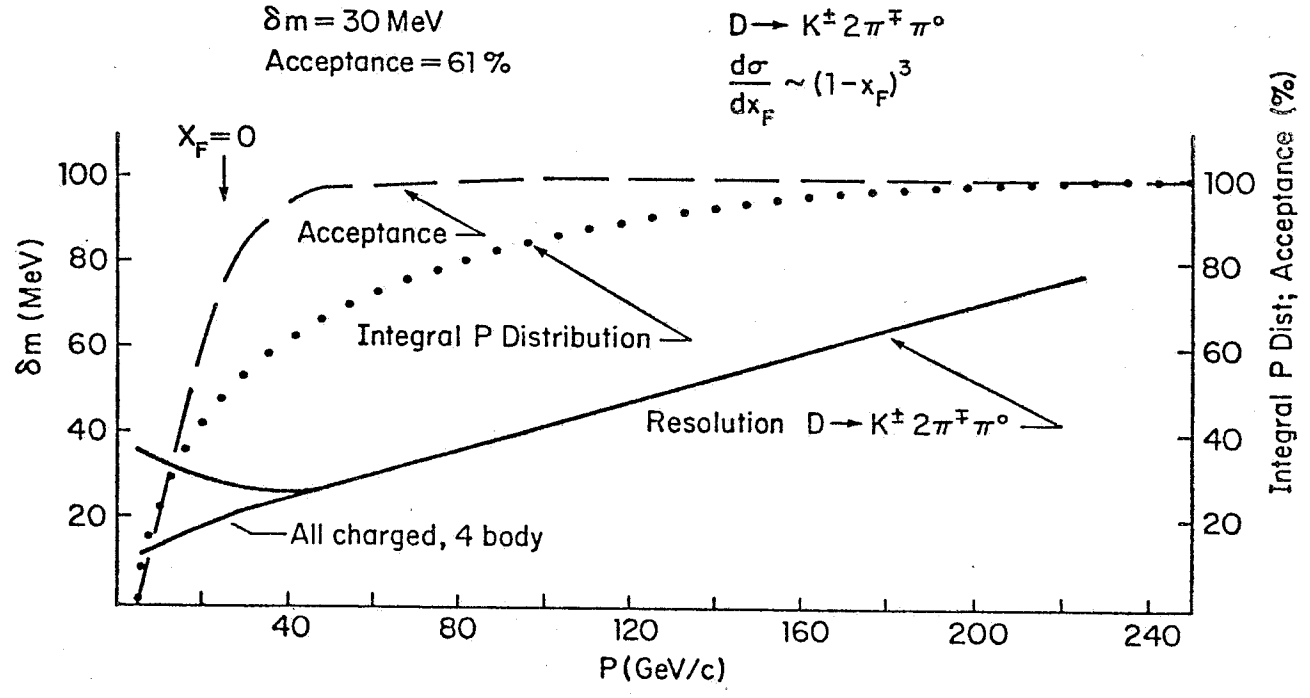
(b) Mass Resolution, Charm
δm = 30 MeV
Acceptance = 61 %
D → K± 2π∓ π°
dσ/dx_F ~ (1−x_F)³
X_F = 0
Acceptance
Integral P Distribution
Resolution D → K± 2π∓ π°
All charged, 4 body
δm (MeV)
Integral P Dist; Acceptance (%)
P (GeV/c)
100
80
60
40
20
100
80
60
40
20
40
80
120
160
200
240

FIGURE II-1

Spokesperson: Neville W. Reay
Department of Physics
Ohio State University
Columbus, Ohio 43210
614-422-7436
FTS 8-940-7436

P-653

A PROPOSAL TO MEASURE CHARM AND B DECAYS VIA HADRONIC PRODUCTION IN A HYBRID EMULSION SPECTROMETER

N. Ushida
Aichi University of Education, Kariya, Japan

M. Johnson
Fermi National Accelerator Laboratory, Batavia, Illinois

T. Ando, G. Fujioka, H. Fukushima, Y. Takahashi, C. Yokoyama
Physics Department, Kobe University, Kobe, Japan

Y. Homma, Y. Tsuzuki
Faculty of Liberal Arts, Kobe University, Kobe, Japan

S. Y. Bahk, C. O. Kim, J. N. Park, J. S. Song
Korea University, Seoul, Korea

H. Fuchi, K. Hoshino, K. Niu, K. Niwa, H. Shibuya, Y. Yanagisawa
Department of Physics, Nagoya University, Nagoya, Japan

J. Dunlea, J. Kalen, S. Kuramata, N. Reay,
K. Reibel, R. Sidwell, N. Stanton
Department of Physics, Ohio State University, Columbus, Ohio

K. Moriyama, H. Shibata
Faculty of Sciences, Okayama University, Okayama, Japan

G. Kalbfleisch, P. Skubic
Department of Physics and Astronomy, University of Oklahoma, Norman, Oklahoma

M. Chikawa, T. Hara, O. Kusumoto, Y. Noguchi, T. Okusawa, T. Omori, M. Teranaka
Osaka City University, Osaka, Japan

J.-Y. Harnois, C. D. J. Hebert, J. Hebert, B. McLeod
Department of Physics, University of Ottawa, Ottawa, Ontario, Canada

H. Okabe, J. Yokota
Science Education Institute of Osaka Prefecture, Osaka, Japan

S. Tasaka
Institute for Cosmic Ray Research, University of Tokyo, Tanashi, Tokyo, Japan

B. J. Stacey, T.-S. Yoon
Department of Physics, University of Toronto, Toronto, Ontario, Canada

J. Kimura, Y. Maeda
Yokohama National University, Yokohama, Japan

June, 1981

Table of Contents

Table of Contents continued

List of Figures

A. Summary of the Experiment

We propose an experiment which employs a hybrid emulsion spectrometer to measure lifetimes and decay properties of beauty particles (B) and charmed particles (C) produced by interactions of high energy hadrons. Emulsion is the highest resolution detector (by more than an order of magnitude) for observing short lifetimes, and the electronic detection system is needed to select events, locate them within the emulsion and provide information about decay products.

A similar technique has proven successful in measuring the lifetimes [1,2,3] of neutrino-produced charmed particles (Fermilab Experiment 531). We believe that the experience therein gained will permit us to switch to hadronic production, where there are more beauty and charmed particles to be found.

The key to this experiment is a new form of solid-state detector which we are developing. With this detector as part of the hybrid emulsion system we should be able to obtain, in a four-month run with modest beam, 15,000 charmed-particle decays, and based on a 50 nanobarn cross section, about 200 B decays. Nearly 30 tau decays should also be observed.

Completing the development work on the new detector will require a year, so that data taking could begin late in 1983. Since the technique we propose has many novel features, we request "shakedown" running on whatever machine (conventional or Tevatron) exists at that time.

B. Physics Motivation

We wish simultaneously to search for B-particle decays and to make a high statistics measurement of charm decays.

The latter measurement provides an acceptable and secure motivation for the experiment. A $\pm$ 10% knowledge of lifetimes permits conversion of branching ratios into absolute partial decay rates without loss of precision. A current experiment [1,2,3] shows hints of two neutral lifetimes and the possible existence of weakly decaying neutral charmed baryons. Definitive studies of these effects, plus the possibility of observing sequential F → tau → other lepton decays, creates interest in a high statistics charm measurement. Observation of visible decay lengths also provides a relatively background-free sample of charmed particles for studying decay modes and production dynamics.

Of even greater interest than these charm measurements, however, is the opportunity to measure the lifetime of particles (B) carrying the b quark, for which strong evidence now exists [4], and to search for other new phenomena which may be associated with lifetimes down to 10^{-15} sec. This experiment will have a sensitivity of 4 events/nanobarn for detecting such interesting events. Should B-particles be produced at this level, their sequential B → charm → strange decays should be topologically striking and relatively background-free once the secondary and tertiary vertices are identified.

Measurement of B lifetimes and relative branching ratios into charm would, in the "standard" Kobayashi-Maskawa six-quark model [5], permit determination of the extended Cabibbo angles θ_2 and θ_3. In the approximation of small θ_i and CP-violating phase δ, we may write

$$\sin \theta_i = s_i, \quad \cos \theta_1 = \cos \theta_2 = \cos \theta_3 = 1$$

If we also assume the ratio,

$$\frac{(B \to \text{charm} + X)}{(B \to \text{no charm})} = \left| \frac{s_3 + s_2 e^{i\delta}}{s_1 s_3} \right|^2 >> 1 ,$$

then, $$\tau_B = \left(\frac{M_c}{M_B}\right)^5 \frac{1}{\left| s_3 + s_2 e^{i\delta} \right|^2} \tau_{charm}$$

The θ_i are given in terms of quark mass ratios by many of the higher symmetry models which predict proton decay [6], and charm lifetimes are 10^{-13} to 10^{-12} seconds [1,2,3]:

$$\tau_B = \left(\frac{1.9 \text{ GeV}}{5.3 \text{ GeV}}\right)^5 (10 - 100) \ (10^{-13} \text{ to } 10^{-12} \text{ seconds})$$

$$\tau_B = 5 \times 10^{-15} \text{ to } 5 \times 10^{-13} \text{ seconds}$$

If the Higgs particle comes from a single multiplet, its couplings are flavor diagonal, and its existence would have no effect on the B lifetime. However, if there are multiple Higgs doublets, in general the charged Higgs could couple $B \to H^-$ + (charm). If $M_B > M_{H^-} + M_C$, the B lifetime could be considerably shortened.

A recent theoretical preprint [7] uses CESR data and a conventional six-quark model to set bounds on the B lifetime in terms of the ratio τ (b→u)/ τ (b → c). Recent CLEO data [8] on this ratio then may be used to set an upper limit of 1.3×10^{-13} seconds for the B lifetime. If the B lifetime turns out to be much shorter than expected, it may be that the b quark (and perhaps the tau lepton) are not conventional. In this case, theoretical predictions have even more freedom, and information obtained on B decays could prove

to be even more exciting.

C. Description of the Experiment

1. Design Motivation

The apparatus is a hybrid emulsion spectrometer similar in concept but technically more demanding than the one used successfully in Experiment 531, and it will be operated in a charged hadron rather than in a neutrino beam. Given a reasonable track density ($1000/mm^2$), we can obtain 2.8×10^8 interactions in 100 liters of emulsion, and will rapidly check the emulsion for an interesting subset of 61,000 predicted secondary vertices.

Reducing secondary interactions leads to an emulsion design in which many thin modules 10 cm x 20 cm x 1.5 cm are sequentially exposed in hourly intervals. Each module will be mounted on a precision stage which moves during the beam spill, exposing strips of emulsion.

The design of the spectrometer is motivated by the following requirements:

1) Finding events in the emulsion quickly and efficiently;

2) Large acceptance;

3) Identification and momentum analysis of decay products;

4) Good reconstruction efficiency for the expected high multiplicity, highly collimated events;

5) Minimum path for pion and kaon muonic decays (since our selection criteria depend on $B\bar{B}$ and $C\bar{C}$ muonic decays);

6) Ability to resolve secondary vertices electronically.

2. Solid-State Detectors

It is very difficult to satisfy the above design criteria with existing technology. Drift chambers, for example, fall short of the position resolution required for beam tagging and decay vertex resolution by factors of 10. Even worse, they can achieve track pair resolution no better than 2 mm, so that tracks more closely spaced than this are lost. Since projected angles between tracks of < 1.0 mrad occur with appreciable probability in hadron interactions at 350 to 800 GeV, it is impossible to place drift chambers close to the emulsion target without incurring unacceptable reconstruction losses. Yet, high resolution detectors close to the emulsion target are essential if the apparatus is to be kept short and secondary vertices are to be reconstructed.

We have, therefore, produced a spectrometer design which relies on the rapidly evolving technology of position-sensitive silicon detectors, and are well into a program of prototyping and testing. Details of our progress and a photomicrograph of our prototype with 40 micron strip spacing are given in Appendix I.

Briefly, the detectors are thin silicon wafers onto which are deposited strips with a center-to-center spacing of 40 microns, as shown in fig. 1. When they are reversed-biased, the ionized electrons resulting from charged-particle passage are collected on individual strips, as shown in the figure. In the region of highest track density individual strips will be read out, and resistive interpolation [9] (with taps every 3-10 strips) will be employed in regions with lower track density. For the spectrometer, we have assumed detectors with the following characteristics: 6 cm diameter active area, 0.3 mm thickness, position resolution of at least $\pm 40/\sqrt{12}$ ($= \pm 12$) microns, two-track separation of 40 microns, and the ability to function in magnetic fields

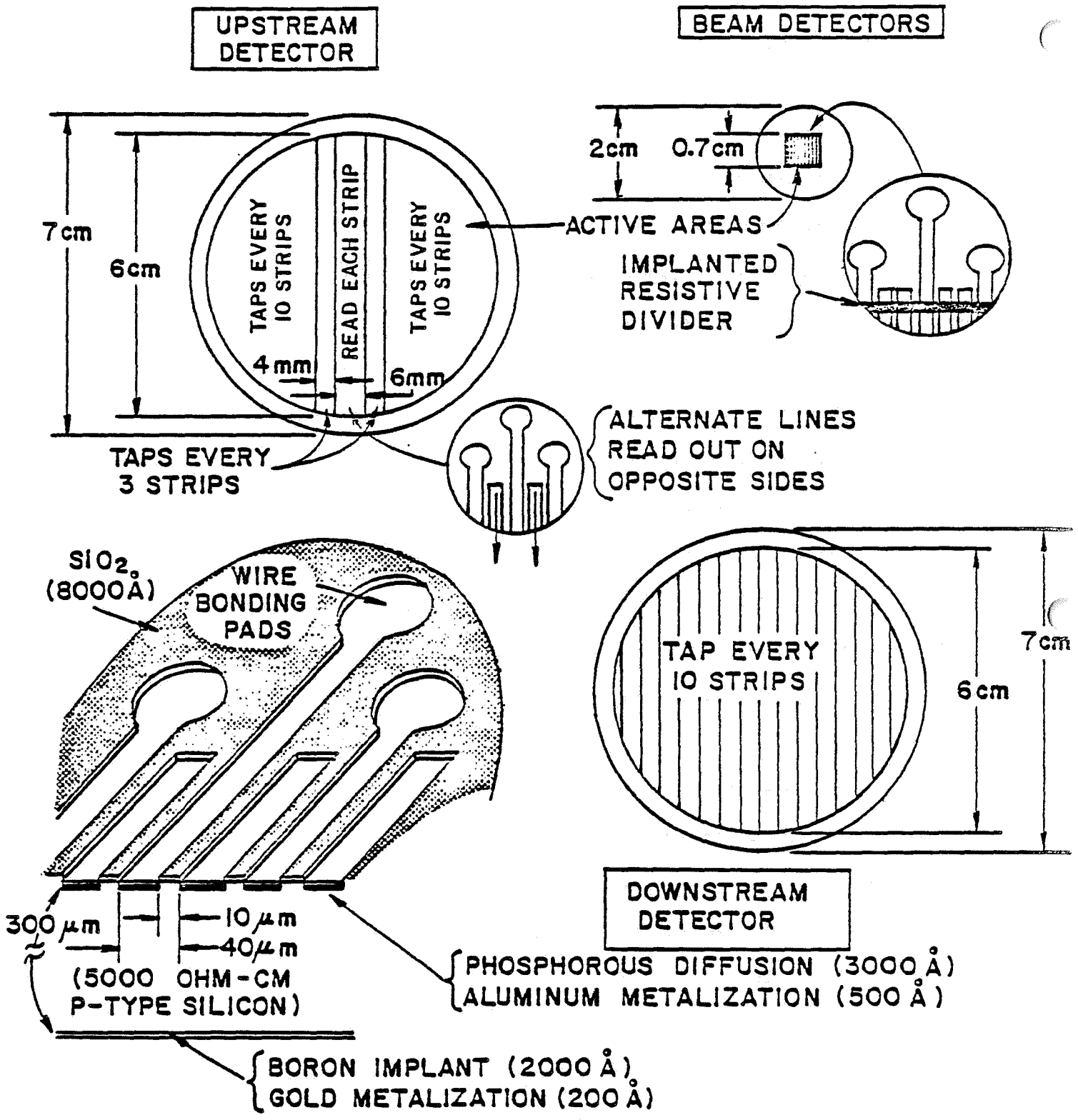
UPSTREAM DETECTOR
BEAM DETECTORS
7cm
6cm
TAPS EVERY 10 STRIPS
READ EACH STRIP
TAPS EVERY 10 STRIPS
4mm
6mm
TAPS EVERY 3 STRIPS
2cm
0.7cm
ACTIVE AREAS
IMPLANTED RESISTIVE DIVIDER
ALTERNATE LINES READ OUT ON OPPOSITE SIDES
SiO2 (8000Å)
WIRE BONDING PADS
TAP EVERY 10 STRIPS
7cm
6cm
DOWNSTREAM DETECTOR
300 μm
10 μm
40 μm
(5000 OHM-CM P-TYPE SILICON)
PHOSPHOROUS DIFFUSION (3000 Å)
ALUMINUM METALIZATION (500 Å)
BORON IMPLANT (2000 Å)
GOLD METALIZATION (200 Å)
SILICON SOLID STATE DETECTORS

Figure 1.

up to 0.7 Tesla.

These requirements are all achievable using "old fashioned" solid state technology.

3. Discussion of Apparatus

A schematic elevation view of the experiment is shown in fig. 2 , and an enlarged view of the charged particle spectrometer is given in fig. 3. Note that the total length of the apparatus between the emulsion target and the upstream side of the calorimeter is less than 3.5 m. The major components are the beam and beam detectors, emulsion target, vertex detector, charged-particle spectrometer, charged-particle identifiers, gamma detector, neutral hadron detector, muon identifier, and trigger counters.

a. Beam and Beam Detectors. We require a hadron beam of about 5 x 10^4 /second with a small (3 mm x 3 mm) focus and a halo integrated over 10 cm x 20 cm which is less than about 7% of the beam intensity. The momentum spread of the beam is relatively unimportant. For B production at 400 GeV, a pion beam would be preferred. For charm production at any energy and B production at Tevatron energies, a proton beam is preferred, as the spot size and halo requirement are more easily satisfied. Possible locations are discussed in Appendix II . The beam coordinates (angles) will be determined to $\pm$6 microns ($\pm$ 7 microradians) by sets of small silicon detectors as shown in fig. 2. The relative positions of all electronic detectors will be calibrated continuously on the high momentum beam tracks.

b. Emulsion. Nuclear emulsion is the only detector which can observe

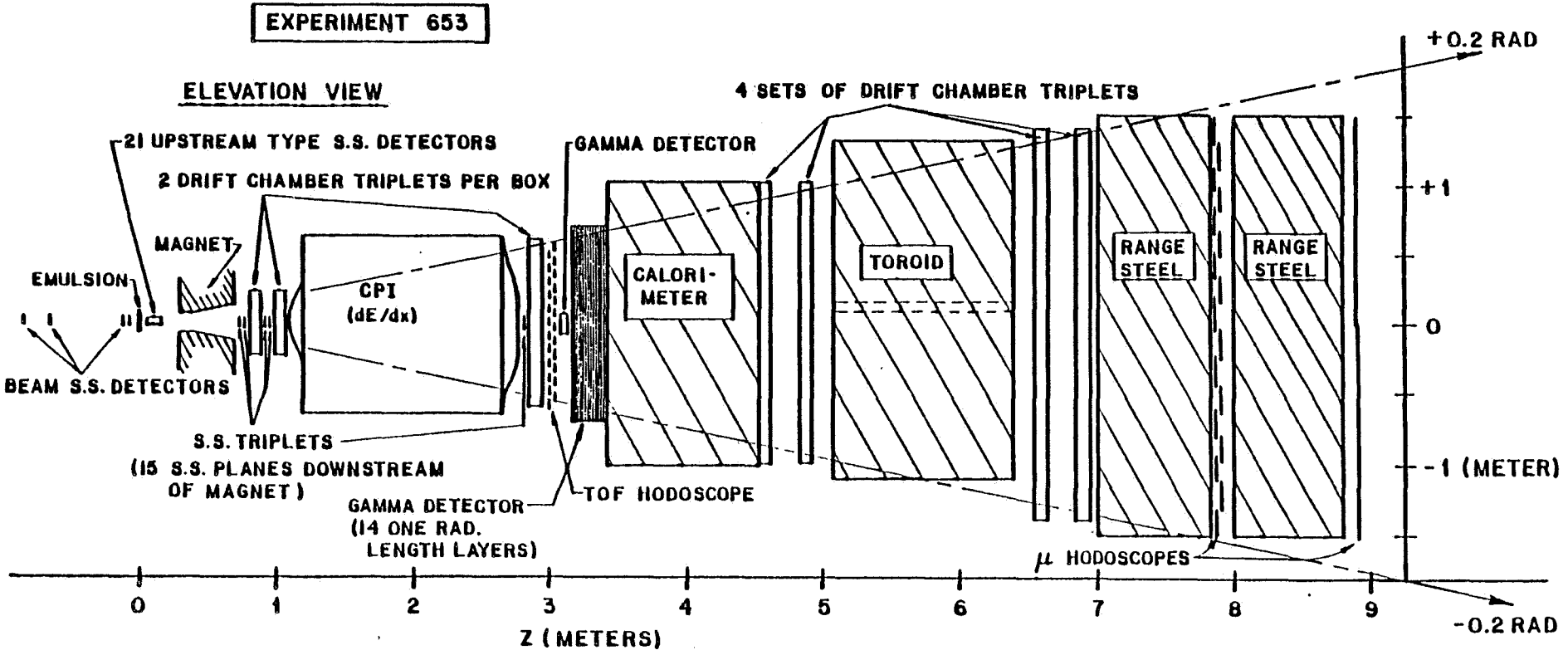
EXPERIMENT 653
ELEVATION VIEW
21 UPSTREAM TYPE S.S. DETECTORS
2 DRIFT CHAMBER TRIPLETS PER BOX
MAGNET
EMULSION
BEAM S.S. DETECTORS
CPI
(dE/dx)
S.S. TRIPLETS
(15 S.S. PLANES DOWNSTREAM
OF MAGNET)
GAMMA DETECTOR
(14 ONE RAD.
LENGTH LAYERS)
GAMMA DETECTOR
CALORI-
METER
TOF HODOSCOPE
4 SETS OF DRIFT CHAMBER TRIPLETS
TOROID
RANGE
STEEL
RANGE
STEEL
μ HODOSCOPES
+0.2 RAD
+1
0
-1 (METER)
-0.2 RAD
0
1
2
3
4
5
6
7
8
9
Z (METERS)

Figure 2.

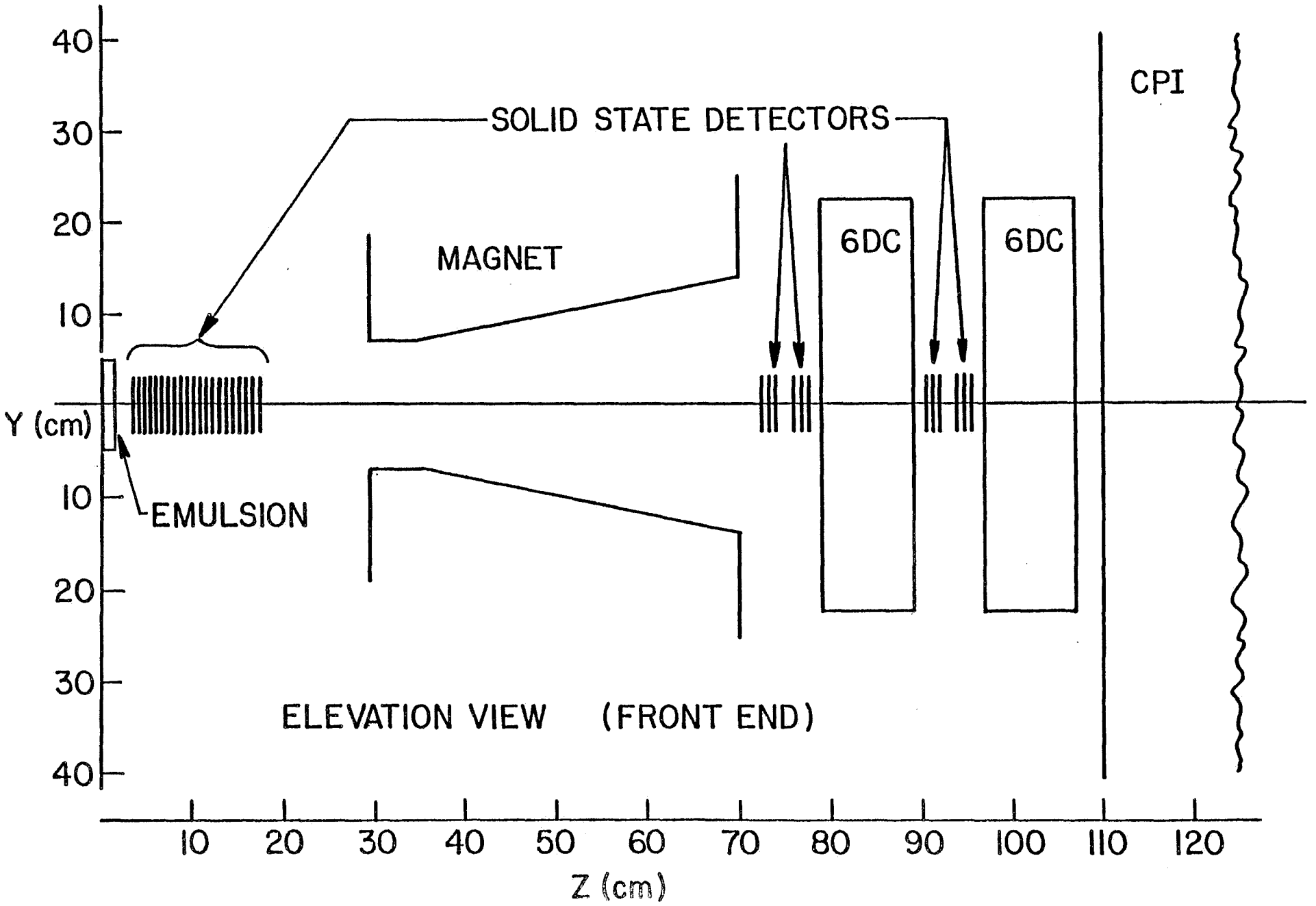
SOLID STATE DETECTORS
CPI
MAGNET
6DC
6DC
EMULSION
Y (cm)
Z (cm)
ELEVATION VIEW (FRONT END)
40
30
20
10
10
20
30
40
10
20
30
40
50
60
70
80
90
100
110
120

Figure 3.

short-lived particles with lifetimes down to 10^{-15} sec with high efficiency. In this experiment we will use as much emulsion as possible and as high a track density as tolerable to get good sensitivity to rare events. The pouring facility built at Fermilab for E531 can produce 32 liters of emulsion modules per month, so that an exposure of 100 liters is well within our capability. Maximum track density is a slightly subjective number, but the Nagoya group has experience from E531 with densities of 225/ mm^2, and from NA-19 at CERN with densities of up to 10,000/ mm^2. The maximum reasonable intensity appears to be about 1000/mm^2, which will give 2.8×10^8 interactions in 100 liters.

Historically, a serious drawback to the use of nuclear emulsion in studying rare processes has been the limited number of events which can be examined under the microscope. A breakthrough of this limitation has been made by the Nagoya group, who have developed a microscope with a TV monitor and computer-controlled digitized stage. This system has already shown its power in analyzing E531 neutrino interactions, and has been extended to handle 6,000 fully-measured events for the second E531 exposure; good progress is being made toward the goal of 10,000 measured events per year. Furthermore, the techniques described below, which take advantage of the excellent resolution of the silicon detectors, make it possible to eliminate uninteresting events quickly, so that the scanning rate should approach 40,000 events per year.

Fig. 4 is a schematic drawing of the emulsion mounting stage and a module of the "vertical" type, in which the sheets are mounted perpendicular to the beam. The emulsion volume is divided into modules 10 cm x 20 cm in area by 1.5 cm thick. This thickness, 0.04 interaction lengths, is a compromise which provides sufficient fiducial volume to observe decays and minimize edge losses, while also keeping secondary interactions and gamma conversions to

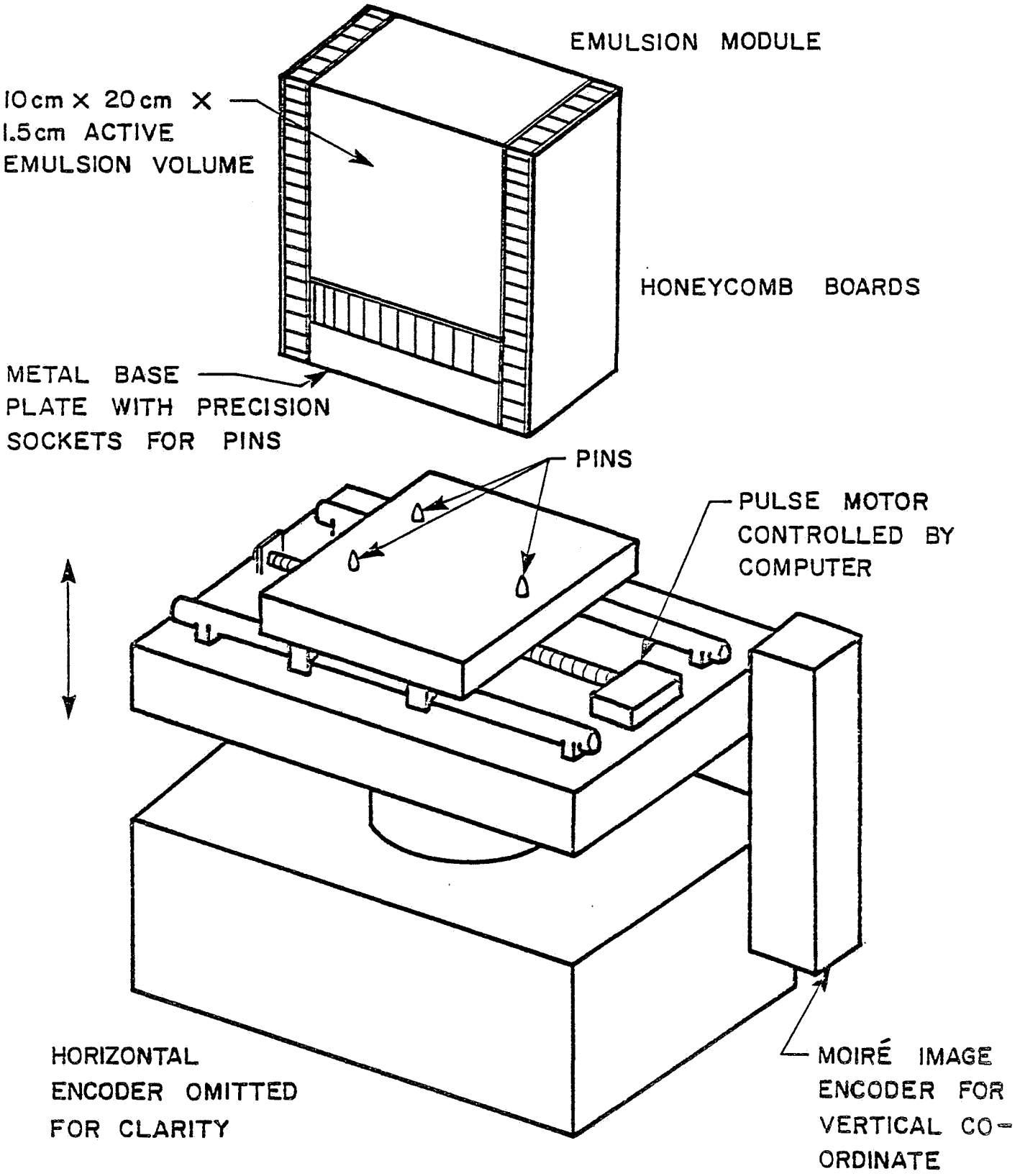

SCHEMATIC DRAWING OF EMULSION STAND

Figure 4.

a tolerable level. Each module contains 40 10 cm x 10 cm x 0.73 mm sheets of plastic- backed emulsion.

In order to maintain the desired track density with a 3 mm x 3 mm beam spot of optimum intensity, it is necessary to have the emulsion mounted on a precision microscope-type stage which moves continuously during the beam pulse, uniformly exposing a band 10 cm high x 3 mm wide. This stage is driven by computer controlled motors, and its position is monitored with standard Moiré image encoders which digitally record the position of the stage at each event with 1 micron accuracy. In E531 the individual emulsion sheets were registered with each other mechanically to $\pm$ 50 microns. Improving this tolerance will substantially reduce the time required to follow tracks from one sheet to another. To do this, we will use the heavy-ion technique already tested successfully by the Nagoya group. The assembled modules will be exposed to a low-intensity heavy ion beam (2 GeV/nucleon Ne, few/cm^2) which provides easily-recognized local fiducials. Relative sheet registration will then be limited mainly by the mechanical stability of the package between exposures, which should be held to a few microns.

The solid state detectors will be able to locate vertices to better than $\pm$ 10 microns in the plane of the emulsion sheets and to $\pm$ 0.2 mm along the beam direction. This defines a scanning volume 1000 times smaller than we used in E531, and means that a predicted vertex will certainly fall within one microscope field of view (100 microns x 100 microns at high power), and within $\pm$ 1 emulsion sheets. Finding a predicted primary or secondary vertex under these circumstances will take approximately 4 minutes. As discussed in section D, we intend to select events with charm decays by reconstructing and resolving the secondary vertices with the solid-state detectors. Because

of this very short time required to find a predicted vertex in the emulsion, these electronic predictions of a decay can be quickly verified. Most vertices from secondary interactions will have dark nuclear breakup tracks and can be immediately rejected. Primary vertices will be even easier to find because one has the additional option of scanning along a beam track. B selection does not rely on electronic prediction of a B-decay secondary vertex. However, if the B lifetime is less than the charm lifetime as expected, most B decays will occur in the same emulsion sheet and microscope field of view as the primary vertex, and can be found simply by varying the depth of focus of the microscope.

In order to use the high precision of the emulsion and the solid state detectors the two systems must be registered with each other to an accuracy small compared with the transverse distance between interactions. This was done to $\pm$ 50 microns with the thicker modules and drift chambers of E531 using the fiducial sheet technique [1,2,3]. In this experiment we will expose four 10 cm x 3 mm bands in each module at 1/20 normal intensity (comparable to the integrated beam halo), during which the spectrometer will run with a total interaction trigger. The interactions in these low-intensity bands can be unambiguously identified by both position and event topology; once found, they provide local calibration good to the 6 micron accuracy of the beam detectors.

c. Vertex Detector. The vertex detector locates events in the emulsion, and also plays a key role in event selection by reconstructing more than half of the secondary vertices from charm decay. It consists of 21 silicon strip detectors spaced 0.7 cm apart, with 7 detectors measuring each of 3 projections rotated 60 degrees from each other (x,u,v). Each silicon wafer (fig. 1) has

an active area of 6.0 cm diameter and is only 0.3 mm thick to reduce multiple scattering. In the central 0.6 cm band of each detector every strip is read out separately to maintain 40 micron track pair resolution in the region of high track density. On either side of this central band the charge interpolation technique [9] is used, with pulse height information being read out from taps every 3 to 10 strips, thus preserving the spatial resolution of ±12 microns but relaxing the track pair resolution where it is not needed.

We have studied the track pair resolution performance of this system by generating Monte Carlo events which contain a $B\bar{B}$ pair cascading through $D\bar{D}$ and contributing 10 charged particles, together with an additional (typically) 10 "ordinary" tracks distributed like hadronic interactions at an energy equal to that left over from the $B\bar{B}$ pair. It was then asked what fraction of the charged tracks from B or D decay was compromised by shadowing from the 20 other tracks. It was found that such a track was shadowed (by another track hitting the same or an adjacent strip) in 2 or more views only 4% of the time, and in all 3 views only 0.5% of the time. Shadowing of a track in only one of three views should not present a serious problem since the ionization is being measured, thus signaling the presence of two overlapping tracks.

This reliable performance at high track density is an enormous improvement over drift chamber technology, in which electronic dead time leads to missing or grossly shifted hits for nearby tracks. In areas of high track density drift chamber discriminators refire at regular intervals equal to the minimum track separation so that a hit may not lie on any true track, as shown below:

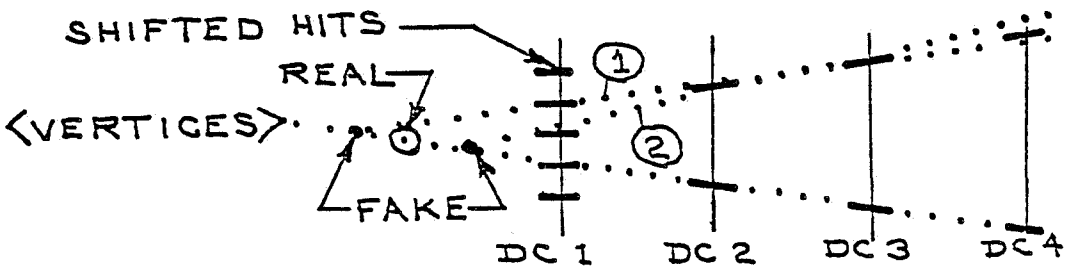

Note that in this example neither hit adjacent to the track in DC 1 is real, so both tracks 1 and 2 are incorrect. From our experience with the drift chambers in E531 it has become evident that most spurious secondary vertices are generated by this effect.

The silicon strip detectors do not refire, have a two-track resolution 50 times better than drift chambers, and reveal multiple tracks by ionization. We believe that this improved performance will allow reliable reconstruction of secondary vertices with a very low percentage of fakes, so that resolving vertices will be limited only by the 12 micron measurement accuracy and multiple scattering. As discussed in Section D, this ability to recognize charm decays with an electronic detector is an enormous advantage in efficient selection of events to be looked at in the emulsion.

d. Charged Particle Spectrometer. In order to achieve maximum aperture and minimum depth we have designed the spectrometer around the small iron magnet shown schematically in fig. 3 and discussed in more detail in Appendix III. This magnet has a pole-piece depth of only 40 cm and allows a vertical (horizontal) aperture from the target of $\pm$200 (240) mrad. By having the pole pieces open vertically outward a transverse kick of 0.20 GeV/c is obtained with a maximum field of 1.7 Tesla; a kick of 0.30 GeV/c seems quite feasible (Appendix III).

The directions of charged particles downstream of the magnet are measured by silicon detectors at small angles and by drift chambers similar to those used in E531 at larger angles (fig. 3). Pairs of drift chamber xuv triplets located 84, 102 and 290 cm from the target cover the full magnet exit aperture. Tracks within 30 mrad of the beam are picked up by two pairs of silicon detector

triplets which cover the region in which the track pair resolution of the drift chambers is inadequate. An additional silicon triplet at 283 cm gives a very long lever arm for very stiff tracks. If one uses the rule of thumb that tracks from B and C decay have transverse momenta around 1 GeV/c, this small-angle system catches tracks above about 80 GeV/c. All downstream silicon detectors are 6 cm in diameter and use charge-interpolation readout with taps every 10 strips.

The momentum resolution of the spectrometer is shown in fig. 5; it is dominated at all but the highest momenta by the constant multiple scattering contribution of $\pm 2\%$, and is still only $\pm 5\%$ at 300 GeV/c.

It is clear that to use the excellent resolution of silicon detectors to full advantage we must build stable mounting hardware and monitor the alignment carefully. Our experience with the much larger apparatus in E531 was that drift chamber positions could be held stable to ± 25 microns over 1-week intervals, and that absolute survey discrepancies between the drift chambers and the emulsion fiducial sheet were ± 50 microns [2]. In addition, we will now have the powerful survey tool of stiff beam tracks passing through the central regions of all the high resolution devices.

e. Charged Particle Identification. Identification of charged particles will use two complementary techniques familiar to us from E531: dE/dx in Ar-CO_2 to distinguish particles in the momentum range 5-30 GeV/c, and time of flight for softer tracks.

Even with an 800 GeV/c beam more than 20% of the charged tracks from charm decays have $p < 5$ GeV/c. More than 80% of these soft tracks can be cleanly

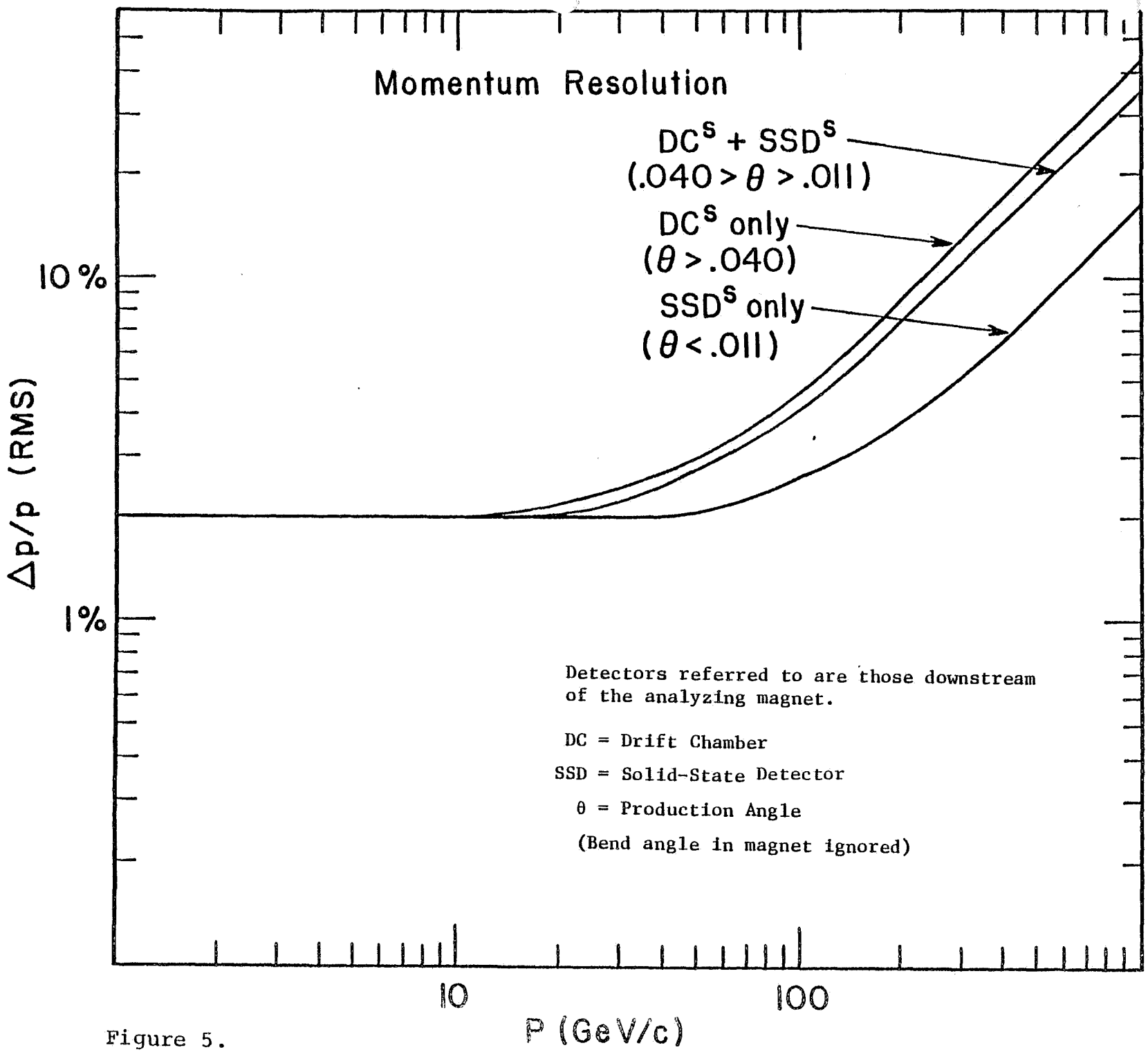
Momentum Resolution
DC^S + SSD^S
(.040 > θ > .011)
DC^S only
(θ > .040)
SSD^S only
(θ < .011)
10 %
1%
Δp/p (RMS)
Detectors referred to are those downstream of the analyzing magnet.
DC = Drift Chamber
SSD = Solid-State Detector
θ = Production Angle
(Bend angle in magnet ignored)
10
100
P (GeV/c)

Figure 5.

identified in the TOF system over a 3 m flight path for a time resolution of $\pm$65 ($\pm$95) picosec for the case of single (multiple) tracks crossing a scintillator. This resolution is a reasonable extrapolation from that achieved in E531 ($\pm$100, $\pm$150 picosec) with much larger scintillators. For this experiment, the downstream hodoscope will consist of a bank of 30 Pilot F scintillators 1.4 m long x 4.0 cm wide x 2.5 cm thick, viewed at both ends by phototubes of modest quality. A start time resolution of $\pm$30 picosec is easily obtained with 3 small beam counters upstream of the target.

The dE/dx charged particle identifier (CPI) will identify at least 60% of the B,C decay tracks in the momentum range 5-30 GeV/c. Since the requirement of a short spectrometer limits the available length to 1.5 m, it is necessary to run the chamber at a pressure of 3 atm absolute, and to sample ionization every 1.0 cm along the tracks in order to obtain the necessary resolution. The empirically determined [10] resolution is

$$\sigma_{Emp}\ (FWHM) = .96\ N^{-.46}\ (xP)^{-.32}$$

where N=number of samples, x=sample size in cm, and P is the absolute pressure in atm. For a CPI with 150 1.0 cm samples at 3 atm a resolution of $\pm$ 3.4% is reached, allowing a 3 S.D. separation of pions and K's at 30 GeV/c.

The proposed design of the CPI consists of two cells, one on either side of the beam axis, allowing the beam and the unresolvable forward jet from hadronic events to pass through a region with no electric field. Ionization from tracks outside this 10 mrad region is collected on 150 sense wires in each cell. The expected track pair resolution is 6 mm, and the necessary sampling clock speed is around 40 MHz. Possible readout and compaction schemes are discussed in Section 3j.

f. Gamma Detector. The design of the electromagnetic shower detector for electron identification and gamma detection is shaped by the same concerns about high track density which motivated the spectrometer design. A similar solution was chosen: conventional technology at large angles, and solid state detectors at small angles. Ideally, the detector should measure both conversion position and energy for each incoming electron or photon; since fully developed showers are likely to overlap, we have emphasized getting conversion points early in the shower development.

The detector is located 3.1 m from the target and has an active area of 1.4 m x 1.4 m. The conventional portion consists of alternating layers of lead converter and extruded aluminum proportional ionization chambers (EPIC). A similar device has been used successfully in the second run of E531. The EPIC tubes will have a cross sectional area of 1 cm x 1 cm, and will be run at a pressure of 10 atm. To measure accurate and unambiguous conversion points the first three sections of the detector will each consist of a 1.5 radiation length (r.l.) converter followed by three crossed planes (xuv) of EPIC tubes. The remaining 9.0 r.l. will consist of 1.0 r.l. converters each followed by one EPIC plane (x or u or v). Tubes in this section will be ganged longitudinally, with all corresponding wires from each projection summed and read out in common. The number of data lines for this conventional detector is 1320. Because of sharing of shower ionization between adjacent tubes we expect a position resolution of $< \pm 1.5$ mm. An energy resolution of $\delta E/E = 0.30/\sqrt{E}$ has been achieved by similar devices using multiwire proportional chambers at 1 atm with 1 r.l. sampling [11]. The factor 10 increase in pressure should improve this value to $0.20/\sqrt{E}$.

Masking of one shower by another grows rapidly more serious at small angles. Beyond 3 cm from the beam, however, monte carlo studies based on bubble chamber events [12] indicate that 98% of the showers will be separated by 2 or more tube spacings in this conventional detector.

One third of the gammas from pi zero decay are less are less than 3 cm from the beam at 3.1 m. The conversion points (and a rough measure of the energy) of these small angle showers will be obtained by a miniature gamma detector placed just upstream of the conventional one. This detector, 6 cm in diameter, will consist of alternating layers of tungsten and silicon wafers with 1 mm strip spacing, using a pattern of radiators and rotated planes similar to that in the large detector. Because the wafers are so thin the device is quite dense, and the shower spread is small. To estimate this shower size the monte carlo program "EGS" was used to generate electron-induced showers. Ten slabs of lead [13] 5.6 mm thick, each followed by an empty space of 3.0 mm represented the detector. Fig. 6 shows the average number of charged particle crossings (from 10 showers) vs. transverse position at the exits of converters 1,3,5 and 9 for incident 25 GeV electrons. At the third space the ionization density is down a factor of 10 from its central value only 0.35 mm from the shower center. These calculations indicate that it should be possible to determine conversion positions to a few hundred microns with such a detector, and to resolve conversion points of showers $\gtrsim$1 mm apart. The losses from masking in this detector will be about 13%, thus maintaining the efficiency

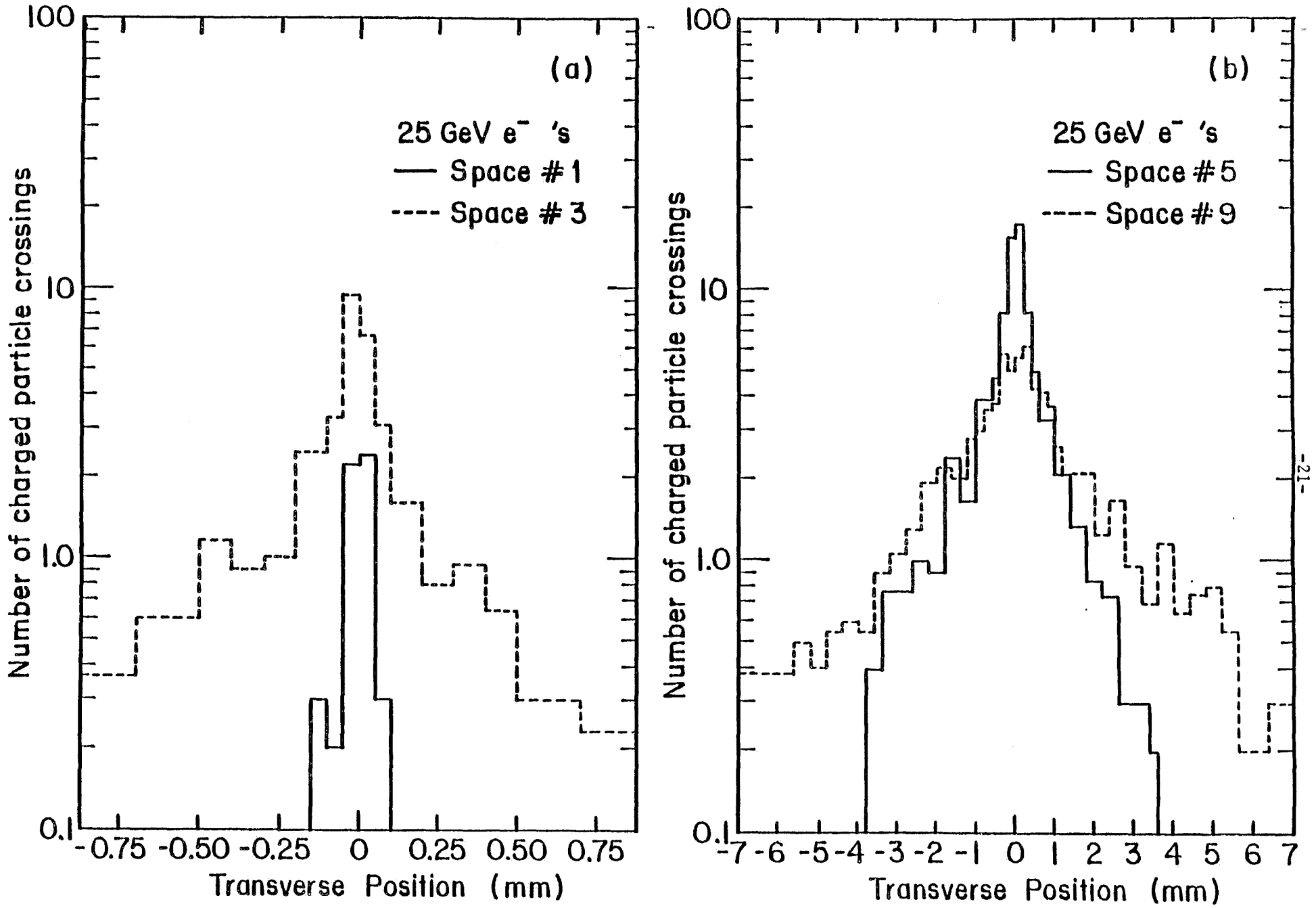

Figure 6. Shower development in the gamma detector after 1,3,5,9 radiation lengths.

of the two complementary detectors at 93%.

g. Hadron Calorimeter. The primary purpose of the hadron calorimeter is to measure the conversion points and energies of neutral hadrons (K^o,Λ^o,n). The position resolution achievable [14] is < $\pm$10 mm, or $\pm$4 mrad at 3.8 m. This angular error makes a smaller contribution to the overall mass resolution than the expected energy measurement error of about $0.7/\sqrt{E}$ for the energies of interest (5-35 GeV).

The proposed detector (fig. 2) consists of alternate layers of iron plates 5 cm thick x 2.4 m high x 3 m wide, and planes of EPIC tubes 1 cm^2 in cross sectional area, operated at atmospheric pressure. The first seven gaps in the iron will be instrumented with pairs of EPIC planes at right angles, with the planes in alternate gaps rotated 45 degrees to give stereo information. The EPIC tubes in these gaps will be ganged transversely as follows: every wire read out for angles < 60 mrad, adjacent tubes added in pairs for angles between 60 and 120 mrad, and adjacent groups of 4 tubes added for angles from 120 to 240 mrad. The final 9 gaps in the calorimeter steel will be instrumented with one EPIC plane each, with alternate planes rotated by 90 degrees. These planes will be ganged transversely like those in the first 7 gaps, and will also be ganged longitudinally, with all x and all y planes in these last 9 gaps read out in common. In all, 1280 amplifiers are required.

The major difficulty in finding neutral hadrons is separating them from the charged hadron background. Monte carlo calculations indicate [15] that showers produced by 30 GeV hadrons typically have transverse size < 20 mm at a depth of 0.5 collision lengths. We have estimated the masking loss contribution to the detection efficiency by using "boosted" [12] bubble chamber data to

generate charged hadron hits on the front face of the calorimeter. A successful identification is assumed if no other tracks have hits within one wire spacing in any direction. The resulting efficiency is shown in fig. 7 as a function of polar angle θ. On the same plot is shown the K^o angular distribution expected from $B \to D(5\pi)$, with $D \to K^o(3\pi)$. We find that more than 80% of the K^o can be resolved under the assumptions above, and 65% with the more restrictive requirement of two wire spacings between showers.

h. Muon Detector. The muon detector has two functions: to reduce the hadron flux enough to give a manageable trigger rate, and to determine from the reconstructed event whether a given track which has traversed the detector is indeed a muon. The first objective is simply accomplished by requiring enough range of iron; 5 GeV of range should be sufficient (see Section D and Appendix IV).

To meet the second objective it is essential to track the muon candidate from the emulsion through the spectrometer, hadron calorimeter and absorber with frequent sampling of position and ionization in the iron to look for evidence of hadronic interaction. It is also very important to make a second momentum measurement after several interaction lengths of iron to be sure that no large energy loss has occurred, and that the correct muon candidate has been tracked through the region of dense hadron showers.

The frequent sampling is performed in the EPIC chambers of the calorimeter. The second momentum measurement is done with a square iron toroid (similar to those in E613) 1.3 m deep and 2.5 m on a side. Assuming low carbon steel (1010 or equivalent), a current of 1000 Amp and 100 turns, one obtains reasonable saturation and a nearly constant magnetic field of 2.0 T. On either

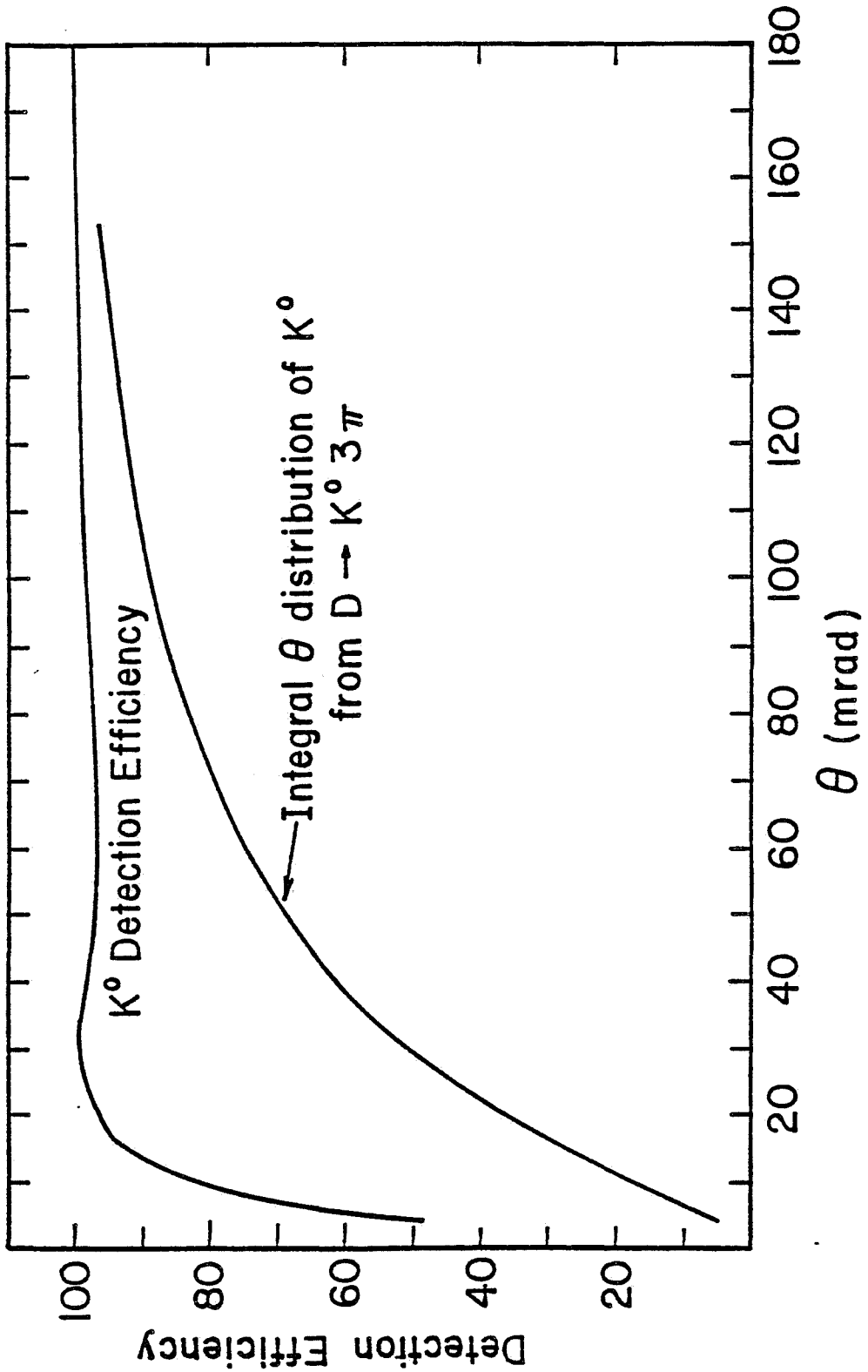
Integral θ distribution (K°) %
Detection Efficiency
100
80
60
40
20
K° Detection Efficiency
Integral θ distribution of K°
from D → K° 3π
20
40
60
80
100
120
140
160
180
θ (mrad)

Figure 7.

side of the toroid are 2 xuv triplets of EPIC chambers instrumented for drift chamber readout using surplus electronics from E531. This system will have a resolution

$$\delta p/p = \left[(.19)^2 + (.01p)^2\right]^{\frac{1}{2}} , \quad (p \text{ in GeV/c})$$

where the first term is the multiple scattering contribution and the second comes from the $\pm$0.5 mm resolution of the chambers. Downstream of the toroid are two identical modules, each consisting of 0.8 m of steel followed by banks of scintillators (as in E531) to complete the range requirement. Muons of 2.8 GeV will penetrate the toroid, and the downstream absorbers transmit 4.0 and 5.2 GeV respectively.

i. Trigger Counters. Since non-zero data from all events from each spill will be stored in a fast buffer memory, we are studying a variety of triggers, many of which require fast processing before recording on tape. Although several techniques appear promising, we present here only the simplest muon trigger, which should be able to lower the rate of recorded events to about 13 per second. This trigger requires a non-halo beam particle to interact in the emulsion, giving rise to a tagged muon stiffer than 5 GeV. The following sketch qualitatively indicates counter locations:

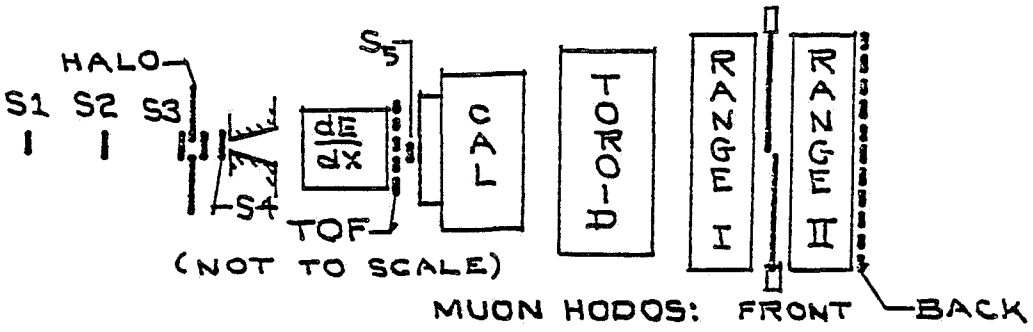

The trigger will consist of

$$\text{Trigger} = (\text{Beam}) \cdot (\text{Interaction}) \cdot (\text{Muon})$$

with components as listed below:

$$\text{Beam} = S1 \cdot S2 \cdot S3 \cdot \overline{\text{Halo}}$$

$$\text{Interaction} = (S4 \geqslant 3 \text{ in pulse height}) \cdot (\geqslant 2 \text{ TOF paddles})$$

$$\text{Muon} = \mu_1 \cdot \mu_2$$

(Note that the TOF hodoscope will have a small hole for non-interacting beam, and also that the muon counters may need shielding against slow neutrons.)

j. Data recording. In this experiment it will be necesary to record information from 9500 solid state detector lines, 520 lines of multi-hit drift chamber wires, 2600 lines of EPIC chambers in the gamma detector and hadron calorimeter, and 300 lines of dE/dx chamber wires. In a 20 second Tevatron spill perhaps 260 events may be recorded. The sheer volume of data necessitates some processing prior to recording on tape, a large amount of buffer storage and use of high density magnetic tape drives.

The solid state detectors (SSD) will be multiplexed in a fashion similar to the proposed Droege system for the Colliding Detector Facility, in which outputs of addressable amplifiers are recorded only if they exceed "table look-up" thresholds. In this way the SSD data should be reduced to typically 1500 2-byte words per event with efficient packing.

The drift chamber multi-hit system already exists and provides efficiently-packed data which will contribute perhaps another 500 words. EPIC chambers may be recorded either with the LeCroy 2280 processor and 12-bit, 48-fold 2282B ADC's, or alternatively with the Droege system. We expect typically 1000 2-byte

words from channels over threshold. More compact recording schemes involving extraction of moments are under study.

The dE/dx chamber in E531 uses CCD pulse height storage and sequential digitization. With the advent of stable flash encoders and inexpensive digital memory it appears feasible to devote an encoder and memory chip to each of the 300 sense wires. We are investigating algorithms to extract the arrival time and integral pulse height of each resolved track from the many time samples of ionization per track obtained from each wire. By compressing time and pulse height information into a single word, the information content from a single event should be reduced to typically 3000 2-byte words.

Such a system may be extended in a natural fashion to encompass more sophisticated trigger processing in the future.

From the above considerations, it is necessary to record (1500+500+1000+3000) = 6000 words per event, or 1.6M words per Tevatron spill. We are developing a fast memory system to buffer several events to smooth statistical fluctuations in data arrival and permit a more uniform rate of permanent data recording.

The exposure of each emulsion module will require approximately one hour. During this time about one 2400 foot reel of 6250 byte/inch data tape will be written. The system is thus well-matched to high density recording, but we will require at least two such high density drives to avoid reliability problems such as have been experienced by E516.

D. Event Rates and Background

The event rates for $C\bar{C}$ and $B\bar{B}$ pairs have been calculated assuming respective cross sections of 25 microbarns and 50 nanobarns per pair per target nucleon at 800 GeV. (If recently reported preliminary results [16] from CERN are verified, there is a leading particle contribution to B production at the level of a few microbarns, and to charm production at the 100 microbarn level.) To obtain the total number of interactions we use the measured [17] mean free path (MFP) of high energy protons in emulsion, 36 cm, corresponding to a total interaction cross section of 12.1 millibarns per nucleon. For 100 liters of emulsion exposed to a beam track density of 1000 per square millimeter we have:

$$\begin{aligned} \#\text{int.} &= (\text{thickness/MFP})(\text{tracks/area})(\text{area}) \\ &= (\text{volume})(\text{tracks/area})/(\text{MFP}) \\ &= (10^5 \text{ cm}^3)(10^5/\text{cm}^2)/(36 \text{ cm}) \\ &= 2.8 \times 10^8 \text{ interactions} \end{aligned}$$

The number of charm and beauty pairs present in the emulsion is then

$$\begin{aligned} \#\text{ charm pairs} &= (2.8\times 10^8)(25 \text{ microbn})/(12.1 \text{ millibn}) \\ &= 5.8 \times 10^5 \text{ pairs} \\ \#\text{ beauty pairs} &= (2.8\times 10^8)(50 \text{ nanobn})/(12.1 \text{ millibn}) \\ &= 1150 \text{ pairs} \end{aligned}$$

The key to success in this experiment is selection criteria for emulsion scanning which have a high efficiency for finding these charm and beauty events.

All of our selection criteria require a muon from charm or beauty decay. We have calculated distributions in lab momentum p and transverse momentum p_T of these muons with a production model in which charm or beauty pairs result

from decay of a heavy parent of mass M which is centrally produced with a distribution

$$d\sigma/dxdp_T = (1-|x|)^n p_T e^{-bp_T}$$

where for charm (beauty) M=4.23 (11.10) GeV, n=4.0 (3.0), b=2.0 (1.0) GeV^{-1}. Four-body decays such as $B \rightarrow D\pi\mu\nu$, $D \rightarrow K\pi\mu\nu$ generate the muons. Integral muon distributions vs. p_T from this monte carlo calculation are shown in fig. 8 for muons from direct B decay, and from directly-produced and B-cascade D's.

Estimation of background depends on reliable calculation of the number of muons from pi and K decay. This calculation, described in Appendix IV, is based on particle production data from the ISR [18] at energies bracketing 800 GeV lab equivalent; it has been checked successfully against an independent approach which starts from a tape of measured 360 GeV bubble chamber events [12]. The resulting muon fluxes from pi,K per interaction per meter of flight path are shown in figs. 9 ,10. The effective decay path of the apparatus is 3.5 meters. We believe that most of the muons from K decay, and some from pion decay as well, can be eliminated offline by comparison of the track slopes perpendicular to the spectrometer bend plane upstream and downstream of the magnet, and by comparison of the momenta determined by the spectrometer and by the toroid. Therefore only the pion contribution from fig. 9 has been used in the background estimates below.

The electronic trigger will require an interaction in the emulsion, plus a muon of more than 5 GeV/c by range. This should reduce the modest interaction rate of 600/sec to a recordable level of about 13 /sec. Offline, three types of selection will be performed on reconstructed events to obtain the sample

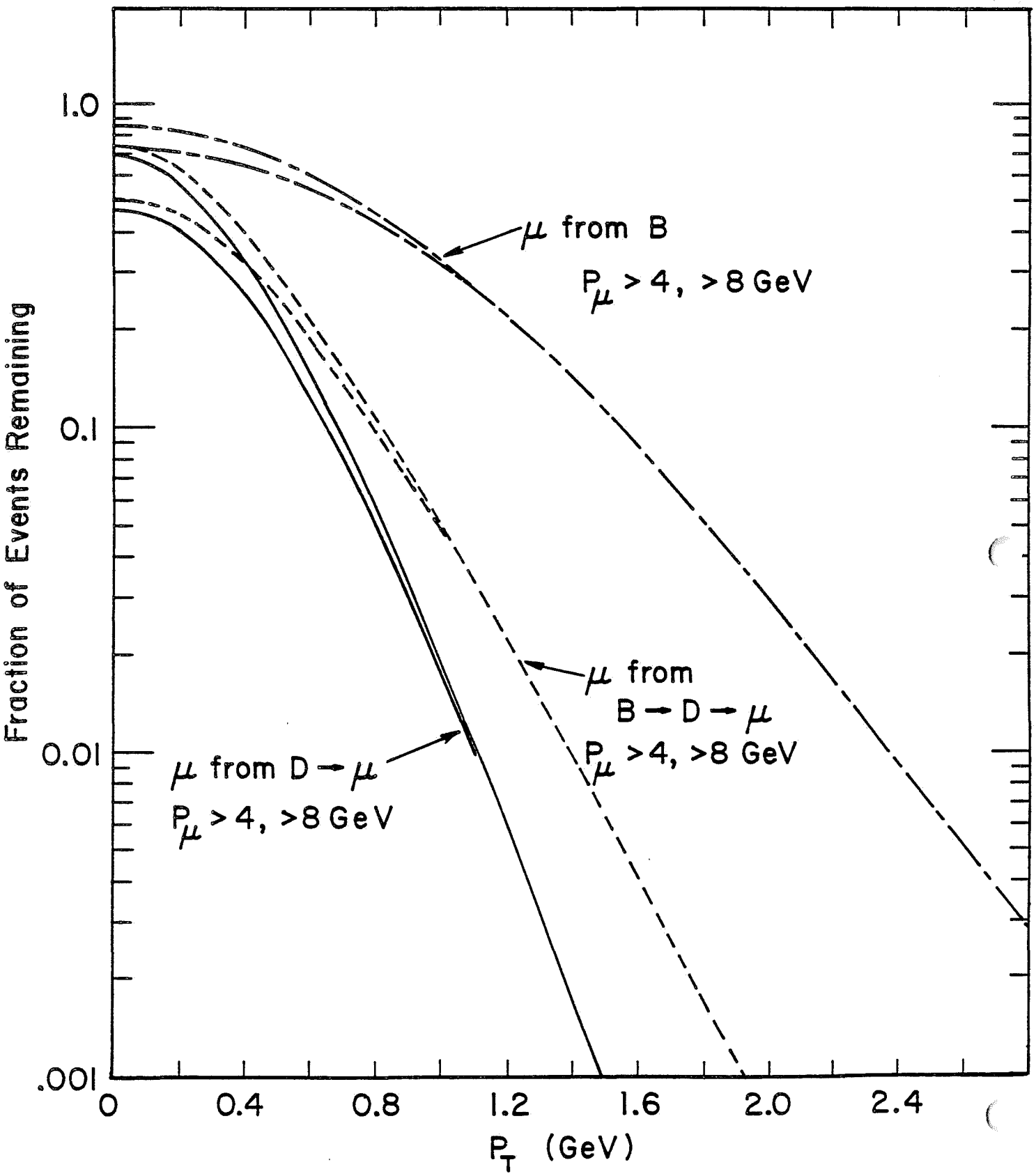
1.0
0.1
0.01
.001
Fraction of Events Remaining
0
0.4
0.8
1.2
1.6
2.0
2.4
P_T (GeV)
μ from B
$P_\mu > 4$, > 8 GeV
μ from
$B \rightarrow D \rightarrow \mu$
$P_\mu > 4$, > 8 GeV
μ from $D \rightarrow \mu$
$P_\mu > 4$, > 8 GeV

Figure 8.

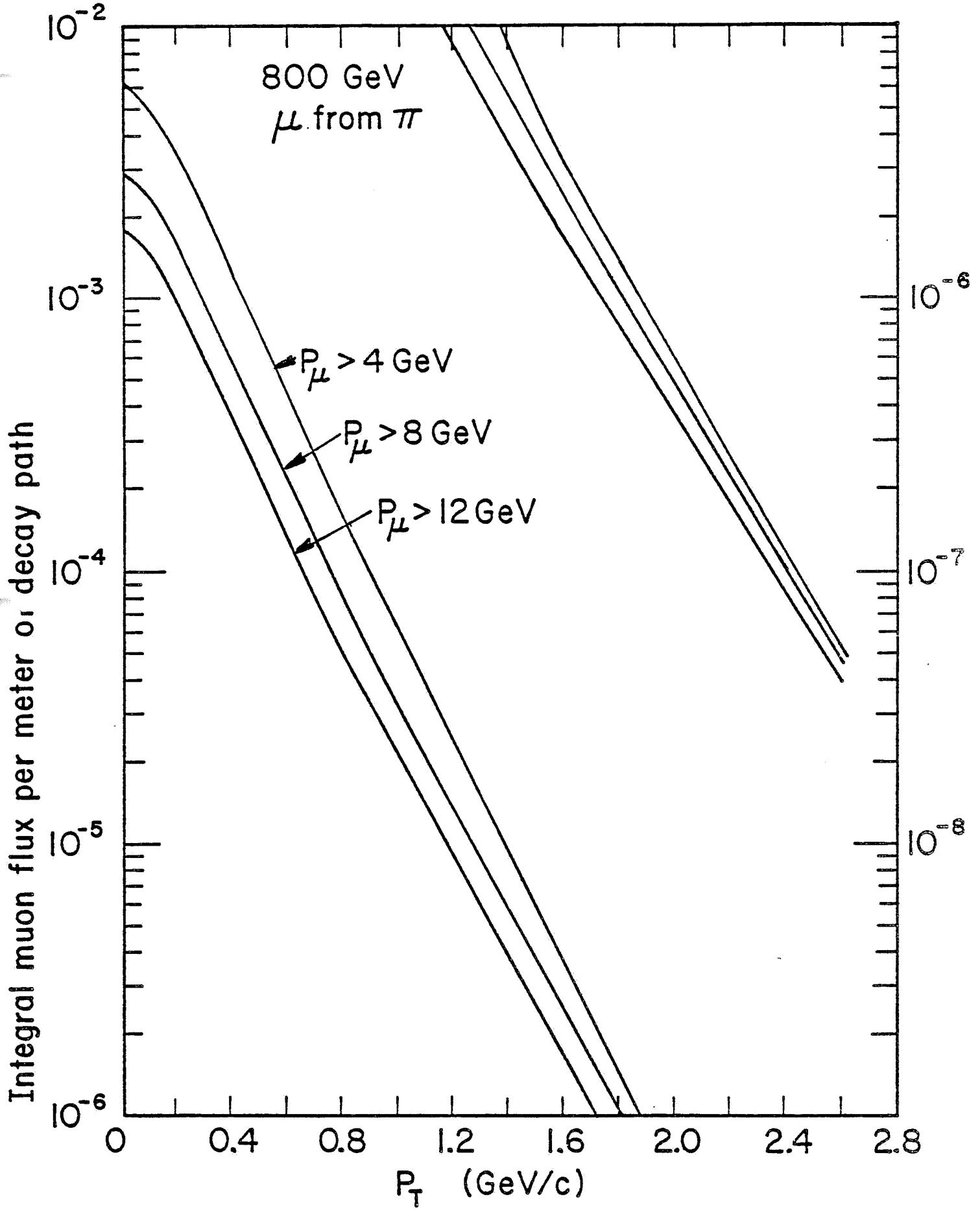

Figure 9. Muons from pion decay.

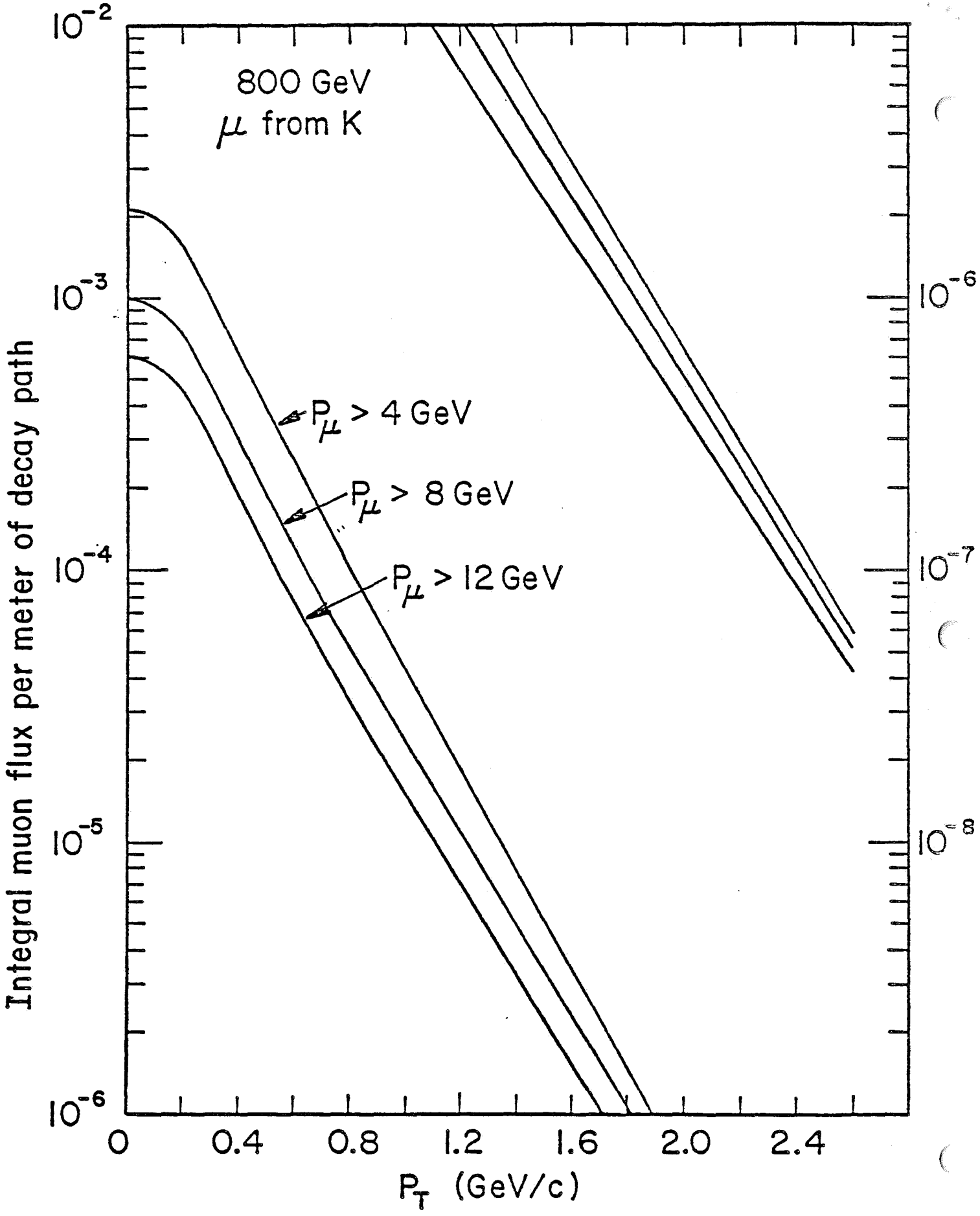

Figure 10. Muons from kaon decay.

to be scanned in the emulsion:

1. Charm Selection. We will capitalize on the excellent resolution of the silicon detectors by requiring an electronically-reconstructed secondary vertex from which a muon of $p > 8$, $p_T > 0.2$ GeV/c emerges. This requirement will pick up not only directly-produced charm, but charm from B decays as well. As shown in fig. 8 , this weak muon cut has an acceptance of 40% (45%) for muons from directly-produced (B-cascade) charm.

We have tested the ability of the vertex detector to resolve secondary vertices with a monte carlo program which simulates multiple scattering in the emulsion and in the silicon detectors, and which generates random measurement errors of ± 12 microns at each detector. Multiprong decay vertices can be located to ± 7.5 microns in the transverse coordinate and ± 220 microns along the parent direction.

Table 1 summarizes the effects of branching ratios and vertex reconstruction cuts on each charmed species. A secondary vertex cut at 4 standard deviations still retains 76% of charged D's and at least half of the others. The abundance-weighted total efficiency for this selection is 0.041 (0.051) for direct (B-cascade) charm.

The yield of directly-produced charm is

$$\begin{pmatrix}\text{Found}\\ \text{charm}\\ \text{pairs}\end{pmatrix} = \begin{pmatrix}\text{Events}\\ \text{in}\\ \text{emulsion}\end{pmatrix}\begin{pmatrix}\text{Muon}\\ \text{cut}\\ \text{survivors}\end{pmatrix}\begin{pmatrix}\text{BR and}\\ \text{vertex}\\ \text{cuts}\end{pmatrix}\begin{pmatrix}\text{Scan}\\ \text{success}\end{pmatrix}$$

$$= (5.8 \times 10^5)(0.40)(2)(0.041)(0.8)$$

$$= 15{,}000 \text{ found charm pairs}$$

The factor of 2 comes from 2 chances of semileptonic decay per pair. The lifetime measurement of one charmed particle per pair is unbiased by this event selection.

Table 1. Data and Assumptions for $C\bar{C}$ Event Selection

Particle		$D^{\pm}$	D^0	F	Λ_c	
Lifetime (10^{-13} sec)	(a)	9.5	3.2	2.0	1.8	
BR to μ		0.20	0.07	~0.04	~0.04	
2 - 6 prongs	(b)	0.52	0.93	~ 0.5	~ 0.5	
Fraction passing vertex cut of 4 S.D.		0.76	0.59	0.5	0.5	
Product of BR, prong and vertex cuts		0.079	0.038	0.010	0.010	
Relative Abundance in $C\bar{C}$ Production	(c)	0.20	0.60	0.10	0.10	
Contribution to finding $C\bar{C}$ pairs		0.016	0.023	0.001	0.001	Total .041
Relative Abundance in $B\bar{B}$ decays	(d)	0.33	0.67	0	0	
Contribution to finding $B\bar{B}$ pairs		0.026	0.025	0	0	Total .051
Contribution if no BR to μ required		0.13	0.37	0	0	Total 0.50

(a) From refs. 2, 3
(b) From ref. 19
(c) Assumes $D^*/D = 3.0$
(d) Assumes $D^*/D = 1.0$

We will also obtain a measurement of the tau lifetime. Assuming 3% of the F's decay to taus, and assuming 10% of the charm sample is F's, we expect 45 taus. This number is reduced to 28 by the smaller efficiency for finding single-prong kinks in the emulsion, as measured in E-531.

The yield of B pairs found from their charm decays is similarly found to be:

$$\text{B pairs found} = (1.15 \times 10^3)(0.45)(2)(0.051)(0.8)$$
$$= 42 \text{ pairs or } 84 \text{ B particles}$$

where 100% decay of beauty to charm has been assumed. Note that both B-particles in the pair are available for unbiased lifetime measurement.

The main background to real charm decays comes from secondary interactions in the emulsion from which one of the outgoing particles has decayed to give the tagged muon. Calculation of this background is discussed in Appendix IV. The probability of a secondary interaction is 0.165, and the chance of a muon from such an interaction passing the p, p_T and multiplicity cuts is found to be 0.13 times that of a muon from the primary vertex, which is (fig. 9) 1.55×10^{-3} per meter per interaction. The background rate is then

$$BG = (0.165)(.13)(.00155 \text{ /m})(3.5 \text{ m})(2.8 \times 10^8 \text{ interactions})$$
$$= 32{,}600 \text{ secondary vertices.}$$

As discussed in the emulsion section, searching the emulsion for a secondary vertex can be limited to one or two sheets and a single microscope field of view, allowing us to look for more than 60,000 such secondary vertices if necessary. Of those resulting from nuclear interactions, 95% can be immediately rejected by the presence of dark tracks from nuclear breakup or recoil [20].

2. <u>$B\bar{B}$ Selection Using a Single Muon with Large Transverse Momentum</u>. This

is the standard type of trigger proposed by many groups. We will require a muon with $p > 8$, $p_T > 1.3$ GeV/c. From fig. 8 ,the fraction of surviving muonic B decays is 0.18. Taking 11% for the BR of B to muons, we have

$$\text{B pairs found} = (1.15 \times 10^3)(2)(0.11)(0.18)(0.8)$$
$$= 36 \text{ pairs, or } 72 \text{ decays.}$$

Each found pair contributes one completely unbiased lifetime measurement and one restricted only in that it is a semileptonic decay.

From fig. 9 , the background is

$$\# \text{ BG} = (2.8 \times 10^8 \text{ int.})(8.5 \times 10^{-6} \text{ muons/m/int})(3.5\text{m})$$
$$= 8300.$$

If the background is unexpectedly high we can, according to figs. 8 and 9, obtain an additional factor of 2.4 rejection at the cost of a factor 1.5 in signal reduction by increasing the p_T cut from 1.3 to 1.5. However, we point out that using a single criterion to cut deeply into both signal and background leads to rate and background estimates which are very model-dependent. For example, our model of muons from B decay gives (2)(0.11)(0.030)=0.0067 B pairs surviving the cut of $p > 10$, $p_T > 2$ GeV/c used in Proposal 694. The model used in that proposal obtains 0.022 for this fraction of survivors. Furthermore, our muon background model gives twice as many muons from an 11 m decay path as their model. Model dependence of the very high-p_T tails has thus introduced a discrepancy of a factor 7 in signal to BG, with our model predicting a signal to background of only 1/1000 for the geometry and cuts of that proposed experiment.

We therefore believe it is desirable to avoid relying too heavily on model-dependent selection criteria, especially those which depend totally on a single criterion. For this reason we are investigating a third event selection

Table 2. Summary of Selection Criteria.

SELECTION	FOUND CHARM DECAYS	FOUND B DECAYS	NUMBER TO BE PARTIALLY SCANNED	NUMBER TO BE FULLY SCANNED
Muon with $p > 8$, $p_T > 0.2$ Plus a Secondary Vertex Containing the Muon	15,000 (~ 30 taus)	84	47,600*	17,000
Muon with $p > 8$, $p_T > 1.3$	---	72†	---	8,300
Muon with $p > 8, 0.7 < p_T < 1.3$ Plus a Secondary Vertex With no Muon	---	72†	13,000	1,000
TOTAL	15,000	200††	60,600	26,300

* Includes both signal and background

† Half are semileptonic

†† The sum has been corrected for double counting

which loosens the p_T requirement but requires in addition a non-muonic secondary vertex.

3. Selection Using a Muon of Moderate Transverse Momentum with a Nonmuonic Secondary Vertex. Reducing the muon p_T cut from 1.3 to 0.7 would increase the B yield 170% over that of selection 2, while increasing the background a factor of 15. Most of this additional background can be eliminated if it is feasible to reconstruct secondary vertices reliably without requiring a muon from a secondary vertex candidate. From Table 1, the fraction of B-cascade charm surviving the prong and vertex cuts, but without the charm muonic branching ratio, is 0.50. We estimate the number of secondary interactions with the right prong number and visible energy to be about 0.5, giving a rejection factor of (0.165)(0.5)=0.08 beyond the muon cut. It is thus reasonable to expect a yield of B's about equal to that of selection 2, with a background of about 13,000 additional events to scan for decay vertices as in selection 1.

Table 2 summarizes the criteria, yield, and background for each of the selection methods.

E. Identification and Reconstruction of Decays

In order to be used to full advantage in studying charm and beauty decays, an apparatus with a high resolution vertex detector must do more than merely see secondary vertices. It must also be able to distinguish decays from interactions, determine the charge of a decaying particle (nontrivial for short decay distances), and reconstruct and identify its species.

As discussed in Section D, the probability of secondary interactions in

the emulsion is about 17% per event. Of these interactions 5% will have no visible nuclear breakup or recoil and a prong number consistent with a decay [20]. The background of fake single charm decays is thus 0.9%. For 50K event candidates containing 15K charm pairs this background is only 3% of the charm signal, and may be further reduced by other considerations such as visible mass. This source of background is also negligible for beauty decays via charm. In the case of B decays without a subsequent cascade, one also has the strong constraint that the visible mass of the decay must be large, so that only for the very small subset of unconstrained beauty decays without charm cascades is there any significant background.

An interesting problem for detectors with resolution appreciably coarser than emulsion is determining the number of prongs emitted by the decay, and thus its charge and species. There are two reasons for this difficulty. First, when an unseen decay vertex must be deduced by measurement, as happens for decay distances so short as to be barely resolvable, forward-going tracks are often ambiguous in their origin. This familiar problem need not be elaborated. A more serious difficulty arises from the expectation that much of charm production is via resonances such as D*. In the particular case of $D^{*+} \rightarrow D^{o} \pi^{+}$, or of $\Sigma_c \rightarrow \Lambda_c \pi^{+}$, the pion is emitted at a very small angle to the direction of the charmed decay product, typically < 5 mrad at Tevatron energies. Since the average decay distance for such events is about 1 mm, the resolution needed to distinguish the decay vertex from the accompanying pion is 5 microns, easy for emulsion but very difficult for other techniques. If the decay vertex is not resolved from the pion the D^{o} looks like a charged decay, and a Λ_c looks like the decay of a doubly charged object.

An important consideration in fitting events is that more than 90% of

the decays throw off one or more neutral hadrons. To obtain unambiguous assignment of these neutrals to a vertex it is necessary not only to detect them in the spectrometer with reasonable efficiency and precision, but also to know with some accuracy the missing transverse momentum at the decay vertex, which is typically 300 MeV for each neutral. In this experiment (as in E531) we will be able to constrain the direction of the decaying particle because the transverse coordinates of both primary and secondary vertices are measured to $\pm$0.4 microns in the emulsion. Thus for a charmed particle with a typical momentum of 70 GeV/c and decay distance of 1 mm, we can constrain p_T to 0.040 GeV/c. In the case of the proposed streamer chamber or NaI detector experiments, the resolution is about $\pm$20 microns in <u>one</u> transverse coordinate, giving 1.4 GeV/c P_T resolution in that projection and no information at all in the other projection. Thus while most decays in the emulsion can be fit with no combinatorial background, this is definitely not the case for detectors in which only one view is available. We note that in the case of LEBC, which has approximately the same resolution as other proposed Fermilab experiments, only one pair decay has so far been fit from a May,1980 exposure of 600K interactions.

We have made monte carlo studies of the mass resolution and acceptance of our spectrometer for $B\bar{B}$ and $C\bar{C}$ events obeying the production model of Section D. Results for the "typical" decays $B \rightarrow D\pi^{\pm}\pi^{\pm}\pi^{\pm}\pi^{o}\pi^{o}$ and $D \rightarrow K\pi^{\pm}\pi^{\pm}\pi^{o}$ are shown in fig. 11. A decay is considered to be within the acceptance of the spectrometer if <u>all</u> secondary products, including gammas from pi zero decay, lie within a cone of half-angle 200 mrad. The integrated acceptance for B (charm) is 73% (64%), and is > 90% for Feynman x > 0. For most events the mass resolution is better than 1.2%.

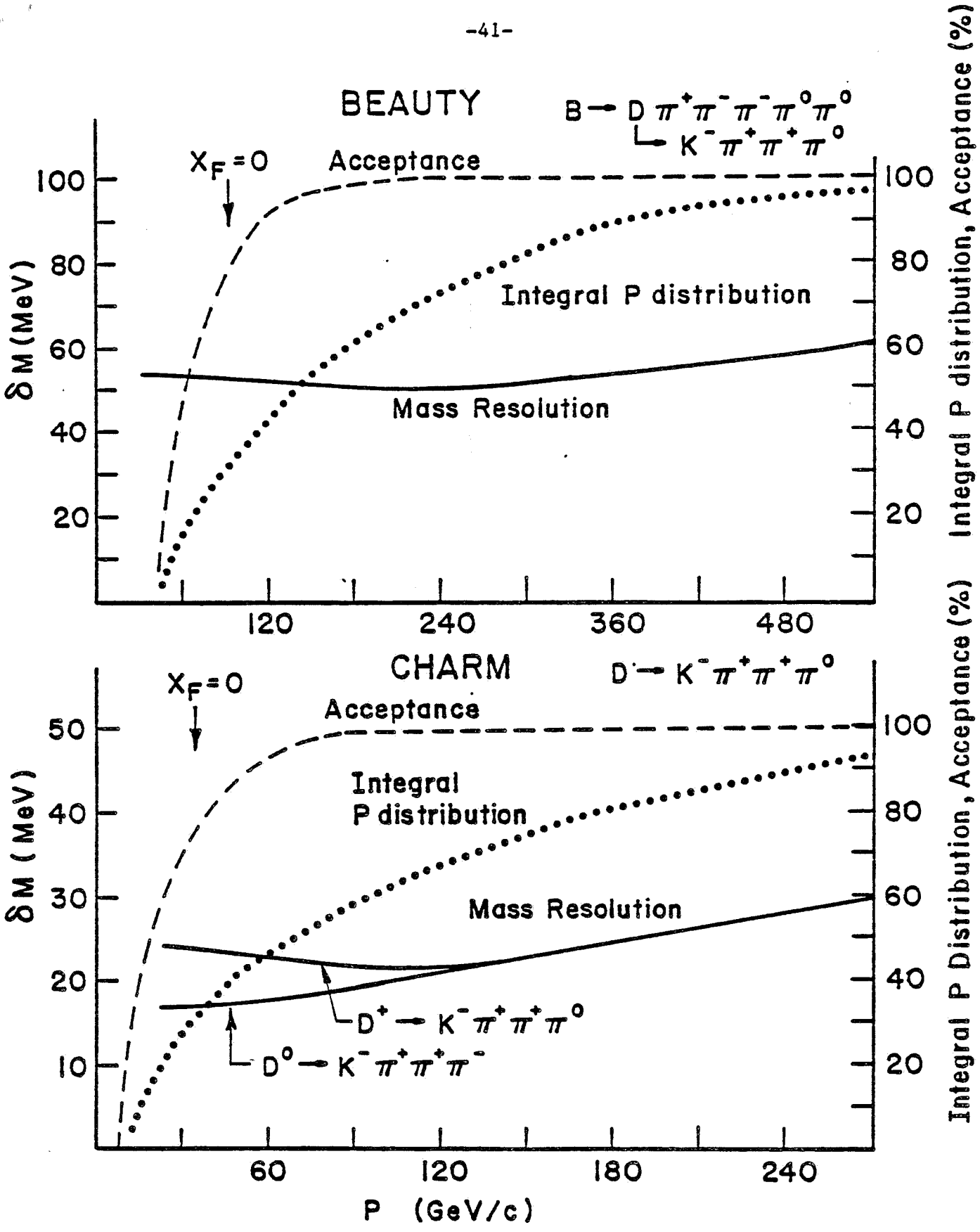
BEAUTY
B → D π⁺π⁻π⁻π⁰π⁰
└ K⁻π⁺π⁺π⁰
X_F = 0
Acceptance
Integral P distribution
Mass Resolution
δM (MeV)
Integral P distribution, Acceptance (%)
100
80
60
40
20
120
240
360
480
CHARM
D → K⁻π⁺π⁺π⁰
X_F = 0
Acceptance
Integral
P distribution
Mass Resolution
D⁺ → K⁻π⁺π⁺π⁰
D⁰ → K⁻π⁺π⁺π⁻
δM (MeV)
Integral P Distribution, Acceptance (%)
50
40
30
20
10
100
80
60
40
20
60
120
180
240
P (GeV/c)

Figure 11.

In addition to those events completely contained in the spectrometer, we can expect to recover events with one or more charged tracks at lab angles > 200 mrad. These slow tracks, typically 1 GeV/c, can be momentum-analyzed by measuring ionization and multiple scattering in the emulsion. The expected mass resolution for charm and beauty decays in this category is about 80 and 190 MeV respectively, and including them increases the acceptance to 80% of all decays.

The acceptance in fig. 11 does not include effects of "pattern recognition" losses such as masking of charged or neutral particles by nearby tracks. These losses are 2% for charged tracks, 7% for gammas, and 30% for long-lived neutral hadrons. Even when these losses are folded in, we still expect more than 65% of all non-leptonic charm decays, perhaps 50% of beauty decays, to be fully constrained, with a negligible (< 5%) fraction of decays having ambiguous fits from combinatorial background. For comparison the fraction of fully constrained non-leptonic multiprong decays in E531 is 54%.

The next question to consider is what fraction of charm decays has the species uniquely identified. We take 5% as an acceptable level of feedthrough. In general, the identification is unambiguous if one or more of the following is true: (a) the resolution in the calculated mass is small; (b) some or all of the decay products are identified by TOF,dE/dx or some other means; or (c) the particle comes from the decay of a resonance such as D* or F*.

If the mass resolution is sufficiently good, no particle identification is necessary to distinguish species because only one kinematic fitting hypothesis is tenable. We have studied the possible ambiguous interpretation of D^+ decays, using for concreteness the $K^-\pi^+\pi^+$ mode and asking how often it could pass for $F \to KK\pi$ or $\Lambda_c \to Kp\pi$. We find that for the 1/3 of events which have

mass resolution better than 10 MeV, only 30% of the generated D's are ambiguous with the F hypothesis, and only 12% are ambiguous with Λ_c. Overall, we find 30% of the events will be cleanly identified even in the absence of particle identification.

However, more than 90% of the charged decay products of charm and beauty have momenta less than 40 GeV/c, and roughly 65% of these can be identified to better than 2 standard deviations by TOF or dE/dx. The majority of charged tracks will be identified for 50% of beauty decays and 75% of charm decays.

The final handle on identifying decays comes from resonance production (D*, F*, Λ_c*,Σ_c). The mass resolution for $D^o\pi^+$, $\Lambda_c\pi^+$ and $D^+\pi^o$ will be of order 2 MeV. We estimate that the backgrounds under the resonance effective mass peaks will be << 5%; it is zero for the 18 D^o decays from E531. Assuming half of charm production to go via resonances, we have 45% of D^o and Λ_c and 30% of D^+, unambiguously tagged by this criterion alone.

To summarize, we estimate that 85% of all constrained and about half of unconstrained charm decays can be identified by one or (usually) more than one of the above methods.

F. Cost Estimates

The following estimates are divided into items which are to be furnished by Fermilab and those which must be furnished by experimenters. For clarity, the worth of existing items has been suppressed in order to focus on new expenditures.

		TOTAL
1.	Fermilab:	
a.	25' x 45' of floor space, along a suitable beam, with power and other utilities.	( )
b.	Village space as provided for E-531	----------
c.	Toroid, estimate 70 tons @$600/ton for cutting and machining, and $5000 for the coils.	$ 47K
d.	Muon and calorimeter steel (already exist in E-531)	----------
e.	Spectrometer magnet estimated at $1.00/lb for machined steel and $3.00/lb for copper, with inclusion of a 30% cost overrun.	$ 30K
f.	PREP electronics	$ 300K
g.	On-line computer (We understand that in 1983-84 the standard on-line computer will be a VAX.)	( )
h.	Off-line analysis (250 hours)	( )
i.	Rigging and surveying	$ 10K
j.	Solid-state prototyping	$ 50K

TOTAL

2. Experimenters:

a. Emulsion

i.	Precision moving target stage	$ 90K
ii.	Emulsion, 100 liters @$6K/liter	600K
iii.	Pouring laboratory (exists at Fermilab)	----------
iv.	Developing laboratory (exists at the University of Ottawa)	----------
v.	Developing costs, @10% of emulsion cost	$ 60K
vi.	Existing scanning laboratories in Canada, Japan, Korea, and the United States	----------
	Subtotal	$ 750K

b. Scintillator Counters

i.	New trigger counters	$ 2K
ii.	Muon hodoscopes (exist from E-531)	----------
iii.	Time-of-flight hodoscope (30 counters)	30K
	Subtotal	$ 32K

c. Solid-State Detectors

i.	Prototyping and construction for 12 beam, 36 spectrometer, and 9 gamma detectors	$ 150K
ii.	Electronics, 10,000 lines @$40/line (from detector to computer)	400K
	Subtotal	$ 550K

		TOTAL
d.	Drift Chambers	
i.	18 spectrometer chambers and supports @$2K/chamber	$ 36K
ii.	12 muon chambers and supports @$2K/chamber	24K
iii.	Multiple hit per wire readout electronics already exist	----------
	Subtotal	$ 60K
e.	Charged-Particle Identifier	
i.	Chamber and supports	$ 25K
ii.	Electronics for 300 wires @$150/wire	45K
iii.	Miscellaneous (power supplies, gas purifiers, etc.)	15K
	Subtotal	$ 85K
f.	Gamma Calorimeter	
i.	Chambers, lead and supports	$ 12K
ii.	Amplifiers and cables for 1300 lines @$20/line	26K
	Subtotal	$ 38K
g.	Hadron Calorimeter	
i.	Chambers and supports	$ 16K
ii.	Amplifiers and cables for 1300 lines @$20/line	26K
	Subtotal	$ 42K

		TOTAL
h. Off-Line Computer Analysis		
i. AMDAHL 470 (Ohio State University)		----------
ii. VAX 11/780 (University of Oklahoma)		----------
iii. VAX 11/780 (University of Toronto)		----------
	Subtotal	$----------
i. Operating Costs, 12 months @$7K/month		$ 84K
	Subtotal	$ 84K
New Costs for Experimenters	TOTAL	$ 1641K

G. Time Schedule for the Experiment*

1)	Spring, 1981	Complete testing of Solid State Devices (SSD) with 1 mm strip spacing.
2)	Summer-Fall, 1981	Further work on Experimental Design
3)	Summer, 1981	Commence testing of 1 cm^2 SSD with 40 μm strip spacing, first reading out every wire and then testing resistive division.
4)	Fall, 1981	Complete testing of 1 cm^2 SSD
5)	Winter, 1982	Commence construction of all Non-SSD equipment
6)	Winter, 1982	Commence construction of Beam and Gamma SSD
7)	Winter, 1982	Commence testing of 25 cm^2 SSD Prototypes
8)	Fall, 1982	Complete all prototype testing and begin construction of spectrometer SSD.
9)	Spring, 1983	Finish all Non-SSD construction
10)	Summer, 1983	Commence rigging of Non-SSD equipment
11)	Summer, 1983	Latest possible date for placing order for more than 100 liters of Fuji Emulsion.
12)	Fall, 1983	Finish rigging of Non-SSD equipment and commence SSD installation.
13)	Fall-Winter, 1983-84	Complete all installation, if possible take 1 month run to "shake down" equipment.

14)	Fall-Winter, 1983-84	Emulsion is received at Fermilab and first modules poured. Pouring of modules also will go on during the data run so as not to pour many more modules than are used.
15)	Winter, 1984	Commence data run, one month for electronic hardware, two additional months to expose emulsion.

We do not show more on the time scale, for if the proposed method were to be successful we would request further running.

* As we have constructed devices similar to all those proposed except the SSD's, we expect the SSD's to be the limiting factor in the time schedule. Accordingly, we have utilized the SSD work to benchmark the construction phase.

Appendix I

Prototyping of Solid State Detectors

The design of the spectrometer for P653 relies heavily on the excellent position and multiple track resolution of position-sensitive semiconductor detectors. These are thin wafers of high resistivity silicon on which are deposited many narrow parallel strips which collect the ionization from charged particle tracks. The size of this signal is about 80 electron-hole pairs per micron of silicon, or 3.8 femtocoulombs for a fully-depleted wafer 0.3 mm thick. Analogue signals may be read out either from individual strips (as is necessary where the track density is high) or from taps every N strips, with the position being inferred from interpolation of the resistively-divided charge [9].

The latter method considerably reduces the instrumentation cost when relatively large areas of detector are needed, as is the case for P653, and maintains the same position resolution as the individual- strip readout in regions of lower track density. In this method strips are connected by constant interstrip resistances R, as shown below:

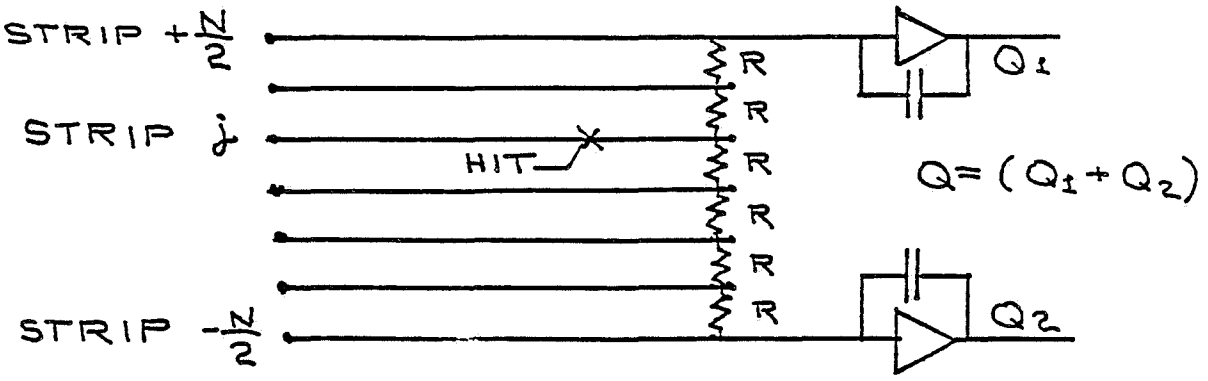

Since the charge-sensitive amplifiers act as virtual grounds, charge deposited by a track passing through strip j is divided according to path resistance

onto only the amplifiers immediately adjacent to that strip. The struck strip is then inferred from the divided charges Q_1 and Q_2:

$$j = \frac{N(Q_1 - Q_2)}{2(Q_1 + Q_2)}$$

For constant interstrip resistance R the error in determining j is

$$\delta j = \frac{(Q_1^2 + Q_2^2)^{\frac{1}{2}}}{Q} N \frac{\delta Q}{Q}$$

where Q is the total deposited charge and δQ is the RMS uncertainty in each signal due to system noise. For N=10, Q=3.8 femtocoulombs (detector 0.3 mm thick), an RMS noise of δQ=0.15 femtocoulombs gives rise to a position uncertainty δj=0.38, comparable to the value of $(12)^{-\frac{1}{2}}$ expected for the case of individually-read strips without charge sharing between strips. There is also a contribution to δj from uncertainty in interstrip resistance which is roughly $(N)^{-\frac{1}{2}}$ $\delta R/R$. Thus for N=10 the fractional error in R must be smaller than 10% RMS to maintain position accuracy. Though not demonstrated here, R must also be kept larger than 2000 ohms if δQ is not to be dominated by parallel resistance thermal input noise to the amplifier.

A. Construction of Position-Sensitive Silicon Detectors

Position-sensitive silicon detectors may be constructed using either surface barrier or diffused junction techniques. In surface barrier detectors the rectifying contact is at the surface between the silicon and the metal deposited on it. They are relatively easy to make by etching away an evaporated metal film to leave the desired pattern of strips. During the past year several groups [21,22,23] have reported successful source or beam tests of surface barrier detectors with strip spacings of 600 microns down to 40 microns.

We have chosen to use the diffused junction technique in which the rectifying junction is buried below the surface, occurring between the silicon and an implanted impurity such as phosphorus on which the metal strips are laid (similar to the construction of commercial IC's). Although requiring specialized equipment, this method has several advantages:

1) The buried junctions are more stable against deterioration and the resulting increase in noise, and the area between the strips is rendered inert by a layer of oxidized silicon. The resistance between the strips is high and stable, as required by the charge division readout. Achieving a uniform resistance for this application is much more difficult in surface barrier detectors.

2) Strip spacings smaller than 40 microns appear to be quite feasible with optical masking techniques, as witnessed by the few-micron line widths routine in IC fabrication.

3) The p-type semiconductor used in our diffused-junction device can easily handle the radiation in this experiment. No impairment of performance occurs for doses of minimum ionizing particles of $10^{14}/cm^2$. This feature is important for possible future high-rate applications.

Prototype diffused junction detectors are being made for us by the Silicon Solid State Group at Lawrence Berkeley Laboratory. We are now in the second generation of prototypes. The first round of detectors, having 0.8 mm strips with 1.0 mm center-to-center spacing, were built mainly to gain experience in diffused junction strip technology; results of tests on these detectors are described below. Prototypes with strips on 40 micron centers have recently been fabricated,and at least 6 of these should be ready for testing early this

summer.

The 9 mm x 9 mm active area of this 40 micron prototype and its printed circuit fanout board are shown in fig. I-1. Photomicrographs of parts of the area are shown in fig. I-2; one can see the strips, the underlying implants and the pads which will be connected with ultrasonically bonded, 20 micron gold wires to the traces on the fanout board.

B. Testing of Prototypes

The first generation of prototypes (1 mm spacing, 1 cm x 1 cm area) has been tested with Ru^{106} electrons (3.5 MeV endpoint) at Fermilab, the University of Toronto, and the University of Oklahoma (UO), with the different groups trying different amplifier and readout schemes. Results from the Fermilab tests using a modified version of the Droege electronics (designed for liquid argon detectors) are shown in fig. I-3. A very clean separation of signal and noise peaks is apparent.

A stack of three of these detectors is being tested both with the 3 MeV source and in the beam from a 30 MeV electron linac by the UO group. Four strips from each of the 3 wafers are read out via FET-cascode amplifiers into standard ADC's. Typical pulse height spectra are shown in fig. I-4. A clear electron peak is observed at 3.2 fc average charge. Noise contributions were present from the amplifier alone (0.1 fc) and from the amplifier-detector combination (0.24 fc). These were increased to 0.4 fc by the noisy RF environment of the linac.

The main questions to be addressed by this multi-detector test are: 1) How often does a particle give a signal in adjacent strips; 2) What is the overall efficiency; and 3) Is the space between metal strips alive or dead?

Some preliminary results are available at this time. Correlations of hits between wafers are shown in fig. I-6a,b for both source and linac data. For perfectly aligned strips, no multiple scattering and no sharing between strips, only the diagonals of these correlation matrices would be populated. Although the multiple scattering from the source is approximately 1 mm, that from the 30 MeV linac beam is only 0.1 mm (comparable to the gaps between strips), and the angular divergence of the beam is much smaller than the mean multiple scattering angle. As is clear from fig. I-6b the 30 MeV data are in fact markedly more peaked at the diagonal. The small subdiagonal population implies a misalignment of about 1/7 strip spacing between planes. Both sets of data are in good agreement with the monte carlo simulations in figs. I-6c,d, which assume no signal sharing between adjacent strips. There is thus already evidence for clean 3-point trajectories.

An estimate of the inefficiency can be made by asking how often neither of the two central strips in the middle wafer failed to record tracks seen by the corresponding strips in both front and back wafers. Two misses were seen in 92 events, giving an efficiency (97±2)%. This high efficiency, together with the known misalignment of 1/7 strip, implies that the 0.2 mm gap between the 0.8 mm metal strips is essentially live. If it were dead (e.g. from increased collection time) one would expect an inefficiency of about 20%.

We are now preparing to test the second generation 40 micron prototypes at LAMPF, starting in July,1981. Four wafers with 30 instrumented strips each will be used in a closely spaced stack to study sharing between strips, position resolution, efficiency and amplifier performance. With a 550 MeV/c beam we will be able to measure the position resolution to 5-7 microns (standard deviation). Fermilab has agreed to provide a PDP 11 computer with CAMAC interface,

together with a full-time research associate, for this and future beam tests. We would appreciate receiving this support by the beginning of testing in July.

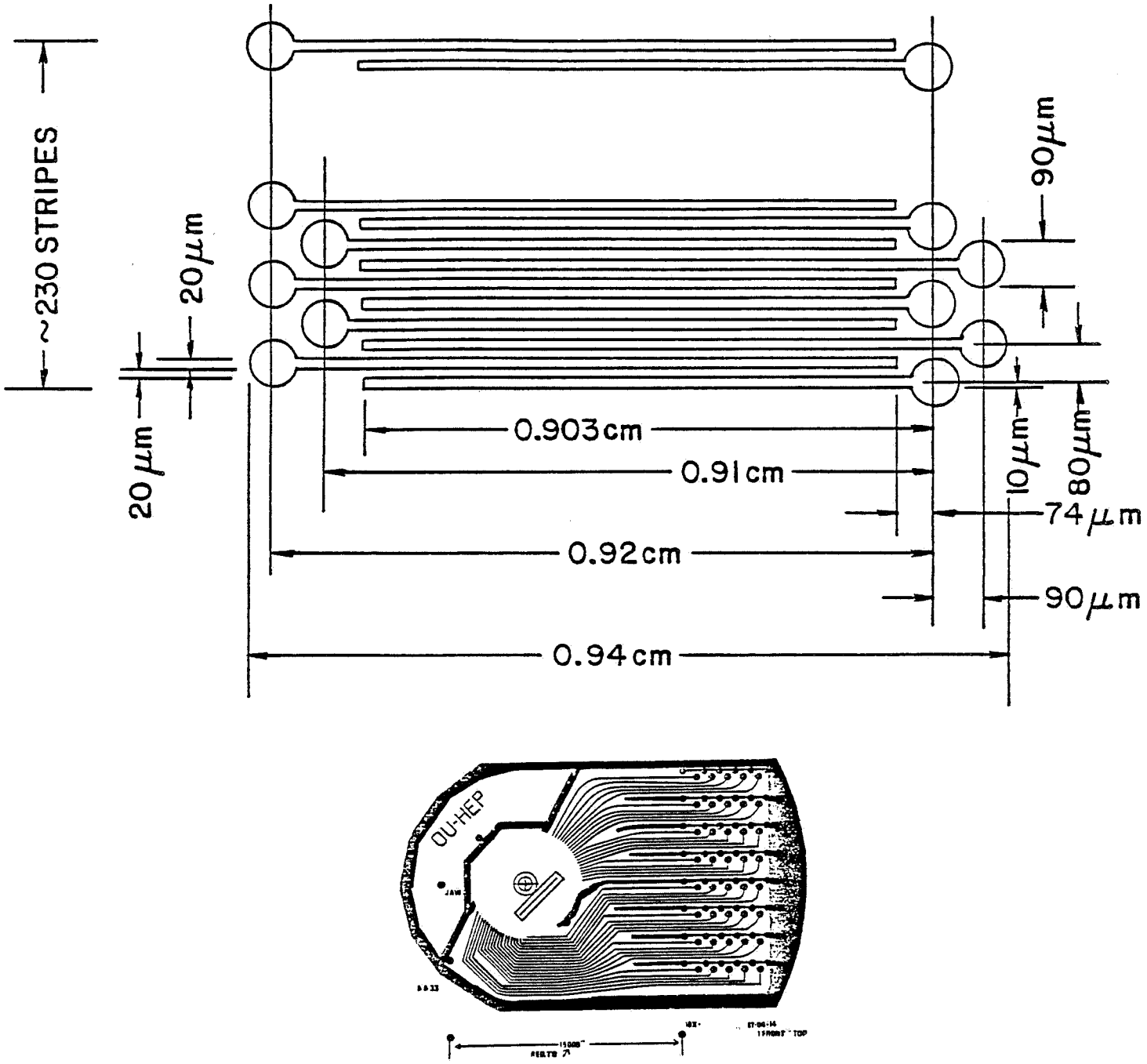

Figure I-1. Layout of stripes and PC mounting board for 40 micron prototype.

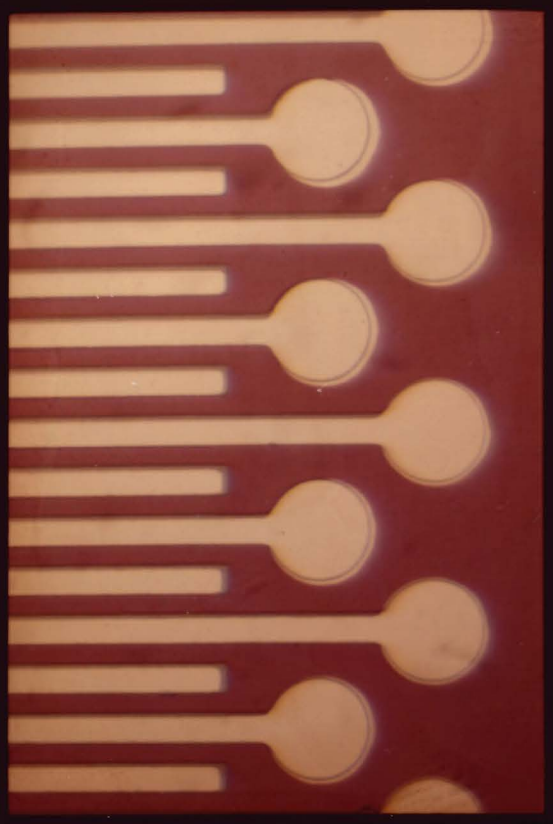

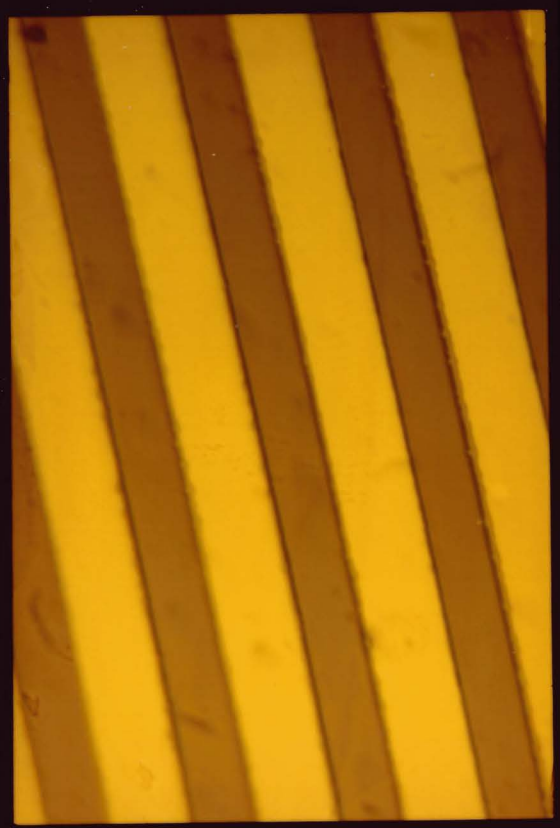

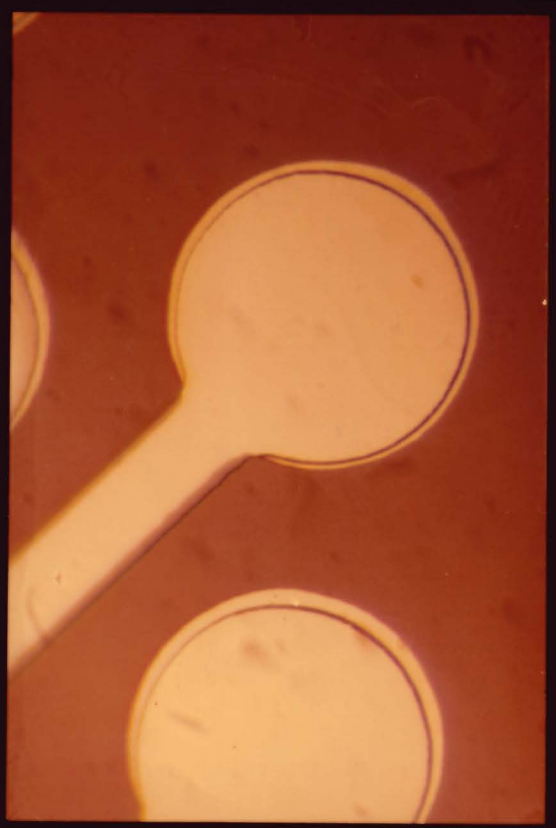

Figure I-2
Photomicrographs of 40 micron (center-to-center) prototype. The color is an artifact. Strip layout shown on page 56.

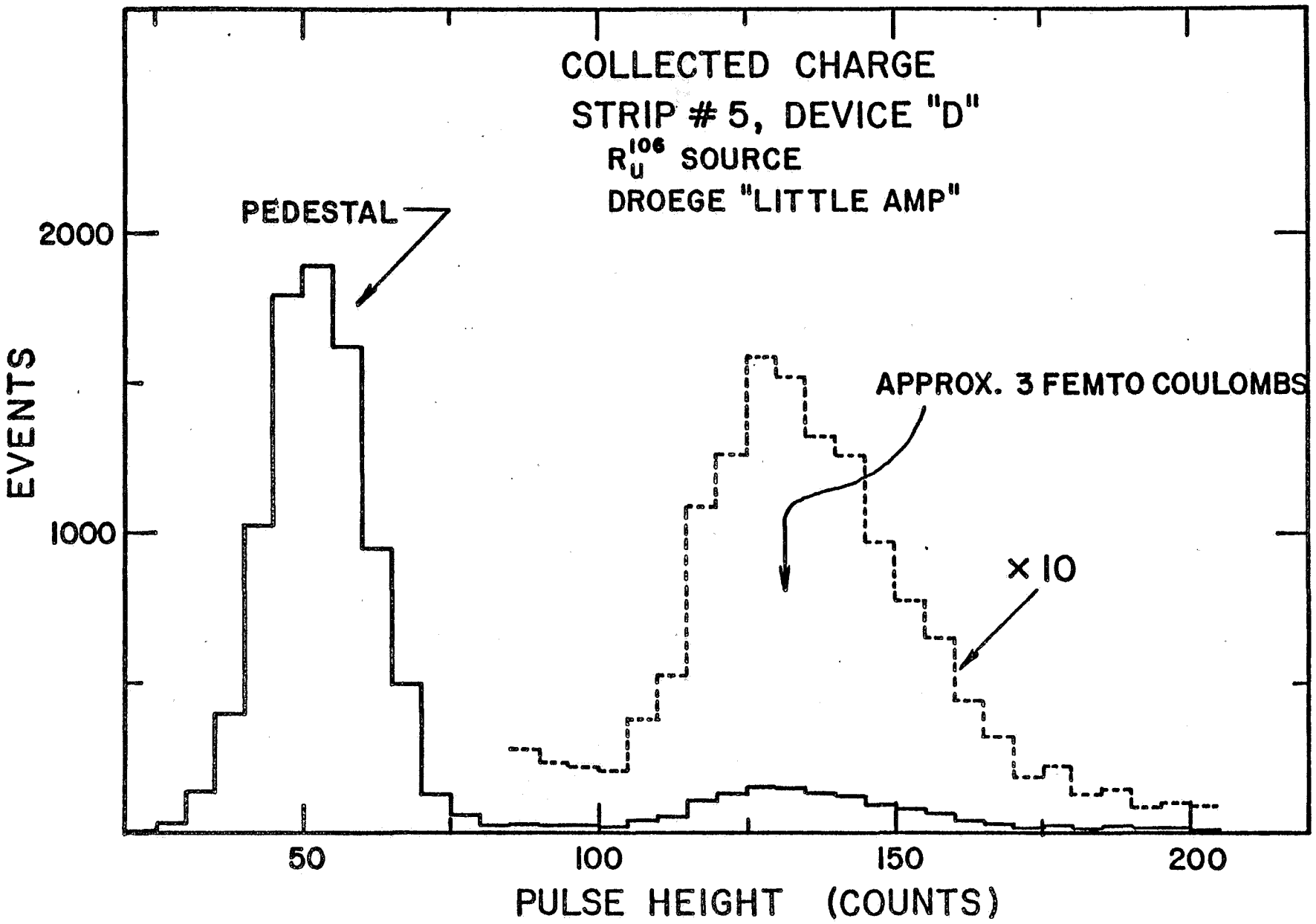

Figure I-3. Pulse height spectrum for one mm prototype.

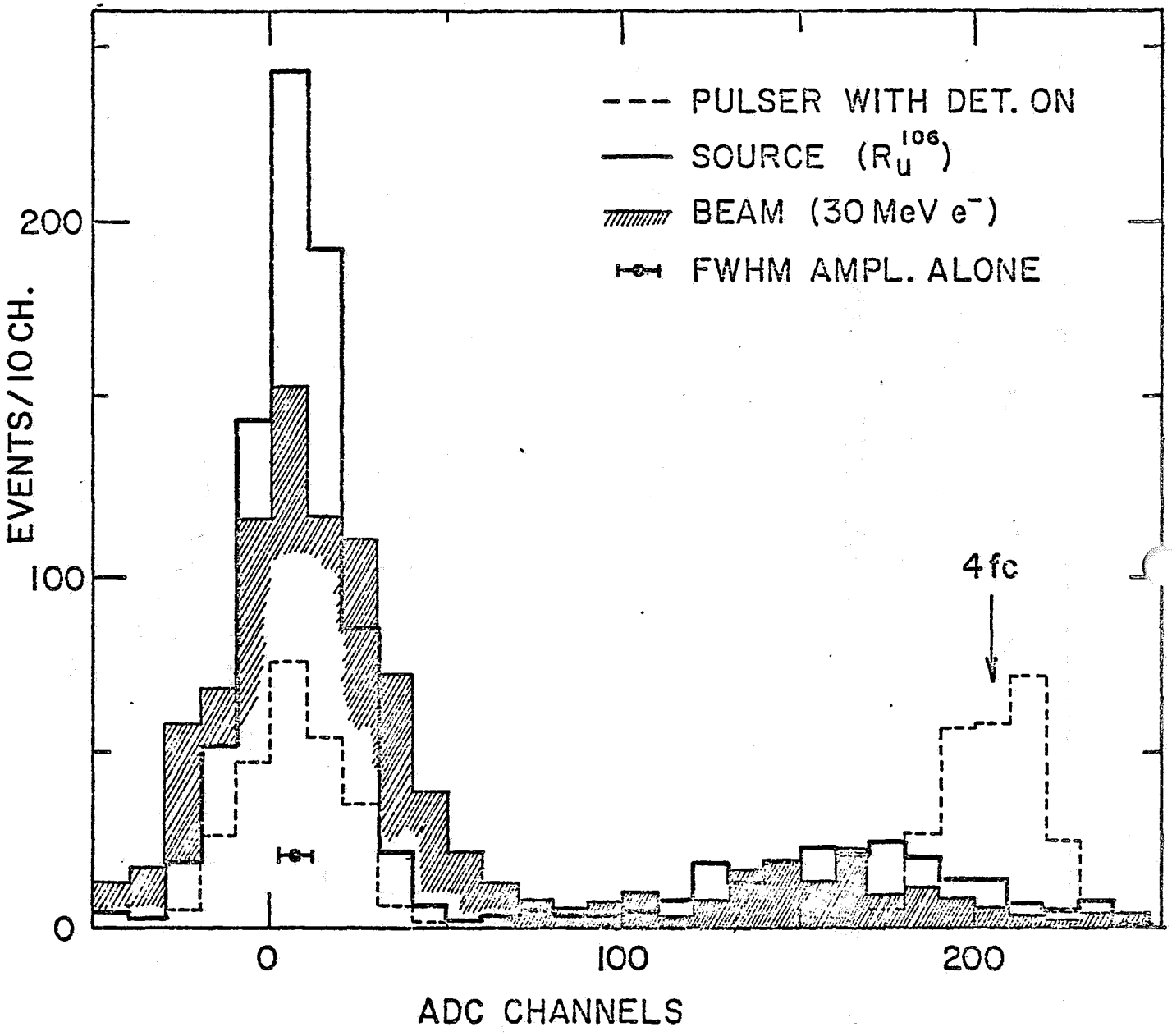

Figure I-4. Pulse height spectrum for one mm prototype.

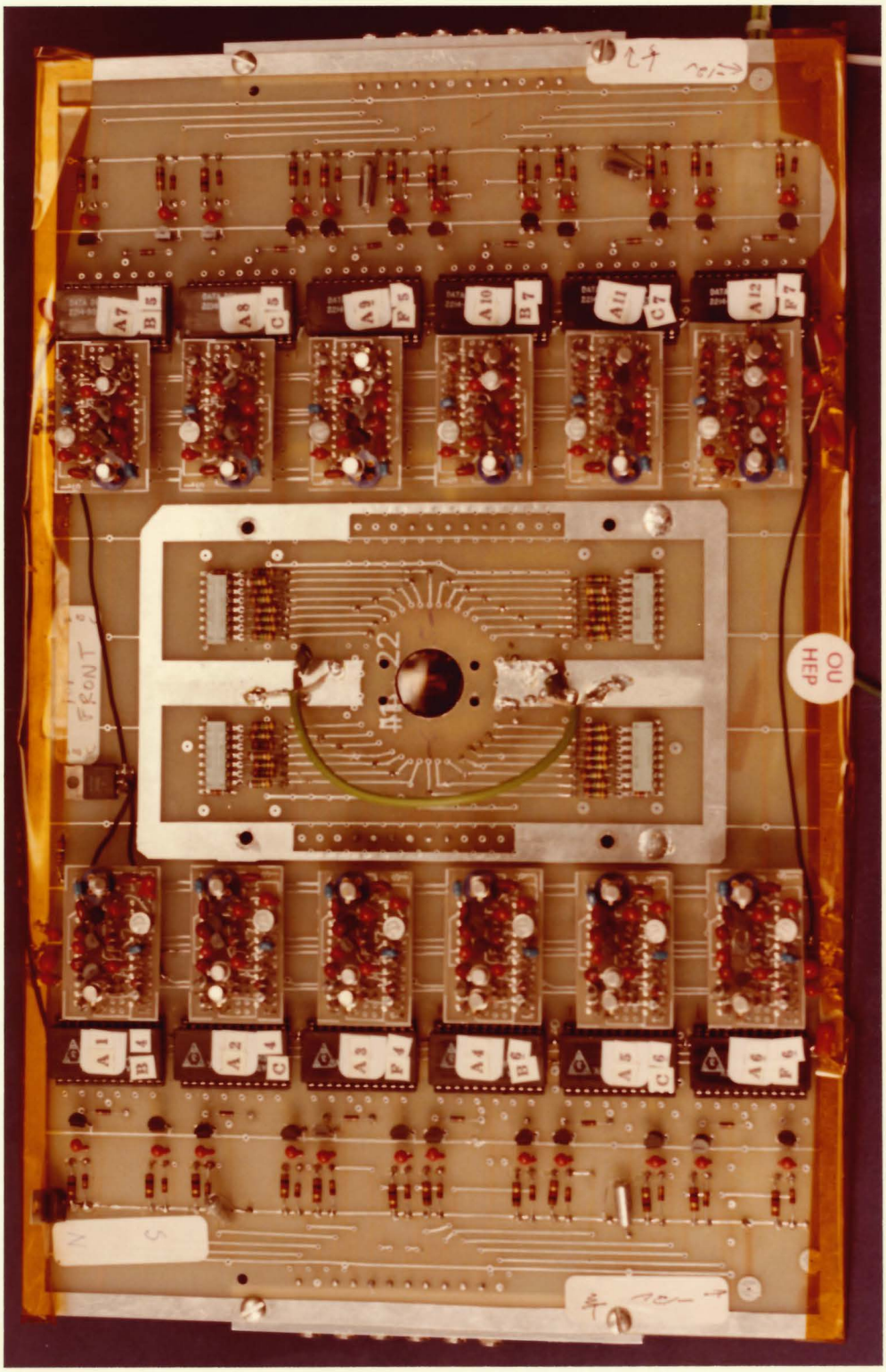

Figure I-5
Amplifier Board

Figure I-6.

Stripe Hit Correlations

Matrix of correlated hits, first plane (1-4)→, second plane ↓ with last detector also hit.

DATA

3 MeV Source

a)

58	10	0	3
18	56	11	0
5	22	69	20
0	0	6	42

220	Diagonal
87	1 Off Diag.
8	> 1 Off
315	

30 MeV Linac

b)

80	2	4	0
15	86	9	3
3	13	174	9
6	4	22	116

456	Diagonal
70	1 Off Diag.
20	> 1 Off
546	

MONTE CARLO

c)

48	9	0	0
14	54	12	1
3	26	54	19
0	7	26	42

198	Diagonal
106	1 Off Diag.
11	> 1 Off
315	

d)

94	0	0	0
20	149	0	0
0	26	149	0
0	0	17	91

483	Diagonal
63	1 Off Diag.
0	> 1 Off
546	

Appendix II

Possible Beam Lines

At least three beam lines (M2, M6W, PC) appear to be compatible with our requirements for both present and Tevatron energies.

We require a beam at or near maximum machine energy which has 2-6 x 10^4/second intensity on a spot size 3 mm x 3 mm, and an integrated halo in a square 10 cm x 20 cm centered on the beam which is at most 7% of the beam intensity. (Note that for a 20-second Tevatron spill we would require roughly 1/2 x 10^6/pulse.)

The remainder of this section will be devoted to a discussion of measurements on the M6 charged beam (provided by P. Garbincius) and on the PC neutron beam (provided by M. Johnson). It is our feeling that the M2 hyperon channel also would be suitable, but we were unable to obtain applicable measurements.

For a 2 x 10^6 positive M6 beam at 100 GeV (2/3π, 1/3P) a spot 6 mm in width and 5 mm high was obtained for the ten percent beam density points. Ninety-eight percent of the beam was contained in a spot of 9 mm x 8 mm.

Halo was determined by three sets of three halo counters, each set mounted in a cloverleaf fashion with a 6 mm x 6 mm hole in the center. The sets of antis were mounted at the second focus and upstream and downstream of the hydrogen target.

The ratio of halo/beam summed over all three sets was 0.075, completely consistent with the fraction of beam overlapping the antis. Spot size and halo did not appear to be a strong function of the momentum setting for the beam, so additional collimation placed at the first focus and along the parallel section should be able to reduce them down to our requirements.

A neutron beam is being commissioned in Proton Center for E-630. They have obtained 0.3 x 10^6 neutrons per pulse in a spot sized 1 mm x 7 mm. The ratio of halo/beam = .04 for halo outside 2 mm x 9 mm. This beam may be converted to a diffracted proton beam of suitable intensity by targetting the main beam at a

small angle into a new curved channel. An additional set of three 10-ft. benders placed downstream of the hyperon magnet would be run with polarity opposite to that magnet, partially correcting for momentum dispersion. K. Stanfield and P. Garbincius believe that a diffracted proton beam could be constructed with a suitable spot size and a halo/beam ratio at least as low as that measured for the neutron beam.

In summary, we believe that our beam requirements are quite minimal and could be satisfied by several existing and proposed Tevatron beam lines with minimal additional cost to Fermilab. Furthermore, our experiment uses less than 15 meters of floor space and could be designed to move in and out of the beam in a day of rigging.

Appendix III

Spectrometer Magnet

Our compact geometry imposes definite constraints on the spectrometer magnet. To get the largest possible field integral we use a tapered vertical magnet gap which opens from 14 cm to 28 cm over a distance of 40 cm. To reduce interference of the coils (and their attendant fringe fields) with the silicon detectors and their amplifiers and connector boards, we propose to put two coils around the sides of an H-frame magnet rather than around the pole-tips as is usually done. A total of 500 kiloamp turns will produce a maximum field of 1.7 Tesla and a transverse momentum kick of 0.2 GeV/c. We are studying the feasibility of using Fe-Co pole tips (saturating at 1.5 times higher field) to increase this kick to 0.3 GeV/c.

Although we can accomplish these goals with conventional coils, fig. III-1 shows the improved geometry possible with superconducting coils. The dimensions of the two cryogenic cans containing such coils are 0.4 m ID by 0.6 m OD by 0.3 m high. The coils are circular and take up their own Lorentz forces by tension, permitting a simple support structure design. If one adds the saving in electric power, the superconducting option looks very attractive. The OU group of our collaboration has sufficient technical expertise and manpower to design the coil, cryostat and magnet but would need the cooperation of Fermilab to provide it with superconducting cable, transformer iron and other materials. Since this magnet requires only about 500 liters of liquid Helium per week it could be kept cold using Dewars; however, a refrigeration system, if one were available, might be a useful alternative.

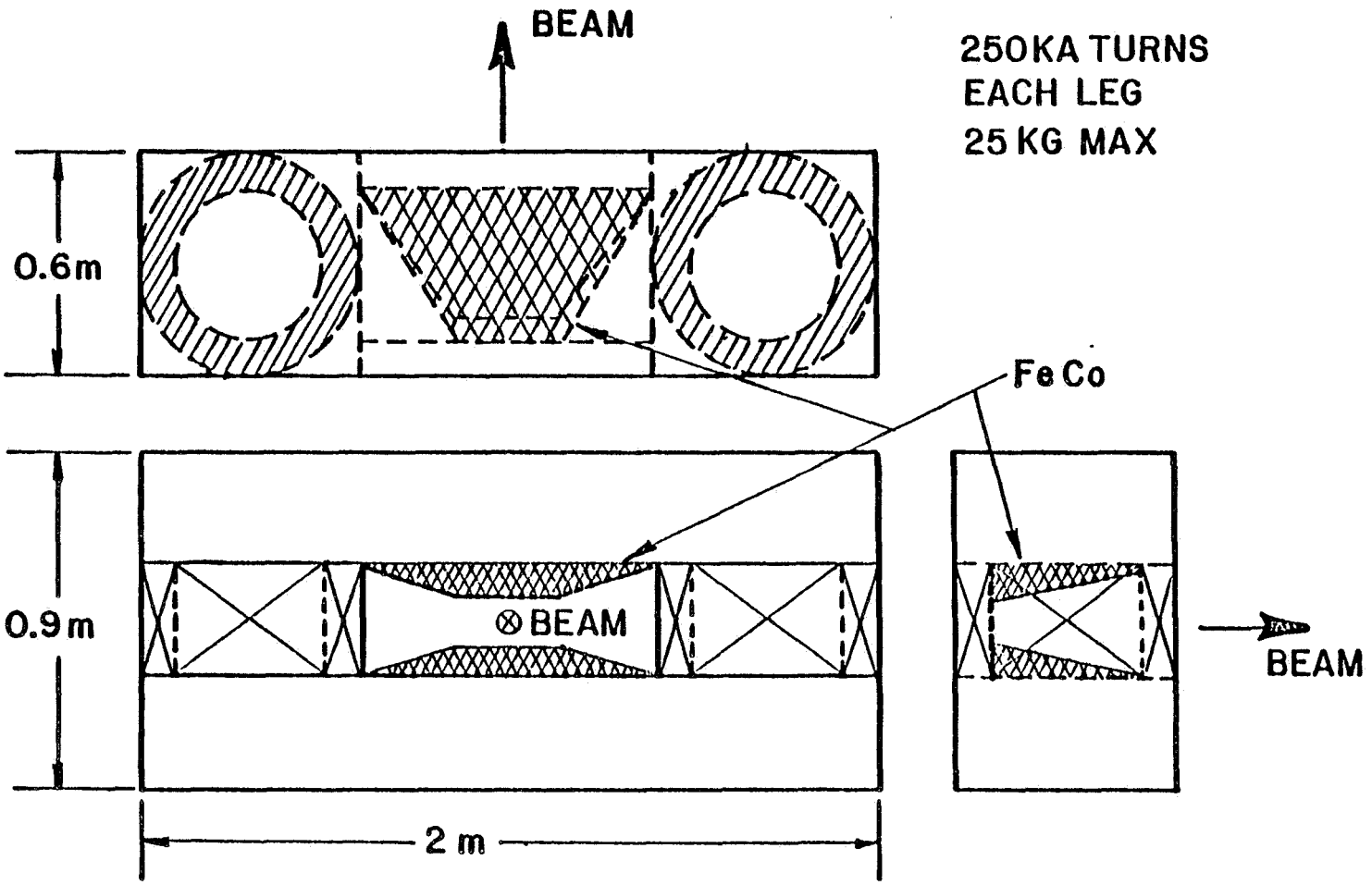

Figure III-1. Spectrometer magnet, drawn for superconducting coils.

Appendix IV

Calculation of Muon Background

The muon background from charged pion and K decay was calculated from ISR production data [18] at center of mass energies of 31 and 53 GeV. Special care was taken in parametrizing this data to be sure the behavior at high transverse momentum P_T was correctly described, since event selection depends at least in part on high-p_T muons. Comparison of the model with data at rapidity y=0 are shown for pions and K's in figs. IV-1a and IV-1b. The model also works well for nonzero y out to very near the edge of phase space.

Laboratory cross sections $d^2\sigma/dpdp_T$ were then calculated with this parametrization on a grid of p, p_T. In each bin of this grid the fraction of pion or K decays per meter is then $m/(c\tau p)$, where τ is the lifetime of the decaying particle of mass m. In each bin of p,p_T of interest a number of monte carlo decays ($\pi \rightarrow \mu\nu$, $K \rightarrow \mu\nu$) were generated proportional to the number of parent decays in the bin. The resulting integral muon spectra are plotted vs. p_T in figs. 9 , 10 for several cuts on lab momentum p. Note that the contributions from pion and K decay are comparable for $p_T > 1.2$ GeV/c.

An independent check on this calculation was provided by a tape [12] of 360 GeV π^-p bubble-chamber events. Charged tracks from these real events were assumed to be pions, and monte carlo decays were generated. The muon yield from this approach agrees with the above calculation to better than 10%.

For the background estimates in Section D; it is necessary to know the number of muons from <u>secondary</u> interactions in the emulsion passing the muon p, p_T cuts. The lab momentum spectrum of pions from 800 GeV interactions is known from the production model described above. It was assumed that this model is also approximately correct for interacting pions down to 10 GeV/c, and the

muon background program was run for "beams" with selected momenta between 10 and 800 GeV/c, corresponding to the interacting secondaries. The yield of muons passing the cuts for each such bin of secondary momentum was then weighted by the momentum spectrum of pions from 800 GeV interactions. The largest contribution to muons passing the cuts was from secondaries of order 100 GeV/c, which make about 6 charged prongs per interaction. We thus estimate that limiting charm decay vertex candidates to < 7 prongs will eliminate 40% of this interaction background.

The probability of a muon from a secondary interaction passing the p, P_T and prong cuts was found to be 0.13 times that of a muon from the primary vertex. This number must be multiplied by the probability of a secondary interaction. We assume 9 charged prongs plus 2 long-lived neutral hadrons per 800 GeV interaction, and use the pion mean free path [17] of 50 cm and an effective path in emulsion of 0.75 cm to obtain 0.165 secondary interactions per event.

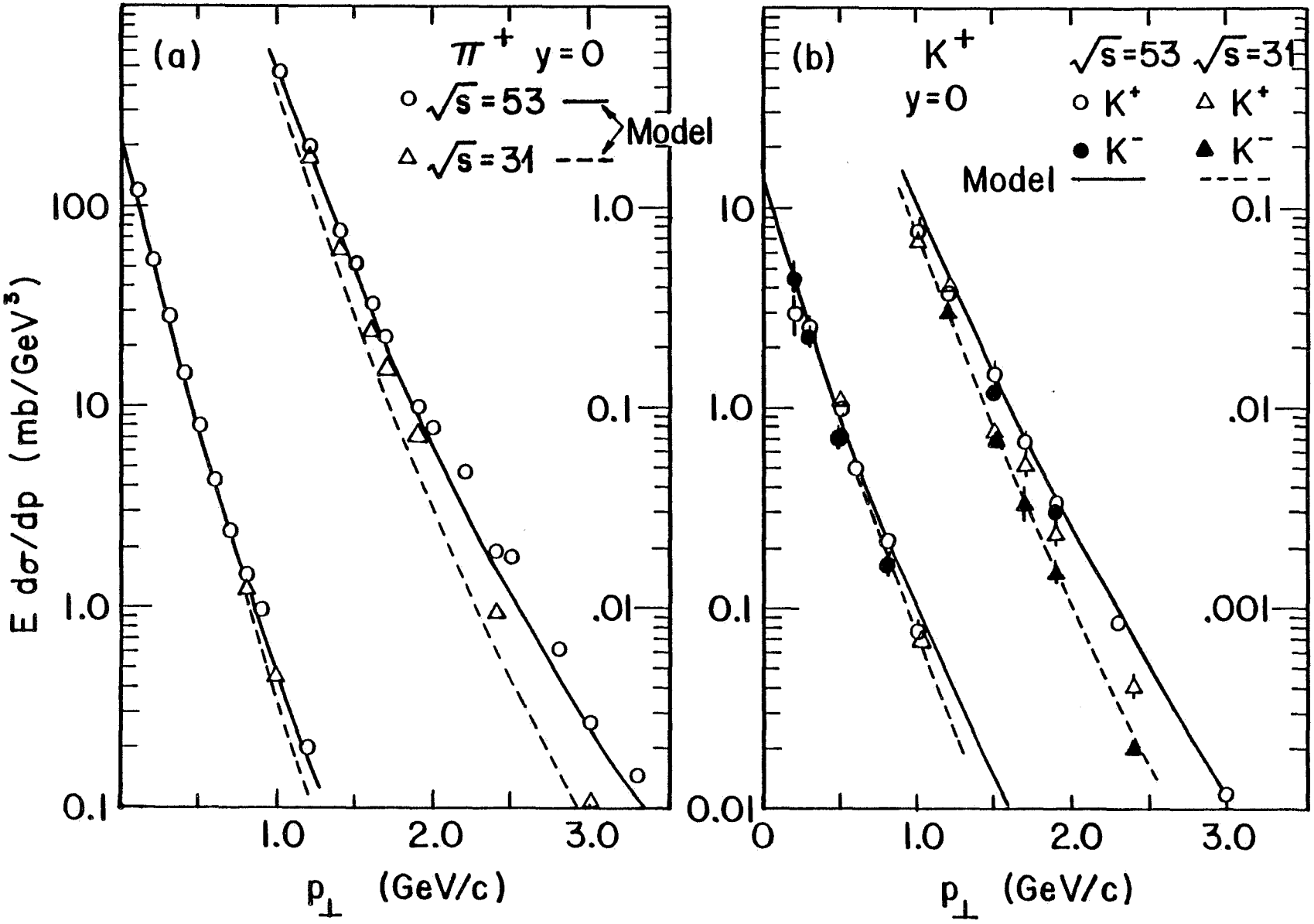
(a)
π⁺ y=0
○ √s=53
△ √s=31
Model
E dσ/dp (mb/GeV³)
100
10
1.0
0.1
1.0
.01
1.0
2.0
3.0
p⊥ (GeV/c)
(b)
K⁺
y=0
√s=53 √s=31
○ K⁺ △ K⁺
● K⁻ ▲ K⁻
Model
10
1.0
0.1
0.1
.01
.001
0.01
0
1.0
2.0
3.0
p⊥ (GeV/c)

Figure IV-1.

REFERENCES

1. N.Ushida et al., Phys.Rev.Lett. 45, 1049(1980); N.Ushida et al., Phys.Rev. Lett. 45, 1053(1980).
2. S.M.Errede, Ohio State University Ph.D. Thesis(in preparation).
3. M.J.Gutzwiller, Ohio State University Ph.D. Thesis(1981).
4. D.Andrews et al., Phys.Rev.Lett. 45, 219(1980); G.Finocchiaro et al., Phys. Rev.Lett. 45, 222(1980).
5. M.Kobayashi and K.Maskawa, Prog.Theor.Phys. 49, 652(1973).
6. See, e.g., John Ellis, "Status of Gauge Theories," CERN preprint Th-2701(1979); S.K.Nandi and K.Tanaka, Phys.Lett. 92B, 107(1980); J.A.Harvey, P.Ramond and D.B.Reiss, Phys.Lett. 92B, 309(1980).
7. H.Tye, "B Decays in the Weinberg-Salam Model," Cornell preprint CBX-81-9(1981).
8. E.H.Thorndike, "First Results on Bare b Physics," Proceedings of XX International Conference on High Energy Physics, Madison Wisconsin(1980), P.705; CLEO collaboration, "Charged and Neutral Kaon Production at the Upsilon 4s," CLNS 81-483(1981). It should be noted, however, that the large kaon signal at the upsilon 4S is not unambiguous evidence for dominant B→ charm(B.Gittelman, private communication), so that this upper limit on B lifetime is not rigorous until this important experimental question is settled.
9. V.Radeka and R.A.Boie, IEEE Trans.Nucl.Sci.27, 351(1980).
10. See, e.g., review by J.N.Marx in "Proceedings of Summer Institute on Particle Physics," SLAC Report No.239(1981), p.215.
11. S.L.Stone, et al., Nucl.Inst.and Meth. 151, 387(1978); See also Ref.14 .
12. We wish to thank J.Whitmore of Michigan State for providing us a tape of 360 GeV π^-p events from the 30-Inch bubble chamber. For 800 GeV design studies, these events were given an appropriate Lorentz boost, and were augmented by extra tracks generated by Monte Carlo to give the correct average multiplicity. Neutral pions(and their decay gammas) with the same p, p_t distribution as charged tracks were also generated by Monte Carlo for each bubble chamber event.
13. The EGS calculations were performed with lead rather than tungsten because lead parameters were "hard wired" into the program. Tungsten radiators will give even less shower spread than lead.
14. See, e.g., review by H.A.Gordon and S.D.Smith in "Proceedings of Summer Institute on Particle Physics," SLAC Report No.239(1981), p.241.
15. T.A.Gabriel and W.Schmidt, Nucl.Instr. and Meth. 134, 271(1978).
16. A.Zichichi, in talk presented at Physics in Collision Conference, Blacksburg, Va.(May, 1981).
17. The measured interaction mean free path for 200 GeV protons in emulsion is 35.5 ± 0.8 cm (J.Hebert, private communication). The MFP for high energy pions will be larger by a factor of about 1.5.
18. B.Alper et al., Nucl.Phys. B100, 237(1975)
19. J.Kirkby, "Review of e^+e^- Reactions in the Energy Range 3 to 9 GeV," in Proceedings of the International Symposium on Lepton and Photon Interactions, Fermilab(1979) p.107.
20. H.Winzeler, Nucl.Phys.69, 661(1965).

References continued

21. S.R.Amendolia et al., "A Multielectrode Silicon Detector for High Energy Physics Experiments," PISA 80-2(1980); Nucl.Inst. and Meth. 176, 457(1980).

22. E.H.M.Heijne et al., "A Silicon Surface Barrier Microstrip Detector Designed for High Energy Physics," CERN/EF/BEAM 80-6(1980); Nucl.Instr. and Meth. 178, 331(1980).

23. J.B.A.England et al., "Capacitative Charge Division Read-Out with a Silicon Strip Detector," CERN-EP/80-218(1980).

FERMILAB E-653

"MEASURING CHARM & B DECAYS VIA HADRONIC PRODUCTION IN A TAGGED EMULSION SPECTROMETER"

1. OBTAIN 200 B^0, B^+ DECAYS (BASED ON A 50 nb σ)
   IS THE b-QUARK NORMAL?
   ONLY EMULSION SEES DOWN TO 10^{-15} SECONDS.
2. LOCATE ~ 15,000 CHARM DECAYS:
   i. $D^0 \leftrightarrow \bar{D}^0$ MIXING:
   $\begin{cases} \omega/\Gamma < .002 \text{ (90\% CL)} \\ \Delta m/\lambda < .05 \end{cases}$
   ii. $F \to \tau \to X$ (AS IMPORTANT AS BEAM DUMP EXPTS IN DETERMINING EXISTENCE OF ν_τ)
   iii. NEW B.R., GROUND & EXCITED STATES TAGGED BY DECAY LENGTH.

AICHI UNIVERSITY OF EDUCATION:
USHIDA

UNIVERSITY OF CALIFORNIA AT DAVIS:
KO, LANDER, MOKTARANI,
RUMIANSIV, YAGER

CARNEGIE-MELLON UNIVERSITY:
EDELSTEIN, FORSYTH, GAMARNIK, LIPTON,
NICHOLS, RUSS, WINKLER

UNIVERSITY OF GIFU: TASAKA

KOBE UNIVERSITY: FUJIOKA,
FUKUSHIMA, HARA, TAKAHASHI,
TSUZUKI, YOKOYAMA

NAGOYA UNIVERSITY: CHIBA, HOSHINO,
KAWA, MIYANISHI, NAKAMURA, NIU, NIWA,
OHASHI, SHIBUYA, TORII, YAMAKAWA,
YANIGASAWA

OHIO STATE UNIVERSITY: DUNLEA, GAUTHIER,
KALEN, KURAMATA, OLEYNIK, REAY,
REIBEL, SIDWELL, STANTON

OKAYAMA UNIVERSITY: MORIYAMA, SHIBATA

UNIVERSITY OF OKLAHOMA: BOL,
KALBFLEISCH, SCUBIC, WHITE, WILLIS

OSAKA CITY UNIVERSITY: KUSUMOTO, NOGUCHI,
OKUSAWA, TERANAKA

SCI. EDUC. CTR. OF OSAKA PREF.: OKABE, YOKOTA

TOHO UNIVERSITY: KAZUNO

YOKOHAMA NATIONAL UNIVERSITY: MAEDA

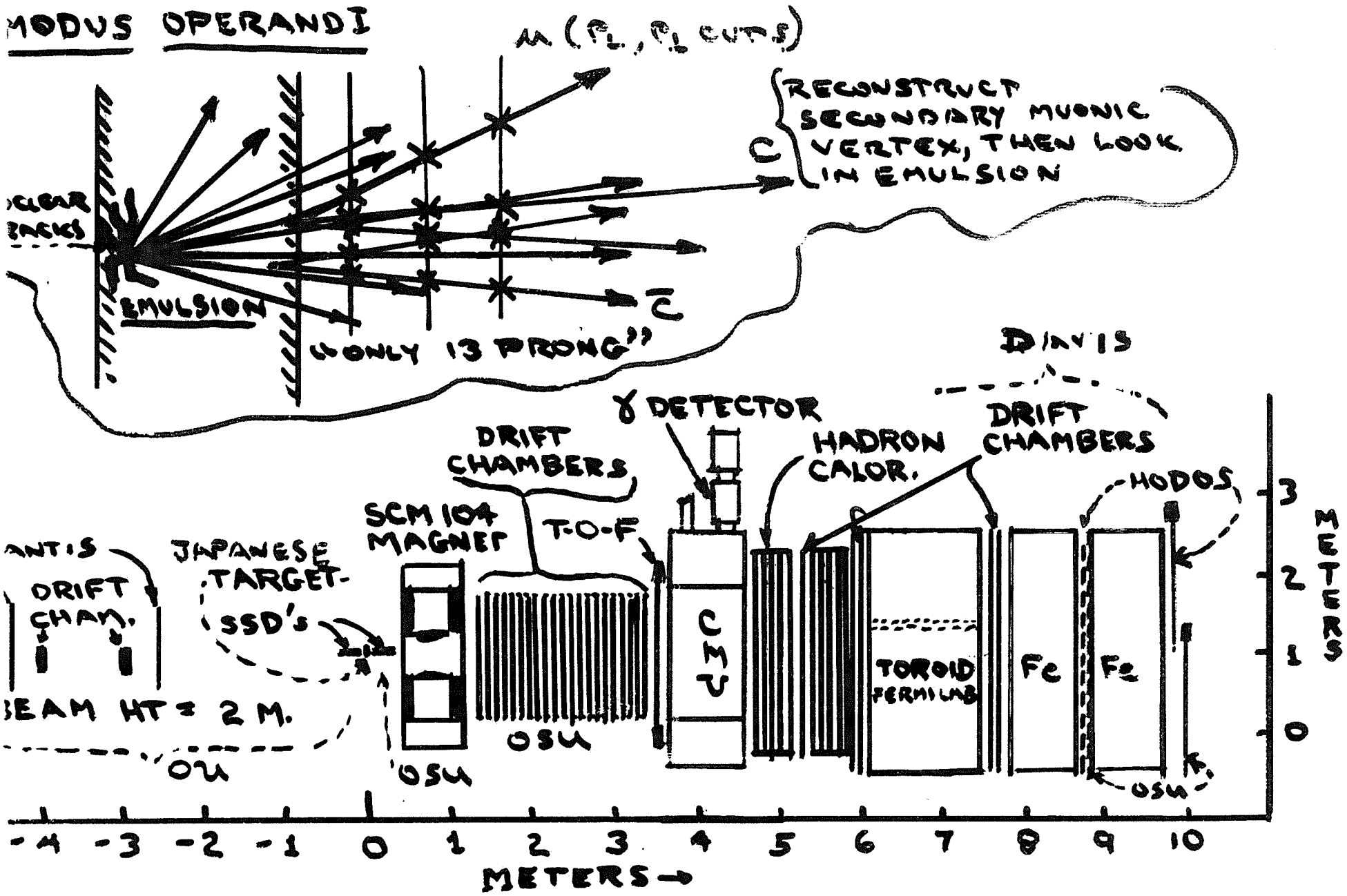

E-653 ELEVATION VIEW
(IN NEW N3 CHARGED BEAM)

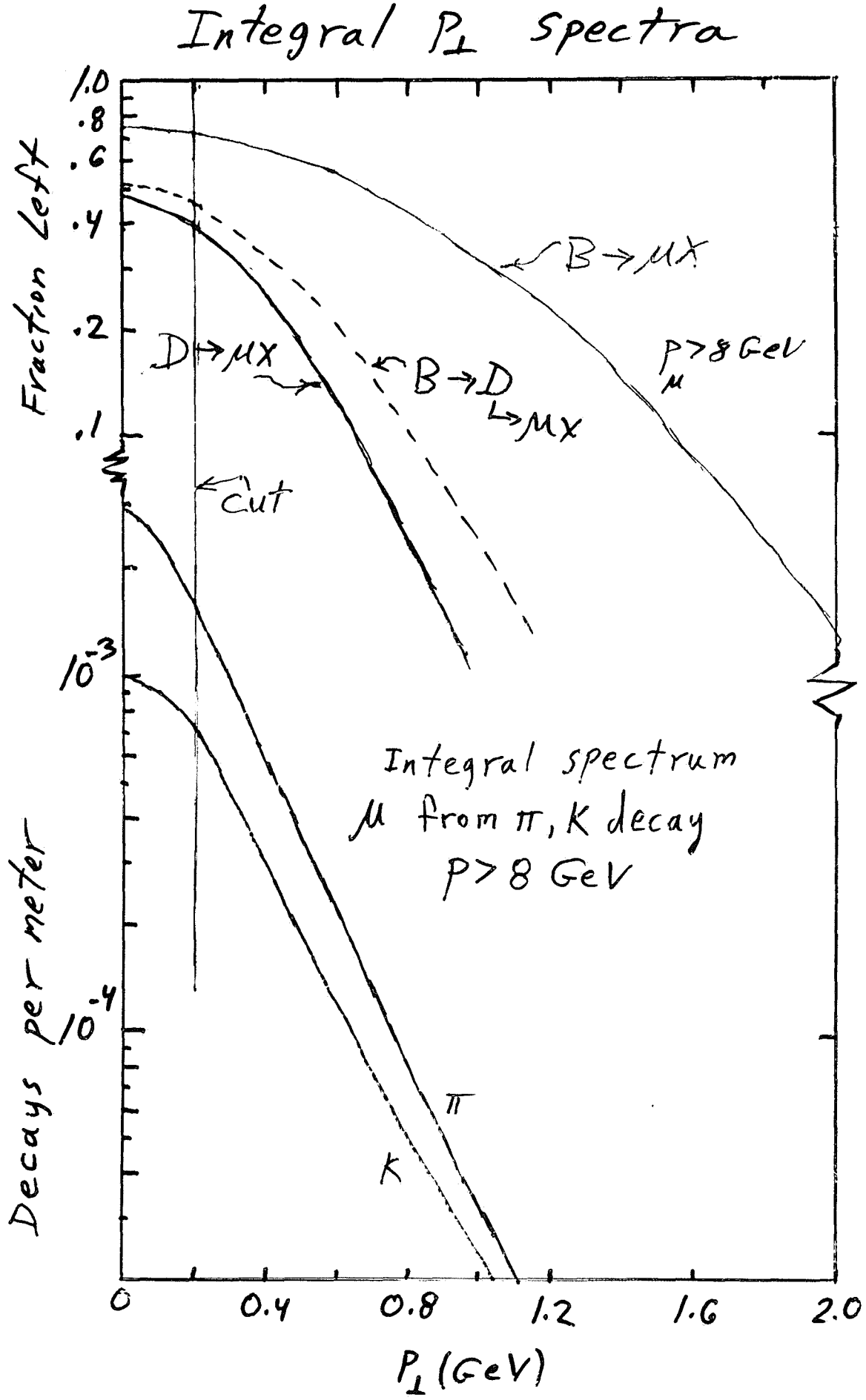
Integral $P_\perp$ Spectra
Fraction Left
1.0
.8
.6
.4
.2
.1
10^{-3}
10^{-4}
$B \to \mu X$
$P_\mu > 8$ GeV
$D \to \mu X$
$B \to D \to \mu X$
cut
Integral spectrum
μ from π, K decay
$P > 8$ GeV
π
K
Decays per meter
0
0.4
0.8
1.2
1.6
2.0
$P_\perp$ (GeV)

YIELD VERSUS CUTS

PRESENT IN 100 ℓ OF EMULSION:

TRACK DENSITY = $10^3/mm^2$

2.8×10^8 INTERACTIONS

5.8×10^5 { CHARM PAIRS
(25 μbn

1,150 B PAIRS (50 nb)

PRESENT ON TAPE:

MUON ($P_L > 8$ GeV/c, $P_T > 0.2$)

(x 0.01)	2.8×10^6	INTERACTIONS
(x 0.088)	3.8×10^4	CHARM PAIRS
(0.25)	288	B PAIRS

AFTER OFFLINE

BACKGROUND	7×10^4
CHARM	1.9×10^4
B → C	90
B → ALL	200

AFTER EMULSION SCAN:

CHARM	1.7×10^4
B → C	80
B → ALL	? ~ 180

COMING ATTRACTIONS

1) SOLID-STATE MICROSTRIP DETECTORS:
G. KALBFLEISCH (U. OF OKLAHOMA)

2) EMULSION:
K. NIU (NAGOYA U.)

3) MUON DETECTION:
P. YAGER (U of CAL, DAVIS)

4) ANALYSIS:
N. STANTON (OHIO STATE U)

5) SPECTROMETER:
R. LIPTON (CARNEGIE-MELLON U.)

6) DATA ACQUISITION ELECTRONICS:
C. RUSH (OHIO STATE U.)

7) SCHEDULE:
R. EDELSTEIN (CARNEGIE-MELLON U.)

E-653 REQUIRES FINDING MANY EVENTS IN EMULSION

1) E531 ⇒ HIGH EFFICIENCY

2) E653 NEEDS HIGHER STATISTICS
⇒ SMALLER SCAN VOLUME (δV)

(BILL REAY 1980) SSD MICROSTRIPES
$\delta V \rightarrow 10^{-3}$!

(3) PROFESSOR NIU WILL DISCUSS >10 X EMULSION SCANNING & MEASURING !)

MAJOR EFFORT — SSD PROTOTYPING

1 cm^2 SQUARE — LBL (81-82) FULLY TESTED

8 cm^2 RECTANGULAR + CENTRONICS (82)

LAMPE TESTING IN PROGRESS

NEXT

SQ. 25 cm^2 UDT# (OSU BENCH TESTING) & CENTRONICS (~ 2 MOS.)

FINAL ~35 cm^2 # 12 SIDED POLYGONS (ORDER WINTER).

+ USE "BEAM SSD's"

" " VTX SSD's" (N. STANTON ...)

TEST GOALS: 1) Q - COLLECTION

2) TRACK POINT RESOLUTION

3) VTX. RECONST. "

"M5" BEAM TEST (FNAL)

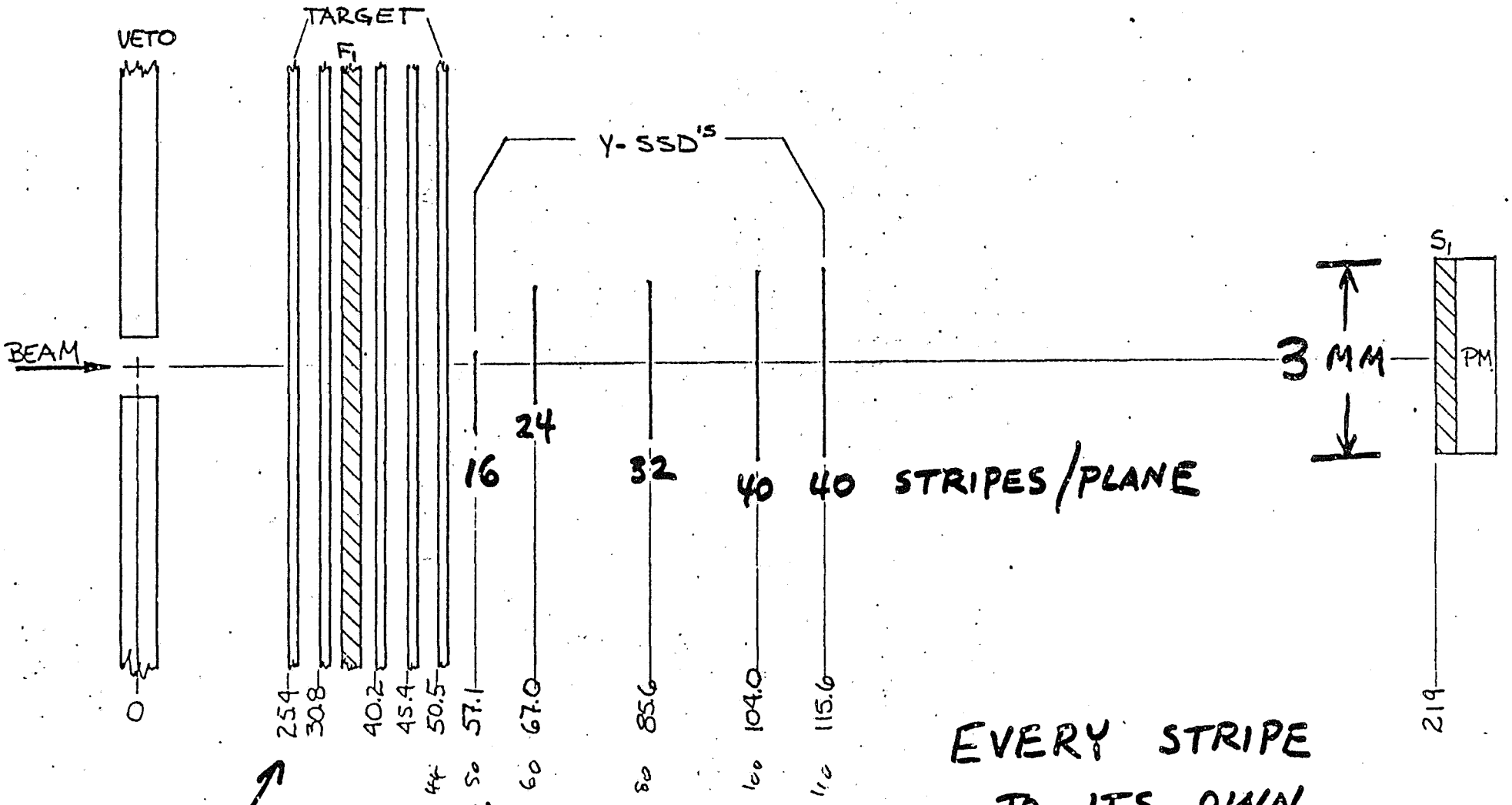

5 - 1/16" (1.6 MM) THICK BRASS

EVERY STRIPE TO ITS OWN AMPLIFIER - & ADC. (156 TOTAL).

mmx10 mmx1 SCALE

1) Q

46 GeV/c π^-

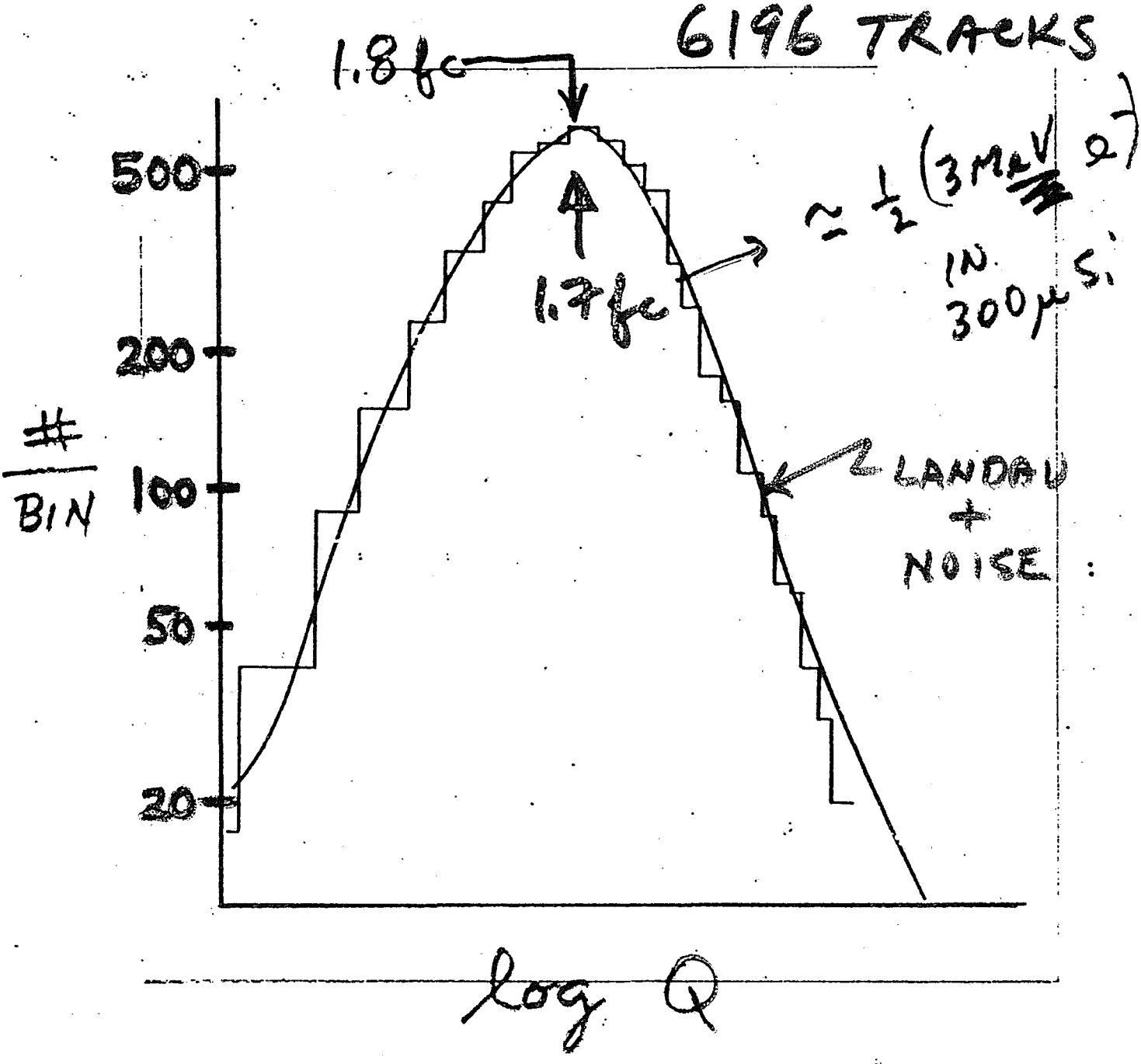

PLANE 4

(LAMPF)

650 MeV/c PROTONS

3905 TRACKS

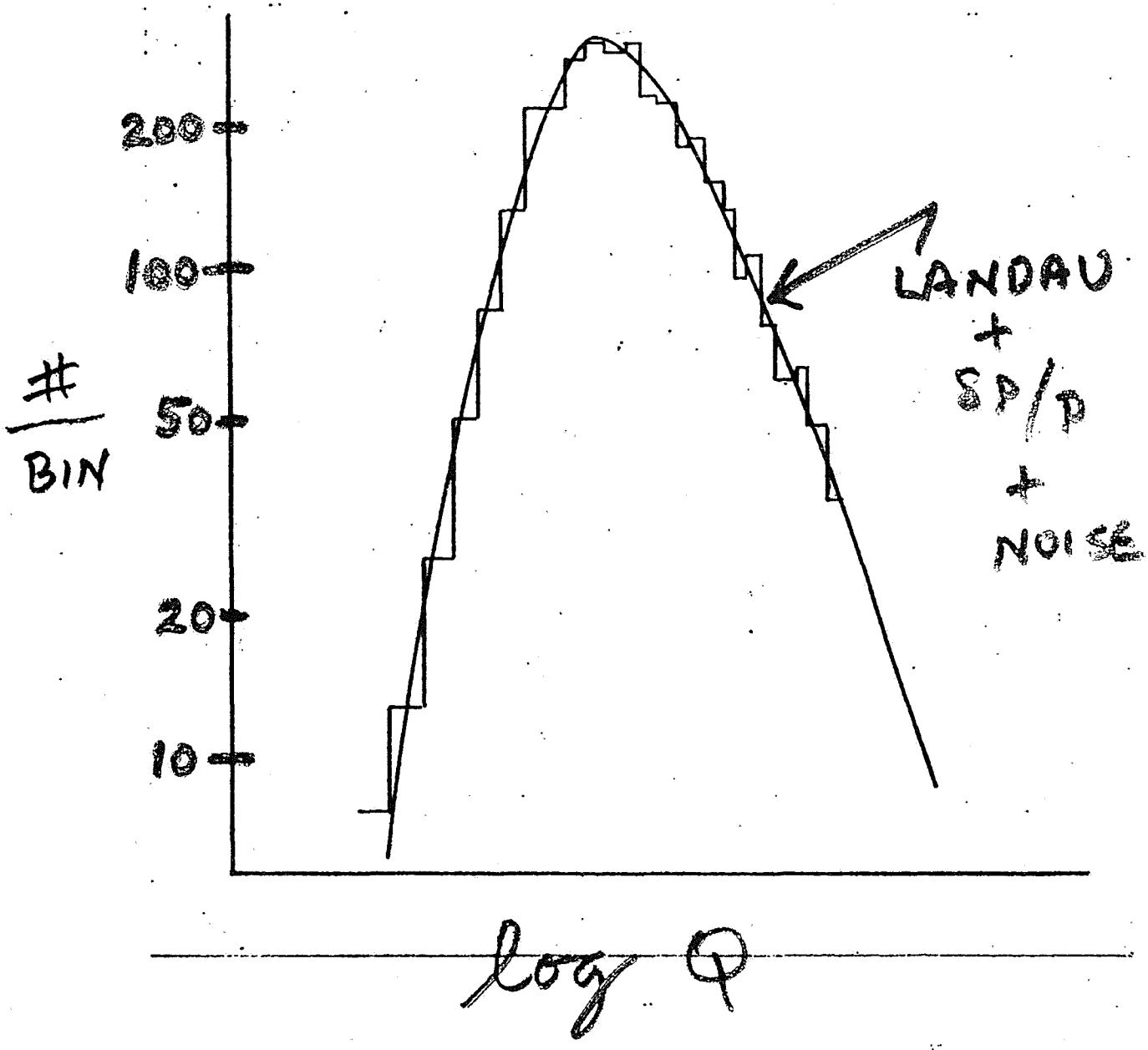

3905

PLANE 4

$\frac{650\ p}{550\ \pi} = 2.7 \pm 0.2$ VS 2.6 (TH.)

$\chi^2 = 12 \sum_i \delta_i^2$ (TH: $\sigma = \frac{\text{PITCH}}{\sqrt{12}}$)

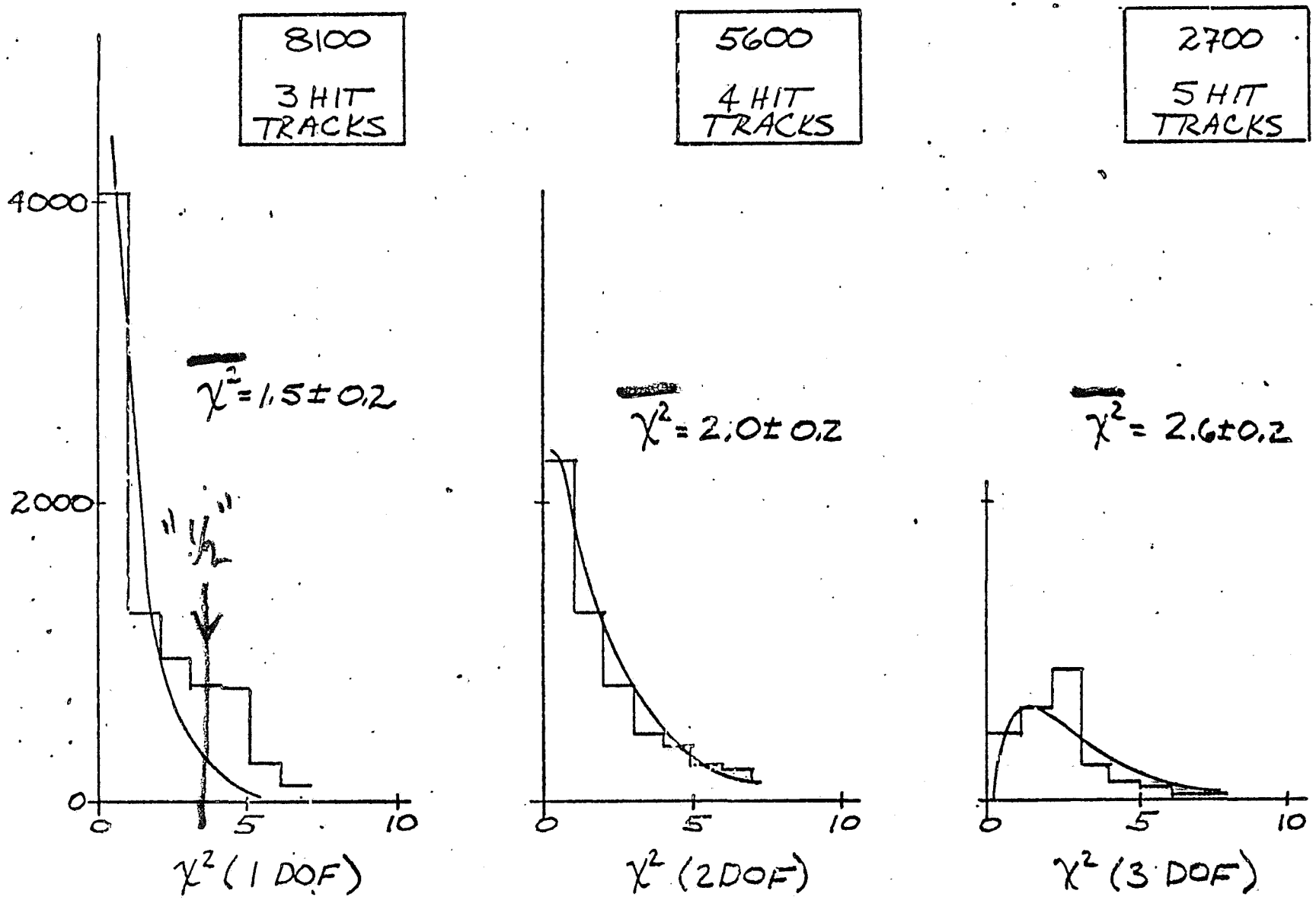

2) TRK-PT. RESOLUTION

$\langle \chi^2/\text{DOF} \rangle = 1.2 \pm 0.2 \Rightarrow$ OK TO (10 ±10,

INCLUDING RESIDUAL MISALIG

3) VIX RECONSTRUCTION

TRANSVERSE

VETO '137 SHADOW

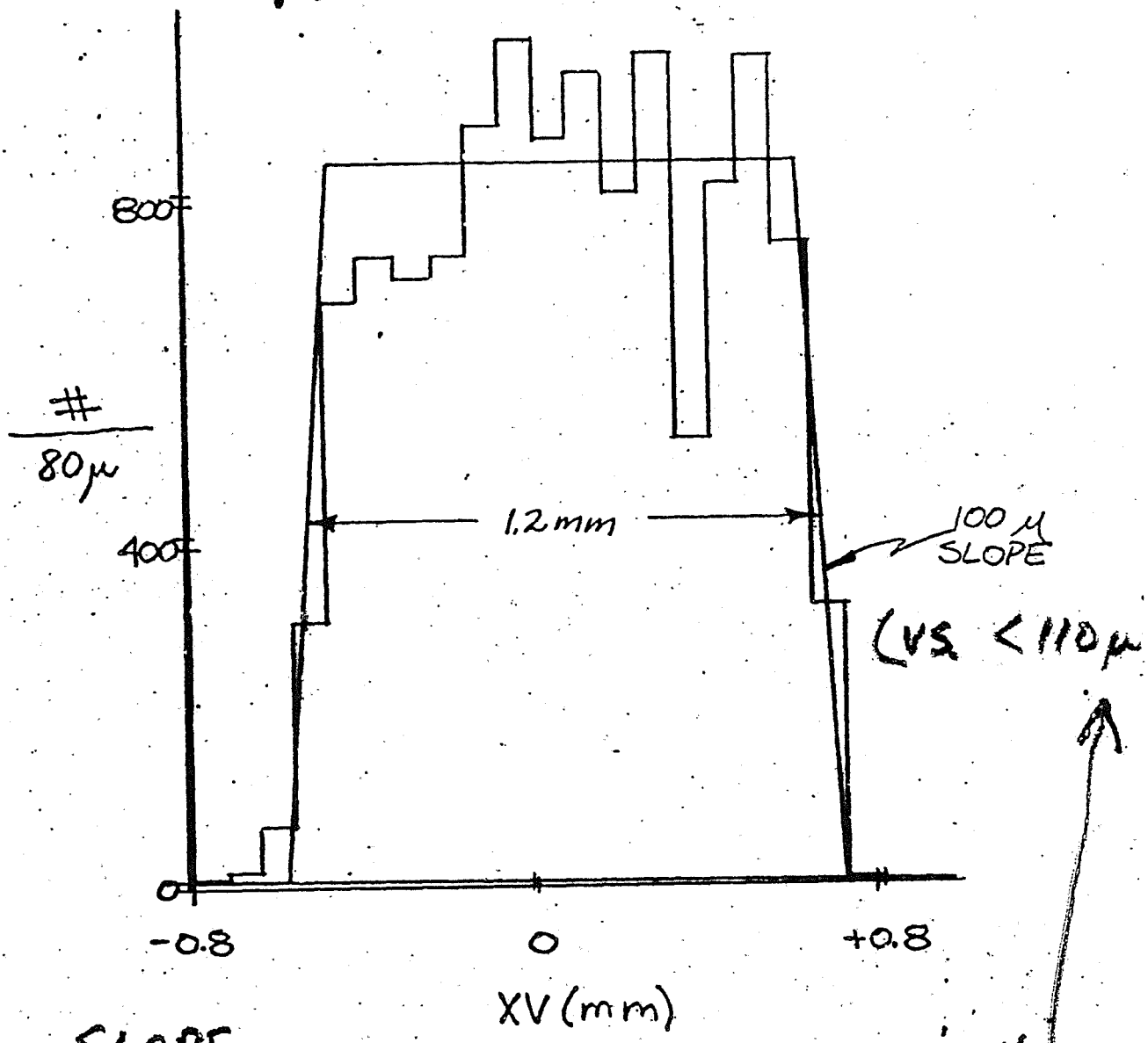

SLOPE

BEAM DIVERG.	<80μ
VETO ALIGN.	<60μ
M.S. BRASS	~20μ
SSD FIT ERRORS	~30μ

EVENT NUMBER = 190 FILE = 46

NASH 71 80

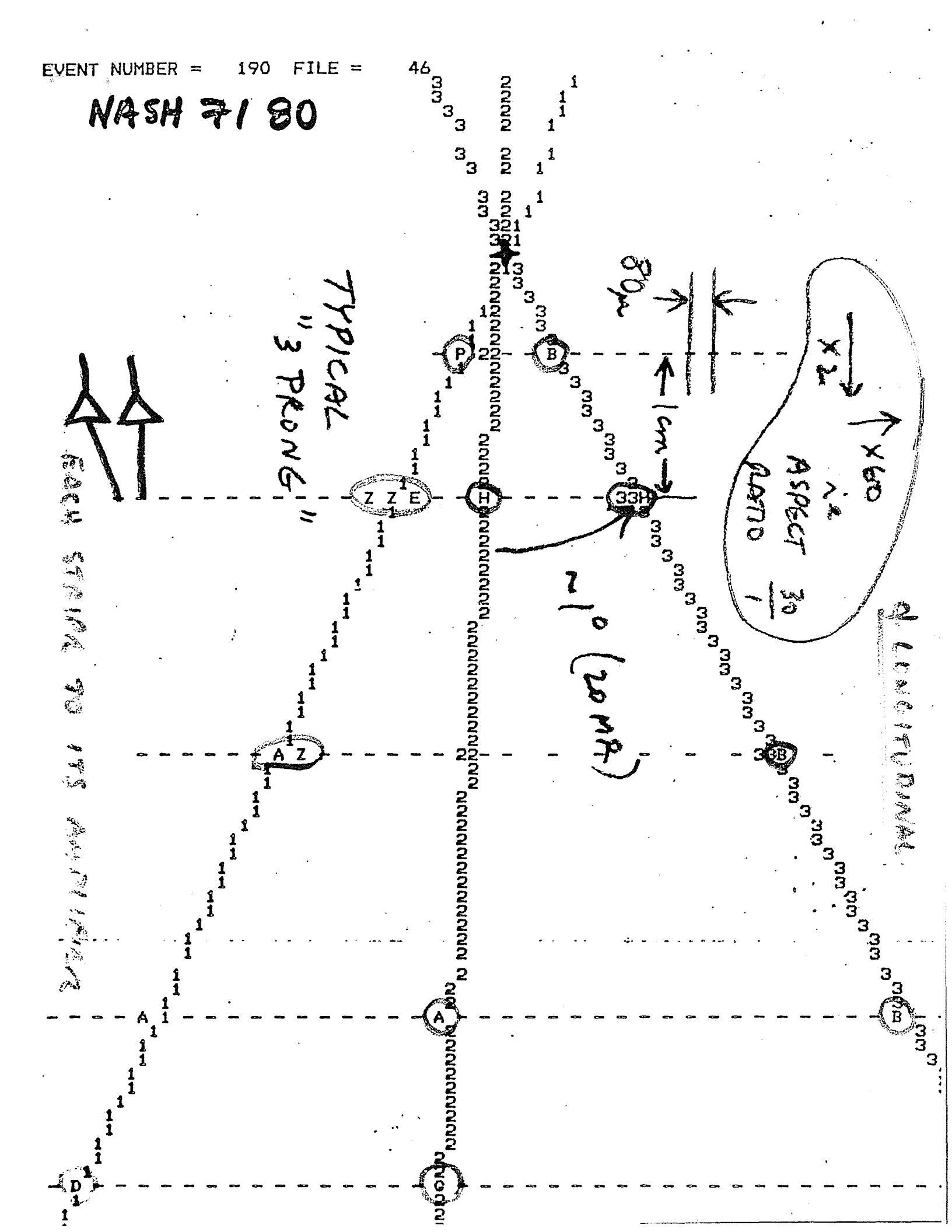

THE δZ_{VERTEX} (RMS)

(500μ FOR $\theta_{12} = 50$ mr)

WILL SCALE LINEARLY

WITH 1) PITCH ($80\mu \rightarrow 40\mu$)

2) $1/\theta_{12}$ (50 mr $\rightarrow$ 70 mr B,C 1/2)

3) Δz TO EMULSION (SAME)

± 2

$$\frac{500}{2\sqrt{2}} \rightarrow$$

$\pm 200\mu$
AS PER THE PROPOSAL

(END "SINGLE STRIPE")

OHIO STATE (REAY)

SPRING 1982

CENTRONICS + 2 CHANNELS AMPLIFIER

σ_{A+D} ~ .05 fc (300 ELECTRONS)

$\Longrightarrow S/N > \frac{50}{1}$!!

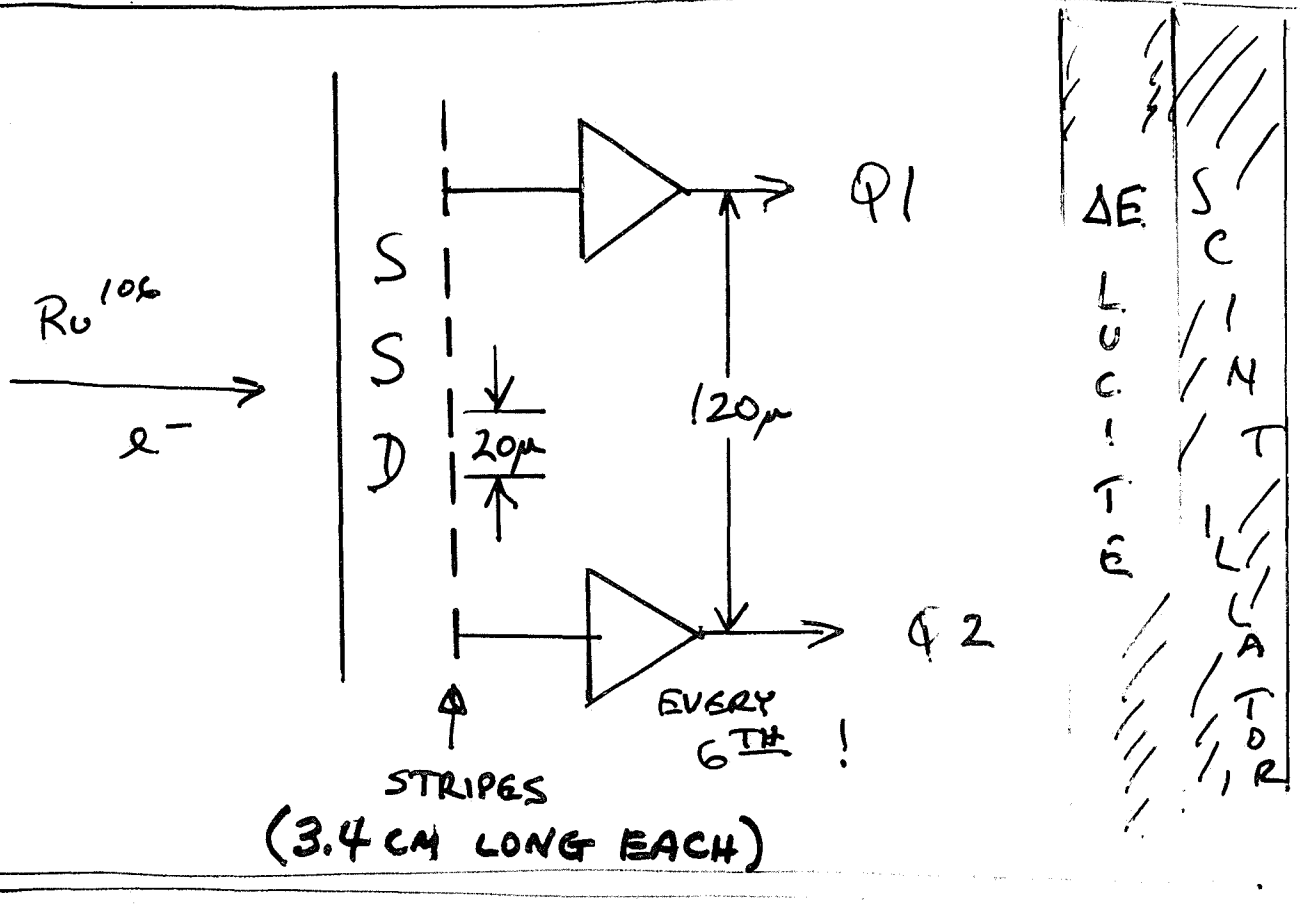

TRIGGER: $\{ ① = (Q1 > T1) \cdot S \}$ $\{ ② = (Q2 > T2) \cdot S \}$ → ADC

$\Sigma_1 = ① + ②$ → TOTAL Q (SOFTWARE!)

CORRELATION: $(Q1 + Q2)$ vs $(Q1 - Q2)$

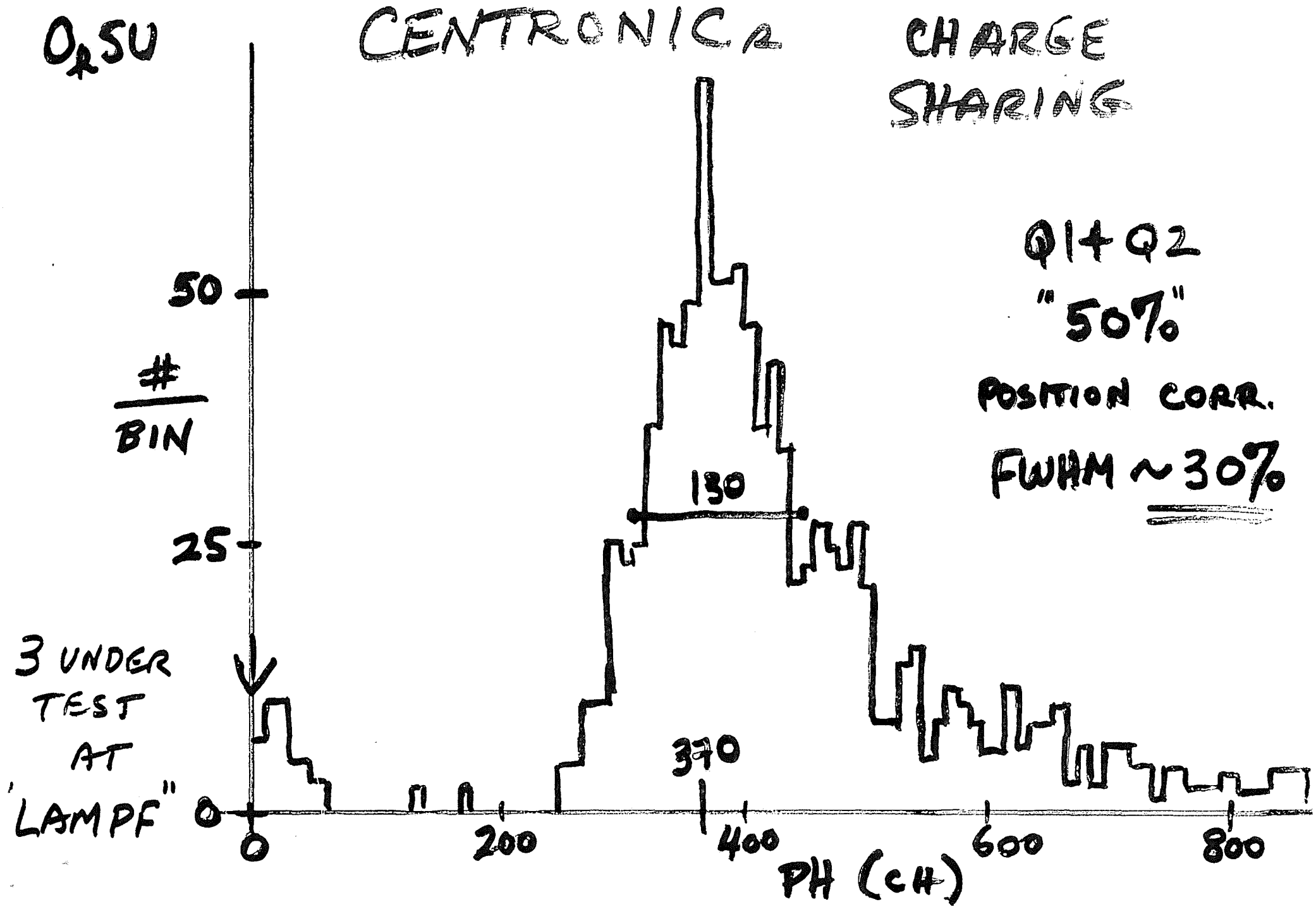
OSU
CENTRONICS
CHARGE SHARING
Q1+Q2
"50%"
POSITION CORR.
FWHM ~ 30%
50
#/BIN
25
130
3 UNDER TEST AT "LAMPF"
0
370
0
200
400
600
800
PH (CH)

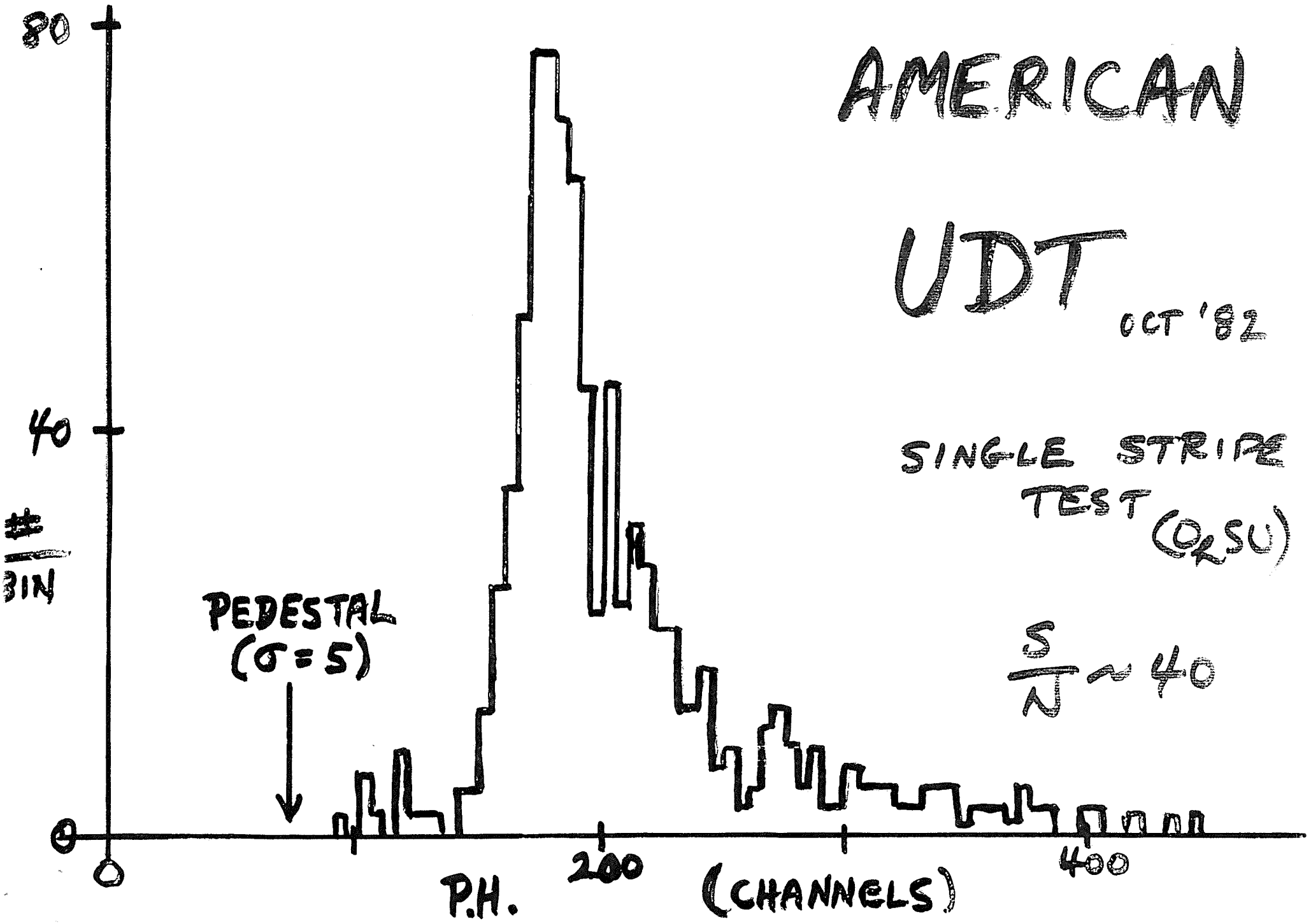
80
40
0
/ BIN
PEDESTAL
(σ = 5)
200
400
P.H. (CHANNELS)
AMERICAN
UDT
OCT '82
SINGLE STRIPE
TEST (QRSU)
S/N ~ 40

WE HAVE GAINED

NEEDED EXPERIENCE

SSD MICROSTRIPES

LOW NOISE AMPLIFIERS

CHARGE COLLECTION / SHARING

& THE WHOLE "GAMUT" OF

ASSOCIATED SOFTWARE

(& STILL RUNNING FAST !)

E653 Emulsion

	E531 ν-beam		E653 hadron-beam	
	1st run	2nd run		
Emulsion	23 ℓ	32 ℓ	100 ℓ	$10^5/cm^2$
Interaction	1200	3000	$\sim 10^{8\sim9}$	need good selection
Charm	50	150	$\sim 10^4$	
Beauty			$\sim 10^2$	
Charm/all	$\sim \frac{1}{20}$		$\sim \frac{1}{1000}$	
Analysing power	$5\cdot10^2$ evts/y	10^3 evts/y	$* 10^4$ evts/y	need at least ×10 grade up
New Tech.	Track Follow in Vertical Emulsion Semi auto. scan-measure Syst.		Mini-plate Matrix Full auto scan-measure Syst. Multi Track Measurement.	

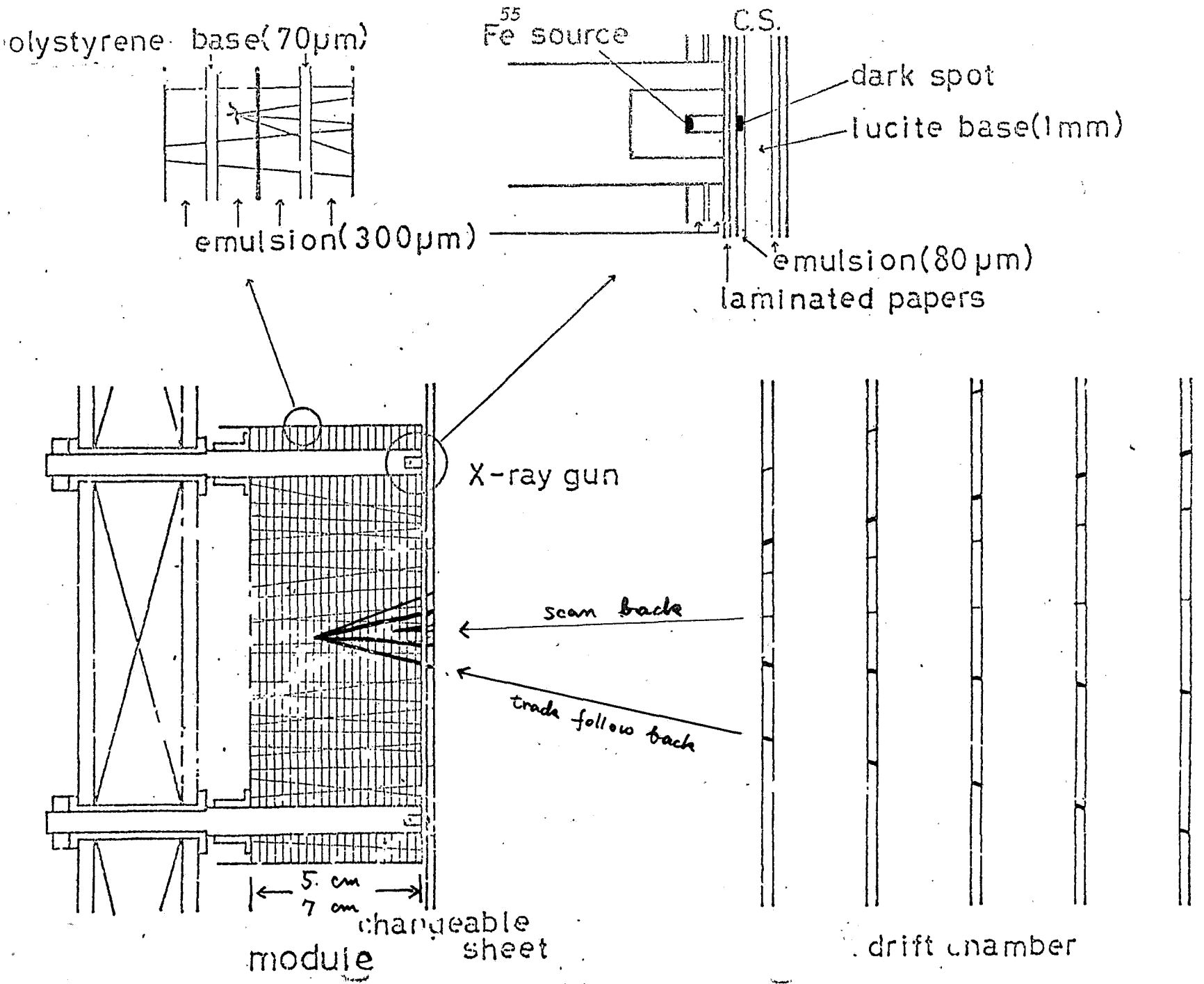
olystyrene base(70μm)
emulsion(300μm)
55Fe source
C.S.
dark spot
lucite base(1mm)
emulsion(80μm)
laminated papers
X-ray gun
scan back
track follow back
5 cm
7 cm
changeable sheet
module
drift chamber

Fig. 11

NGY-574 529-3013 Z-PROJECTION

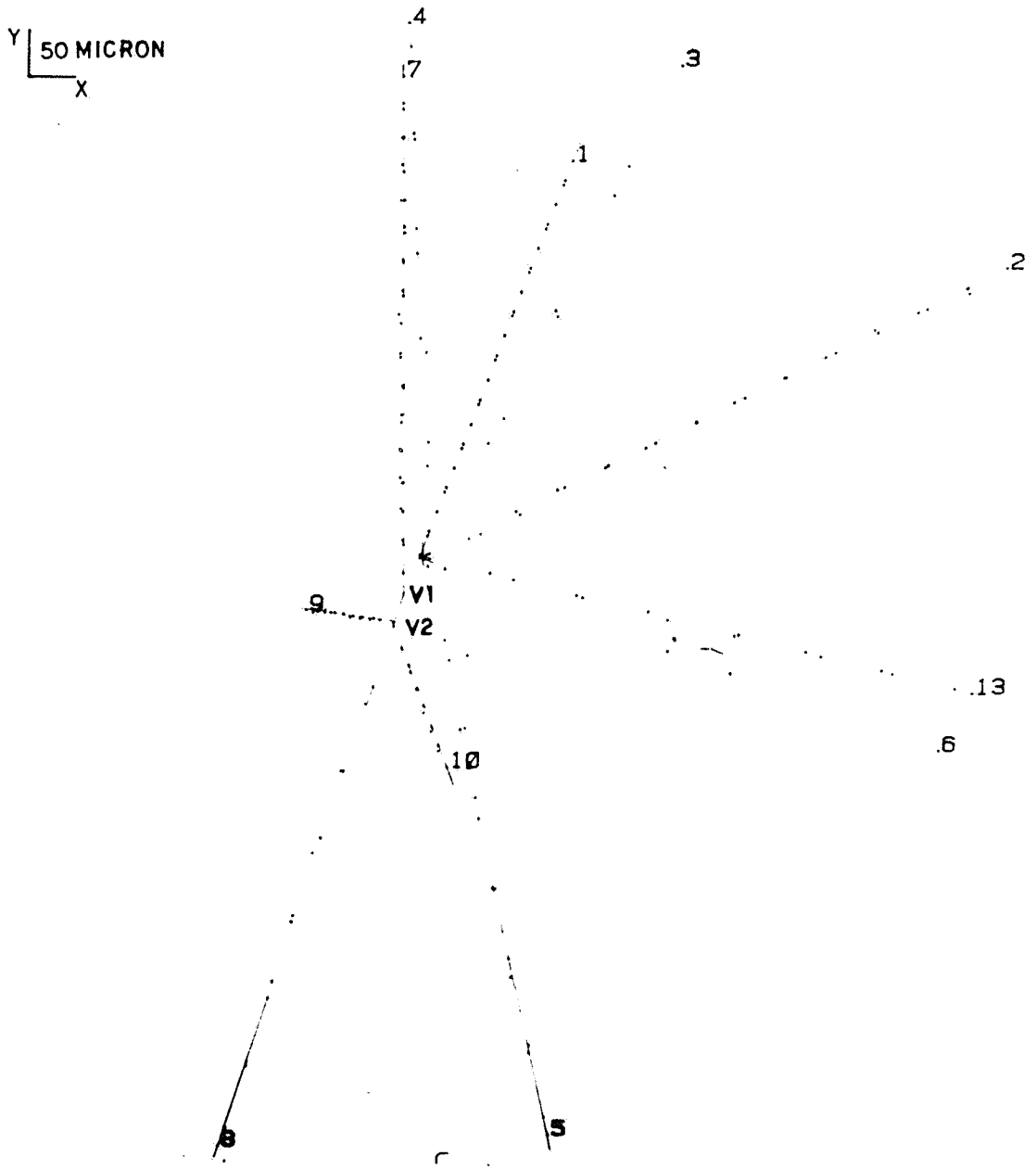

NCY-574 529-3013 X-PROJECTION

200 MICRON
600 MICRON

Y-PROJECTION

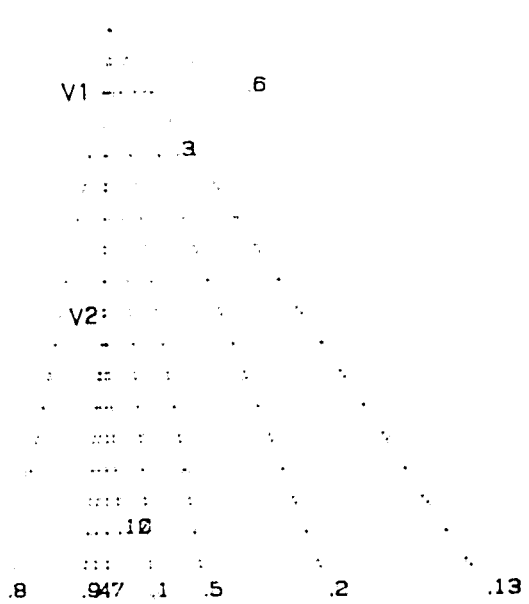

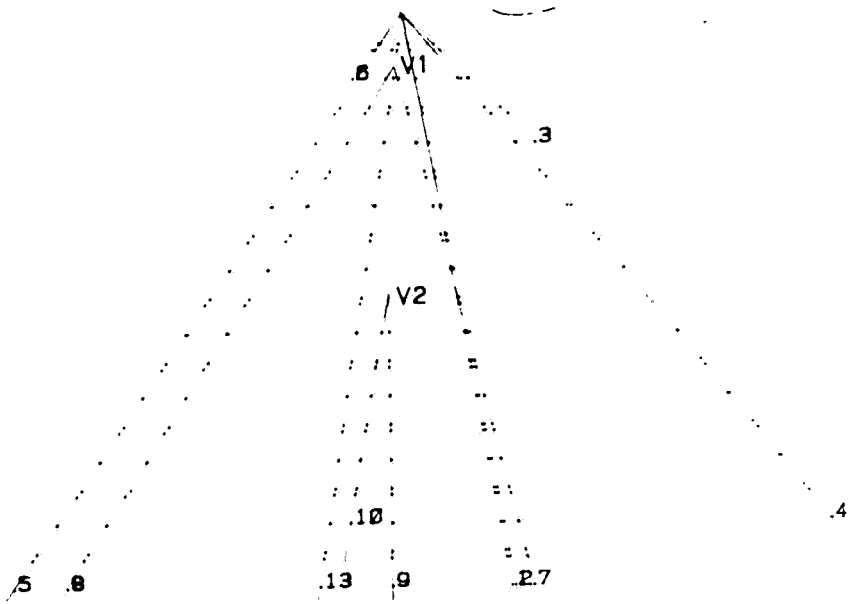

NSY = 1071

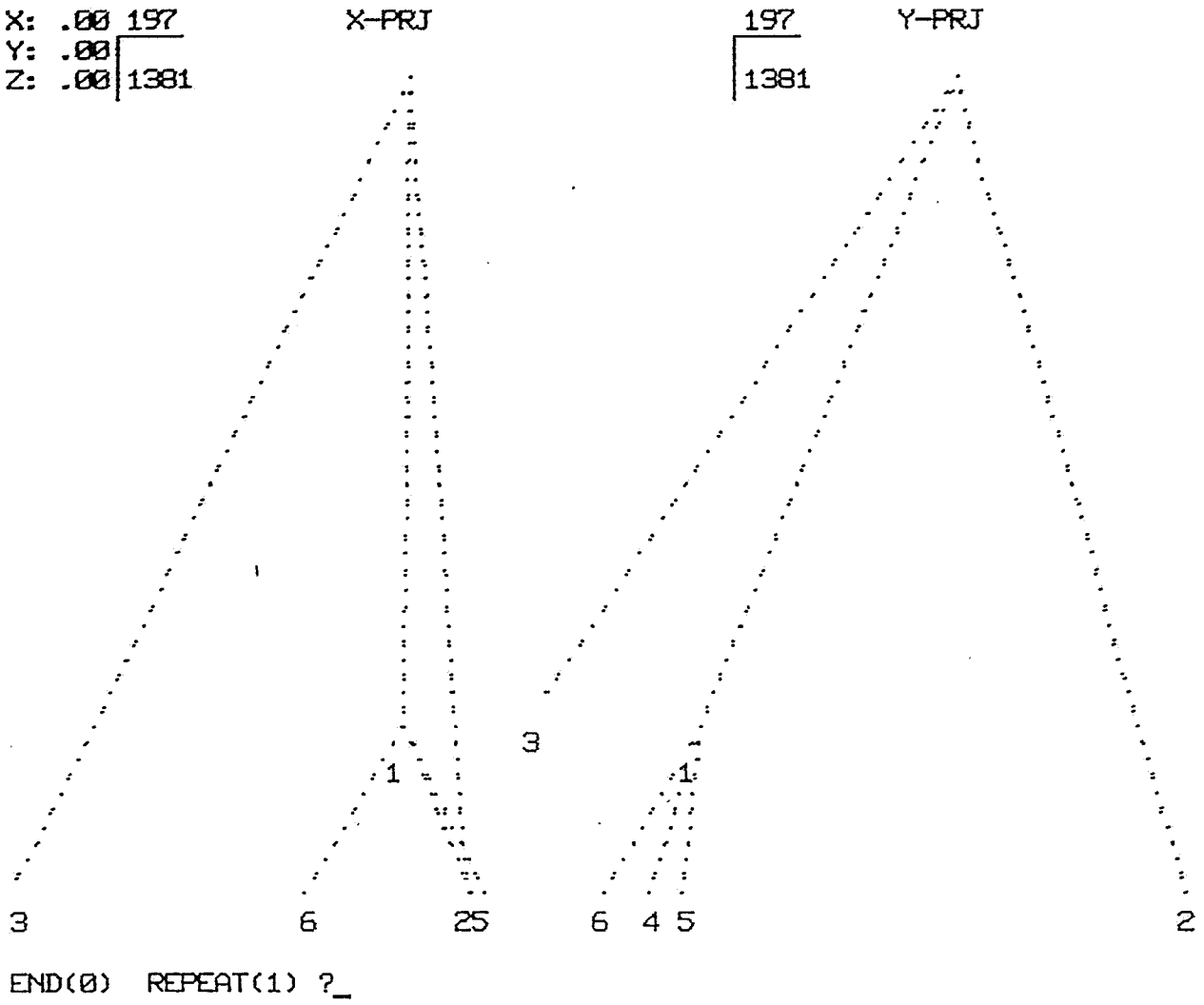

END(0) REPEAT(1) ?_

How to get grade up of $\times 10$

	E 531 Semi auto	E 653 Full auto
Location of events Decay scan to 1mm	90 min	5 min
Follow down, Angle measure Charged Decay Search to 6mm	130 min	12 min
Scan back Neutral Decay Search $0 \sim 5$ cm $0 \sim 2$ cm	60 min	10 min
	280 min/evt.	27 min/evt.

Measurable events / Machine year: 500 | 5000 (25000 Location only)

Eff. No. of Machine: 2 | 1 (+2 requested) (+ ≥10 Semi auto)

Much better prediction of interaction vertex by N.S.D. $0.1 \sim 1\,mm^3$

New Emulsion Techniques

Miniplate Matrix

Track Following Speed a few sec/plate

Full auto Scan-measuring System with Multi Track measurement

(1) Mother chamber

24 x 24 cm^2, 25 plates,

Net ~1 liter (4 kg),

330 μm emulsion on both side of 70 μm film base.

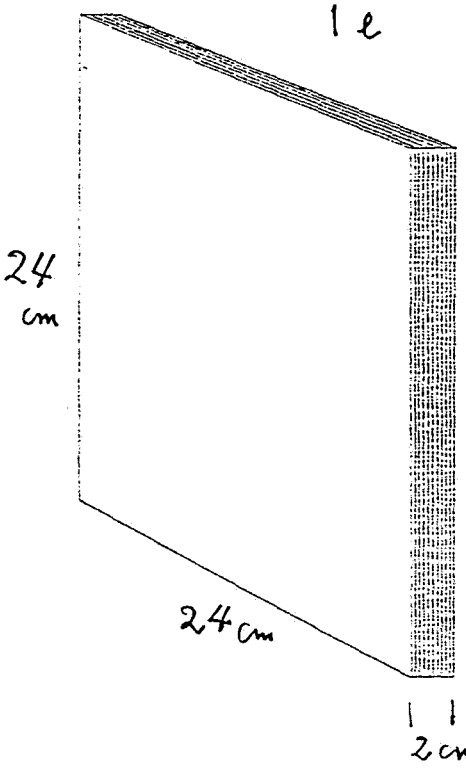

(2) Heavy ion exposure

Ne, Si, or Fe,

≳1 GeV/c/nucleon,

1~0.5/cm^2.

About the role of the CR39 plates see the Note (p.2).

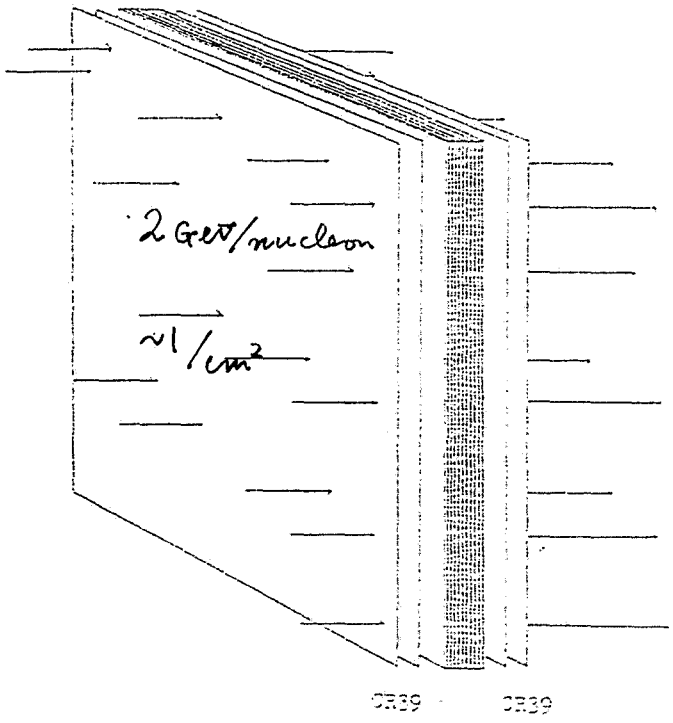

(3) Mini-module

One mother chamber is cut into 8 x 8 = 64 mini-modules.

Each mini-module has 25 mini-plates with the measures of 3 cm x 3 cm.

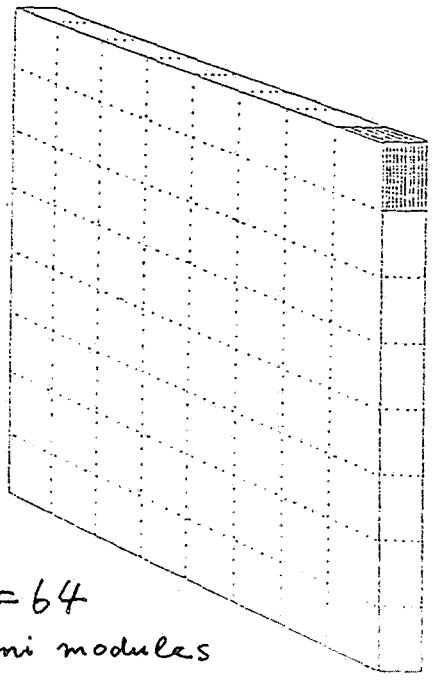

(4) Matrix of 25 mini-plates from the same mini-module

15 cm x 15 cm,
(Supporting plate = 16 cm x 16 cm)

Each mini-plate has 3~6 fiducial heavy ion tracks with the same pattern.

Stroke of the measuring stage should be 15 cm x 15 cm.
Driving speed to the next mini-plate is ~3 sec.

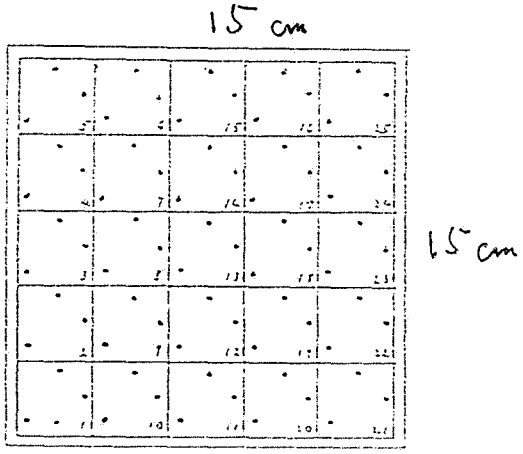

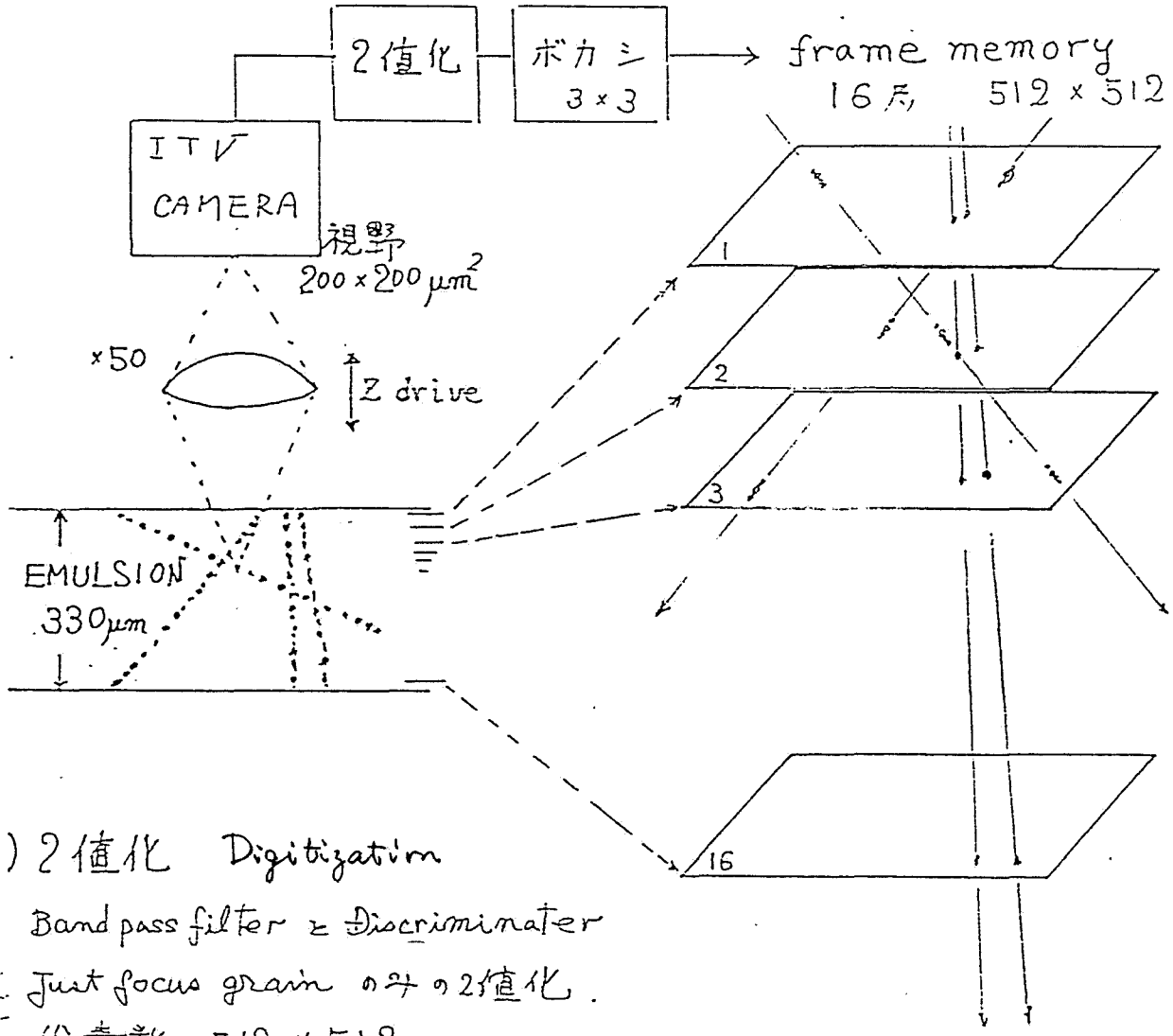

(1) 2値化 Digitizatim

Band pass filter と Discriminater

Just focus grain のみの2値化.

絵素数 512×512.

(2) ボカシ

Hit した各々の 2 値化絵素を 3×3 にぼかす.

(3) Z (objective lens) を変えつつ Recording.
30μm step ごとに 16 枚の絵を Pictures in 16 frame memories に 1 sec
ストアーしていく。 64K DRAM 4ケ (200 nsec)

(4) 16片の絵の同時よみ出し.
TV 方式で 16片同時に (相対的な frame の位置は programable) よみ出して. 飛跡自動認識ロジックに流す.

Processing of 16 frames → Select tracks with 16 different angles.

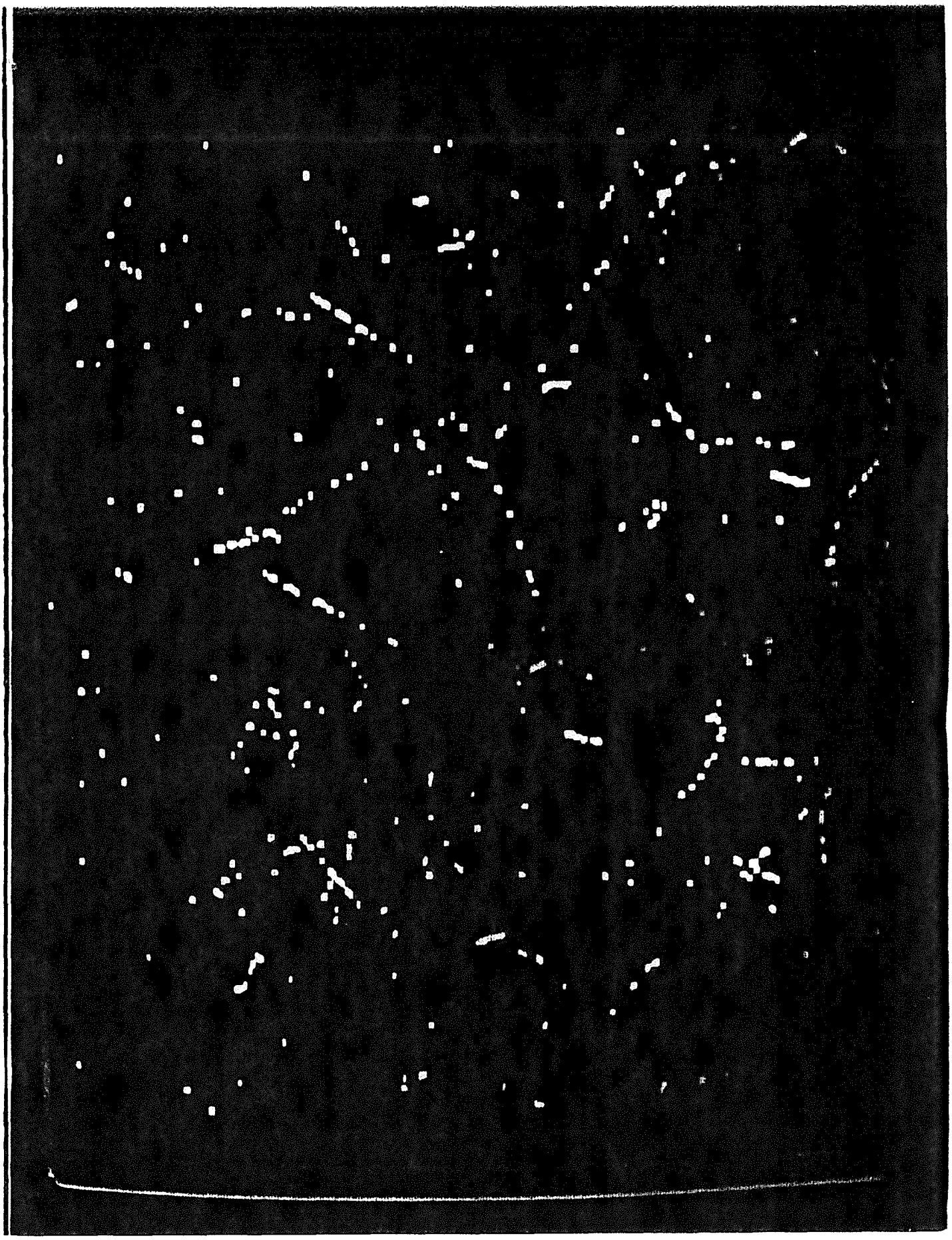

Emulsion Works

1) Production of emulsion modules — FNAL
   pouring, assembling
   (E531 32 ℓ 1 month)

2) Exposure to hadron beam — FNAL
   Target Mover

3) Exposure to heavy ion beam — LBL

4) Processing of emulsion — FNAL
   Processing Facility

5) Heavy ion fiducial measurement
6) Mini plate processing and Calibration
7) Scanning and analysis

} Japan

New Machine(s)

V + n × Semi auto. machines.
n ~ 10

H 3 Semi auto machines
+ 10 Manuals

eam size 3 mm × 3 mm $10^4/cm^2$

mulsion 240 mm × 240 mm

to get $10^5/cm^2$ need Luster Exposure

~ 3 mm/sec

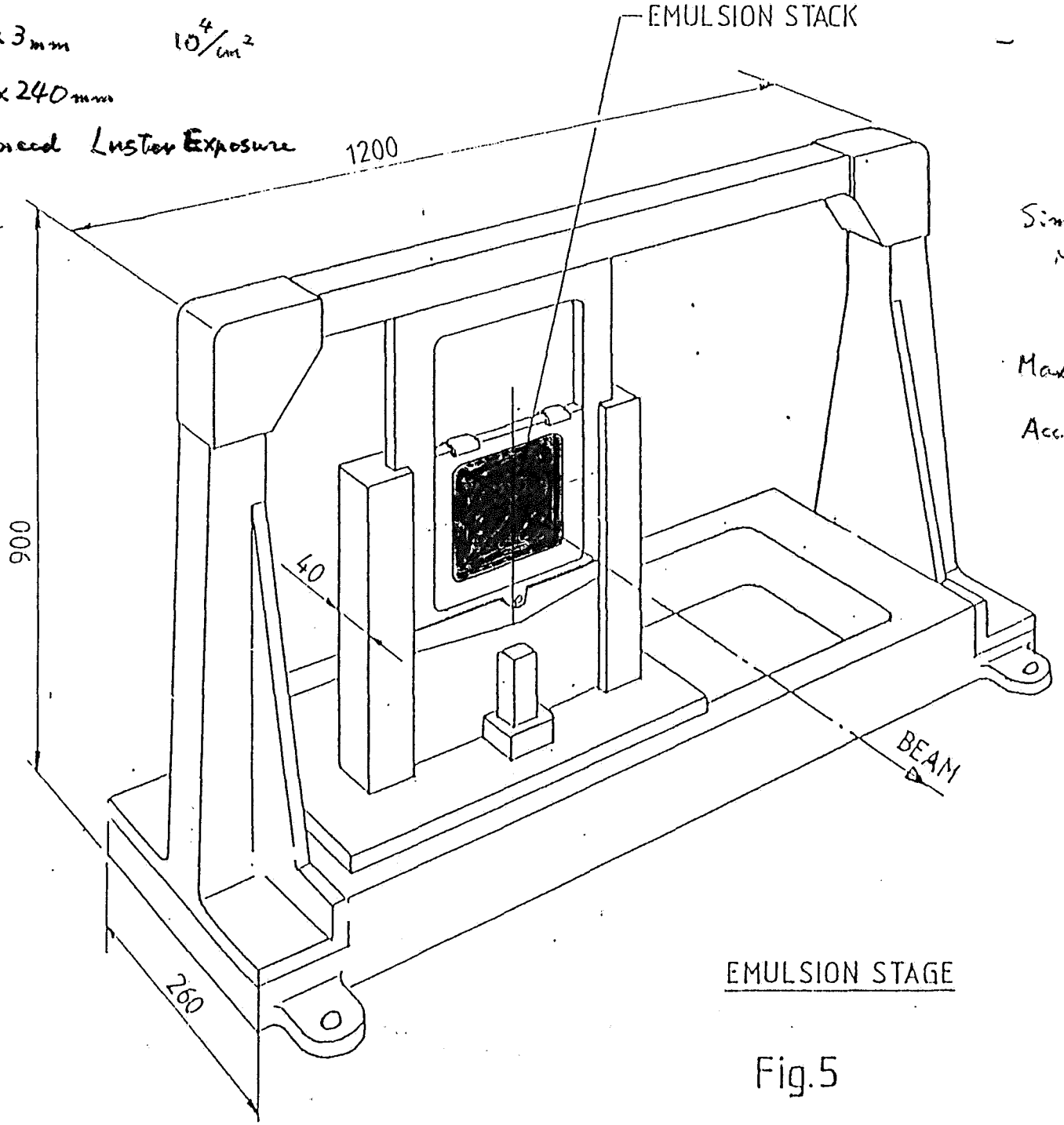

Similar Type to Measuring Stage.

Max. Speed 3 cm/sec

Accuracy ~ μm

EMULSION STAGE

Fig.5

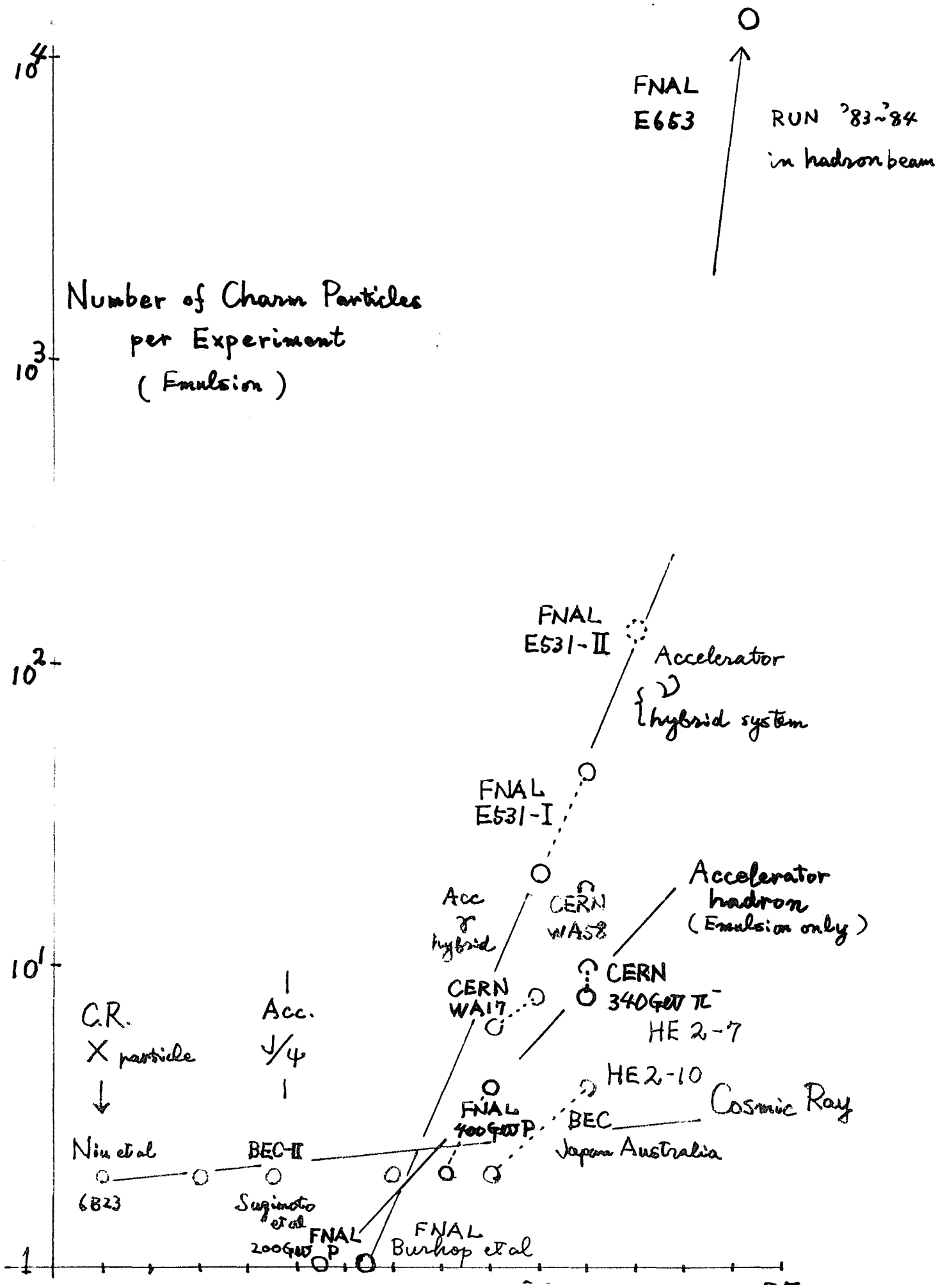
FNAL
E653
RUN '83~'84
in hadron beam
Number of Charm Particles
per Experiment
(Emulsion)
FNAL
E531-II
Accelerator
hybrid system
FNAL
E531-I
Acc
γ
hybrid
CERN
WA58
Accelerator
hadron
(Emulsion only)
CERN
WA17
CERN
340GeV π⁻
HE 2-7
HE 2-10
C.R.
X particle
Acc.
J/ψ
FNAL
400GeV P
BEC
Cosmic Ray
Japan Australia
Niu et al
BEC-II
6823
Sugimoto
et al
200GeV P
FNAL
FNAL
Burhop et al

Processing of Emulsion at FNAL

To avoid { background
fading
transportation problem
{ low temperature package
hand padding
→ loss of emulsion ~15%

Cost

Processing Equipments 55.4 K$

Building (≥ One House) ?
etc

UCD YAGER

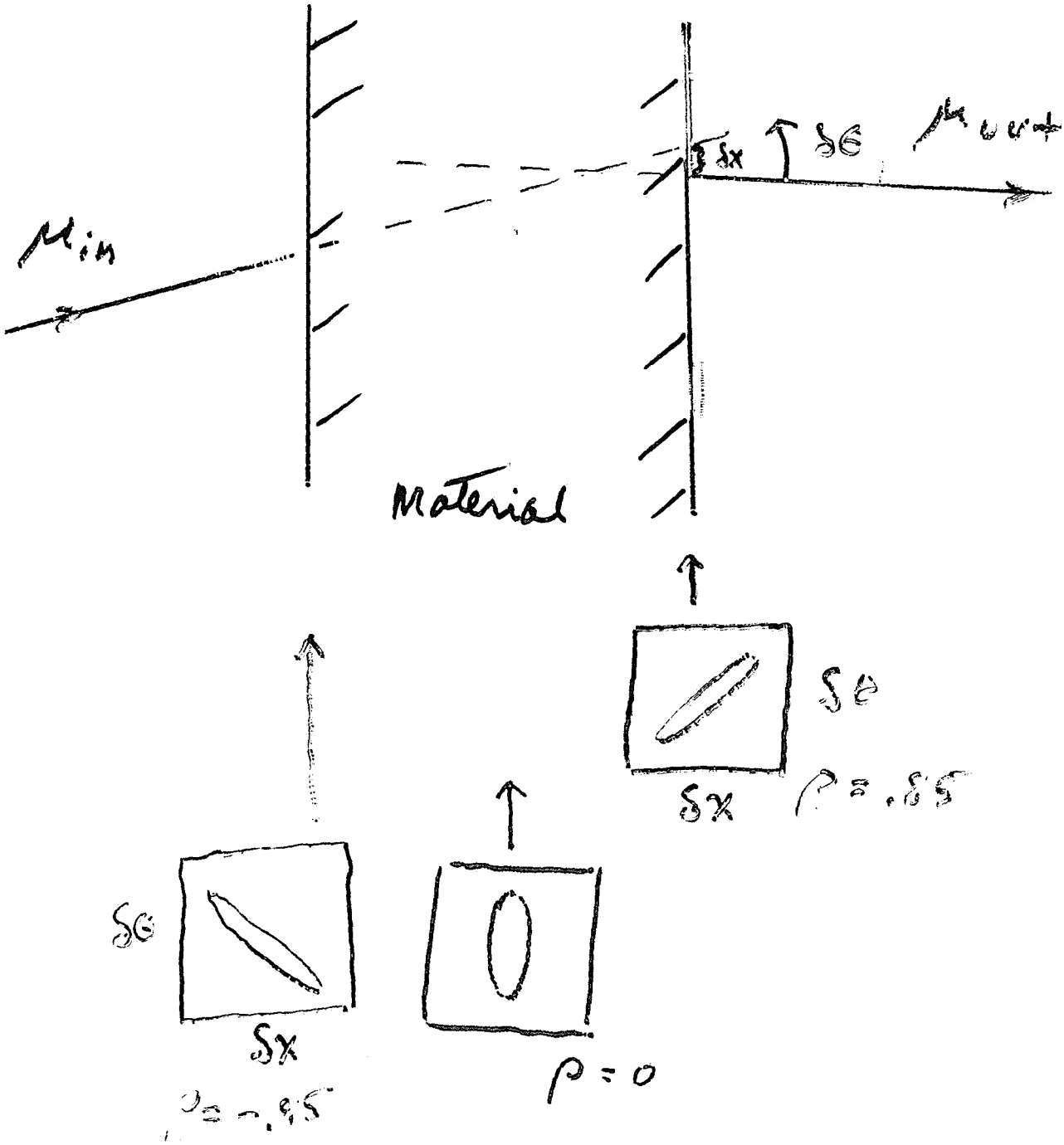

Mid plane equivalent
fully exploits pos. angle in
simplest way.

VCD 2

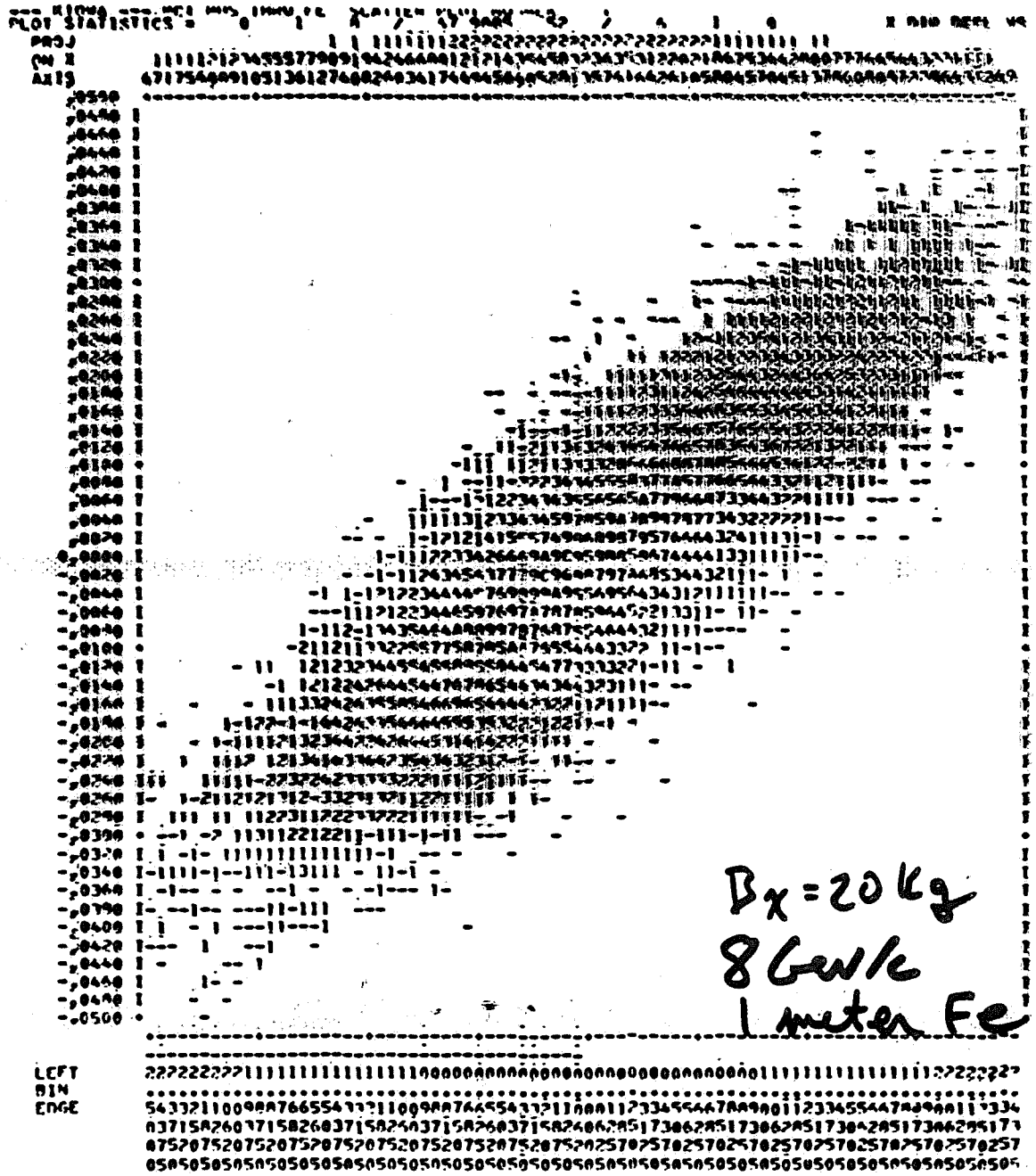

$\delta\theta_x$

$B_x = 20$ kg
8 GeV/c
1 meter Fe

δx at exit plane

$\sigma_x = 0.97$ cm

$\rho = +0.87$

VCD 3

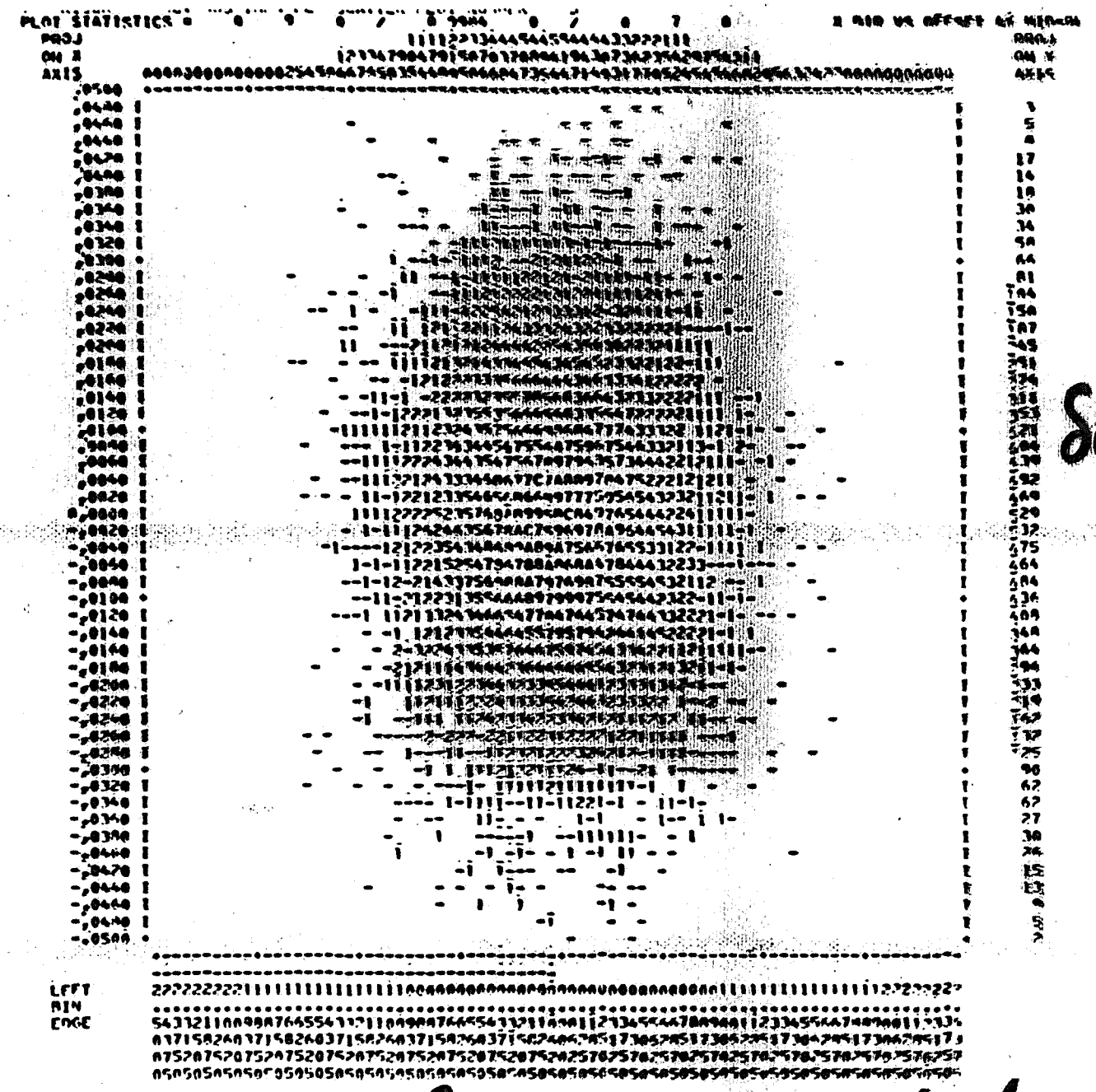

$\delta\theta_z$

δx at mid plane

$\sigma_x = 0.43$ cm

$\rho = 0.01$

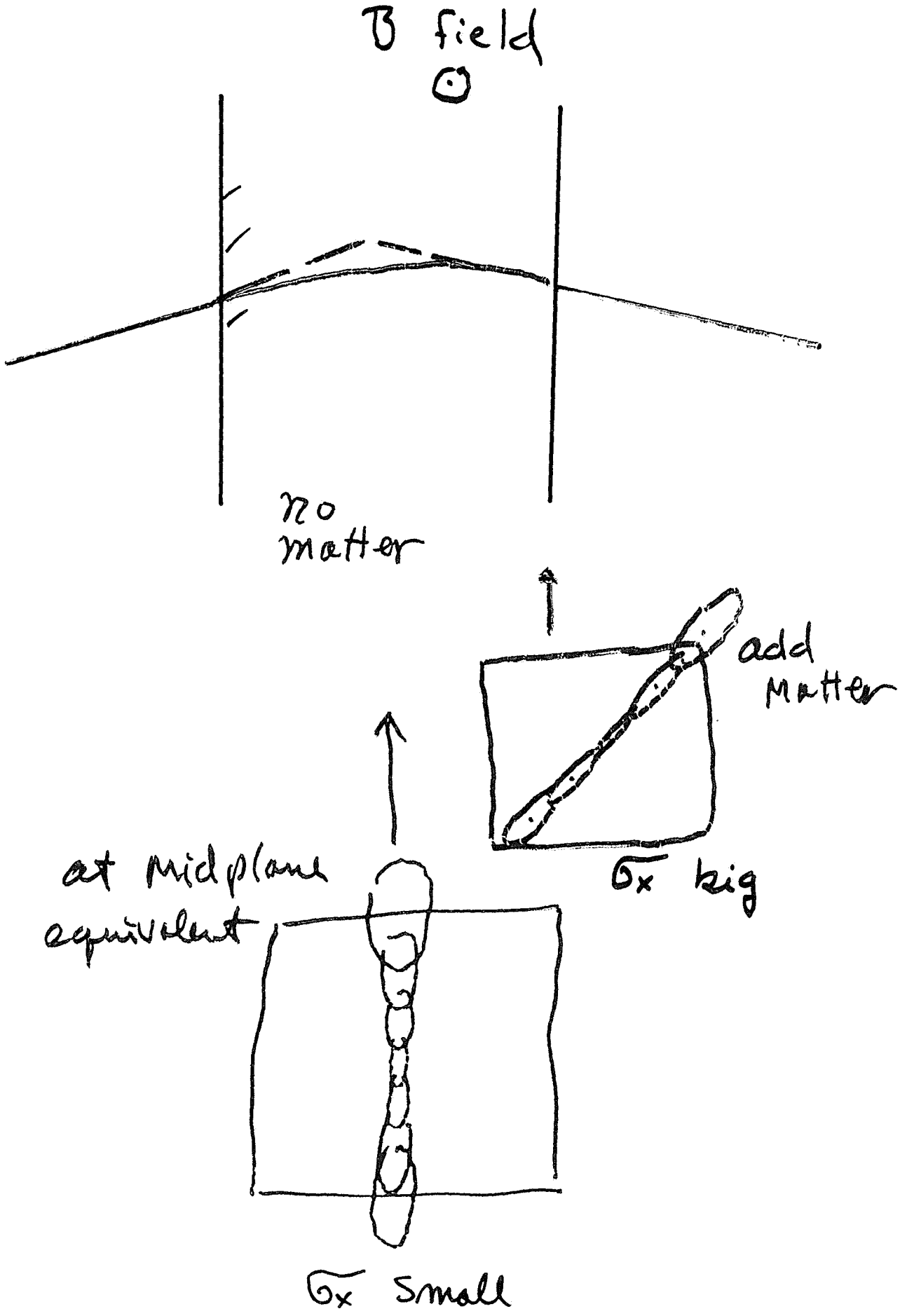
B field
no matter
add matter
at midplane equivalent
σ_x big
σ_x small

UCLA

MUON SYSTEM MAKES USE OF THESE SIMPLE IDEAS USING <u>angle and position</u>.

A) Find μ consistent with production in emulsion target

B) Impose P and P_T cuts to enrich and filter data to tape

C) Provide off-line link-up to tracks in High Resolution spectrometer

---

U.C. DAVIS will build 3m x 3m chambers similar to the 2m x 3m chambers we built for PEP-9 (200μ Resolution)

UCD-6

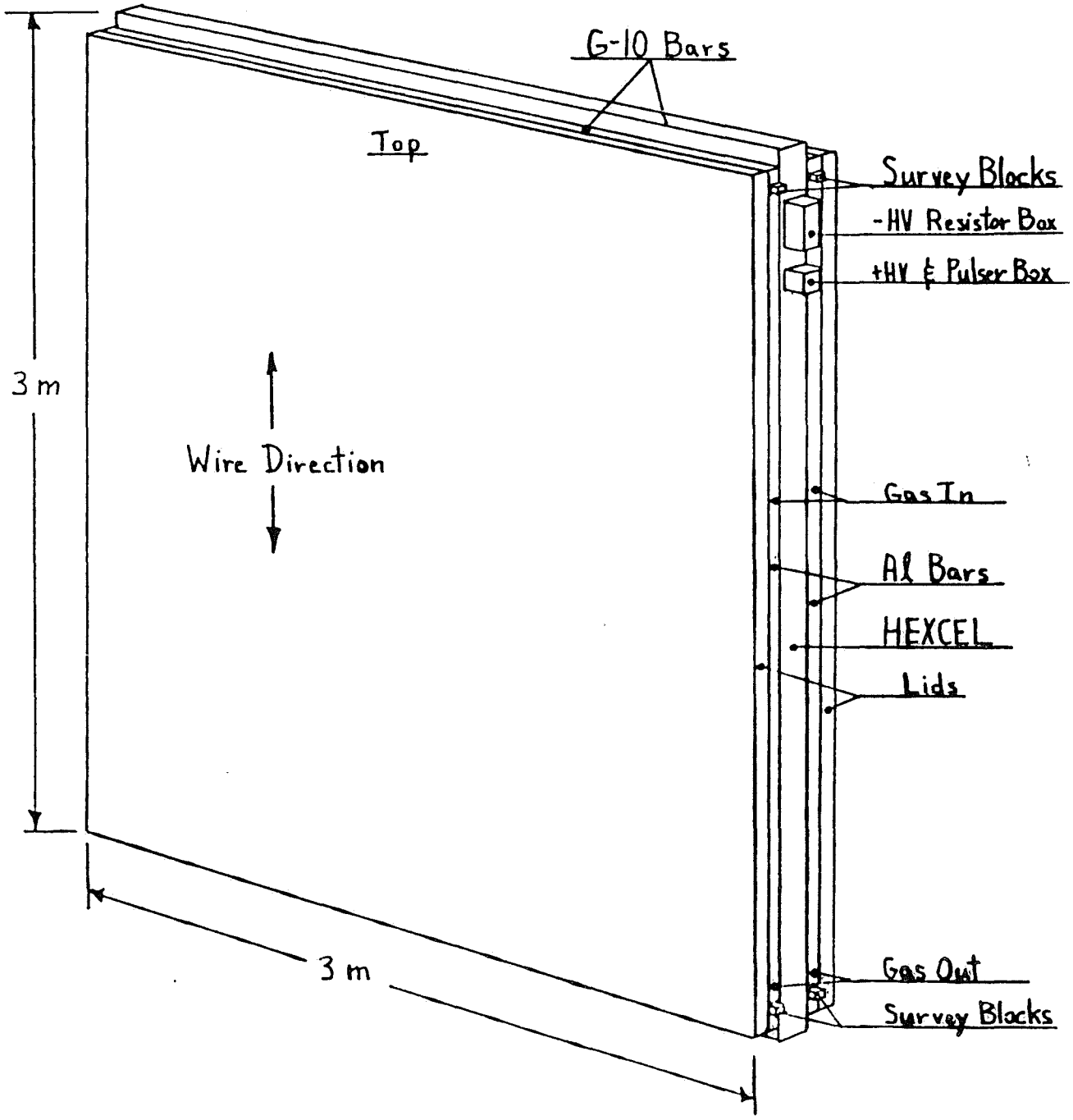

Outside View

(Top)

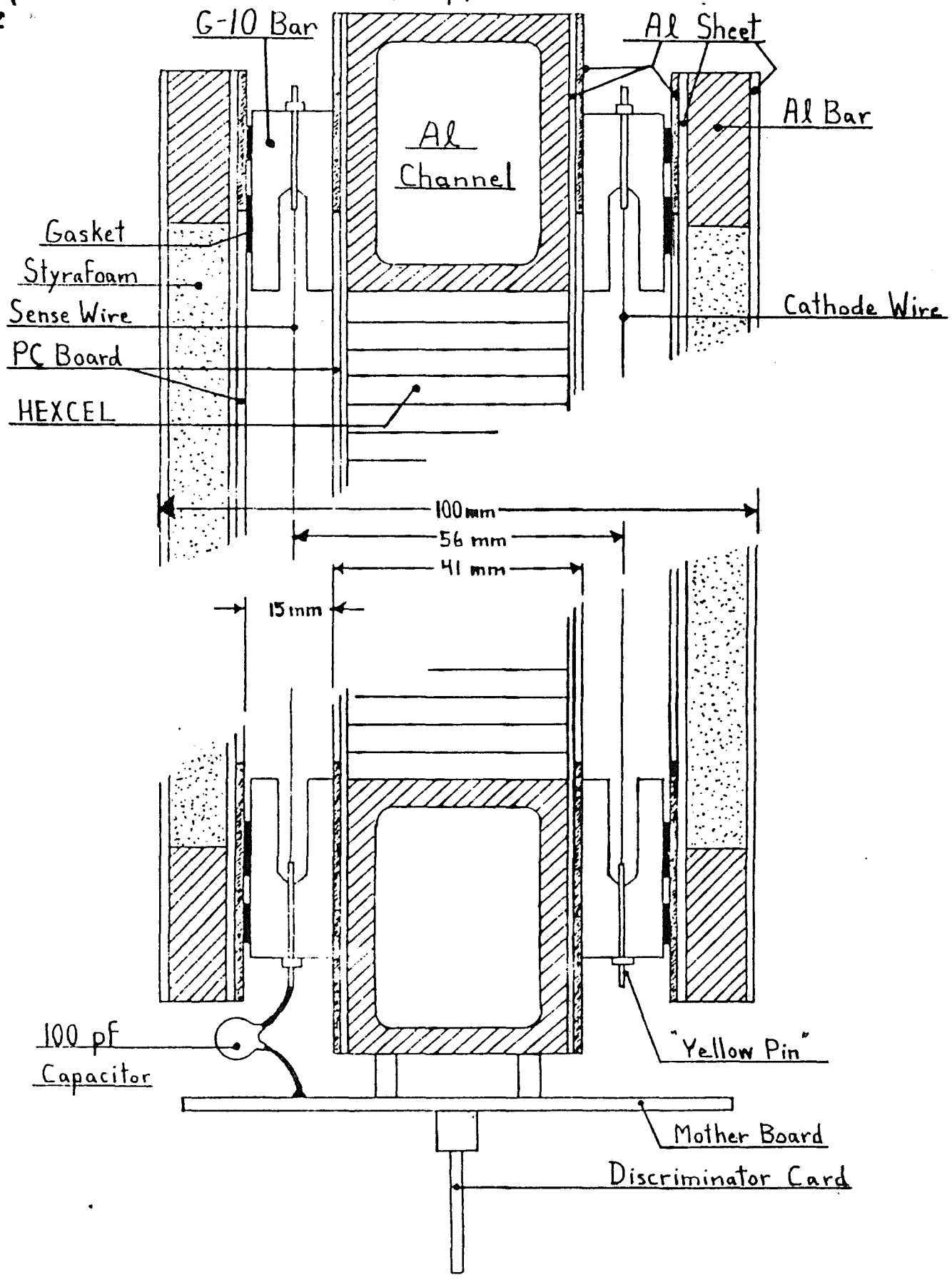

Vertical Cross Section

7 Deploy as follows in 70cm
Gaps on either side of (Fe, $\vec{B}$)

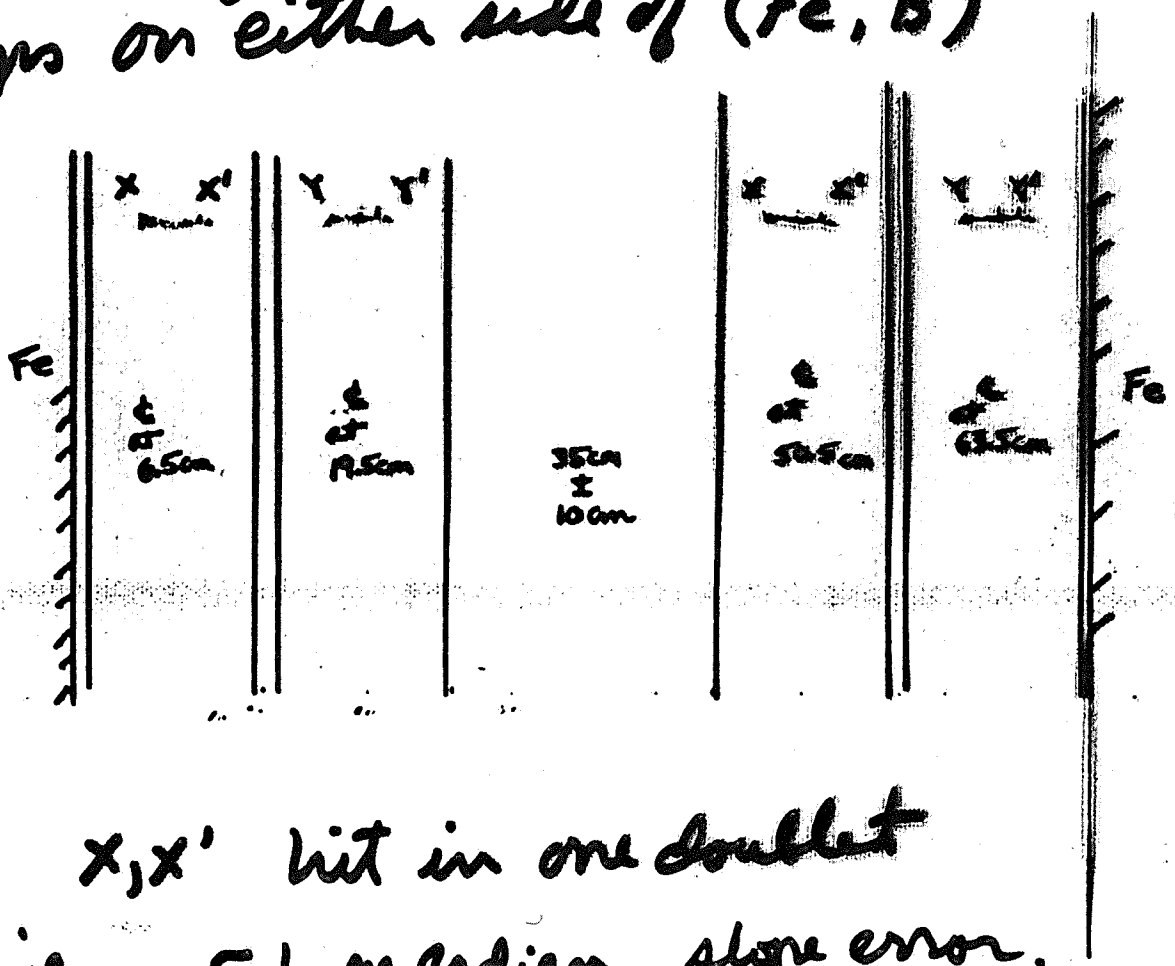

X, X' hit in one doublet
gives 5.1 mradian slope error.

⇒ 0.25 cm Window
in other doublet – speeds
track finding.

UCD-9

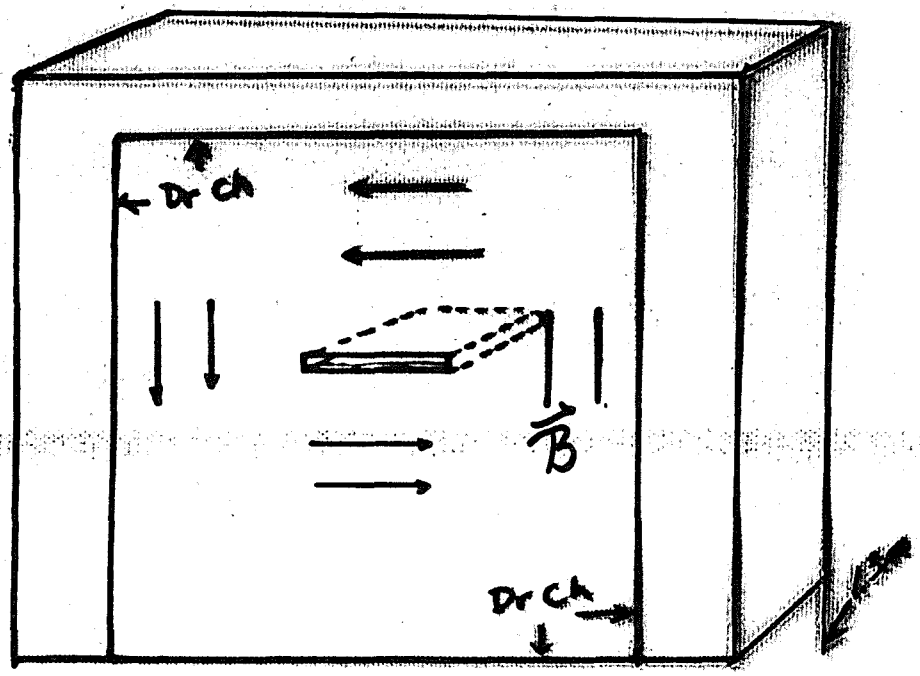

"Toroid" $\frac{\Delta p}{p} \sim 0.2$

Hole above beam line stuffed with lead shot

How can we determine that we have a μ from the vicinity of the target, determine P_μ and find P_T after penetrating so much material.

To us the experiment looks like:

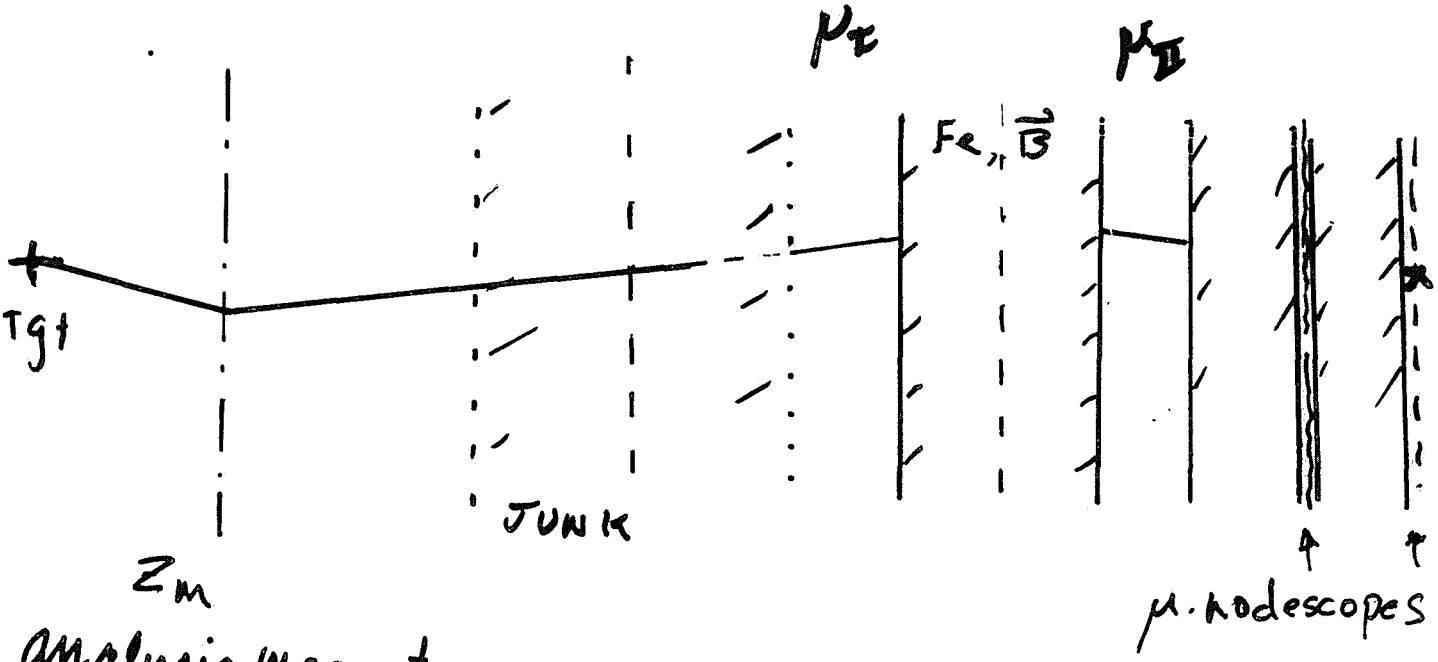

From μ_I & μ_{II} pairs of doublets determine P_μ to 20%

UCD-IC

Example $P_\mu = 16$ gev/c

$\delta x_s = .83$ (Monte Carlo)

$P_T = 1.5$	$\delta P_T^+ = .36$	$\delta P_T^- = .24$
$P_T = 0.8$	$\delta P_T^+ = .22$	$\delta P_T^- = .10$
$P_T = 0$	$\delta P_T^+ = \delta P_T^- = 0.06$	

Conclude

① We can impose P_μ & P_T cuts On-line and record only data consistent with "Prompt" μ.

② For link up, we have

a.) Sign of μ $\sim \frac{1}{2}$

b.) Production angles

c.) Value of P_μ to 20%

d.) a tight spot at Z_s

toward which a candidate must point.

End

Thus if track is consistent with Multiple coulomb scattering limits we have found the production slopes x_0' y_0' and hence P_T!

With $Z_m = 50\,cm$ $Z_s = 450\,cm$

and $P_K = 0.35\,GeV/c$ at the analysis magnet in the x projection

$$P_T = \frac{1}{450}(140 + X_s P)$$

$$\Rightarrow X_s = (450 P_T - 140)/P$$

$$\delta P_T^2 = \left(\frac{P \delta X_s}{450}\right)^2 + \left(\frac{X_s \delta P}{450}\right)^2$$

$$= \left(\frac{P \delta X_s}{450}\right)^2 + \left((P_T \pm .311)0.2\right)^2$$

$P \delta X_s \sim$ constant $\sim 14\,GeV \cdot cm$

first term $\sim (0.03)^2$, small

Outline Event Selection

Present in 100 l of emulsion:

2.8×10^8 interactions of beam
5.8×10^5 charm pairs (25 μbn)
1,150 beauty pairs (50 nbn)

Present on tape: Events with μ, $p > 8$ GeV, $p_t > 0.2$

$\times .01 \Rightarrow$ 2.8×10^6 background
$\times .088 \Rightarrow$ 3.8×10^4 charm pairs with a $c \to \mu x$
$\times .25 \Rightarrow$ 288 B pairs with $B \to \mu x$ ($\sim 60\%$)
or $B \to c \to \mu x$ ($\sim 40\%$)

Note events on tape have B enrichment over c + $D^{\pm}$ enrichment $\sim \times 3$ over other $c \to \mu x$.
Expect 70% of charm pairs on tape have ≥ 1 $D^{\pm}$.

How to find beauty:
→ a) Find the $c \to \mu x$ events, look for $B \to c$
b) Lots of other schemes for getting at the other 60%.
(High p_t μ, 2ndary vertices + high p_t, ...)

How to find charm: Look for visible secondary vertices using SSD's.

Sources of secondary vertices:
Decays
Interactions
Inadequate resolution
Reconstruction screw-ups

Before continuing with yield + BG estimates, look at how reconstruction is done.

Monte Carlo Event Simulator

Generate charm pairs obeying

$$\frac{d\sigma}{dx\,dp_\perp} = (1-|x|^n)\, p_\perp e^{-b p_\perp}, \quad \begin{matrix} n = 4 \\ b = 2.0\ \text{GeV}^{-1} \end{matrix}$$

Energy left over from charm pair (typically several hundred GeV) goes into producing an "ordinary" hadronic interaction.

Put in:

secondary hadronic interactions in emulsion

γ conversion in emulsion

Propagate charged tracks thru emulsion + spectrometer, putting in multiple scattering. Generate hits at detectors.

Put in resolution and track confusion smearing, e.g. if cluster of SSD's is on, use centroid of cluster.

Refit tracks, reconstruct vertices.

→ Work in progress!

X view

Typical $D^+ \bar{D}^0$ Event @ 1 TeV

19 charged tracks

D^+ 89 GeV, $t_0 = 8.7 \times 10^{-13}$ sec

D^0 76 GeV $t_0 = 6.3 \times 10^{-13}$ sec

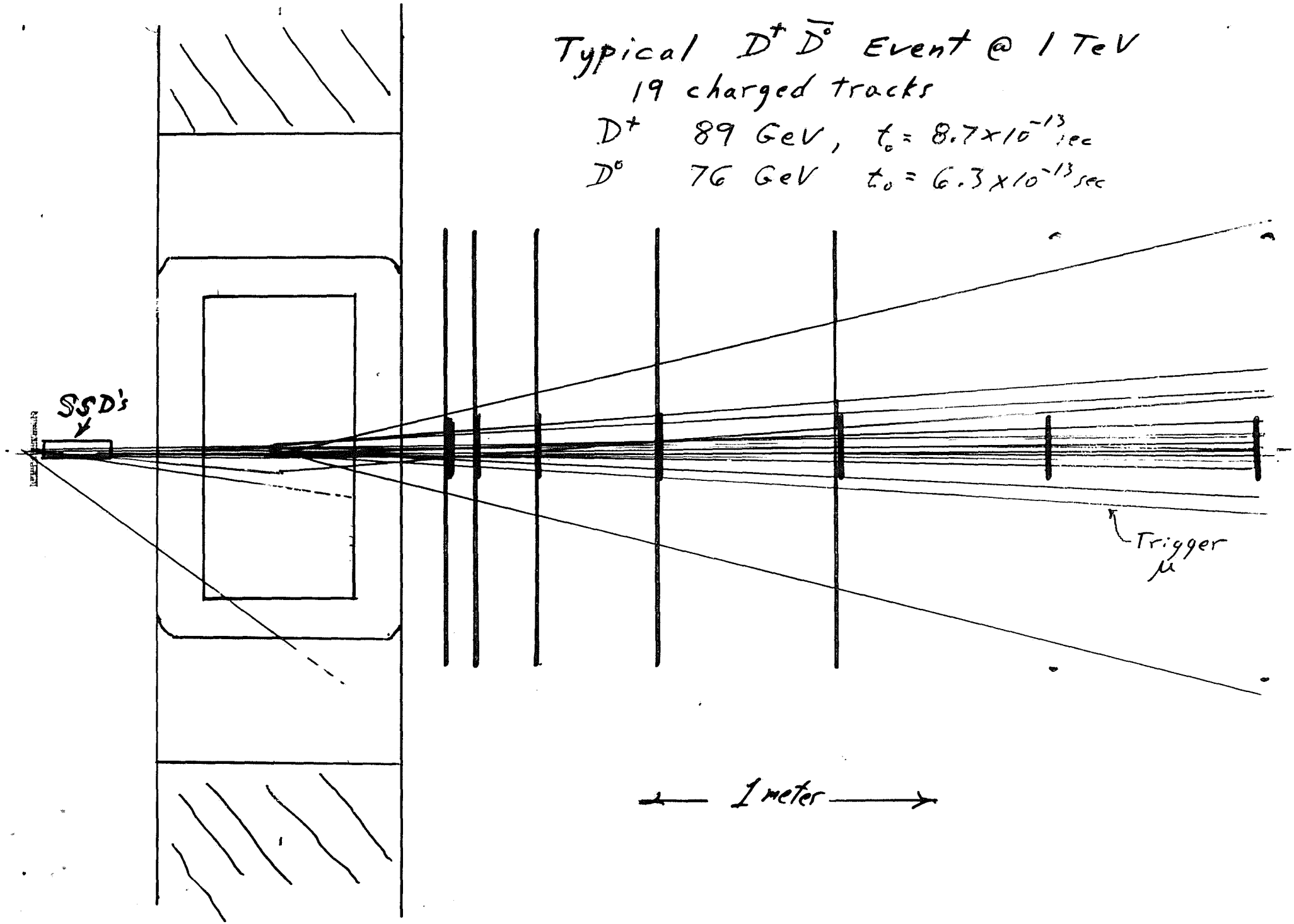

SSD Vertex Detector

X view (one of 3 60° stereo views)

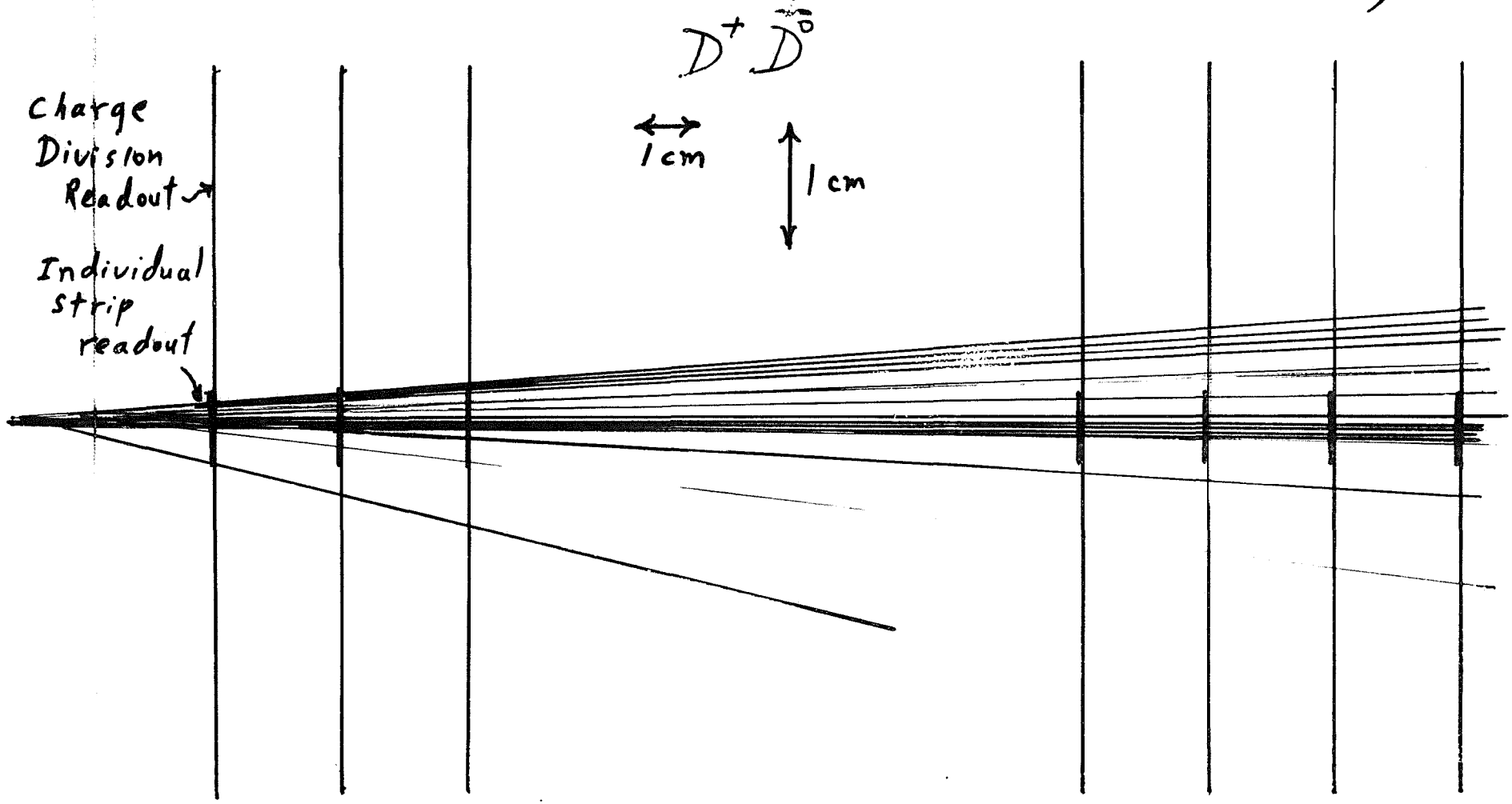

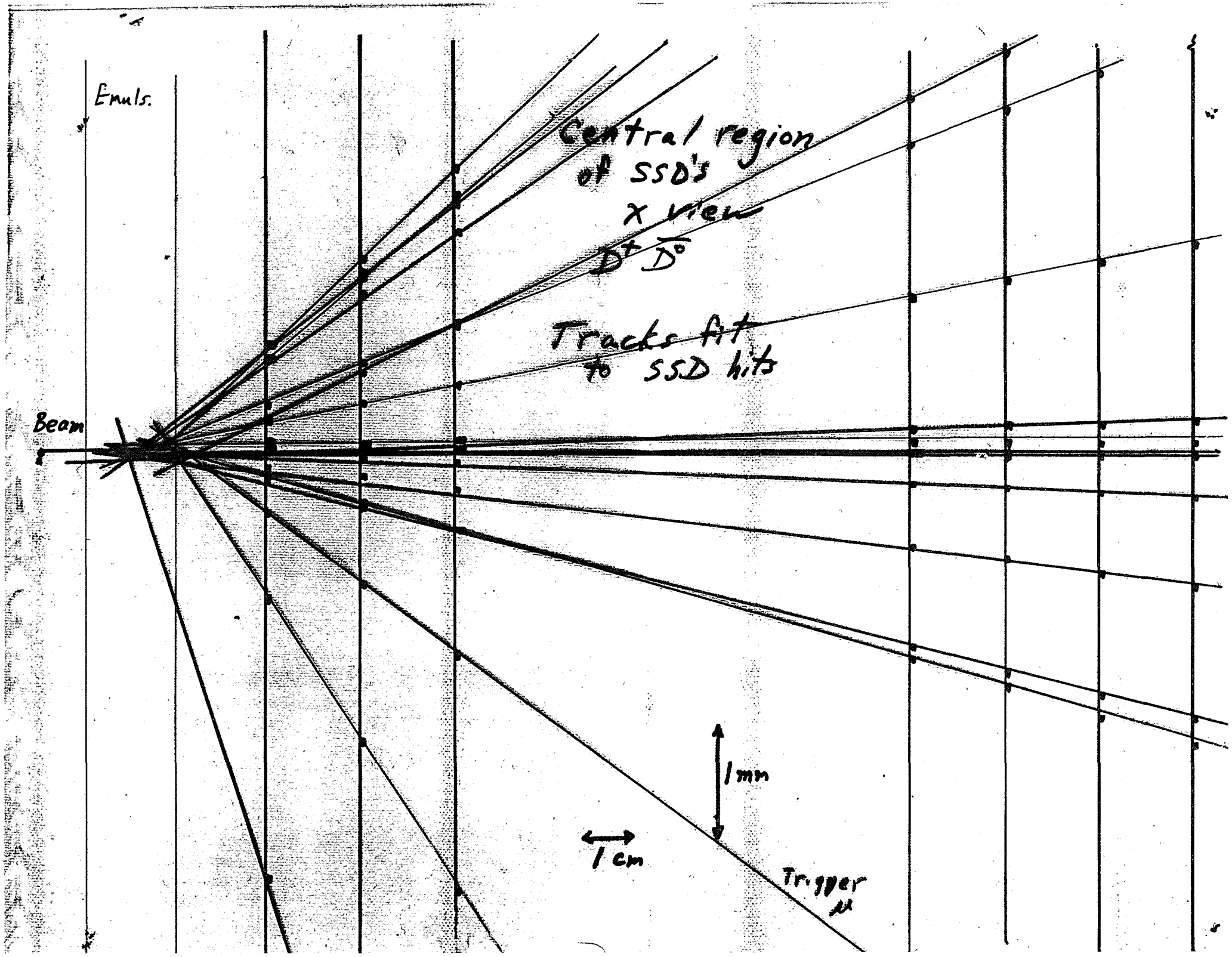
Emuls.
Central region
of SSD's
x view
$D^+ \bar{D}^0$
Tracks fit
to SSD hits
Beam
1mm
1cm
Trigger
μ

Recognizing Secondary Vertices

Typical $D^+ \bar{D}^0$ event. Use all 3 stereo views.

Intersection with beam track: find primary vertex.

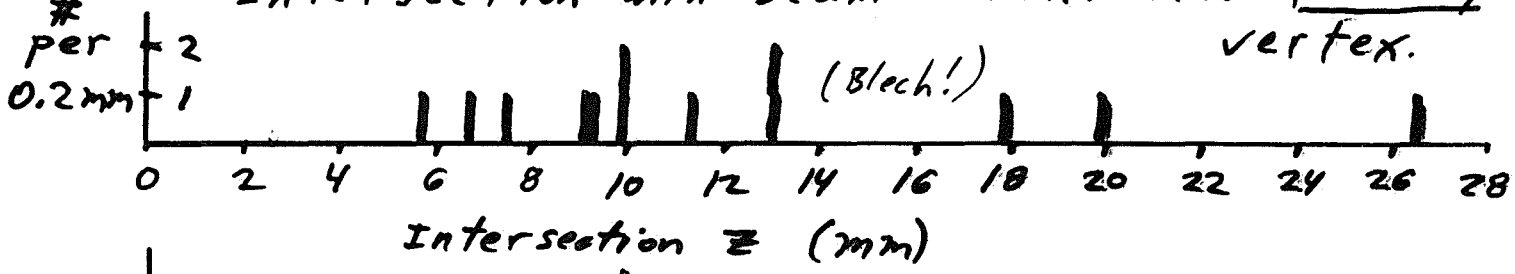

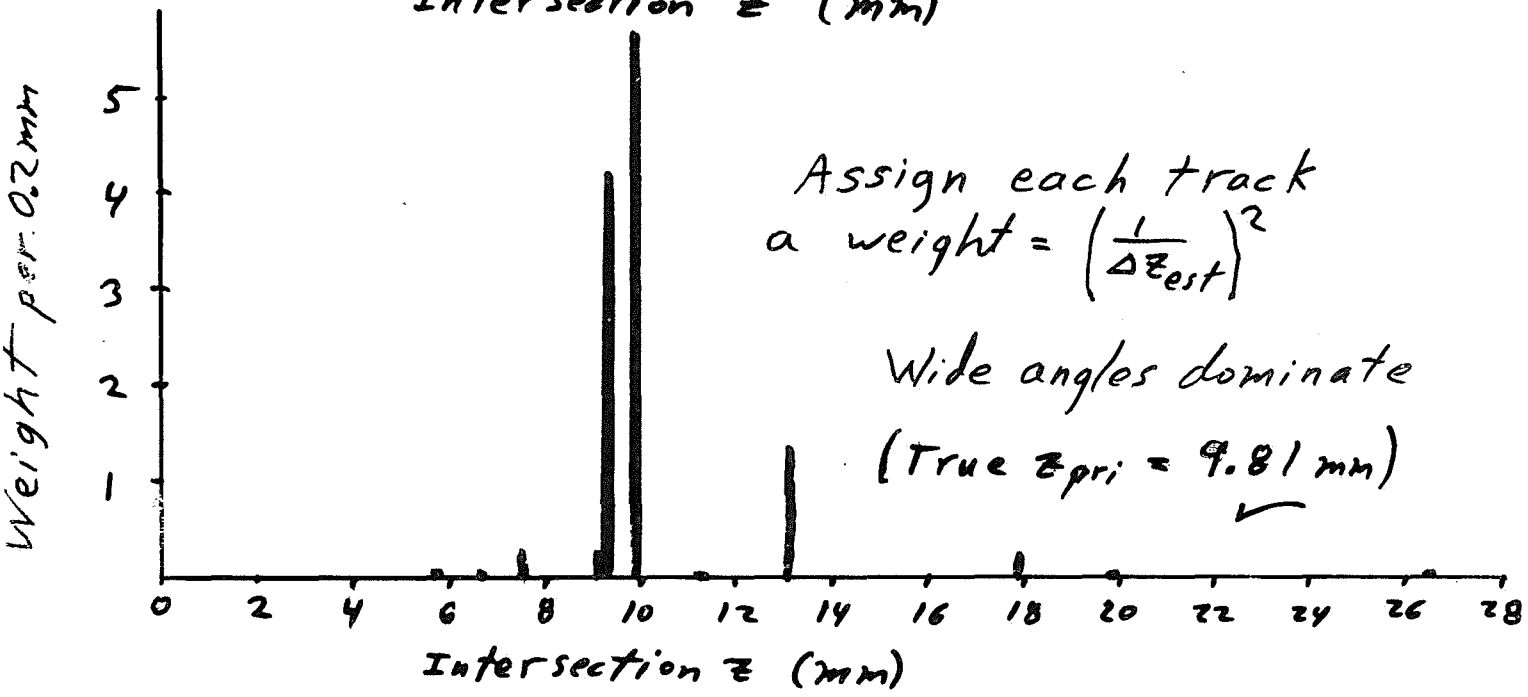

Assign each track a weight = $\left(\frac{1}{\Delta z_{est}}\right)^2$

Wide angles dominate

(True z_{pri} = 9.81 mm)

Now look at impact parameters of all tracks at primary vertex. Let

R = (impact param)/(est. error)

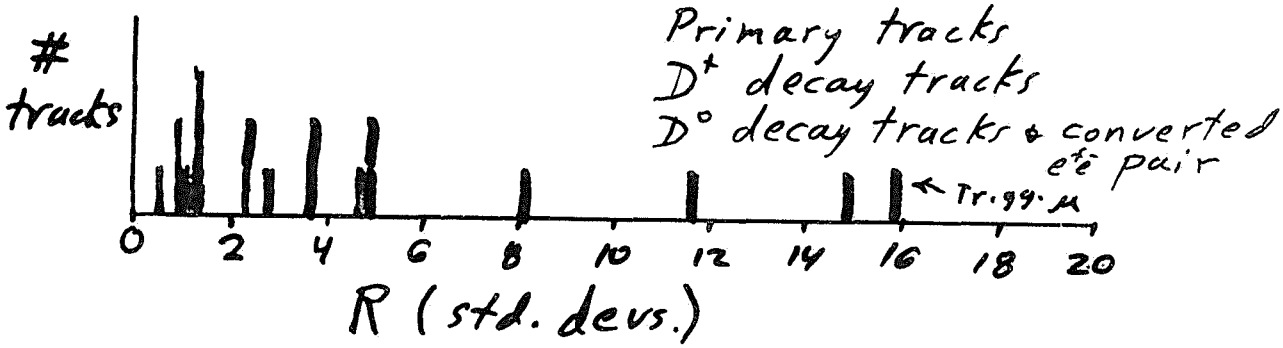

Results from 500 simulated $D\bar{D}$

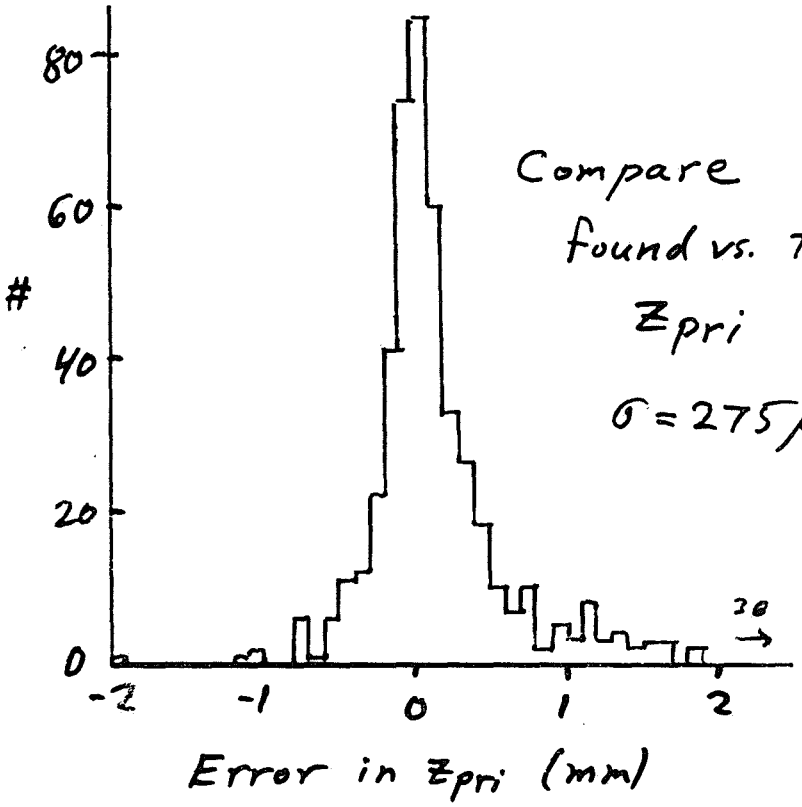

Compare found vs. true z_{pri}

$\sigma = 275\,\mu$

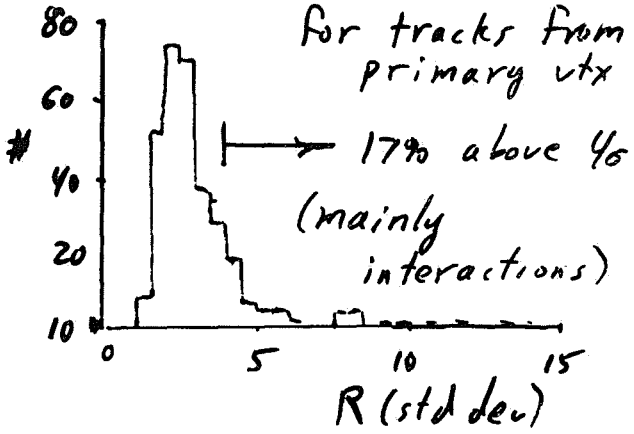

Maximum R for tracks from primary vtx

17% above 4σ (mainly interactions)

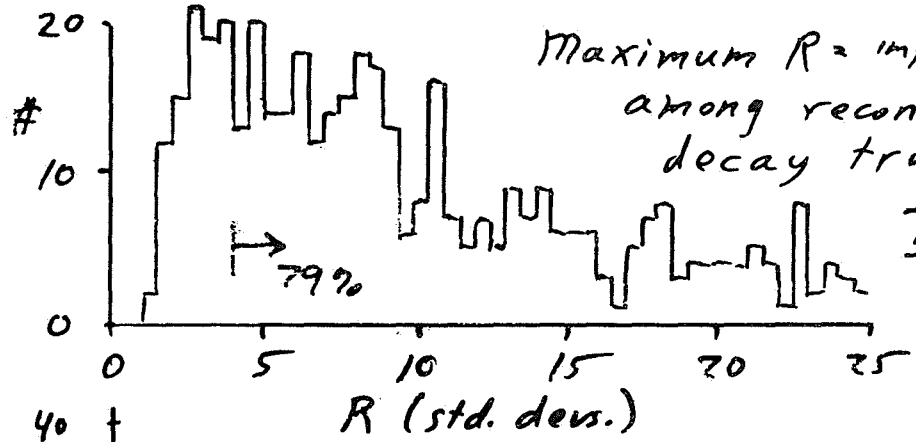

Maximum R = impact/err among reconstructed decay tracks

79% above 4σ (52% for $D^0\bar{D}^0$)

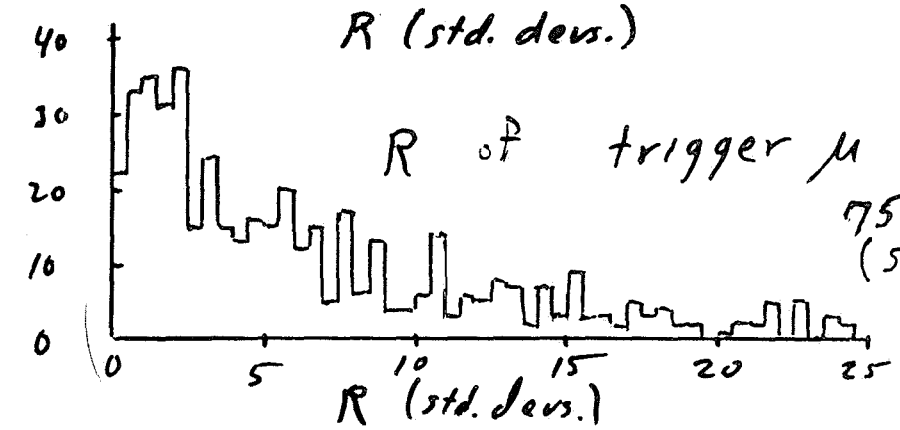

R of trigger μ

75% above 2σ (50% above 1.5σ for $D^0\bar{D}^0$)

Offline Event Selection (continued)

On tape: 2.8×10^6 BG
3.8×10^4 charm pairs with a $C\to\mu X$.

Demanding no kinks in downstr. DC gets rid of most $K\to\mu$
$2.8\times10^6 \to 1.8\times10^6$ BG

$$\#\text{BG with interactions} = \left(\frac{1\text{cm}}{50\text{cm MFP}}\right)\left(11\ \frac{\text{hadrons}}{\text{ev}}\right)\left(1.8\times10^6\text{ ev}\right)$$
$$= 4.0\times10^5 \qquad \text{Too many!}$$

<u>But</u> demand that trigger μ come from a <u>secondary</u> vertex. Prob. of a secondary interaction giving a π, K decay μ passing cuts is small, $\sim .13$ that of a primary interaction.

$$\Rightarrow \#BG = (.13)(4.0\times10^5) = 5.2\times10^4$$

$\Rightarrow$ Need to associate trigger μ with a secondary vertex at $\sim 95\%$ confidence.

E.g, trigger μ has impact parameter $\gtrsim 2\sigma$ $(D^\pm)$

<u>or</u>, trigger μ has impact param $\gtrsim 1.5\sigma$
<u>and</u> another track intersects downstream.

Require also maximum impact parameter in event $\gtrsim 4\sigma$, to get down to level of interactions.

These cuts keep $\sim 60\%$ of $c\bar{c}$ pairs with one charged D. (For $D^0\bar{D}^0$, work still in progress. $\sim 25-35\%$)

$$\Rightarrow \text{Charm pair yield} \approx (3.8\times10^4)(.6f + .3(1-f))$$
f = fraction on tape with ≥ 1 $D^\pm$, $\approx .7$
$$= \underline{1.9\times10^4}$$

$$\#\text{Beauty decays in these events} = 1.9\times10^4\left(\frac{50\times10^{-3}\,\mu\text{bn}}{25\,\mu\text{bn}}\right)2(1.13) = \underline{86}$$

SPECTROMETER

DESIGN DRIVEN BY EMULSION WITH ~1 hour time resolution AND LIMITED SCANNING CAPABILITY - LOW INTEGRATED FLUX

WE WANT MAXIMUM EFFICIENCY FOR WRITING CHARM EVENTS ON TAPE.

- LARGE ACCEPTANCE μ TRIGGER
  forward muon detection

↓

SHORT SPECTROMETER

↓

HIGH HIT DENSITIES ⇒ GOOD 2 TRACK (SHOWER) RESOLUTION

SHORT LEVER ARMS

SIGNIFICANT MULTIPLE SCATTERING + CONV. IN EMULSION + SSD ⇒ measure e^+e^-
⇒ DOMINATES $\delta P, \delta\theta$ AT LOW MOMENTUM

NEED GOOD ϵ FOR $D^* \rightarrow D \pi^{\pm}$

MANY π^0's IN B, C Decay

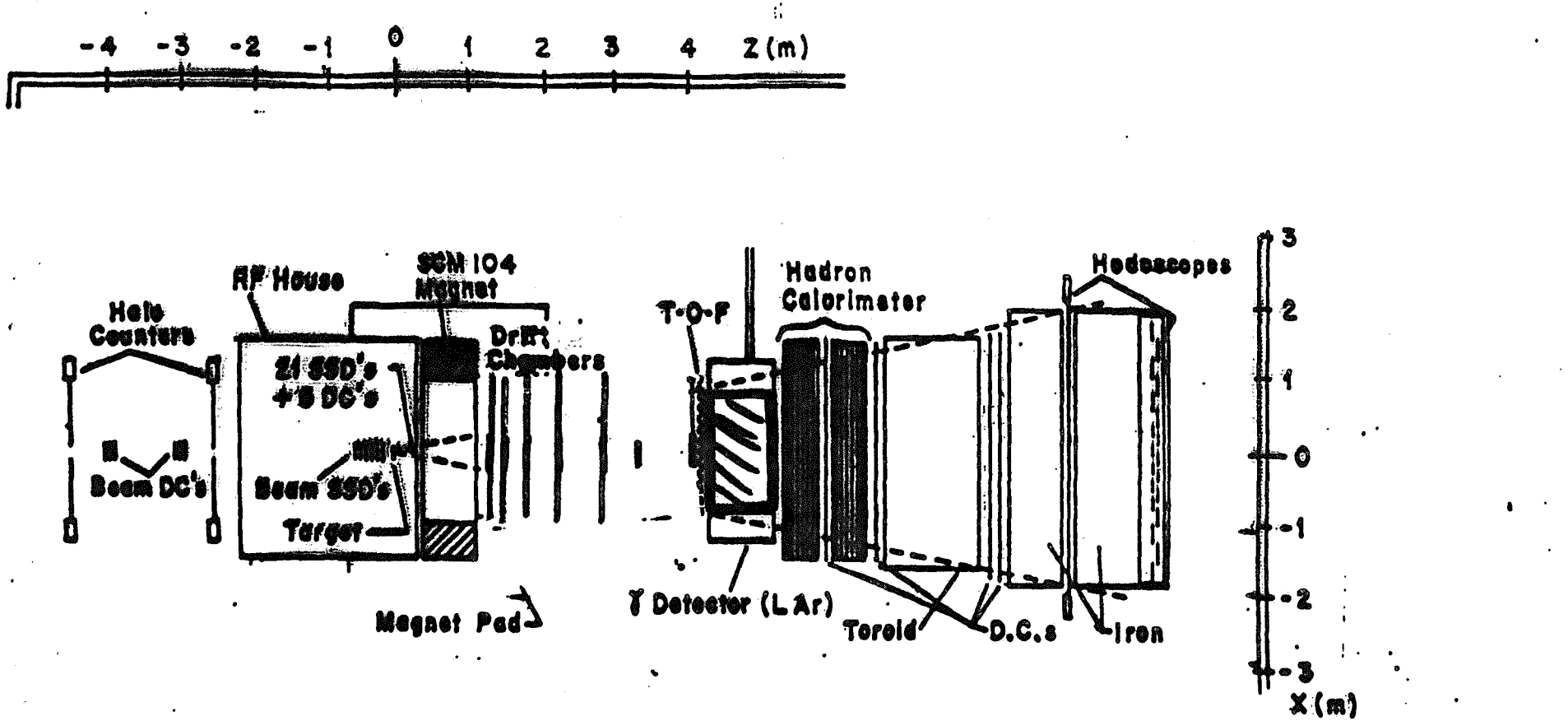
-4
-3
-2
-1
0
1
2
3
4
Z(m)
RF House
SCM 104 Magnet
Halo Counters
Drift Chambers
21 SSD's
+3 DC's
Beam DC's
Beam SSD's
Target
Magnet Pad
T-O-F
Hadron Calorimeter
Hodoscopes
γ Detector (L Ar)
Toroid
D.C.s
Iron
3
2
1
0
-1
-2
-3
X(m)

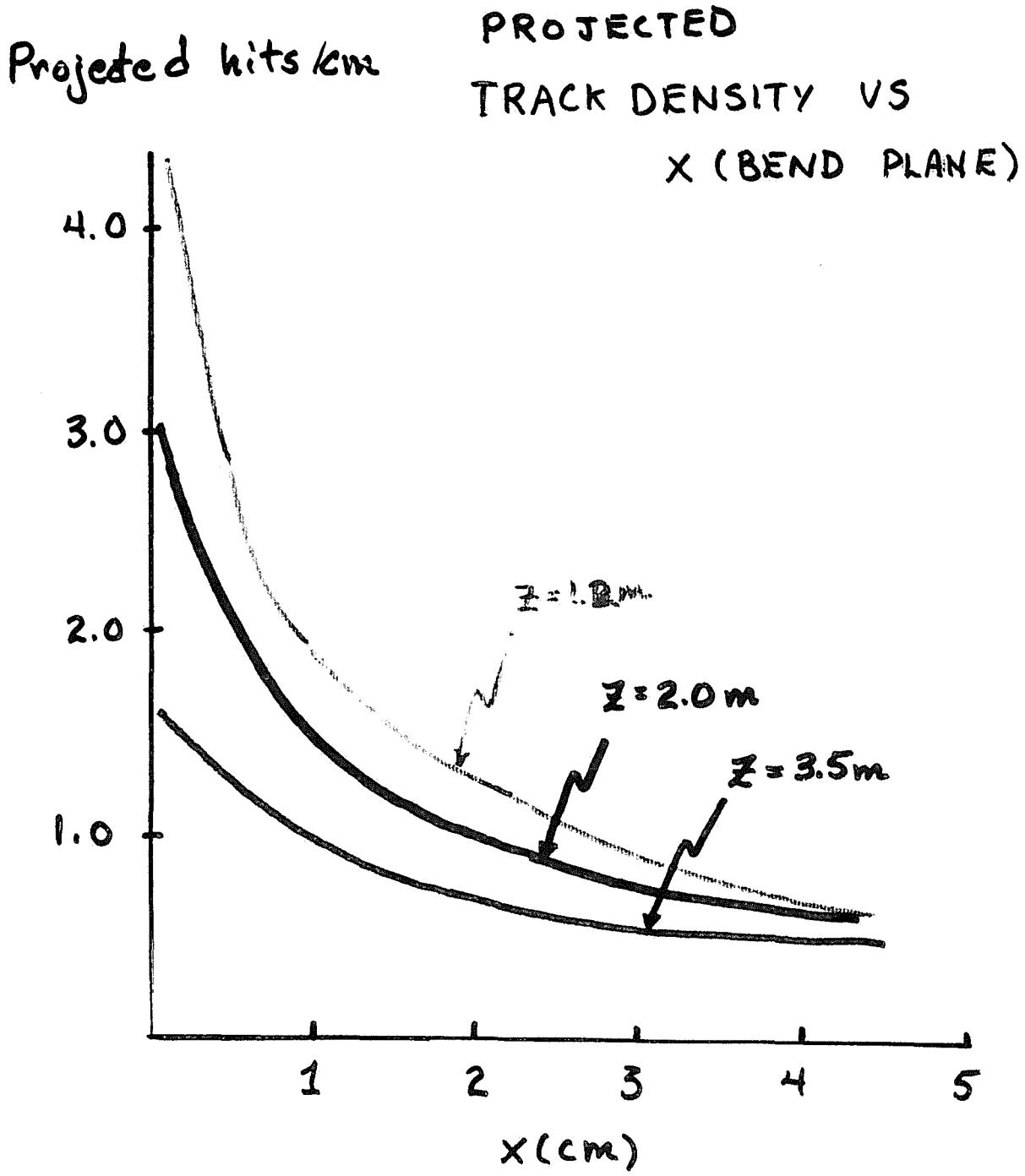
PROJECTED
TRACK DENSITY VS
X (BEND PLANE)
Projected hits/cm
4.0
3.0
2.0
1.0
Z = 1.8m
Z = 2.0m
Z = 3.5m
1
2
3
4
5
X(cm)

DRIFT CHAMBERS

- require excellent multi hit separation

⇒ High pressure (2.5 Atm)
⇒ Fast, multi hit electronics (Platner + LeCroy)
⇒ Inner + Outer sections

20 cm
$\sigma \sim 100\,\mu m$
$\Delta \sim 1mm$
1cm Cells
(region where σ_{meas} is important)

$\sigma \sim 250\,\mu m$
$\Delta \sim 2.5mm$
(E531 $\Delta \sim 2.5mm$)

EM CALORIMETER LIQUID ARGON

- NEED GOOD ENERGY RESOLUTION, 2 shower separation, pattern recog.

⇒ High detector density
⇒ Longtitudinal segmentation (3)
⇒ Transverse segmentation
1/8" strips, PADS
$\Delta = 3mm$ for 15 gev showers

HADRON CALORIMETER - GAS TUBES

- LOW CENTRAL ϵ
⇒ BOTH STRIPS AND PADS

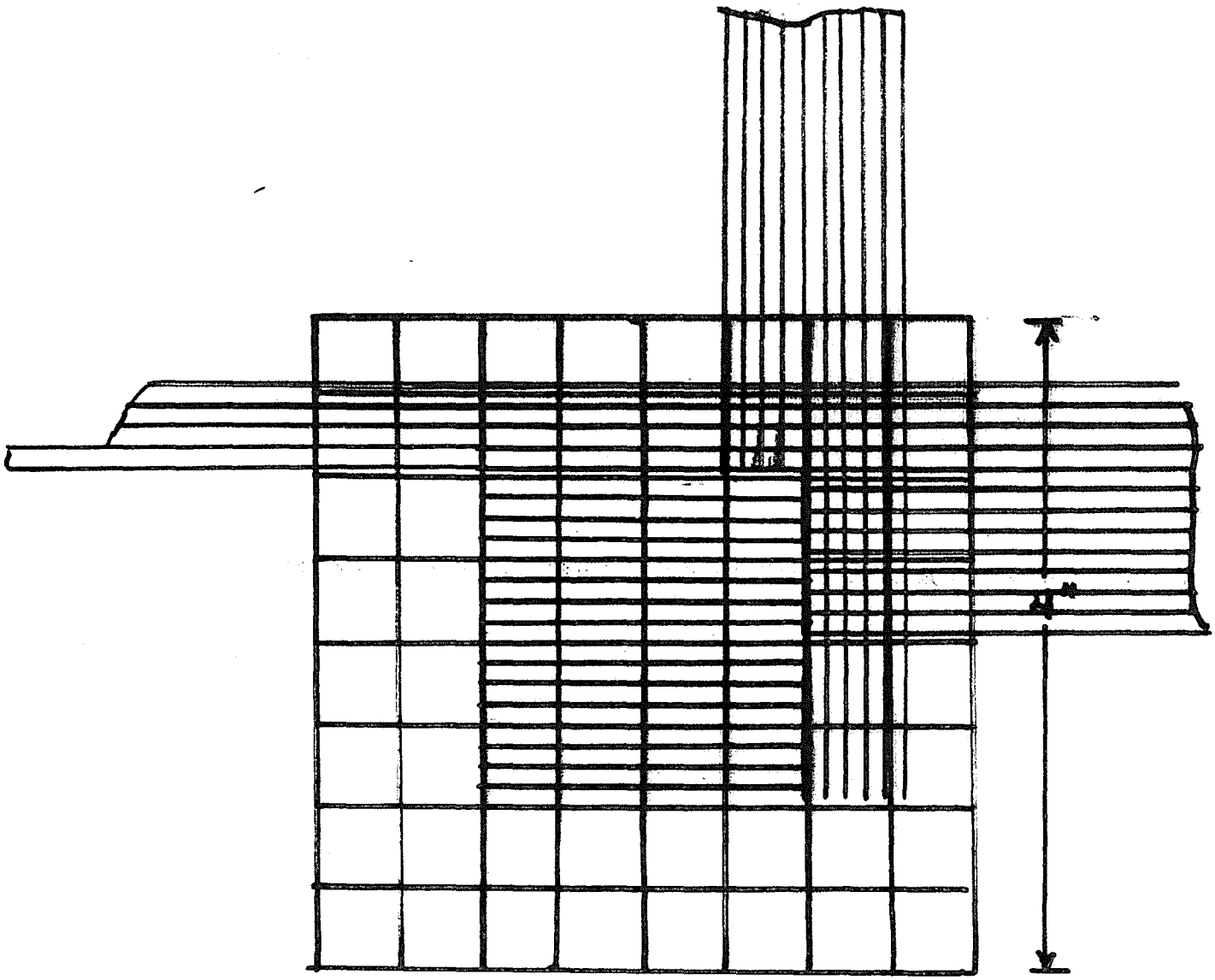

LAC CENTRAL

REGION

H_m
LAC CENTRAL REGION
E_γ
FWHM

FERMILAB

ENGINEERING NOTE

SECTION	PROJECT	SERIAL-CATEGORY	PAGE

SUBJECT: E655 Argon Cal. - Front View

NAME: R. LIPTON

DATE: | REVISION DATE:

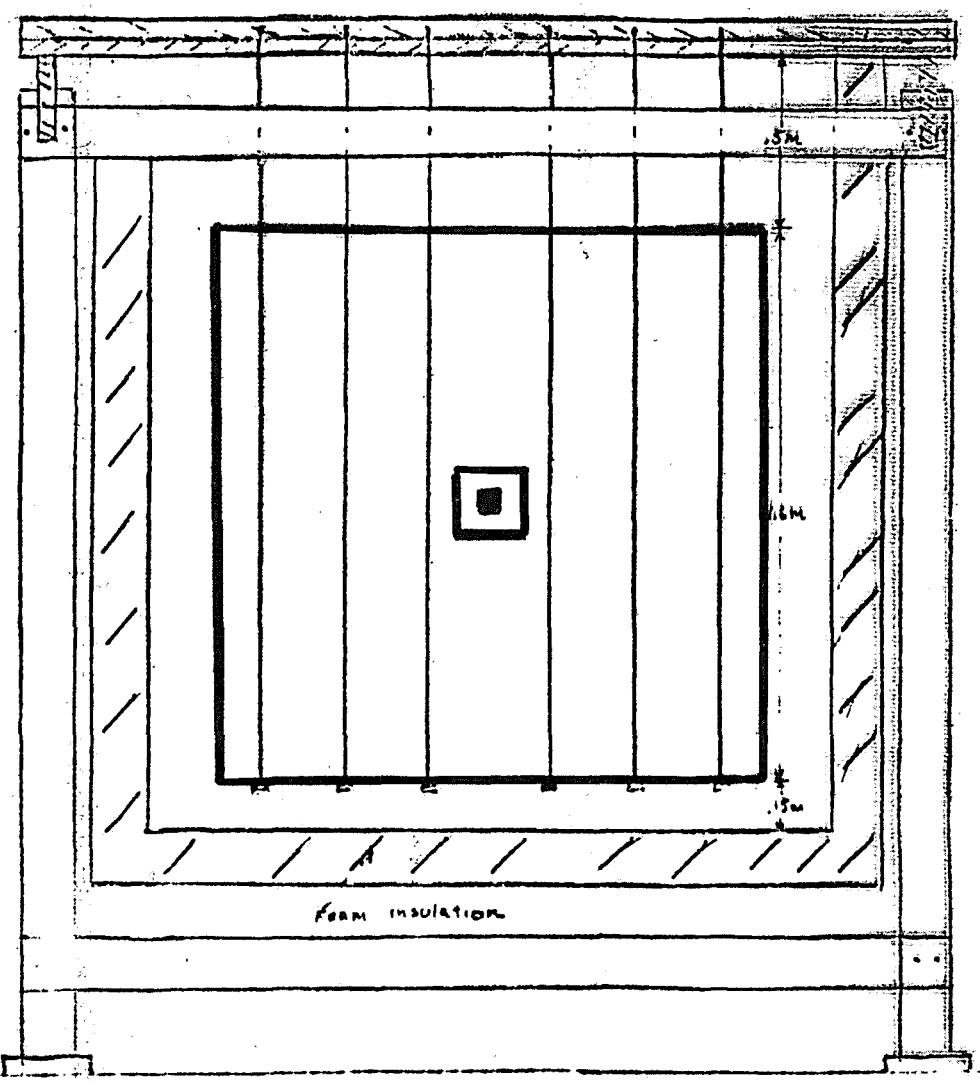

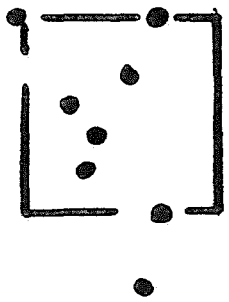

BACKGROUND FROM $p_\perp$-limited phase space

model using residual energy left after $B\bar{B}$ pair is formed. Produce $pp\,\pi^+\pi^-\,\pi^+\pi^-\,\pi^+\pi^-\,\pi^0\pi^0\,\pi^0\pi^0$

(a) $(1-x)^3 e^{-P_\perp}$ dist for $(B\bar{B})$ blob with e^{-5M} mass dist.

(b) $B \rightarrow D^+ \pi^+ \pi^- \pi^+ \pi^- \pi^0 \pi^0$; $\bar{B} \rightarrow$ chg. conj.

$\quad\quad\hookrightarrow K^+ \pi^0 \pi^0$

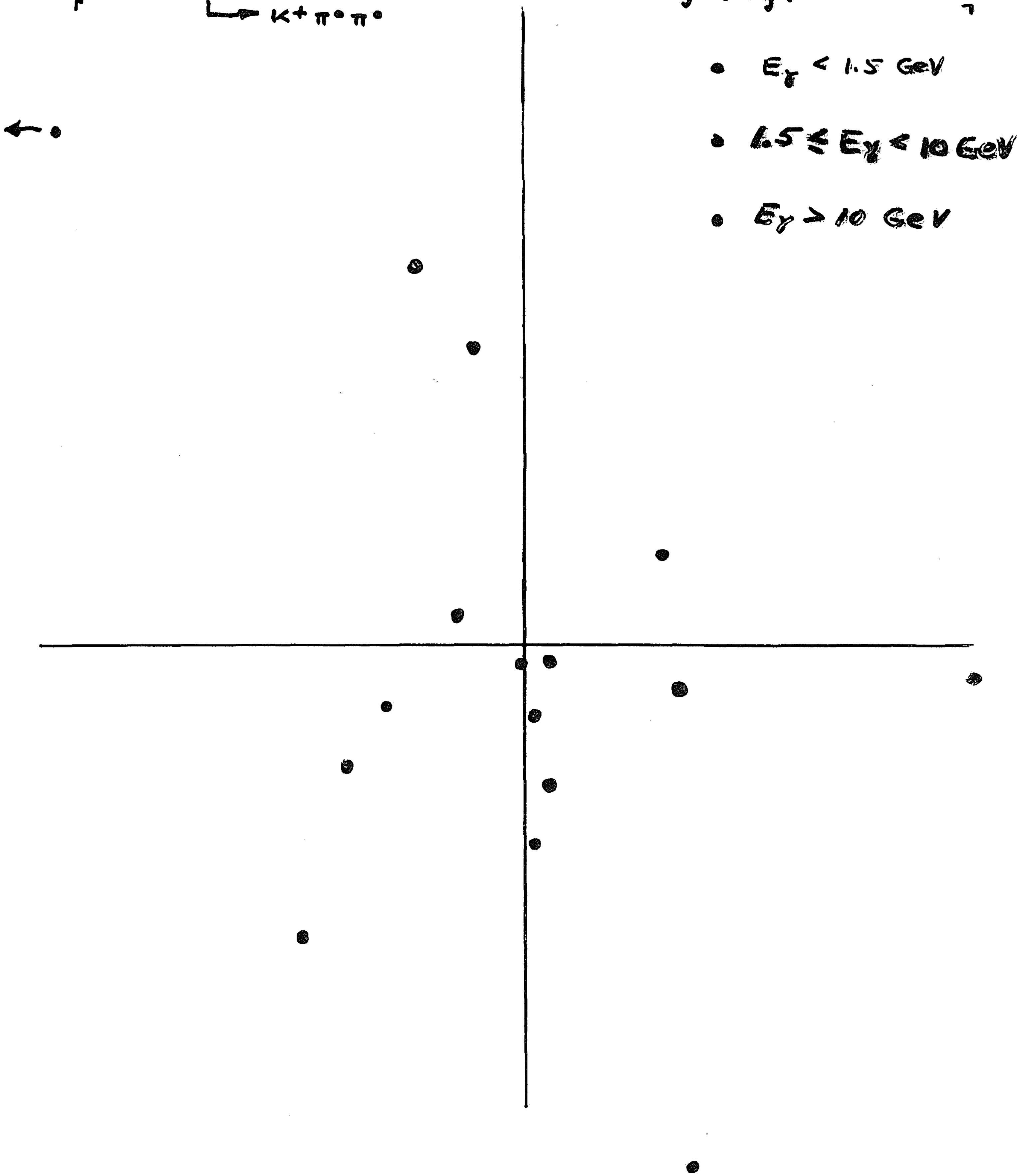

SUMMARY OF SPECTROMETER

Acceptance: ± 200 mr Vertical
± 240 mr Horizontal

Momentum Resolution ~1% at 10 GeV

Mass Resolution ($D \to K\pi\pi\pi\pi$) ~ 14 MeV

Magnet $\Delta P_\perp$ ~ .35 GeV

EM Calorimeter

- active area - 1.6 M x 1.6M
- sampling - .4 X_0
- gap - 4mm
- segmentation - 3x 8 X_0 Longtitudinal
  - 1/8" STRIPS (X, Y),
  - 4 Pad regions Trans.
- # Channels - 4000
- $\sigma(E)/E \sim .15/\sqrt{E}$

TOF

50 counters, $\sigma \leq 100$ ps
p π, K sep. $\leq$ 3 GeV

Drift Chambers

- active area - 1.5m x 1.5m
- 21 Planes
- 2.5 atm

Hadron Calorimeter

Gas avalanche ~ 2400 channels
5 cm sampling

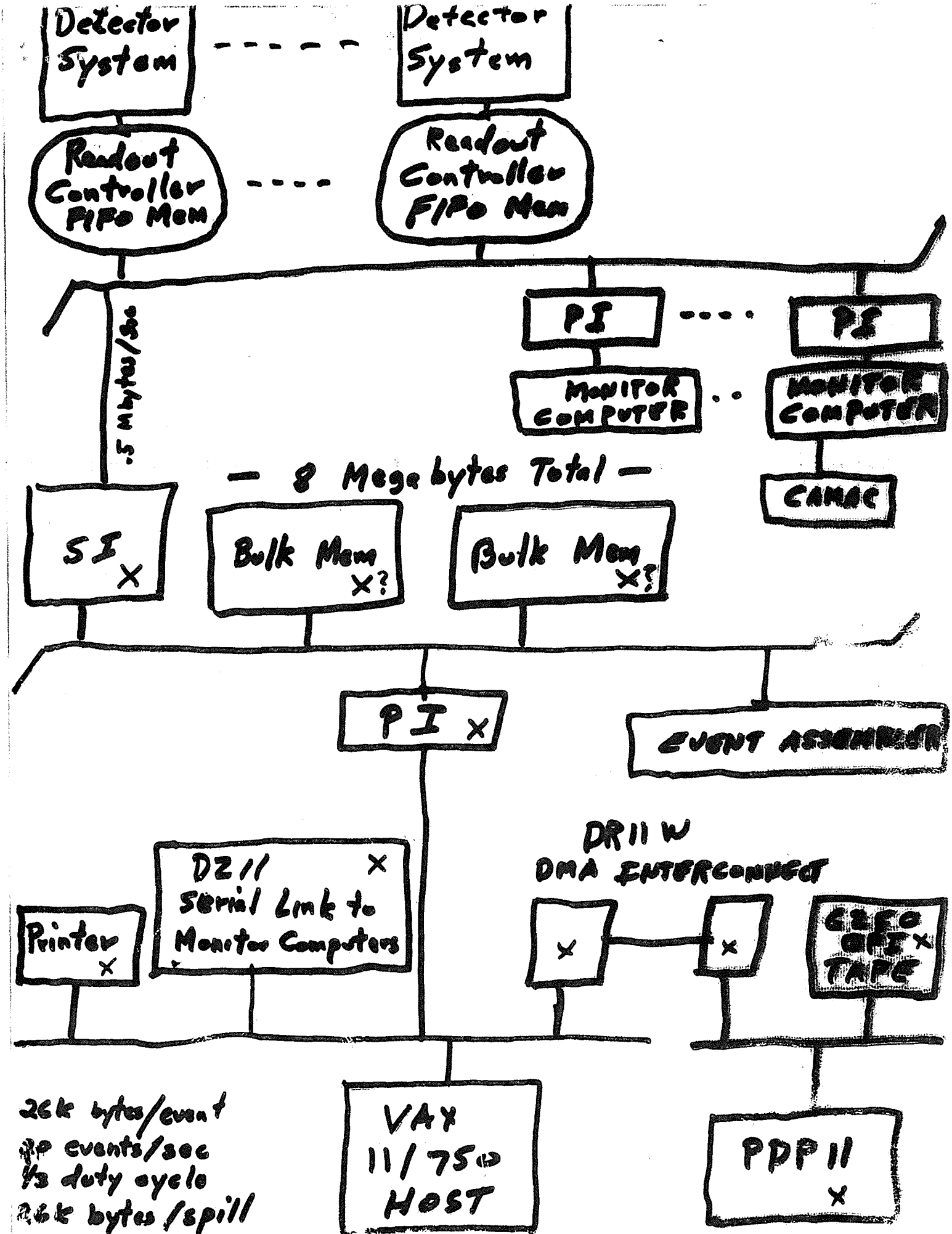
Detector System
Detector System
Readout Controller FIFO Mem
Readout Controller FIFO Mem
4 Mbytes/sec
PI
PI
MONITOR COMPUTER
MONITOR COMPUTER
CAMAC
— 8 Mega bytes Total —
SI X
Bulk Mem X?
Bulk Mem X?
PI X
EVENT ASSEMBLER
DR11 W
DMA INTERCONNECT
DZ11 X
Serial Link to Monitor Computers
Printer X
X
X
CCCO DEC TAPE
VAX 11/750 HOST
PDP11 X
2Ck bytes/event
4P events/sec
1/3 duty cycle
26k bytes/spill
to 4 Mbytes/spill

FERMILAB

→ BLDG

SCM 104 WORK

→ TOROID & STEEL

RIGGING

PREP LIST

→ COMPUTER HARDWARE

BEAM

→ EMULSION LAB

L.A. HANDLING

→ L.A. READOUT ELECTRONICS

OFF LINE COMPUTING

OTHER COMMITMENTS

E 653 PROJECTS

1. EMULSION; JAPAN
2. SSD; OSU, OU
3. DRIFT CHAMBERS; OSU
4. E.M. CALORIMETER; CMU
5. H. CALORIMETER; OU
6. MUONS; UCD
7. DATA ACQUISITION; OSU, CMU
8. COMPUTING
   ON LINE; CMU, OSU
   OFF LINE; .....

SCHEDULE

1. BEGIN TEST 1/84
2. BEGIN DATA TAKING 6/84

E653

DIRECTORS REVIEW - 1986

AICHI UNIVERSITY OF EDUCATION JAPAN
UNIVERSITY OF CALIFORNIA, DAVIS USA
CARNEGIE-MELLON UNIVERSITY USA
CHONNAM NATIONAL UNIVERSITY KOREA
FERMILAB USA
UNIVERSITY OF GIFU JAPAN
GYEONGSANG NATIONAL UNIVERSITY KOREA
JEONBUG NATIONAL UNIVERSITY KOREA
KOBE UNIVERSITY JAPAN
KOREA UNIVERSITY KOREA
NAGOYA UNIVERSITY JAPAN
OHIO STATE UNIVERSITY USA
OKAYAMA UNIVERSITY JAPAN
UNIVERSITY OF OKLAHOMA USA
OSAKA CITY UNIVERSITY JAPAN
OSAKA PREFECTURE SCIENCE
EDUCATION INST. JAPAN
SOOKMYONG WOMANS UNIVERSITY KOREA
TOHO UNIVERSITY JAPAN
WON KWANG UNIVERSITY KOREA

E653

JAPAN - KOREA - USA

10^4 $c\bar{c}$ PLUS 10^2 $b\bar{b}$ COMING FROM PROTON OR PION INTERACTIONS IN EMULSION.

PHYSICS GOALS

1) CHARGED & NEUTRAL LIFETIMES:
   - BARYONS, BEAUTY.

2) PRODUCTION DYNAMICS:
   - σ, x_F, $c\bar{c}$ AND $b\bar{b}$ CORRELATIONS! (MASS, PARTICLE TYPES, ETC.)
   - SEE ALL DECAYS -

3) NEW STATES:
   - BARYONS, EXCITED STATES, EXOTICS.

4) UNUSUAL DECAY MODES:
   - $F \to \tau$ (DOUBLE KINK POSSIBLE BECAUSE WE SEE ASSOC. CHARM.

5) MIXING:
   - EXAMPLE: $D^{\pm}$ BY CHARGE, $D^0 \to \mu^{\pm} X$ ELIMINATES CAB. 2nd SUPP. DECAY FAKING MIXING.

6) SURPRISES:
   - CAN LOOK FOR NAGOYA'S 4 CHARM EVENTS, AS HAVE GOOD EFFIC. FOR FINDING ALL DECAY VERTICES.

MOST EXPERIMENTS FORM MASS PEAK, SUPPRESS BKGND WITH VERTEX INFO.

BKGNDS TYPICALLY ~20% AS ONE DECAY IS MISSED, SO NEED 25-50 EVENTS IN PEAK TO CLAIM SIGNAL.

IN E653, BECAUSE OF EMULSION + ELECTRONIC DETECTION SEE ALL VERTICES, BKGND $\lesssim 1\%$. ASSOCIATED DECAY IS UNBIASED BY TRIGGER.

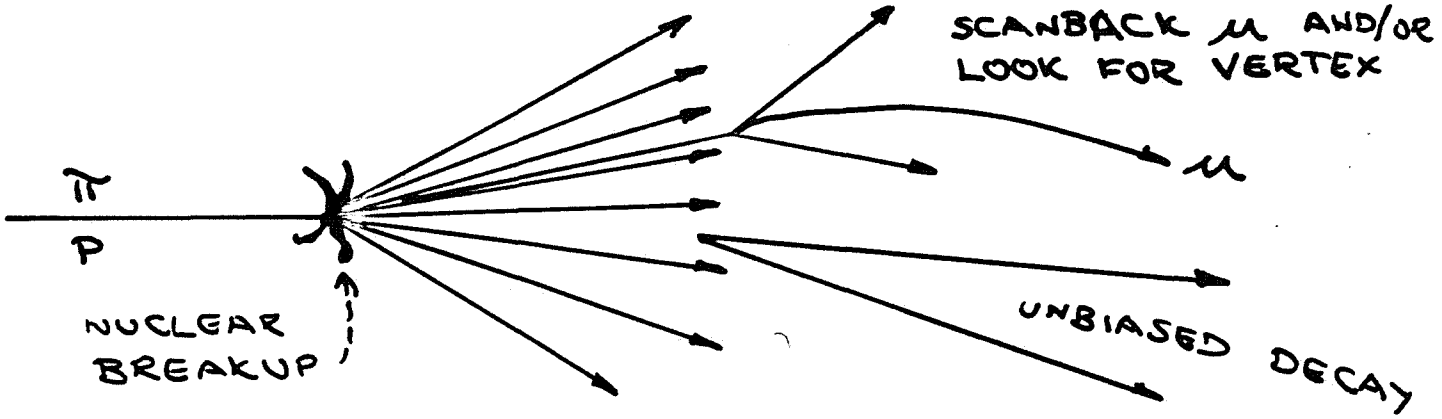

BUILD 2nd VERTEX WITH SPECTROMETER TRACKS NOT MATCHING EMULSION TRACKS COMING FROM PRIMARY.

FOR $B\bar{B}$, { SINGLE MUON CUTS $P > 8$ GeV/c, $P_T > 0.8$ GeV/c, $\ell \gtrsim 40\,\mu$ GIVES $\sim 10^{-5}$ REJECTION.

WITH THIS TECHNIQUE, 5-10 EVENTS IS ENOUGH TO ESTABLISH SIGNAL, CAN DETECT 2, 3, 4 DECAY VERTEX EVENTS WITH GOOD EFFICIENCY.

– AND WE'RE NOW BEGINNING TO DO THIS!

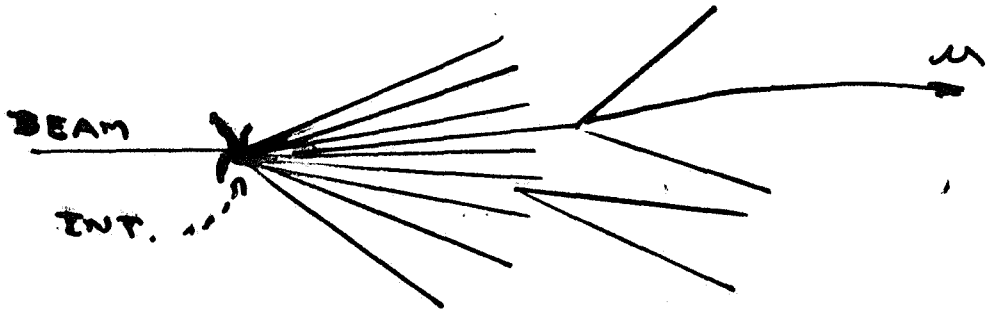

TRIG = BEAM · INT · μ

E-653 PLAN VIEW - FIRST RUN

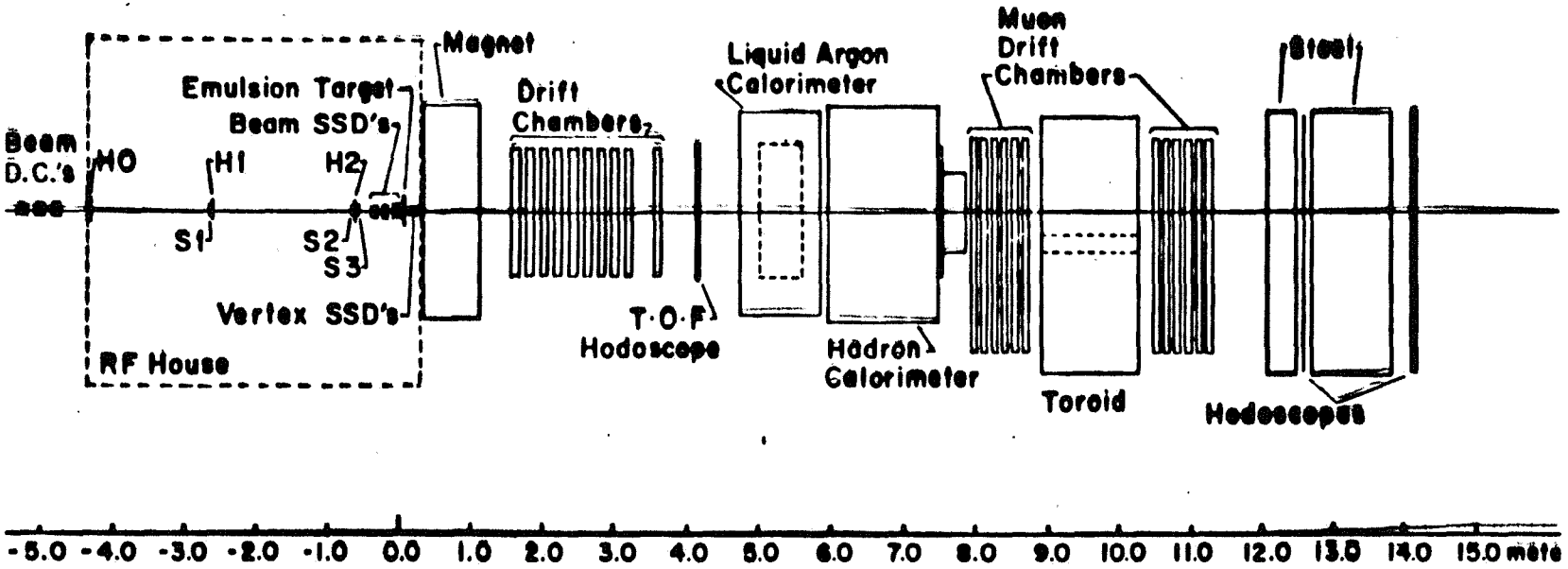

5.4 x10⁶ triggers

1300 tapes

E653 Expectations

ITEM	800 GeV P RUN 1	650 GeV π RUN 2
Total Triggers	5.4×10^6	8×10^6
Triggers after cuts	$\sim 2.0 \times 10^6$	$\sim 4.5 \times 10^6$
Equivalent Interactions	4.2×10^7	1.1×10^8
$\sigma_{c\bar{c}}$ / Nuc	$30 \mu b$	$30 \mu b$
$c\bar{c}$ A dependence	$A^{0.8}$	$A^{0.8}$
$\sigma_{B\bar{B}}$ (WA 78 / WA 75)	~ 8 nb	~ 24 nb
$B\bar{B}$ A dependence	A^1	A^1
$c\bar{c}$ efficiency	.026	.026
$B\bar{B}$ "	.12	.12
$c\bar{c}$ pairs found	~ 2000	~ 8000
$B\bar{B}$ " "	~ 4-5	~ 45

TODAY'S SCHEDULE

I INTRO - REAY (HE'S DONE)

II FIRST RUN

A. TRACKING - SIDWELL

B. EMULSION - NIU
(A LITTLE 2nd RUN CREEPS IN)

C. CALORIMETRY - LIPTON

D. PLAN FOR ANALYSIS - DUNLEA

III PION SECOND RUN

A. IMPROVEMENTS - WILLIS

B. REQUESTS - VOLK

Vertex Finding

Sidwell

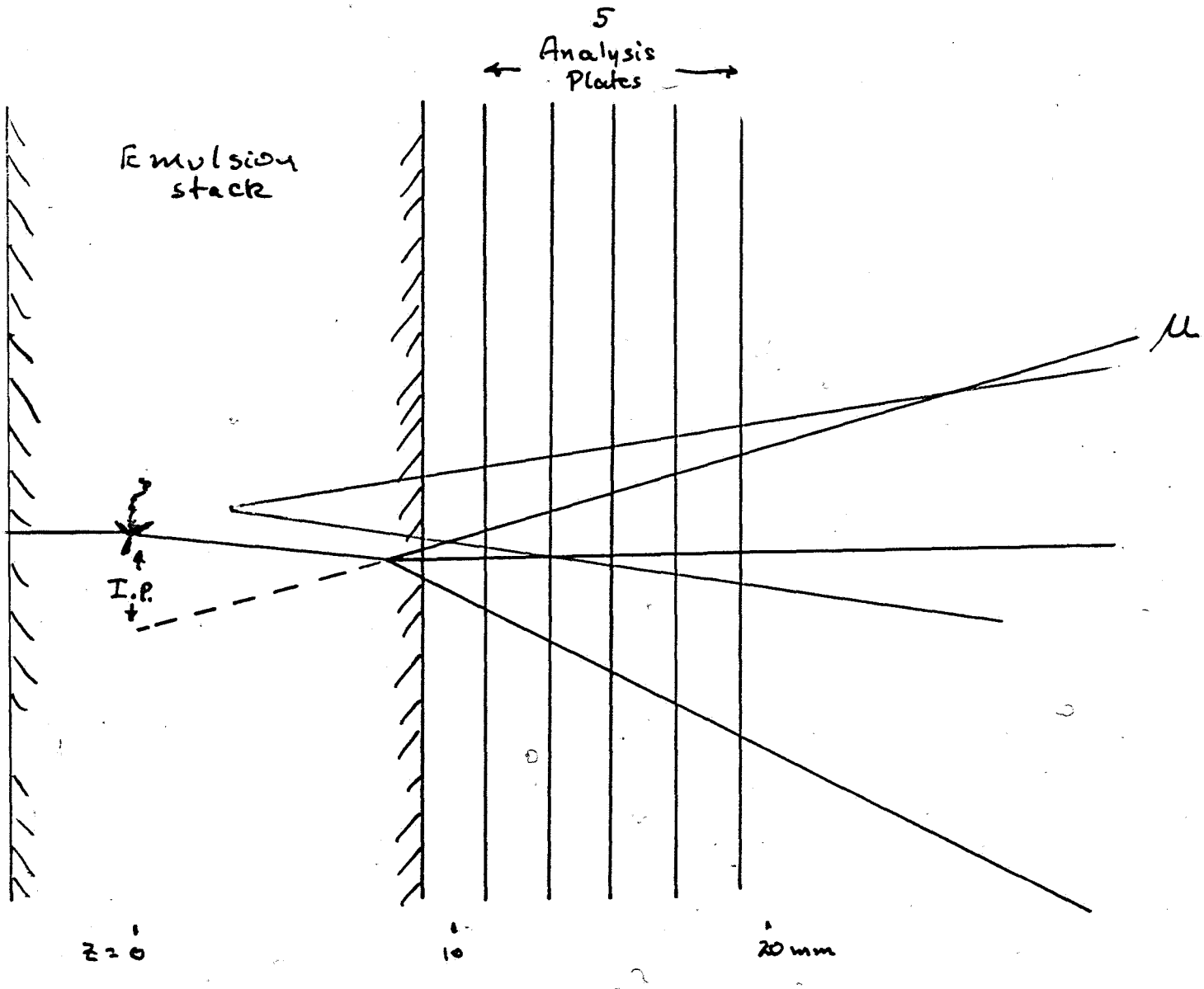

For 40 GeV D^+ ($x_F = 0$):

D.l. ≃ 6 mm

I.P. = 300 μ / track

Interesting events:

Secondary with tagged μν

OR

μν passing modest $P_\perp$, I.P.

PARAMETERS

Detector	# Planes	Resolution / Plane
Beam SSDs	9	8 μ
Vertex SSDs	18	8 μ in center 23 outer strips
Drift Chambers	50	110 - 140 μ
Muon Chambers	24	500 μ

$\Delta p = a p^2$ $\quad a \approx 2.5 \times 10^{-4} \Rightarrow 1.2\%$ at 50 GeV

Primary Vertex : $\quad \delta x, y = 6.5 \mu$ typical

$\delta z \quad 300 \mu$

DATE 05/12/86 NO = 15

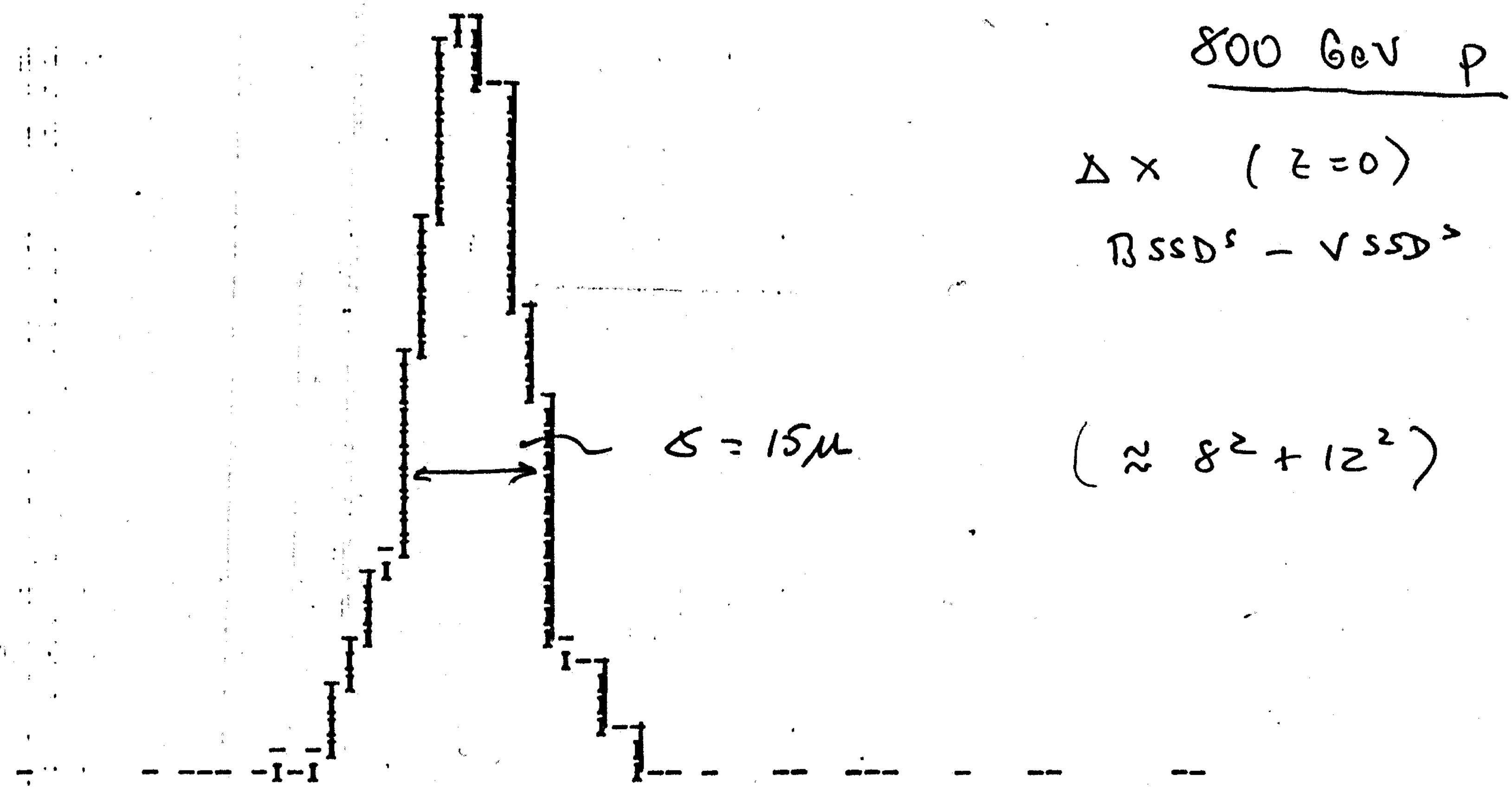


```
  2         3         4         5         6         7         8         9         1
                                                                                    0
67890123456789012345678901234567890123456789012345678901234567890123456789012345678901234567890

                              122456776643111
          1      1 111 24239302017004345312552 1 1    11  111   1    11      21

------------------------------------------------------------
1111111111111111                              11111111111111111111112222222222
7766554433221100998877665544332211   1122334455667788990011223344556677889900112233 44
5050505050505050505050505050505050505 50505050505050505050505050505050505050505050505

ALL CHANNELS = 0.6450E+03      * UNDERFLOW = 0.2100E+02      * OVERFLOW = 0.3000E+02
MEAN VALUE   = 0.2516E+01      * R . M . S = 0.2783E+02      * ABNOR CHA=  0.0000E+00
```

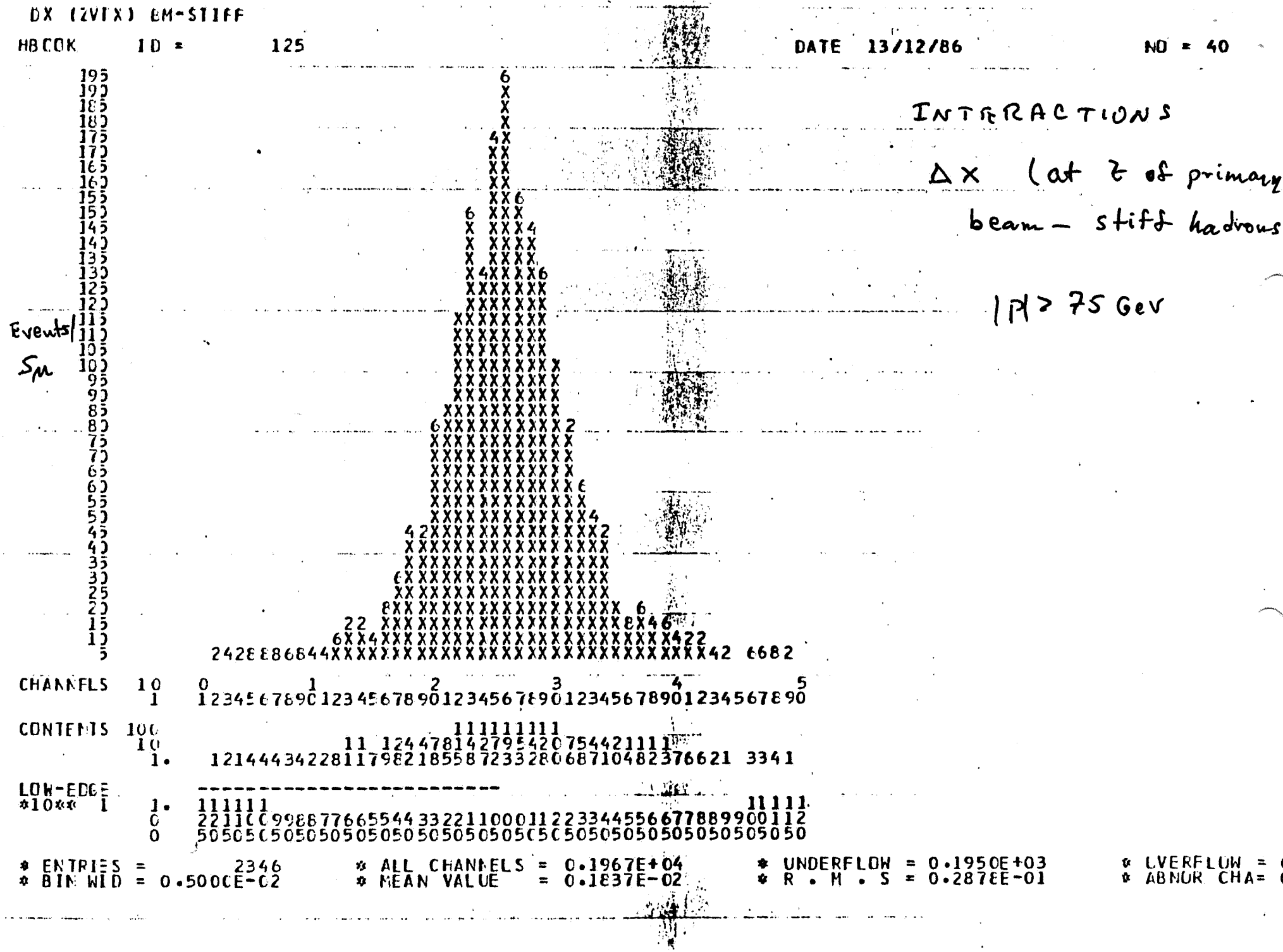
DX (ZVTX) BM-STIFF
HBCOK ID = 125
DATE 13/12/86
NO = 40
Events/
SM
INTERACTIONS
Δx (at z of primary)
beam – stiff hadrons
|P| > 75 GeV
CHANNELS
CONTENTS
LOW-EDGE
* ENTRIES = 2346
* ALL CHANNELS = 0.1967E+04
* UNDERFLOW = 0.1950E+03
* OVERFLOW =
* BIN WID = 0.5000E-02
* MEAN VALUE = 0.1837E-02
* R . M . S = 0.2878E-01
* ABNOR CHA =

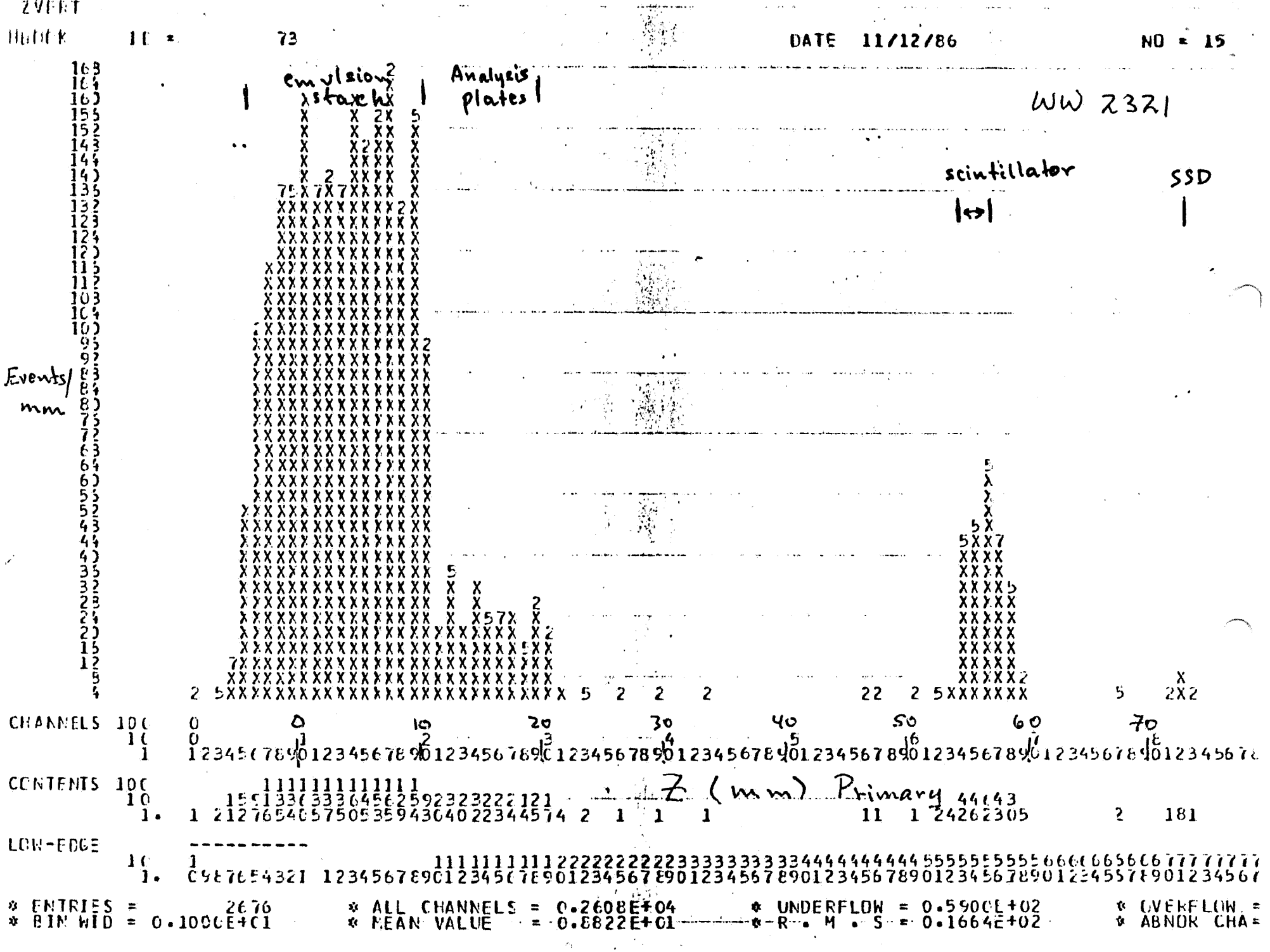
ZVERT
HISTOGRAM ID = 73
DATE 11/12/86
NO = 15
emulsion stack
Analysis plates
WW 2321
scintillator
SSD
Events/mm
Z (mm) Primary
CHANNELS
CONTENTS
LOW-EDGE
* ENTRIES = 2676
* ALL CHANNELS = 0.2608E+04
* UNDERFLOW = 0.590CE+02
* OVERFLOW =
* BIN WID = 0.100CE+C1
* MEAN VALUE = 0.8822E+01
* R.M.S = 0.1664E+02
* ABNOR CHA=

EXPANDED

ID = 74 DATE 11/12/86 WW2321 NO = 16

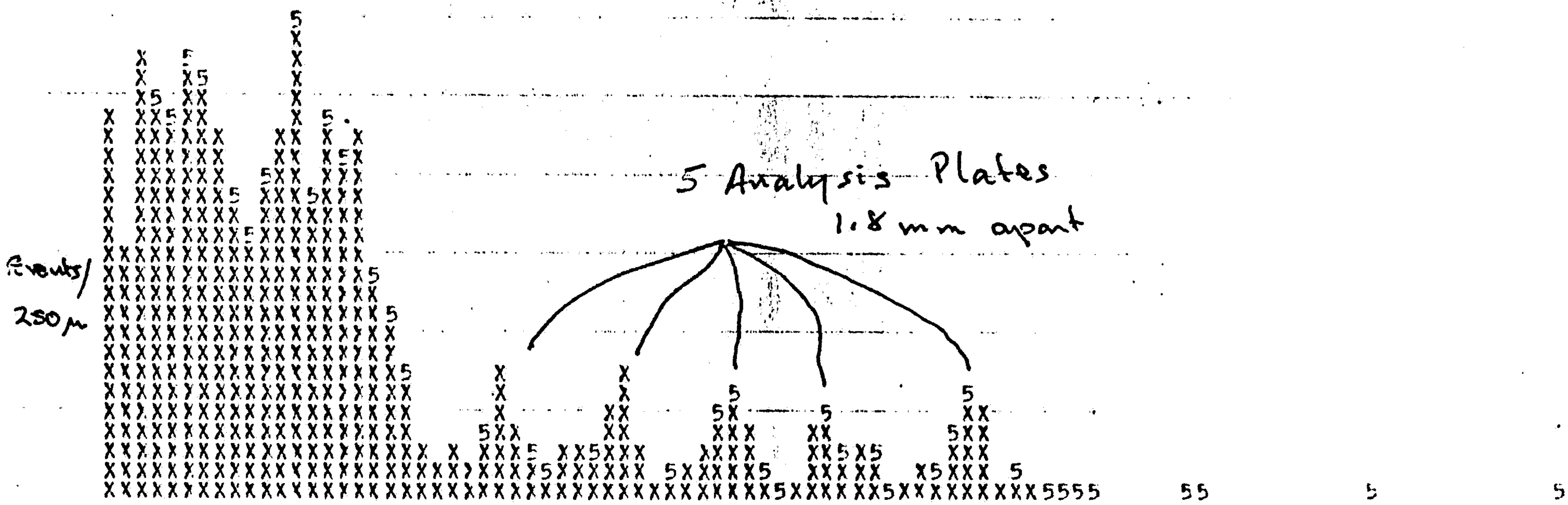


```
100   0                                                                                                   1
 10   0         1         2         3         4         5         6         7         8         9         0
  1   1234567890123456789012345678901234567890123456789012345678901234567890123456789012345678901234567890

 10   42443443323343333211      1     11     1          11
  1.  05619553817389195839364647485366504623469183128956512437102321111       11         1           1

 10                     111111111111111111111111111111111111111111 22222222222222222222222222222222222222222
  1.  55556666777788889999000011112222333344445555666677778888999900001111222233334444555566667777888899999
  0   02570257025702570257025702570257025702570257025702570257025702570257025702570257025702570257025702570
  0   05050505050505050505050505050505050505050505050505050505050505050505050505050505050505050505050505050
```

= 2676 * ALL CHANNELS = 0.9330E+03 * UNDERFLOW = 0.1479E+04 * OVERFLOW = 0.2640E+03

= 0.2500E+00 * MEAN VALUE = 0.9252E+01 * R . M . S = 0.3870E+01 * ABNOR CHA = 0.0000E+00

Z of primaries

TEST EVENT PREDICTION

Analyze 124 IC triggers (30 tapes) in Mid October ⇒ 500 predictions

Results so far:

Primaries — finding effic = 96%

$\Delta x, y \simeq 7-9\mu$

$\Delta z = 300\mu$

17 events with charm candidates

Use to debug + refine algorithms

Extrapolated 1st Run Yield

$$\text{Yield} = \frac{5.4 \times 10^6 \text{ trig}}{1.2 \times 10^5 \text{ trig}} \times 17 = 740$$

improve μ algorithms × 1.75 (November)

Improve I.P., vertex quality × 1.3 ?

1700 pairs

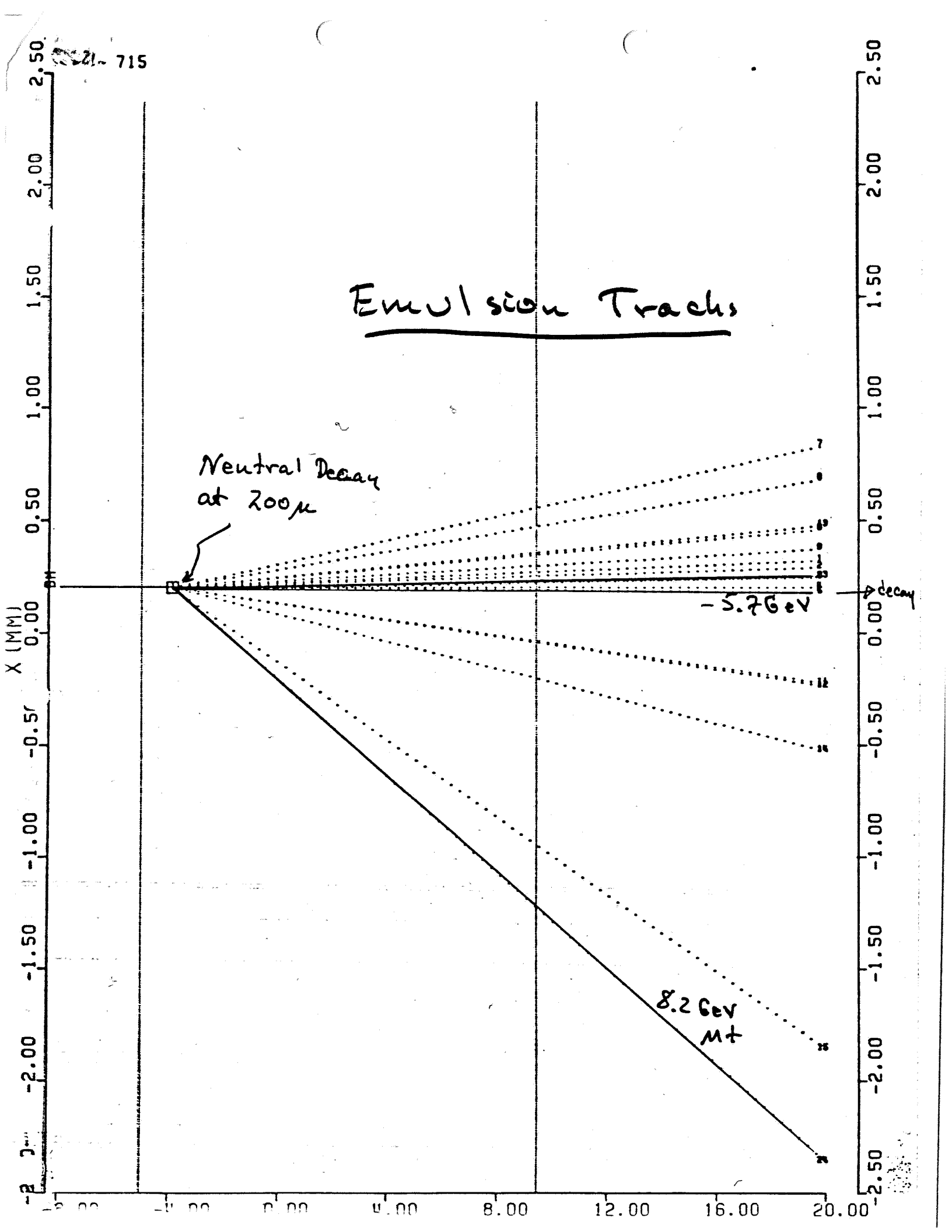
Emulsion Tracks
Neutral Decay
at 200μ
-5.76 eV
8.2 GeV
M+
decay
X (MM)
2.50
2.00
1.50
1.00
0.50
0.00
-0.50
-1.00
-1.50
-2.00
-2.50
8.00
12.00
16.00
20.00

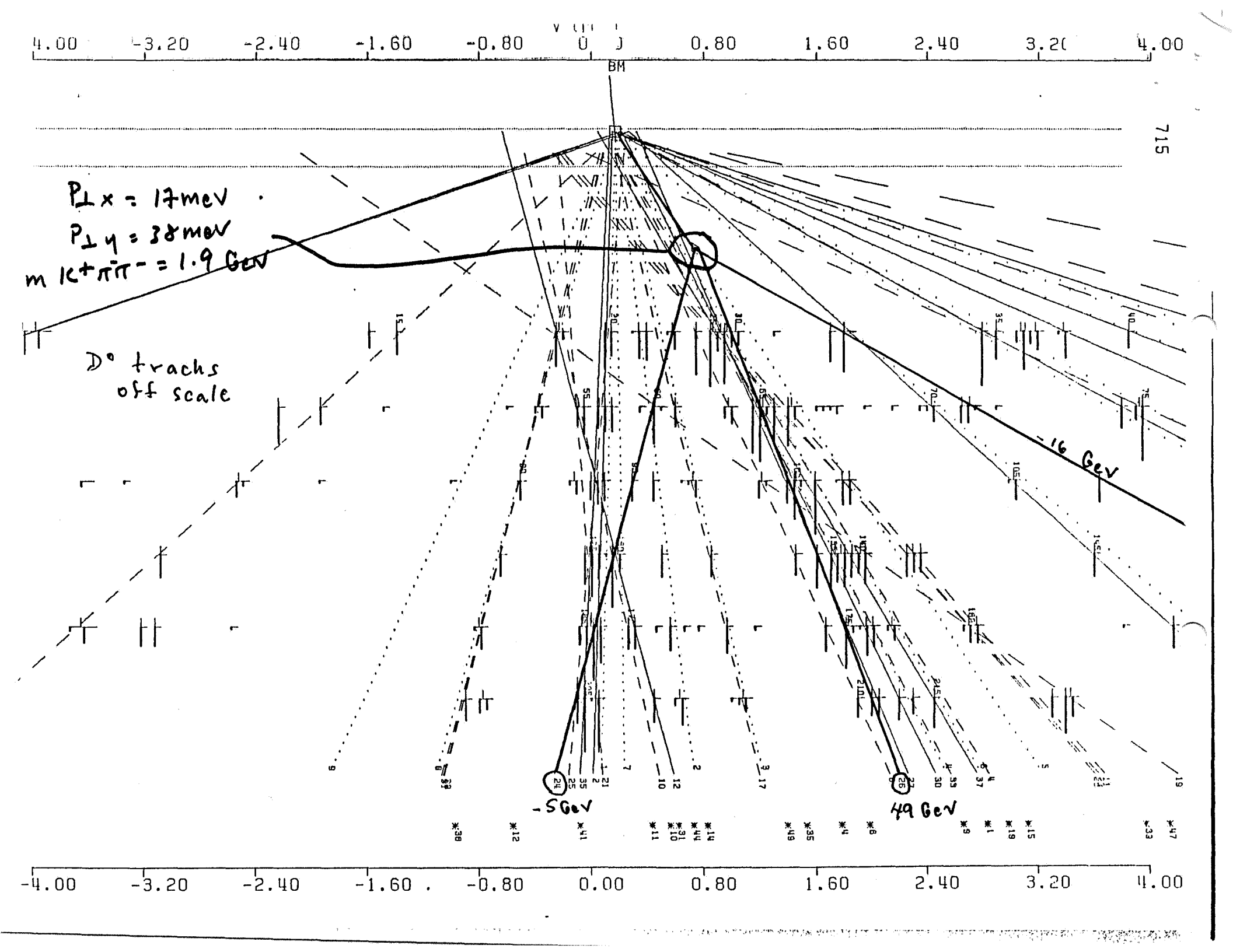
4.00 -3.20 -2.40 -1.60 -0.80 0.80 1.60 2.40 3.20 4.00
BM
715
$P_{\perp x}$ = 17mev
$P_{\perp y}$ = 38mev
m $K^+\pi\pi^-$ = 1.9 GeV
D° tracks off scale
16 GeV
5 GeV
49 GeV
-4.00 -3.20 -2.40 -1.60 -0.80 0.00 0.80 1.60 2.40 3.20 4.00

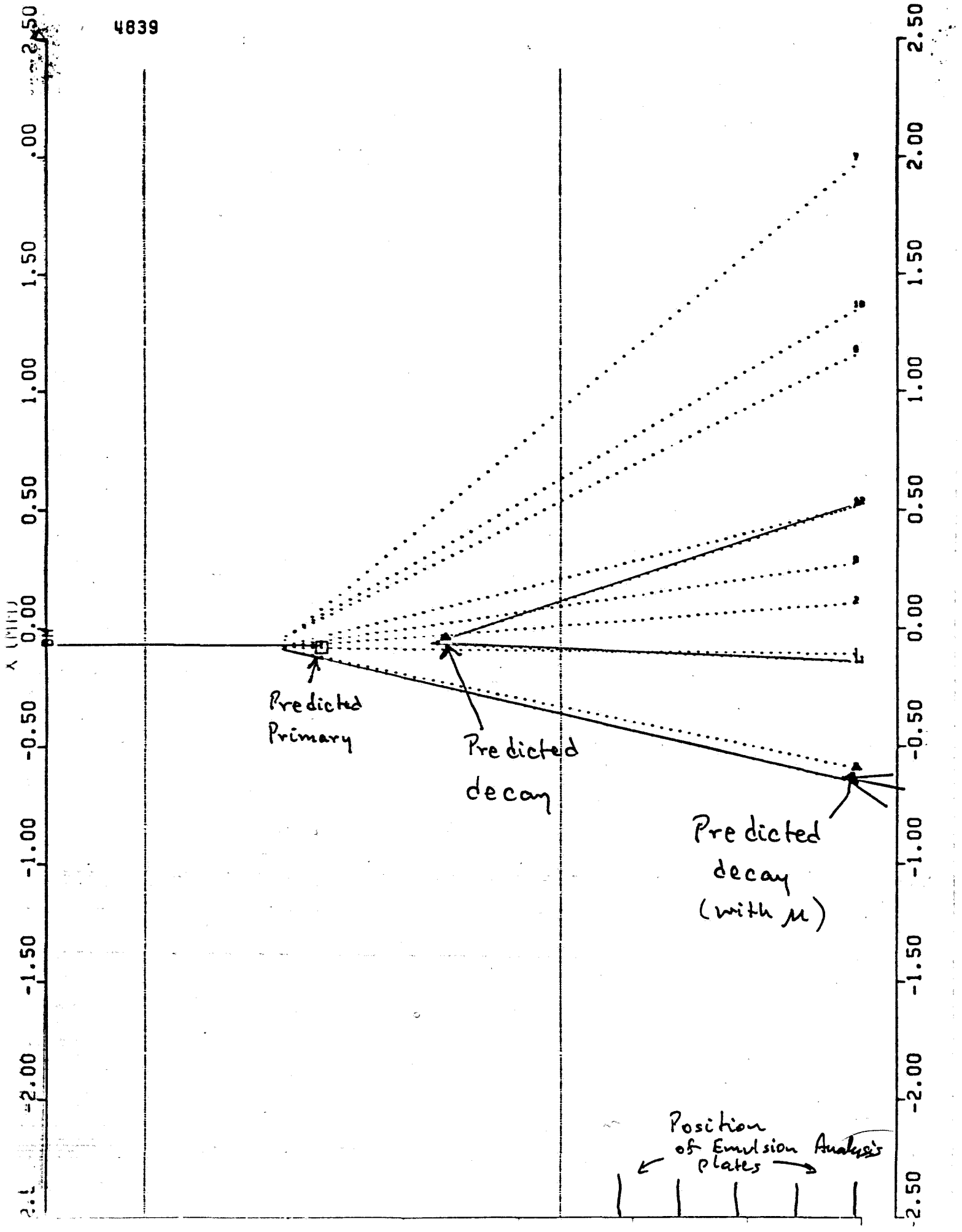
4839
2.50
2.00
1.50
1.00
0.50
0.00
-0.50
-1.00
-1.50
-2.00
-2.50
Predicted Primary
Predicted decay
Predicted decay (with μ)
Position of Emulsion Analysis plates

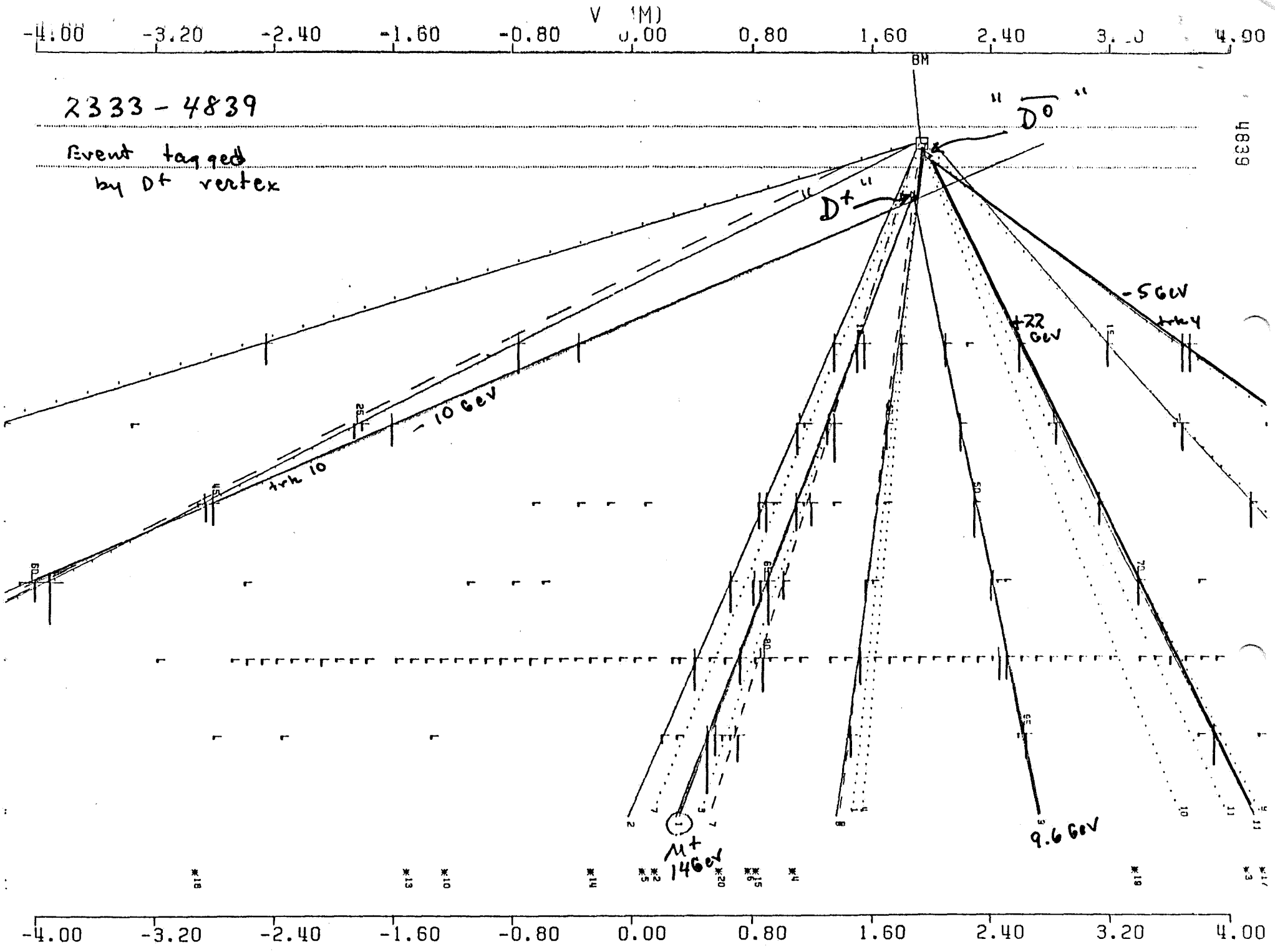
V (M)
-4.00
-3.20
-2.40
-1.60
-0.80
0.00
0.80
1.60
2.40
3.20
4.00
2333 - 4839
Event tagged by D+ vertex
4839
BM
"D0"
D+
-5 GeV
trk 4
+22 GeV
-10 GeV
trk 10
9.6 GeV
μ+ 146 GeV

86/12/18

Emulsion Works in E653 1st Run and A New Emulsion Technique to be used in the 2nd Run

K. Nin

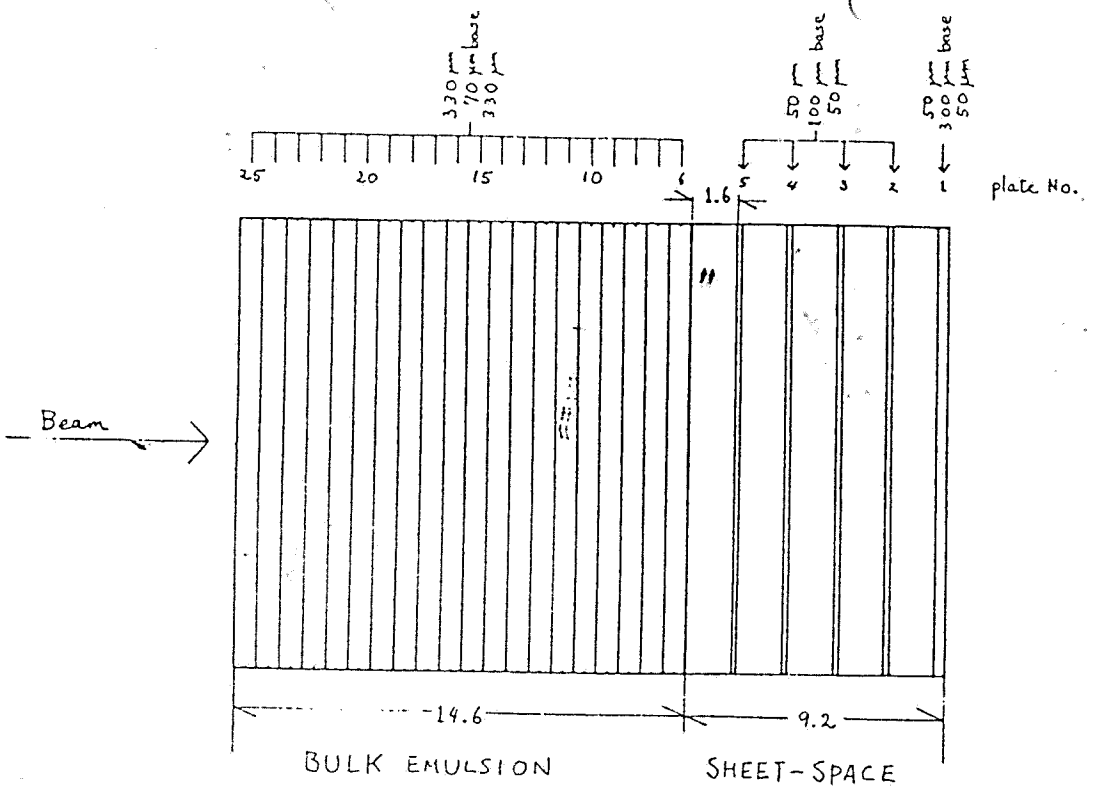

11

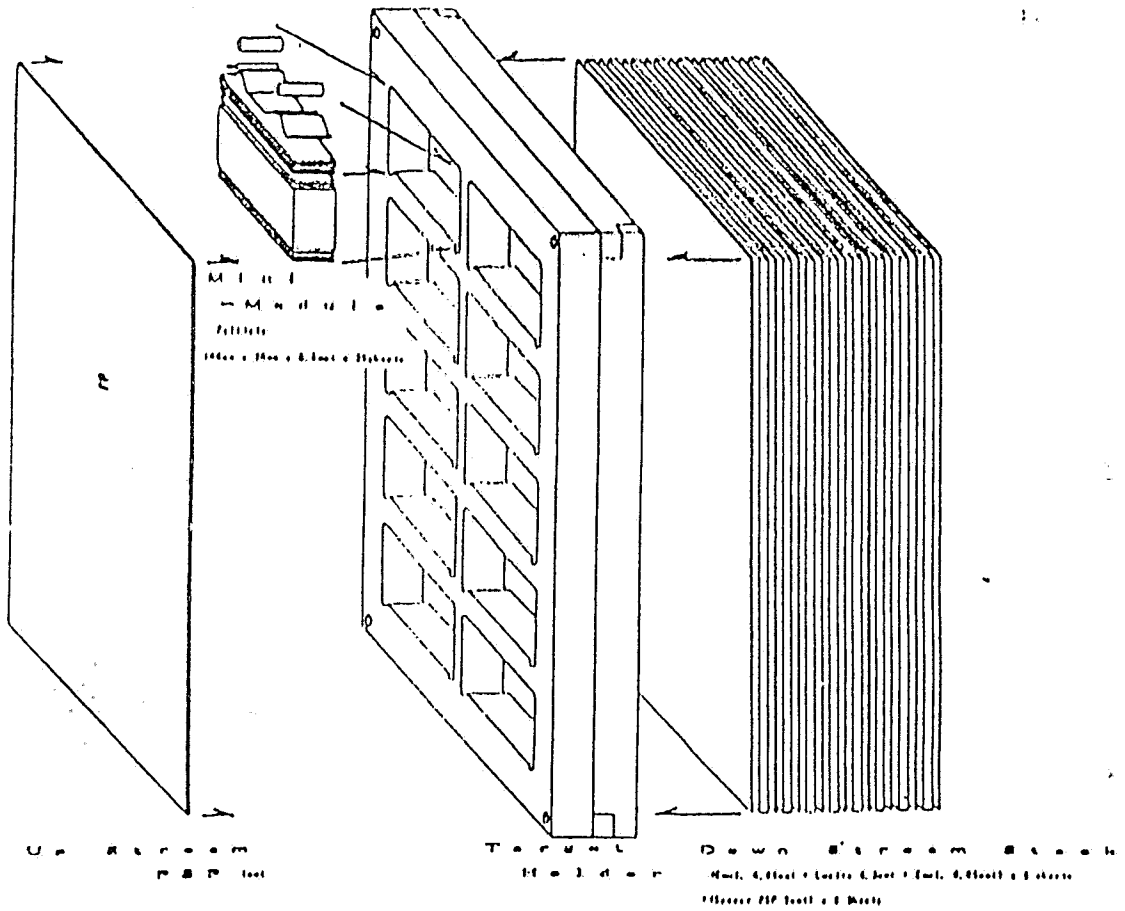

TARGET STRUCTURE
OF HORIZONTAL MODULE

beam 3 mm φ

10^5/spill

spill time 20"

painting

$\rho \gtrsim 10^5/cm^2$

スター ピッチ

	Δρ
3mm	⋮
2mm	⋮
1mm	↓

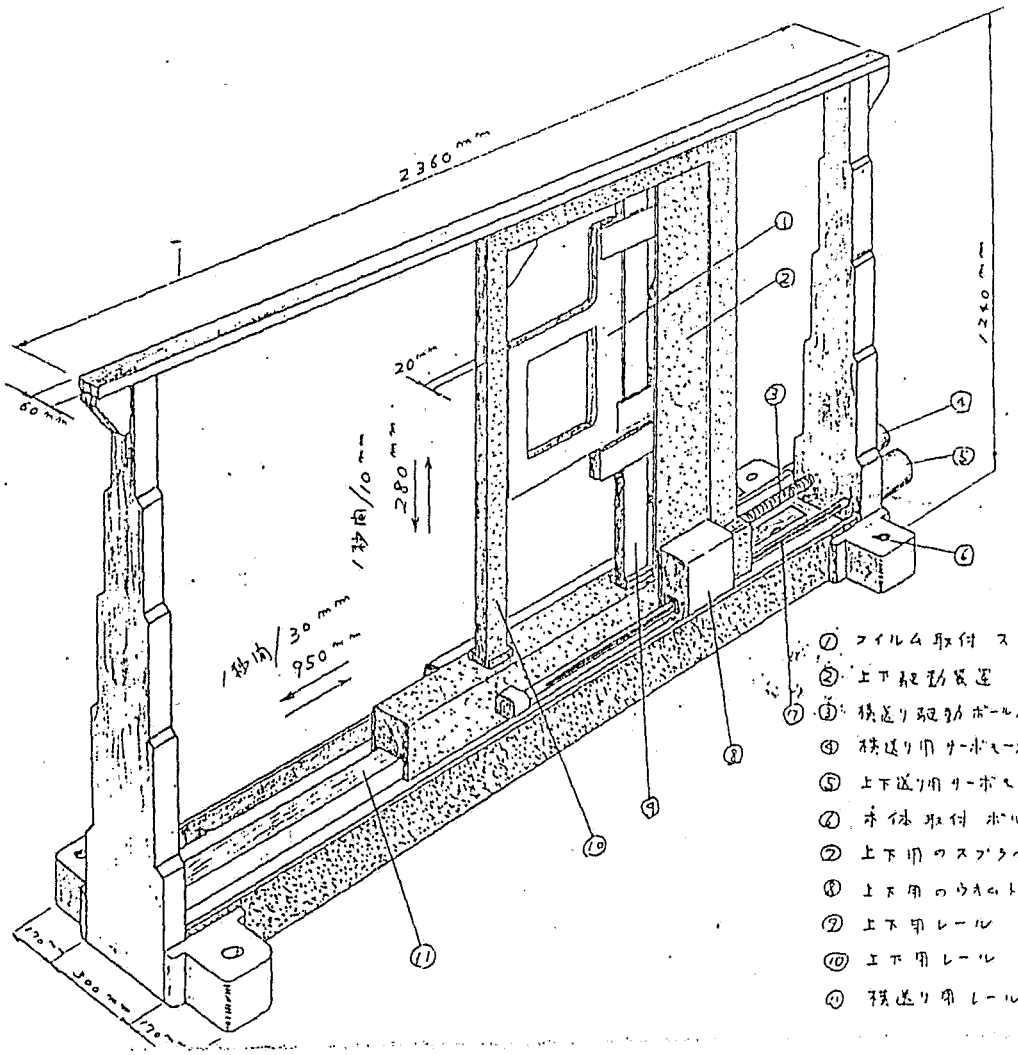

$\Delta Z = Z_{predicted} - Z_{emulsion}$

WITH DECAY
2 ary INT.

15 events

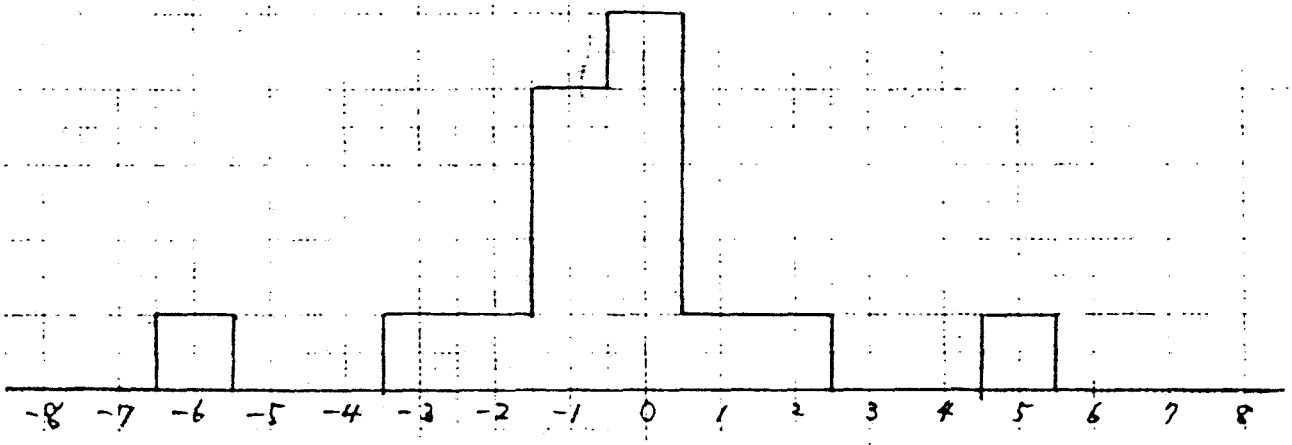

NO DECAY
2 ary INT.

87 events

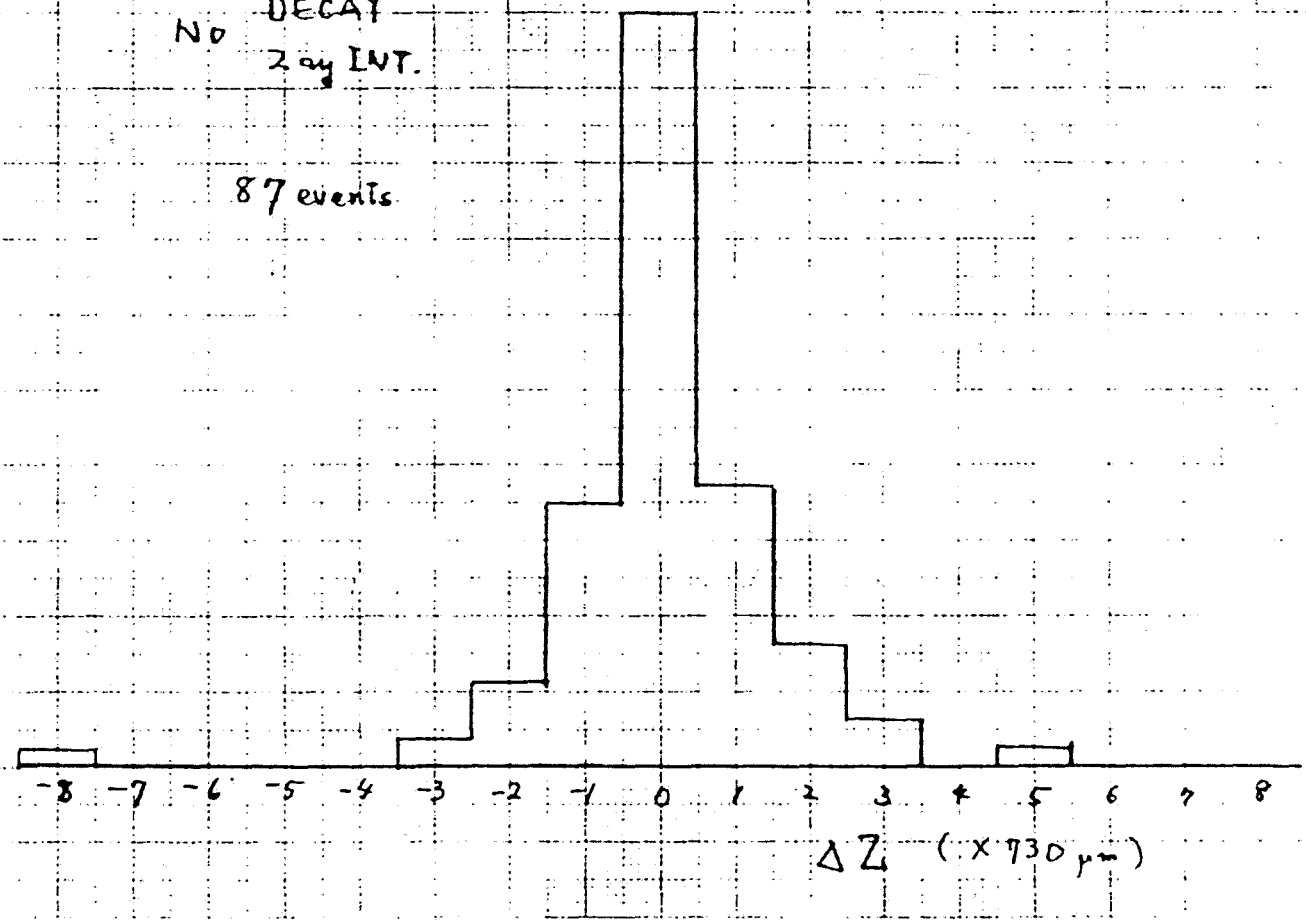

DEPARTMENT OF PHYSICS
NAGOYA UNIVERSITY

DATE .....

NO. .....

	NAGOYA	OSAKA	KOBE		
Decay Search	Follow Down		Scan Back		
Status	almost F.D. ^ Completed (Scan Back not yet)	Very Preliminary		Non VTI-TRK: μon	Non VTI-TRK: others
In Fiducial	237 evts	92 evts	103 evts	38	143 → After Cut
Analysed	237	92	36	33	24
Not Found	1	13		3	5
Found	236	79		30	19
	(99.6%)	(86%)			
μ → 1ry match	197	48		25	19
	(83%)			(83%)	
μ → non match	39	4			
Follow Down	3*				
With 2ry Ints	9	9+7		4	2 → 2ry Int
(Expected)	(9)	(16)			2 → e pair
μ→2ry μ→1ry μ→missing	3 3 19				
With Decay Cand.	11	0 3		1	2 Decay
Pair $\mu \to \{^{N2\cdot N4}_{C3}$	3+1				
" μ → Kink	1				
Single $\mu \to \{^{N2\cdot N4}_{C3}$	2-1			1	
" μ → Kink	1				
Single non μ $\{^{N2\cdot N4}_{C3}$	2 (another μon predicted)	2			1
" non μ · Kink	1 1				1
Pair non μ $\{^{N2\cdot N4}_{C3}$	0	1			
" non μ · kink	1				

Need Scan Back

236 events

EVENT CHECK

(5~10 min)

μ match

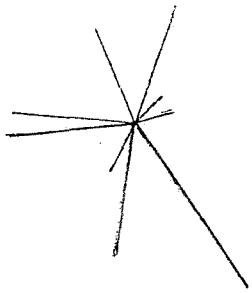

μ non match

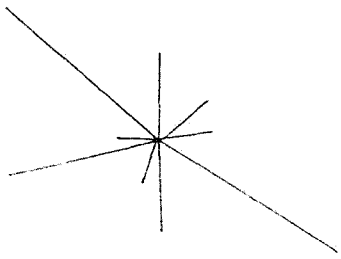

Stop Analysis

197 events

Continue Measurement

39 events

DECAY SEARCH

(1~2 hr)

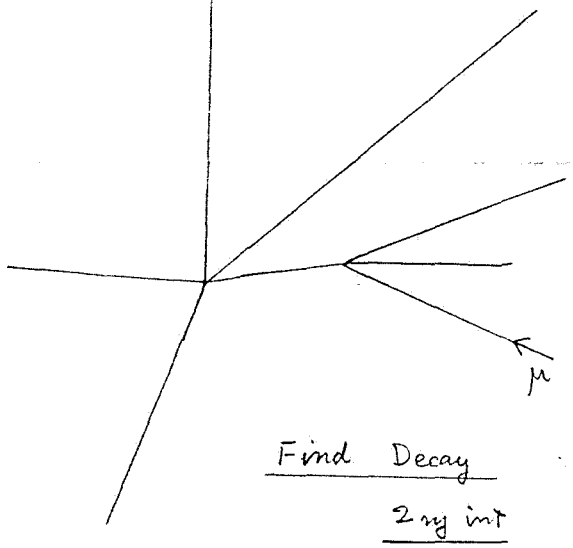

Find Decay

2 ry int

197 × 10 min = 1970 min < 39 × 120 min = 4680 min

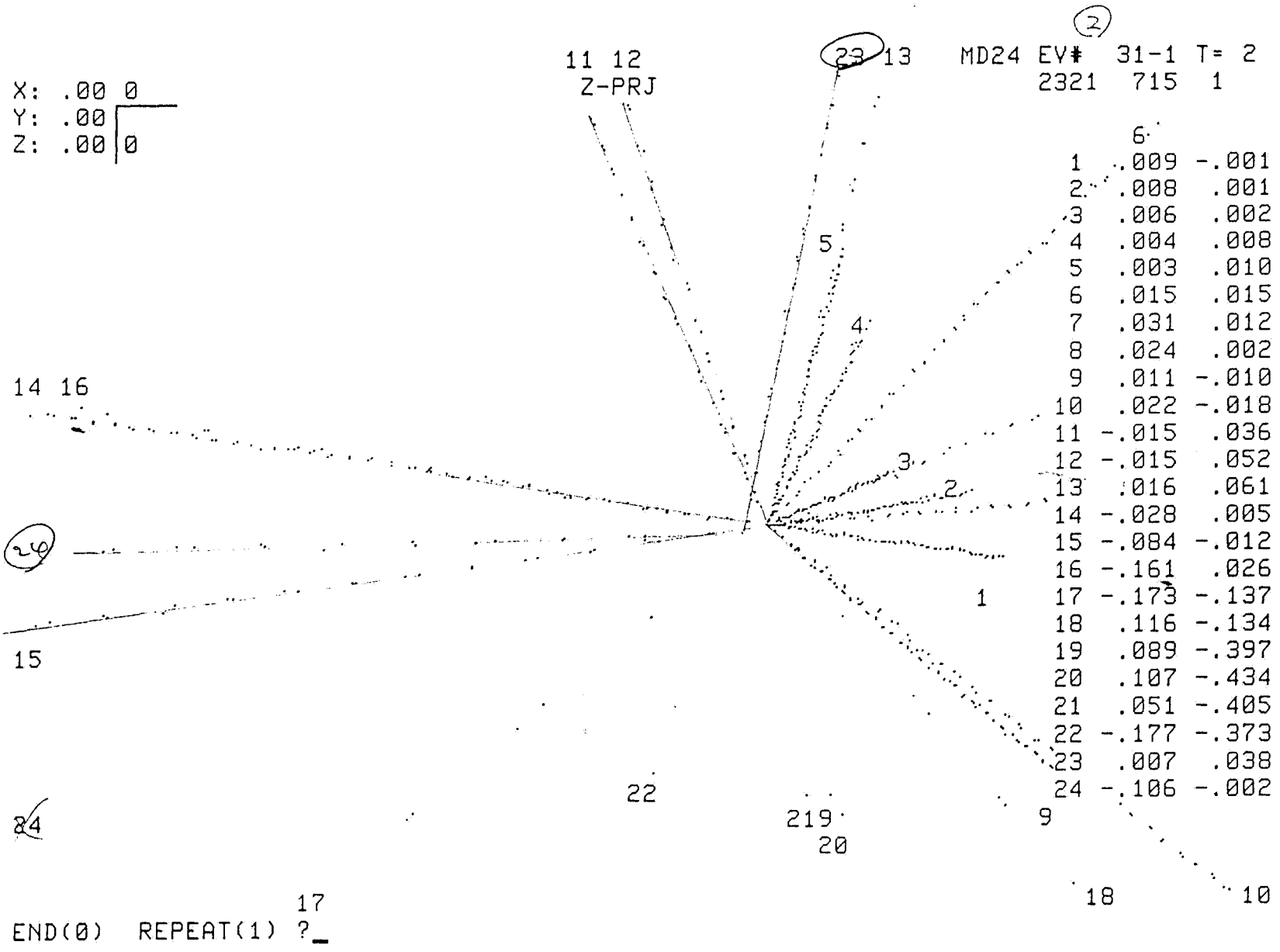
X: .00 0
Y: .00
Z: .00 0
11 12
Z-PRJ
23 13
MD24 EV# 31-1 T= 2
2321 715 1
14 16
15
24
22
219
20
9
18
10
17
END(0) REPEAT(1) ?_
1 .009 -.001
2 .008 .001
3 .006 .002
4 .004 .008
5 .003 .010
6 .015 .015
7 .031 .012
8 .024 .002
9 .011 -.010
10 .022 -.018
11 -.015 .036
12 -.015 .052
13 .016 .061
14 -.028 .005
15 -.084 -.012
16 -.161 .026
17 -.173 -.137
18 .116 -.134
19 .089 -.397
20 .107 -.434
21 .051 -.405
22 -.177 -.373
23 .007 .038
24 -.106 -.002

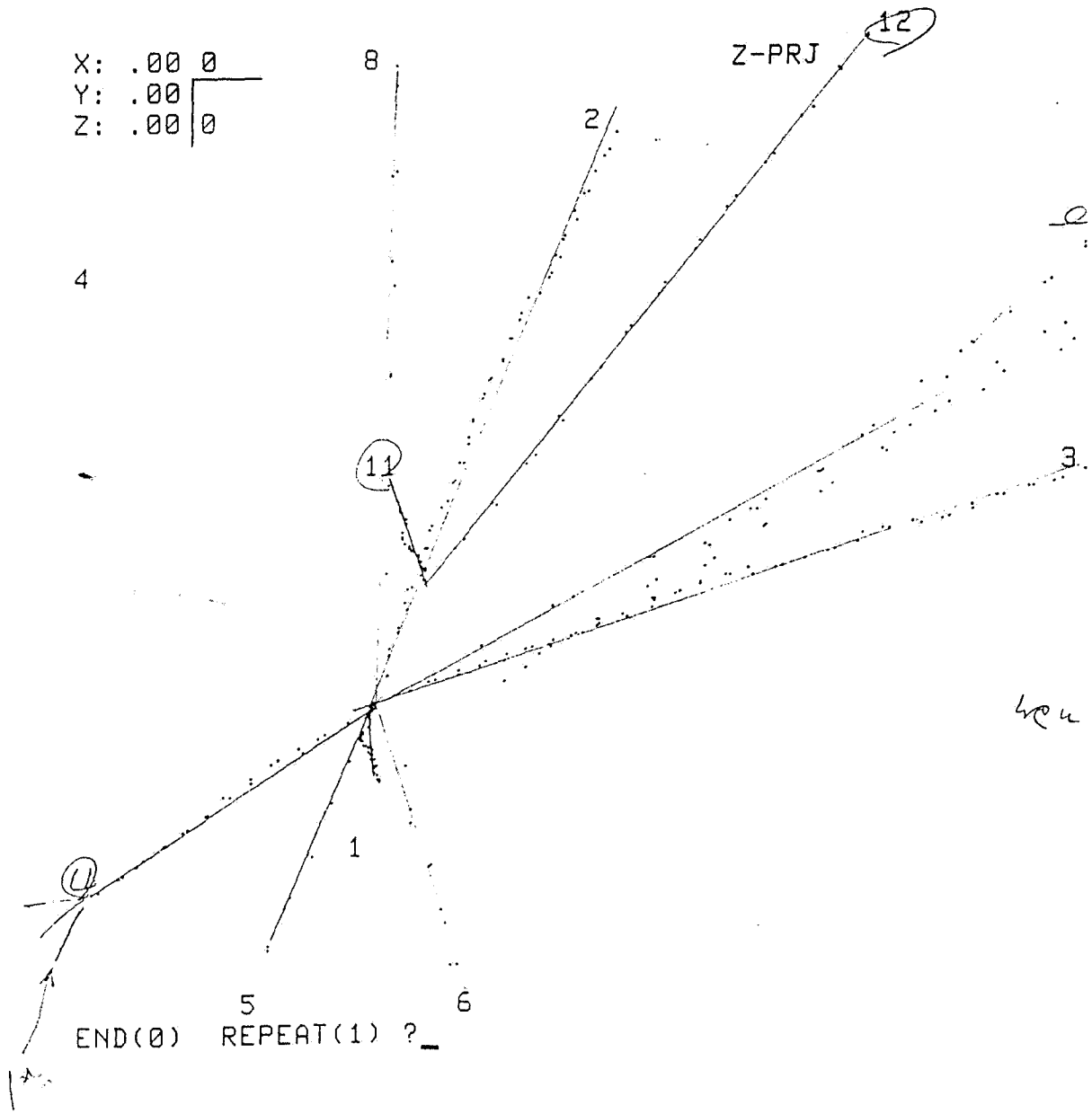

MD24 EV# 217-1 T= 2
2333 4839 3.

1	.000	-7003
2	.011	.025
3	.031	.010
4	-.027	-.019
5	-.023	-.058
6	.020	-.062
7	.102	.051
8	-.000	.128
9	.060	.046
10	.070	.049
11	-.003	.007
12	.041	.052

DECAY CANDIDATE EVENT

RUN-EVENT TYPE FOUND BY
1714-3002 TRIDENT SCAN BACK

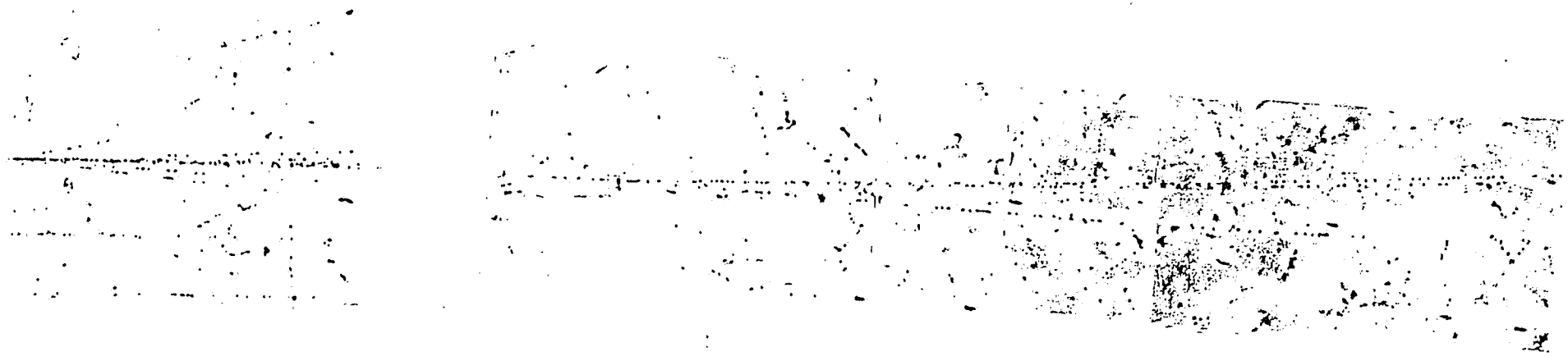

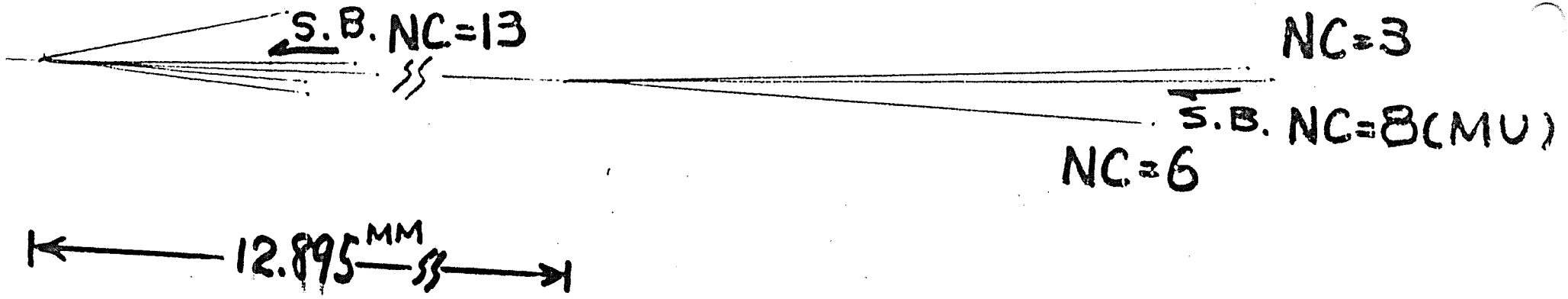

Receiving Reel

{ RESOLUTION 1 μm
{ COMPLETE 2 DIMENSION

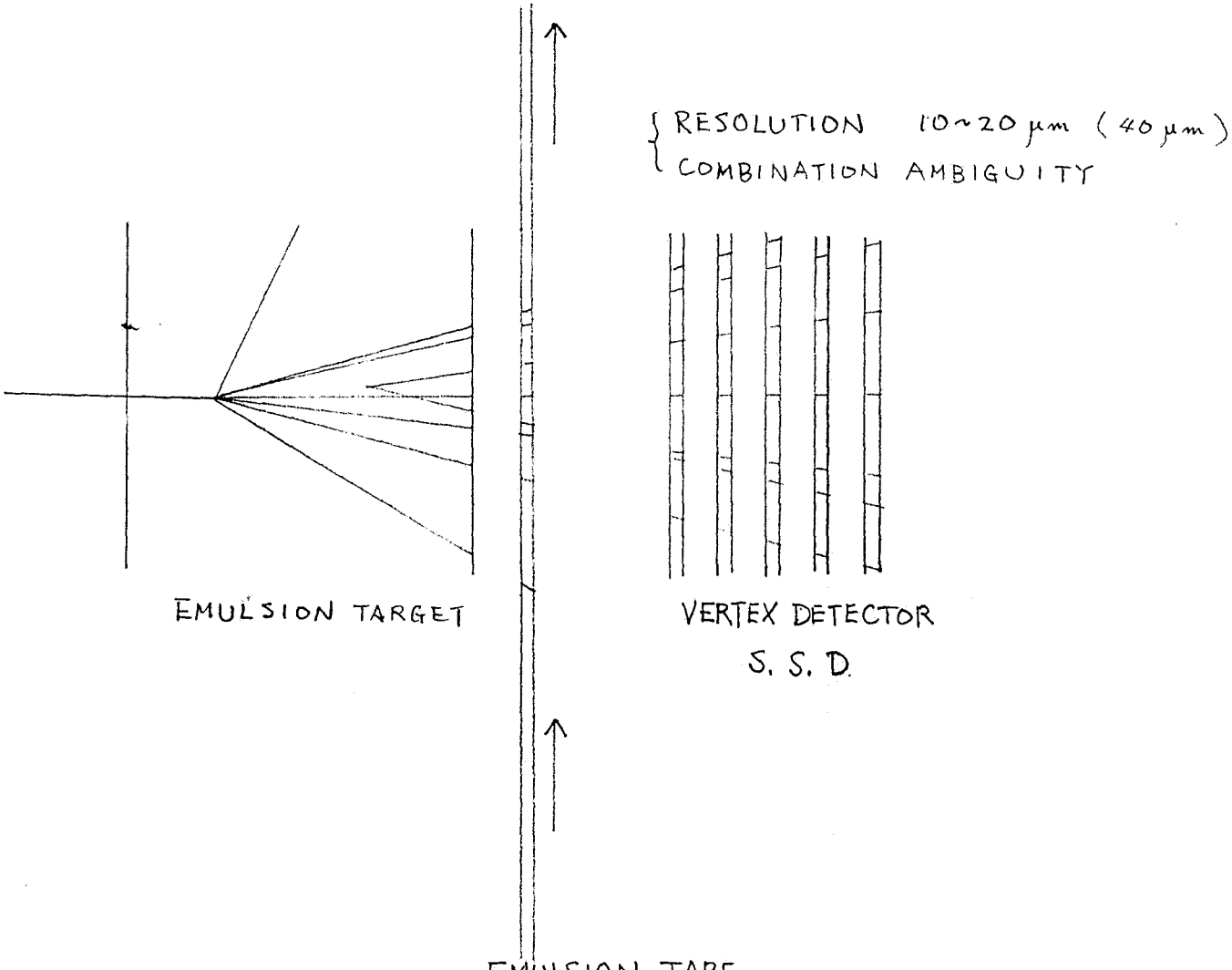

Feeding Reel

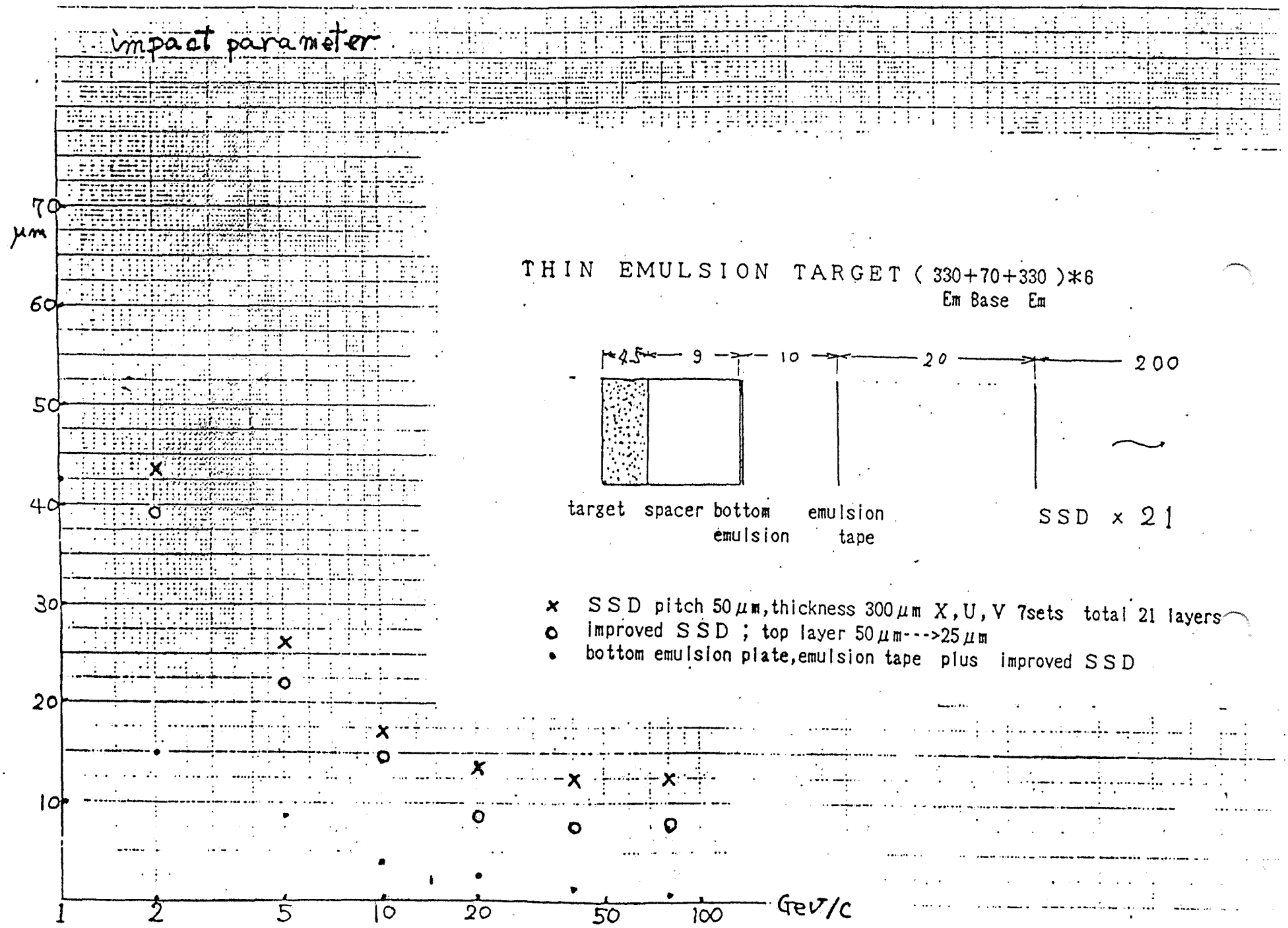
impact parameter
70
μm
60
50
40
30
20
10
1
2
5
10
20
50
100
GeV/c
THIN EMULSION TARGET (330+70+330)*6
Em Base Em
4.5
9
10
20
200
target
spacer
bottom emulsion
emulsion tape
SSD x 21
× SSD pitch 50μm, thickness 300μm X, U, V 7sets total 21 layers
o improved SSD ; top layer 50μm--->25μm
• bottom emulsion plate, emulsion tape plus improved SSD

MOD: U - 24 TAG: 42
RUN: 2321 EVT: 1948 DST: 2 TYPE: 1

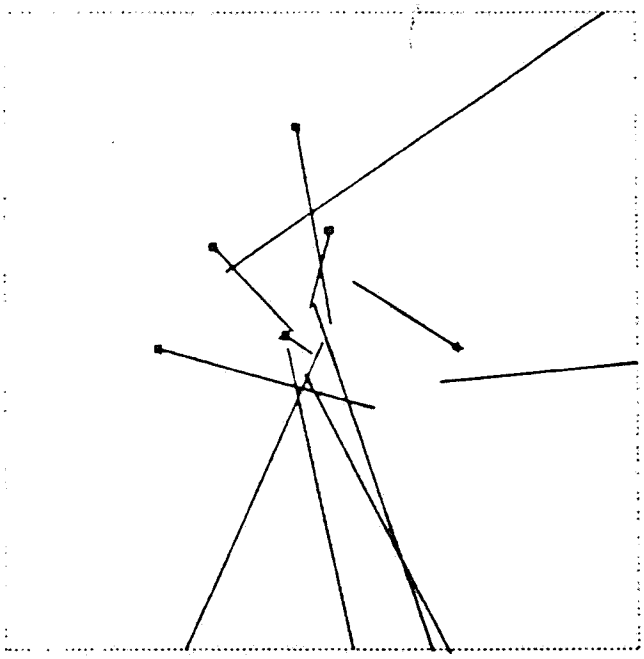

MOD: U - 24 TAG: 42
RUN: 2321 EVT: 1948 DST: 2 TYPE: 1

original

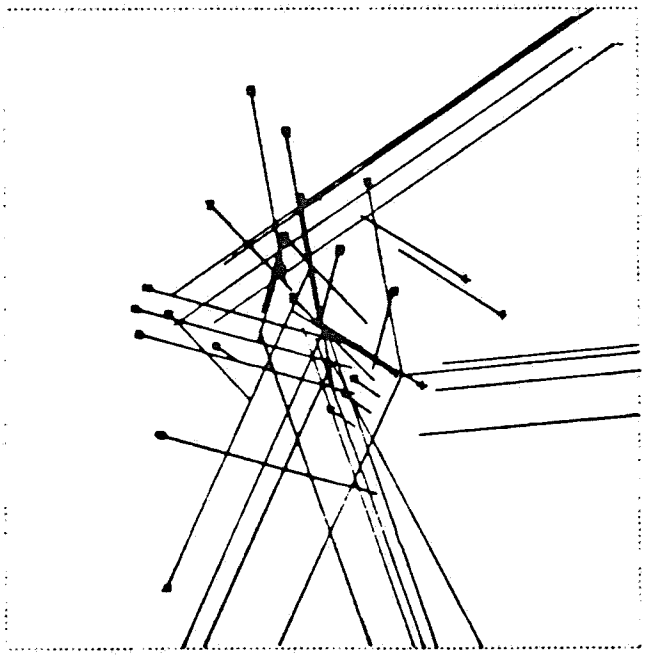

MOD: U - 24 TAG: 42
RUN: 2321 EVT: 1948 DST: 2 TYPE: 1

all of cand tracks

RUN: 2321 EVT: 1948 DST: 2 TYPE: 1

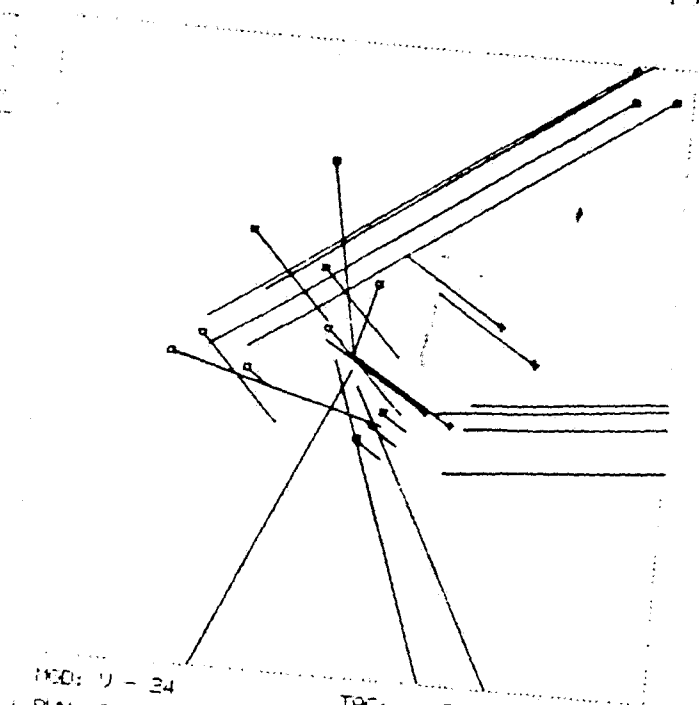

select on VTX tracks

MOD: 0 - 24 TAG: 42
RUN: 2321 EVT: 1348 DST: 2 TYPE: 1

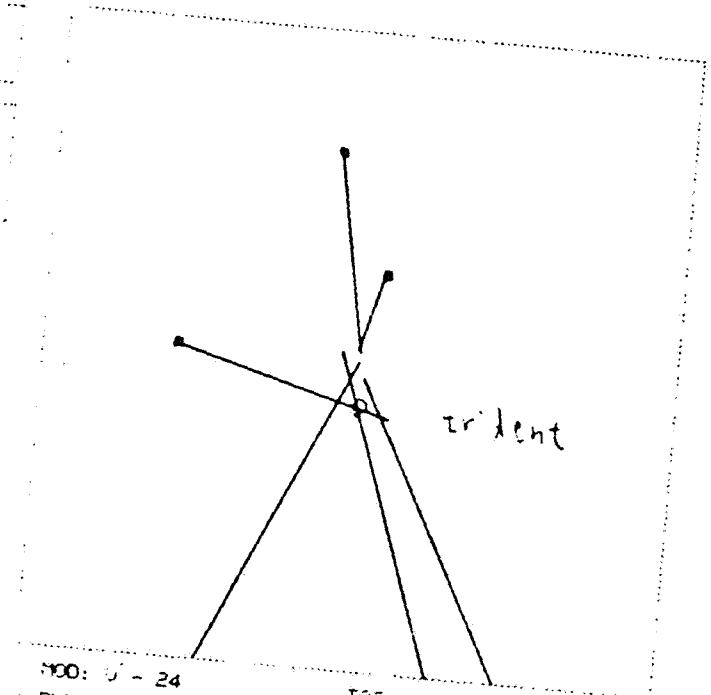

erase ambig. tracks

MOD: 0 - 24 TAG: 42
RUN: 2321 EVT: 1548 DST: 2 TYPE: 1

erase ambig. tracks

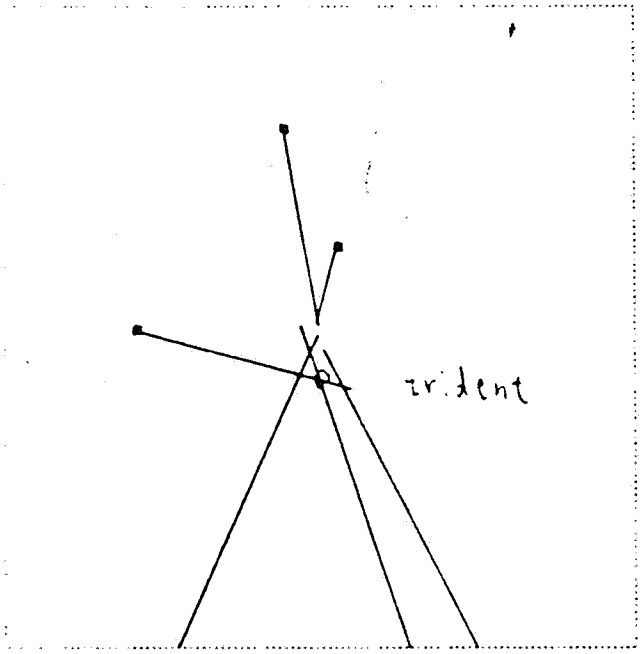

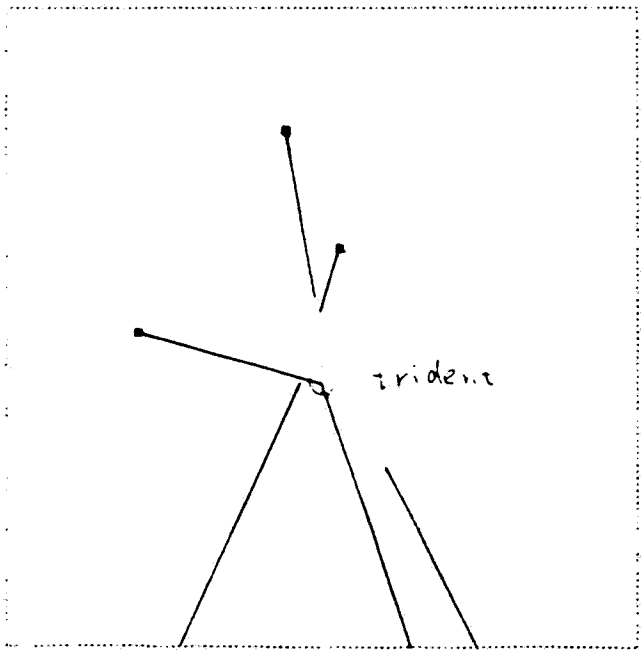

Track Selector

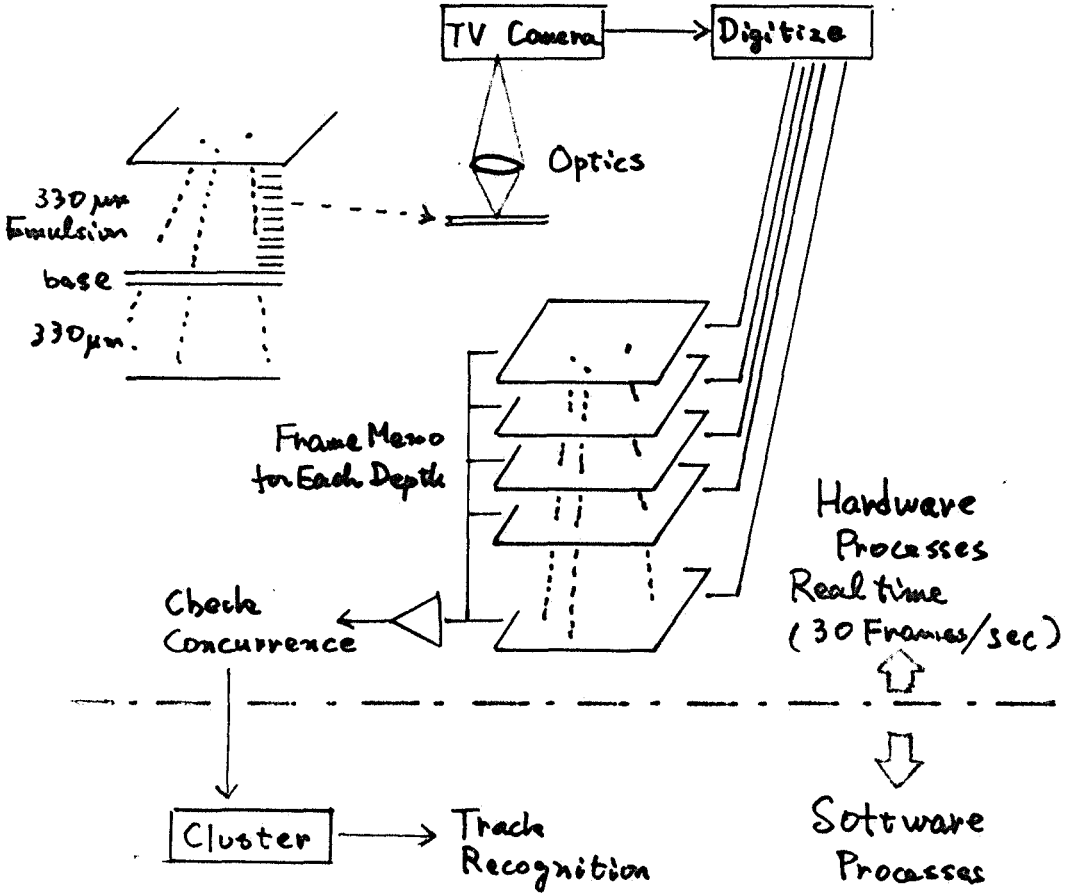

CALORIMETRY

GOALS

- FITS FOR CHARM AND BEAUTY DECAYS WITH NEUTRALS

  - FOR D^0 $44\pm10\%$ $D^0 \rightarrow K^- x$
    16% ALL CHARGED
    23% WITH 1 π°

- ELECTRON IDENTIFICATION (SHORT R.L. TARGET)

  - VERTEX PREDICTION
  - SCANNING
  - SEMI-ELECTRONIC DECAYS

PATTERN RECOGNITION

- 14 RECONSTRUCTED SHOWERS PER EVENT
- 13 CHARGED TRACKS
- SHORT SPECTROMETER
  - 40 GEV SYMMETRIC π
    SHOWER SEPARATION = 3.3 CM
  - SHOWER OVERLAP PROB. HIGH

- PROJECTIVE + PAD GEOMETERY

DETECTOR PARAMETERS

Prop. tube

	LAC	HADRON CALORIMETER
SIZE	1.6M x 1.6M	2.4M x 2.4 M
SAMPLING	.094" Pb	5cm Fe
# OF SAMPLES	39	16
LONGTITUDINAL SEGMENTS	3	4
TRANSVERSE SEGMENTATION	.5cm X,Y + PADS	1.6cm X,Y (anode) + PADS
CHANNELS	3600	2200
RESOLUTION ENERGY POSITION	$12\%/\sqrt{E}+.025\%$ 1.3mm	$\sim 100\%/\sqrt{E}$ $\sim$ 2 cm
	CMU	OU

em showers → well behaved

hadron showers → SPLAT

LAC PAD STRUCTURE

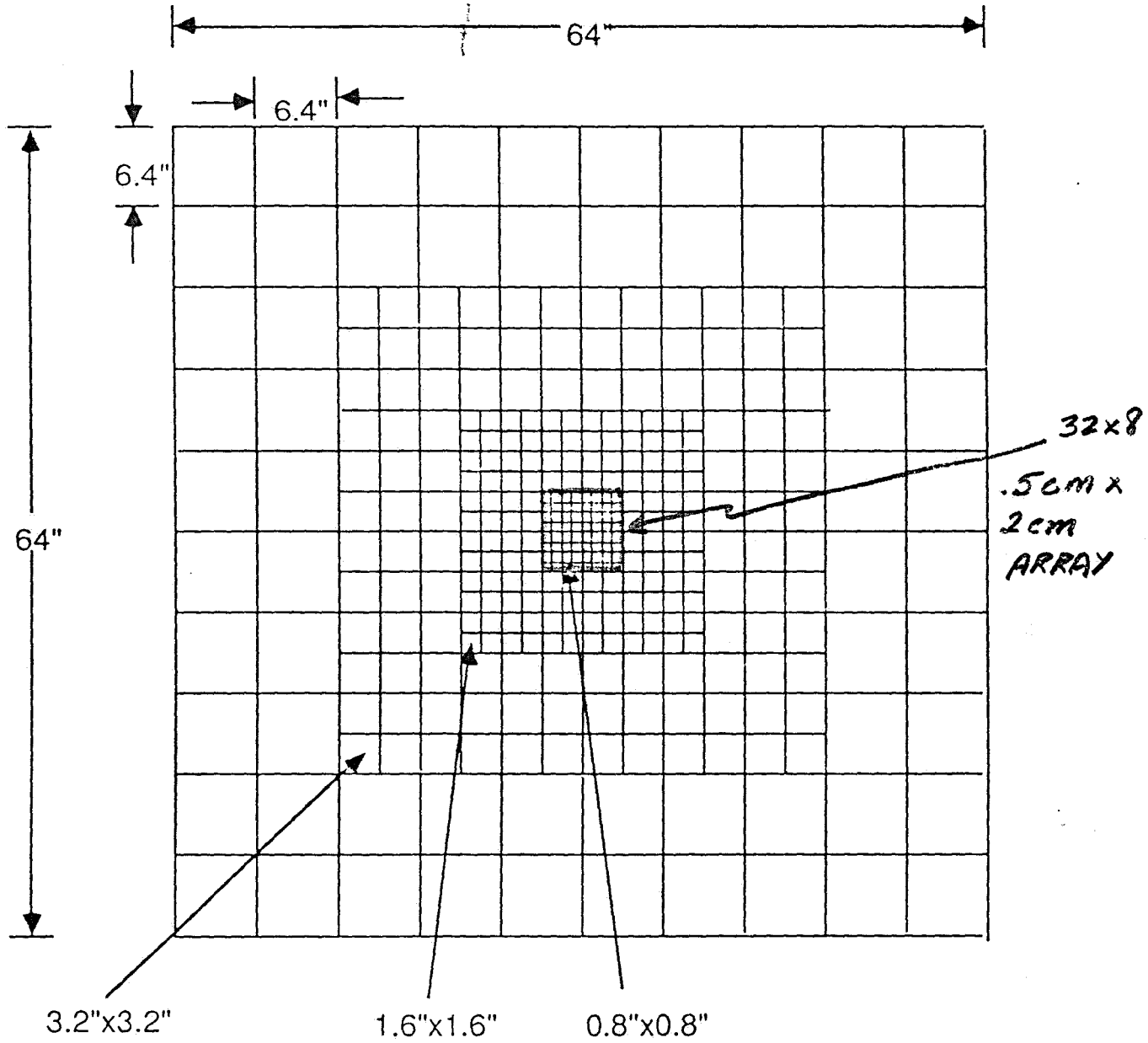

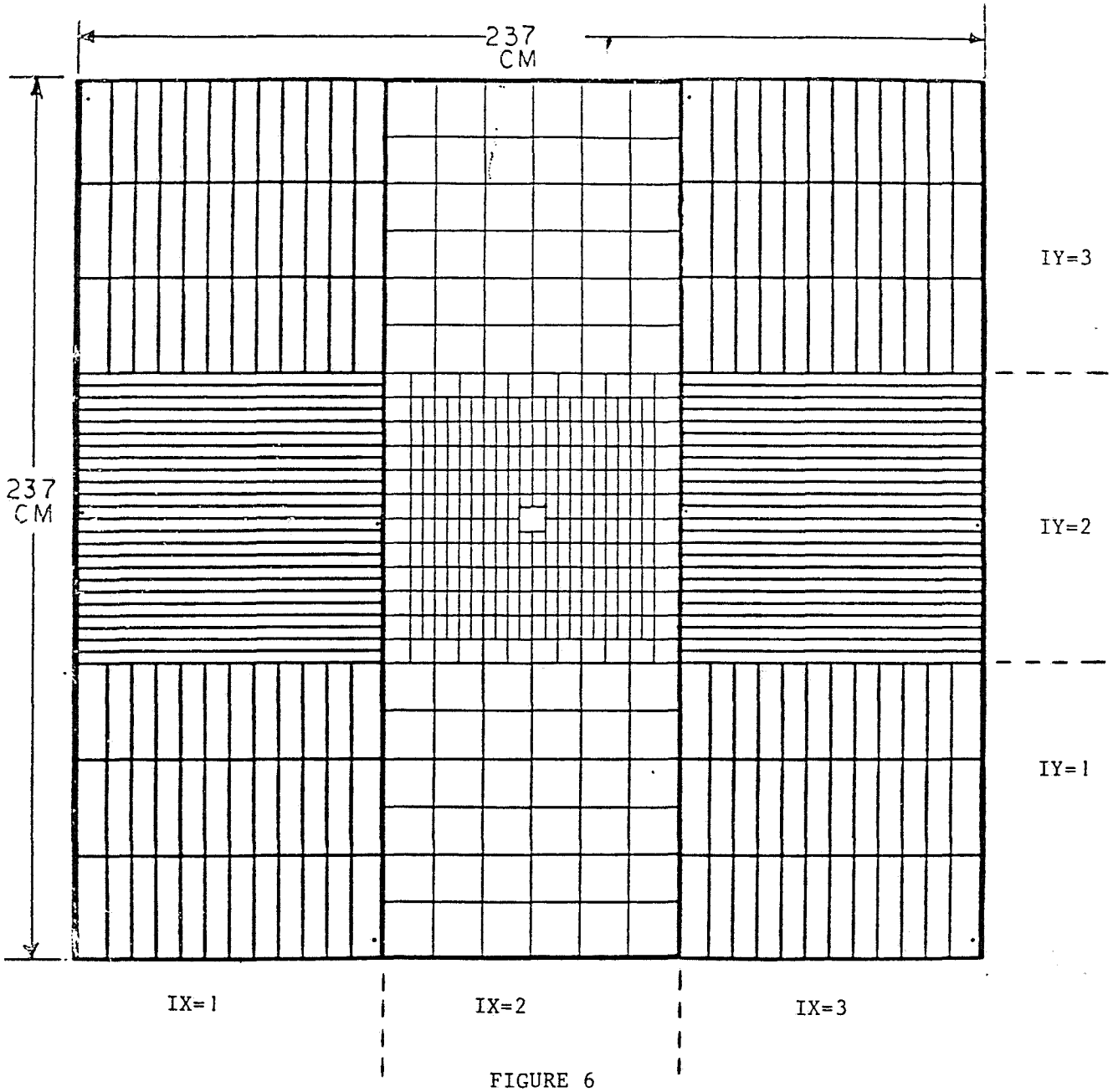

FIGURE 6

The pad pattern for the entire detector for modules in the vertical orientation (view 1). The horizontal modules (view 2) are rotated 90° counterclockwise. For the muon analysis, the detector was divided into nine equal-area regions. The values of the indicies IX and IY specify the individual regions.

Event 715

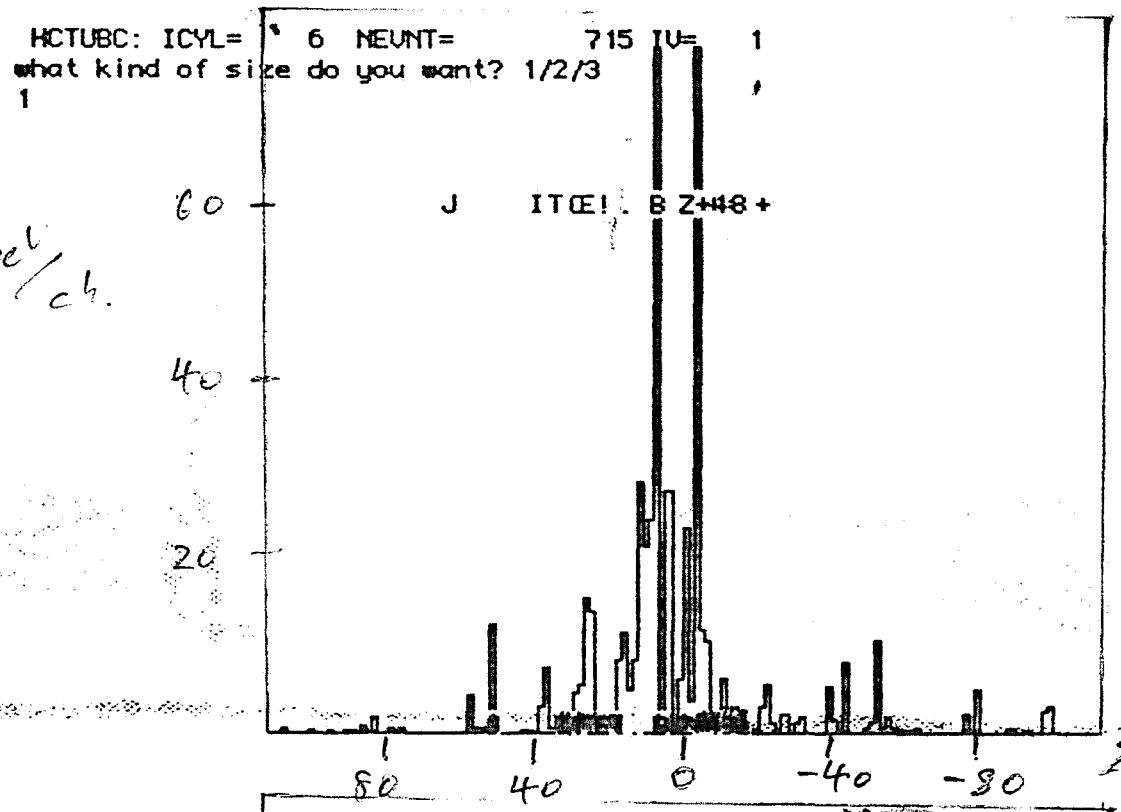
HCTUBC: ICYL= 6 NEVNT= 715 IV= 1
what kind of size do you want? 1/2/3
1
60
40
20
GeV/ch.
80
40
0
-40
-80
X (cm)

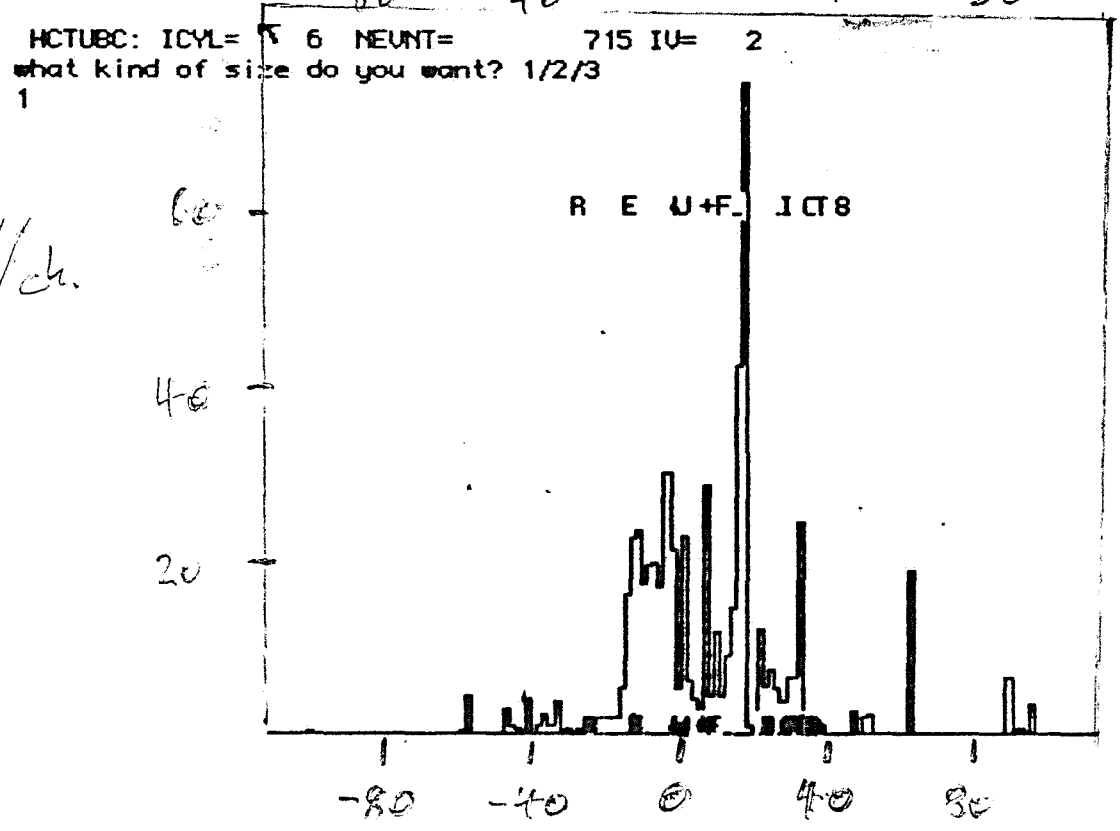
HCTUBC: ICYL= 6 NEVNT= 715 IV= 2
what kind of size do you want? 1/2/3
1
60
40
20
GeV/ch.
-80
-40
0
40
80
Y (cm)

ICYL= 6 NEUNÍ= 715

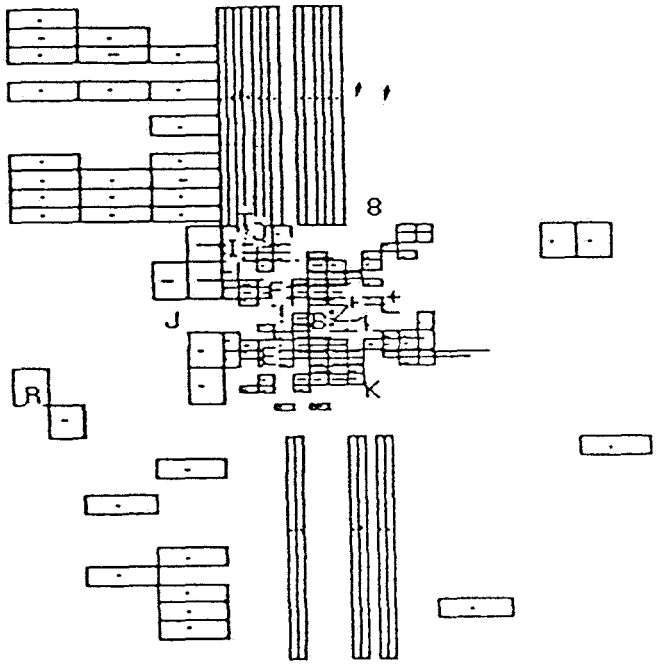

ICYL= 0 NEUNI= 715 nplhc: blowup? 1,2=yes, 0=no 2

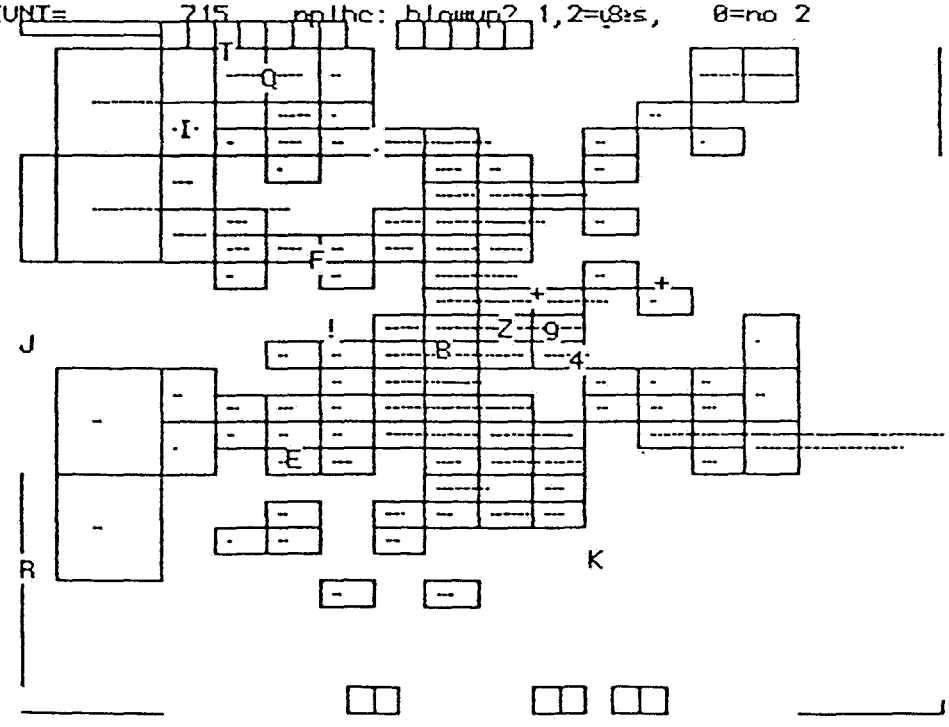

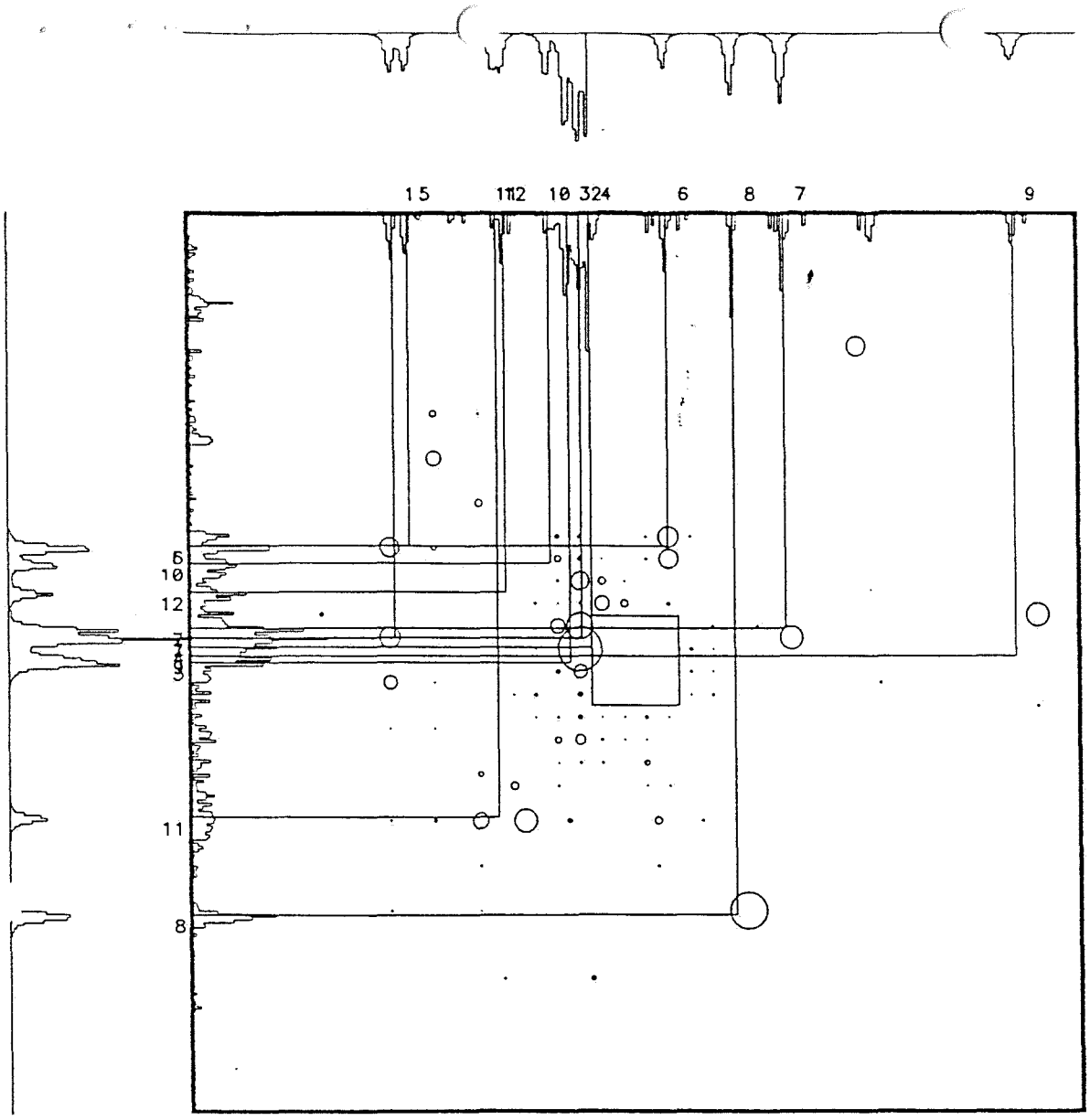

EVENT 715 RUN 2321 IRES 0

XMAX= 154.00000 PMAX= 253.00000

YMAX= 139.00000 SECTION 1

SHOWER	ENERGY	X CENTER	Y CENTER	FTSHWT	CHISQUARE
1	2.174	414.152	-16.734	1.000	1.068
2	11.053	74.719	-16.929	0.436	1.042
3	7.599	96.155	27.027	0.566	0.785
4	10.814	56.492	-0.669	0.411	1.372
5	2.467	387.081	-182.892	0.894	1.983
6	3.104	-83.968	-182.940	0.586	0.895
7	3.799	-298.039	-33.870	0.959	8.195
8	6.024	-205.490	477.269	0.533	2.759
9	1.982	-714.895	15.294	0.986	1.965
10	3.978	131.468	-151.769	0.562	2.056
11	2.160	228.385	301.551	0.869	3.090
12	2.424	213.425	-98.784	0.828	2.570

XMAX= 684 Event 716 Run 2321 SECTION= 1 YMAX= 699

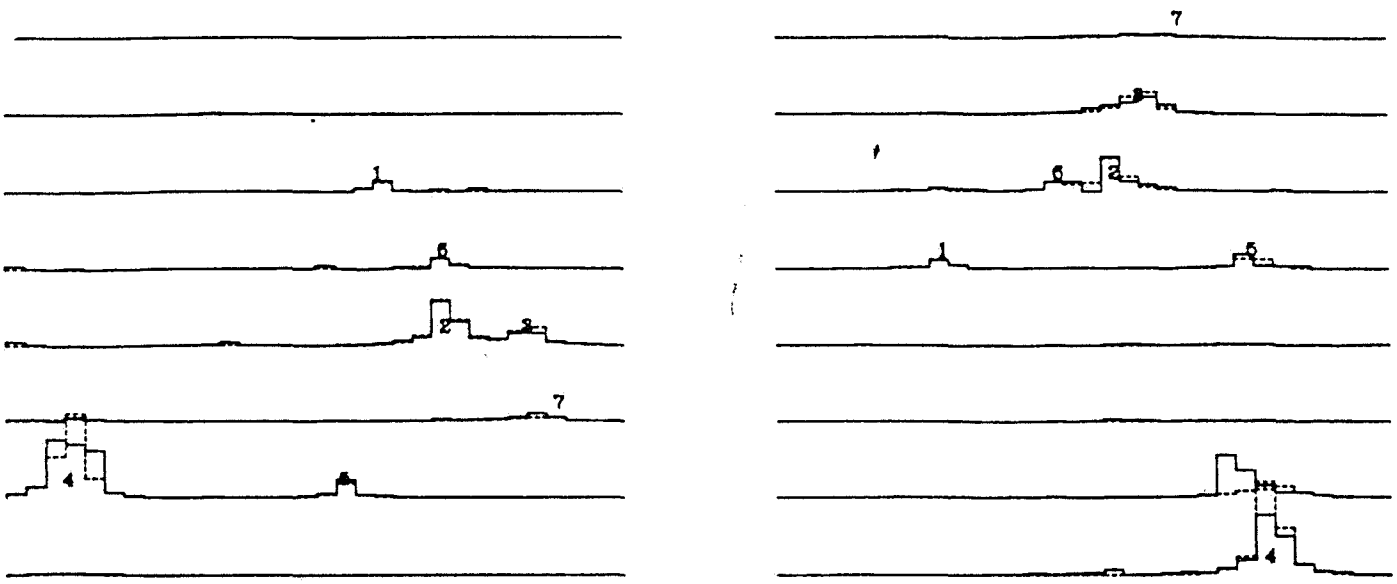

Shower #	X-energy	Y-energy	X-positn	Y-positn
1	3.661	4.170	19.295	6.754
2	15.386	11.334	22.610	17.740
3	6.615	10.168	27.076	19.087
4	28.602	34.686	3.229	25.821
5	4.193	5.627	17.493	24.997
6	2.945	3.821	22.711	14.605
7	0.846	0.778	26.726	21.159

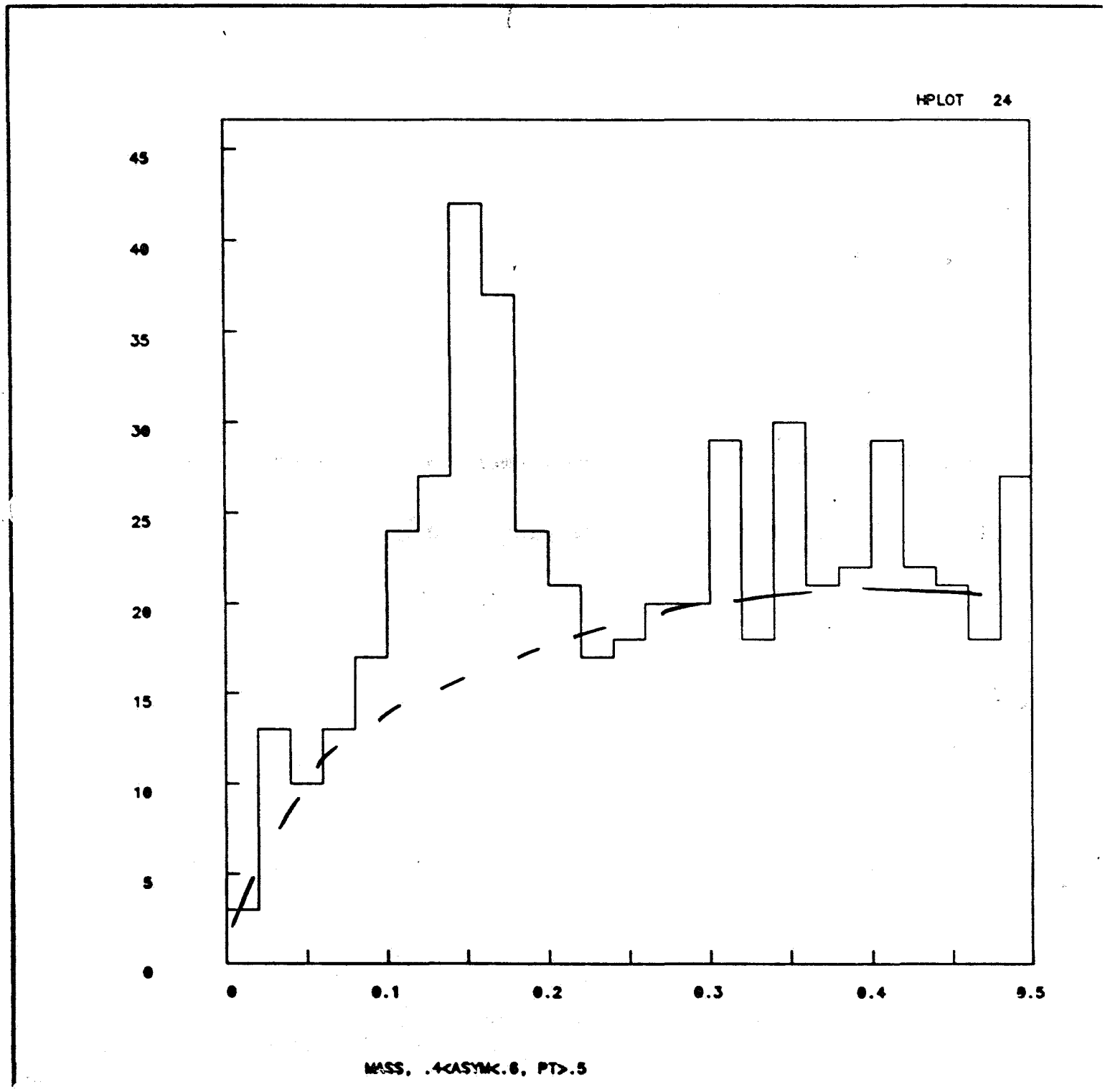
HPLOT 24
45
40
35
30
25
20
15
10
5
0
0
0.1
0.2
0.3
0.4
0.5
MASS, .4<ASYMC.6, PT>.5

STATUS - TO BE DONE

LAC

- REFINEMENTS TO CODE
- STUDY e^+e^- RESOLUTION IN DATA
- MONTE CARLO & STUDY

HAD. CAL

- CALIBRATE WITH HADRON BEAM
- DEVELOP CODE FOR DATA EVENTS

Data Crunch

Vertex Finding

Calibration

Alignment
Drift Times
Spurious Electronic effects

E653 Data Analysis

December 18, 1986

Monte Carlo

Geant 3
Testing Reconstruction Algorithm.
Detector efficiencies.

Event Fitting

Identifying species of the secondary vertices.

Event Fitting

Status: Adapted from an E531 program.

Basic program structure makes use of π°'s and charged tracks. Tests with Monte Carlo complete. Tests with real charm to be completed by January 15th.

Momentum refitting completed by February 14th.

Program for matching tracks between the emulsion and μ-strip detectors - March 15th.

Add missing tracks and K_s near emulsion - March 15th.

Add 0C fit $D \rightarrow \mu X$ and D* fit - March 15th.

At this point we have a structure with which we can do some physics.

We had 1300 tapes in the first run and will have Twice as many in the second run

Rough Benchmarks

Machine	1 Data Tape	Tapes/week
Vax 750	1000 Min.	
Vax 780	620 Min.	
Vax 785	520 Min.	
Vax 8600	160 Min.	
Ohio IBM 3081E	90 Min.	20
Okl. IBM 3081K	60 Min.	25-30

ACP: Each node is equivalent to 60% -90% of a VAX 780

We could spin a tape every 20 Min. Running one week/month with 5 good days in that week, Conservatively ACP can do 200 Tapes/month
So we volunteered to be guinea pigs for the ACP

Status: Our programs have been compiled linked and have run on ACP 68020 nodes.

ACP Schedule:

Tape tests with one tape Complete by January 15th.

Ten tape test finished by February 1st.

100 tape test begins March 15th.

Computers to use	**Comparisons** Rate/month	Time to crunch 1300 tapes
1. OSU IBM	80 tapes	15 Months
2. OK IBM	120 tapes	12 Months
3. OK and OSU	200 tapes	7 Months
4. ACP	200 tapes	7 months
5. ACP & OK	320 tapes	4 months
6. Everybody	400 tapes	3 months

Scenario 5 is the most likely.

IMPROVEMENTS FOR E653 SECOND RUN

3 GENERAL CATEGORIES:

I. IMPROVE SIGNAL/NOISE

II. INCREASE RATE OF DATA-TAKING

II. IMPROVE QUALITY OF DATA

IMPROVE SIGNAL/NOISE

A. 650 GeV/c π^- BEAM

→ b PRODUCTION CROSS SECTION IS LARGER BY ~ ×2-3

→ TOTAL CROSS SECTION IS SMALLER BY ~20%

→ CHARM CROSS SECTION IS APPROXIMATELY THE SAME; MAY BE STIFFER x DISTRIBUTION, SO LARGER FRACTION OF EVENTS WITHIN ACCEPTANCE

NET IMPROVEMENT: ×2½ - ×4 FOR b's
×1.2 FOR CHARM

→ THIS ASSUMES MACHINE ENERGY IS 850 GeV; IF IT IS HIGHER, b CROSS SECTION GOES UP EVEN MORE.

B. REDUCE TRIGGERS FROM INTERACTIONS OUTSIDE EMULSION

→ SILICON WAFER JUST UPSTREAM OF EMULSION WILL VETO UPSTREAM INTERACTIONS

→ INTERACTION COUNTER (SCINTILLATOR) REPLACED BY WAFER - FEWER INTERACTIONS IN IT.

C. EXTRA STEEL IN FRONT OF MUON SYSTEM

→ REDUCES CONFUSION IN CHAMBERS UPSTREAM OF TOROID - 40% OF EVENTS HAVE EXTRA HITS NOW

→ VECTOR DRIFT CHAMBER IN MIDDLE OF STEEL WILL IMPROVE MATCHUP TO UPSTREAM TRACKS

→ MUONS NOW NEED AT LEAST 7 GeV TO TRIGGER SYSTEM (SOFTWARE CUT IS AT 8 GeV)

NET INCREASE IN EFFICIENCY OF MUON SYSTEM: × 1.5

TOTAL INCREASE IN CHARM + BEAUTY

$\sigma_{\bar{b}b}/\sigma_{TOT}$	REQUIRE INTERACTIONS IN EMULSION	MUON SYSTEM EFFICIENCY	MORE TRIGGERS	
b × 3.5				
c × 1.2	× 1.5	× 1.5	× 2	= × 15 b
				× 5 c

NCREASE RATE OF DATA-TAKING

7. 4 MBy 1891's

→ EVENTS ARE NOW LONGER, DUE TO ADDITIONAL DRIFT CHAMBERS AND LARGER SSD's

→ IN ORDER TO TAKE 500 EVENTS/SPILL, WILL NEED A TOTAL OF 6 4 MBy MEMORIES, PLUS 1 SPARE. WE HAD 2 OF THESE IN THE LAST RUN, WHICH MEANS: 5 HAVE TO BE UPGRADED. (LAST RUN'S RATE WAS 300 EVENTS/SPILL)

→ <u>WITHOUT</u> MORE 4 MBy 1891's, RATE WILL <u>DECREASE</u> TO ~200-250 EVENTS/SPILL.

. SMART CAMAC CRATE CONTROLLERS

→ WILL ESSENTIALLY ELIMINATE CAMAC DEAD TIME

C. NEW FASTBUS DRIVER (FNAL)

→ NEED TO SPEED UP SYSTEM THROUGHPUT BY ~ x 1.5

→ SEVERAL OPTIONS ARE CURRENTLY BEING EXPLORED BY US AND THE LABORATORY

IMPROVE QUALITY OF DATA

A. LARGE SSD's

3 10cm × 10cm SSD's WILL REPLACE THE LAST 3 5cm × 5cm ONES IN THE VERTEX STACK

→ WILL INCREASE EFFECTIVE SOLID ANGLE OF PRECISION TRACKING SYSTEM.

FRACTION OF b EVENTS WHERE ALL CHARGED TRACKS ARE IN SSD's WILL INCREASE BY A FACTOR OF 1.25

B. BETTER GAS SYSTEM

→ WILL REDUCE VARIATIONS IN DRIFT VELOCITY. CALIBRATION NOW MUST BE DONE ON EVERY RUN.

ENGINEERING NOTE

E653 VERTEX SILICON STRIP DET. (II)

NAME LUNDBERG

DATE 8-OCT-86

REVISION DATE

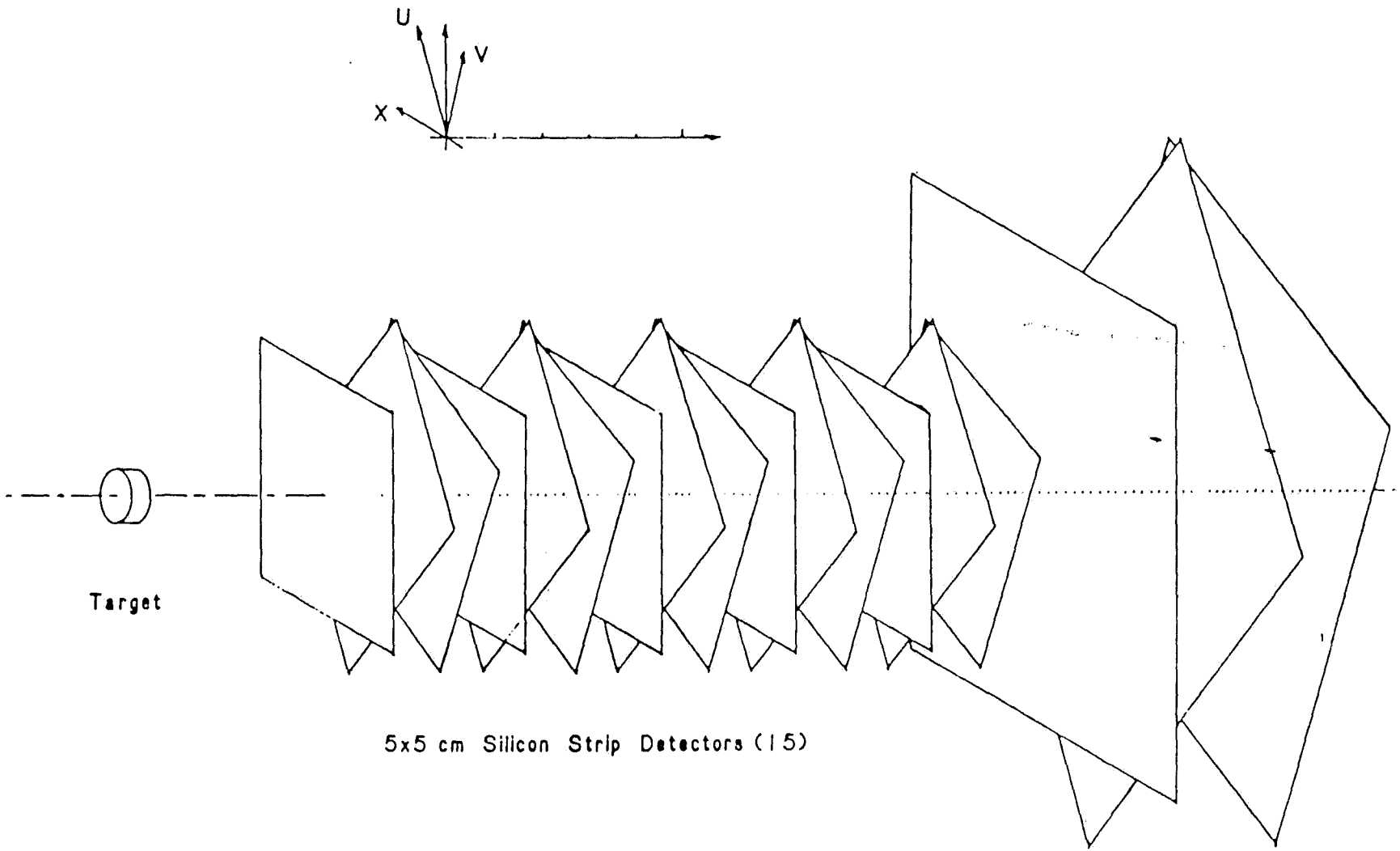

E653 2ND RUN LAYOUT

- NEW FOR 2ND RUN
- MAJOR IMPROVEMENTS FOR 2ND RUN

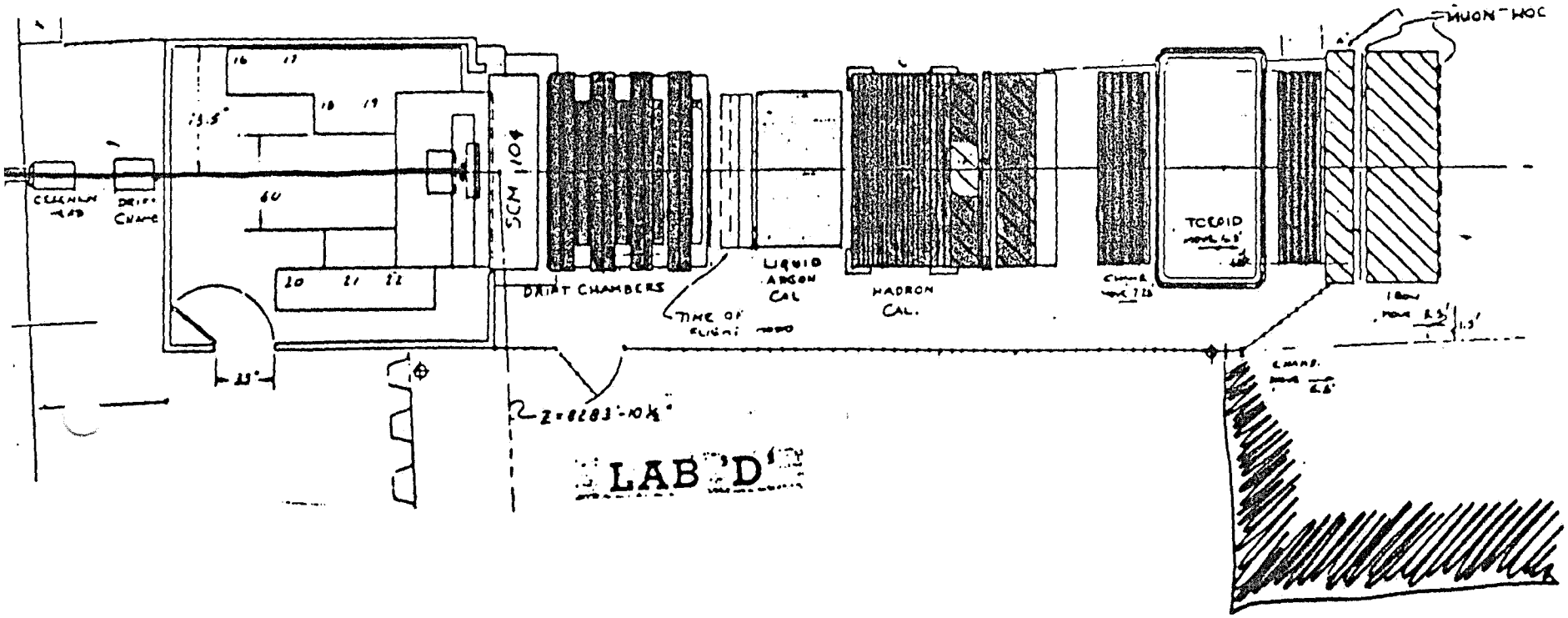

C. Detailed List of All Improvements

1. Equipment
   a. General
      - ★ pion beam
      - ★ extension to building (for new steel)
      - ★ fourth portakamp and associated improvements (clean power, covered access to building, etc.)

   b. Beam System
      - improve drift chamber stand
      - repair bad channels
      - new veto on upstream interactions
      - new interaction counter

   c. SSD's
      - 3 10 cm x 10 cm at downstream end

   d. SCM104 Magnet
      - ★ Hall probes for continuous monitoring and recording of field

   e. Vector Drift Chambers
      - added two - one in stack, one in gap in new steel
      - replaced 2 mil wire in coarse cells with 1 mil wire - can run at lower voltage
      - ★ TDC's in two Fastbus crates - can run coarse and fine cells a different least counts; fewer events are too long for a single crate
      - ★ better gas

   f. Time of Flight
      - improved bases - faster signal, better grounding
      - add start time

   g. Liquid Argon Calorimeter
      - increased shaping amplifier gain - reduces effect of pedestal drift
      - revise plumbing - improve monitoring
      - replace dead amplifiers

   h. Hadron Calorimeter
      - new amplifiers and preamplifiers - can run at lower voltage

   i. Muon System
      - ★ improved field shaping
      - ★ improved amplifiers
      - ★ added steel
      - ★ centered east-west

2. Electronics
   - ★ programmable logic units in trigger - can automatically change trigger type
   - improve scanning DVM, for monitoring of voltages
   - ★ additional Fastbus crate for drift chambers
   - ★ 4 Mbyte 1891's
   - ★ smart CAMAC crate controllers
   - microVAX for monitoring

3. Software
   - ★ Fastbus driver
   - automatic voltage checking for computer-controlled high voltage power supplies

★ MAJOR HELP FROM FERMILAB IN ACHIEVING THESE ITEMS

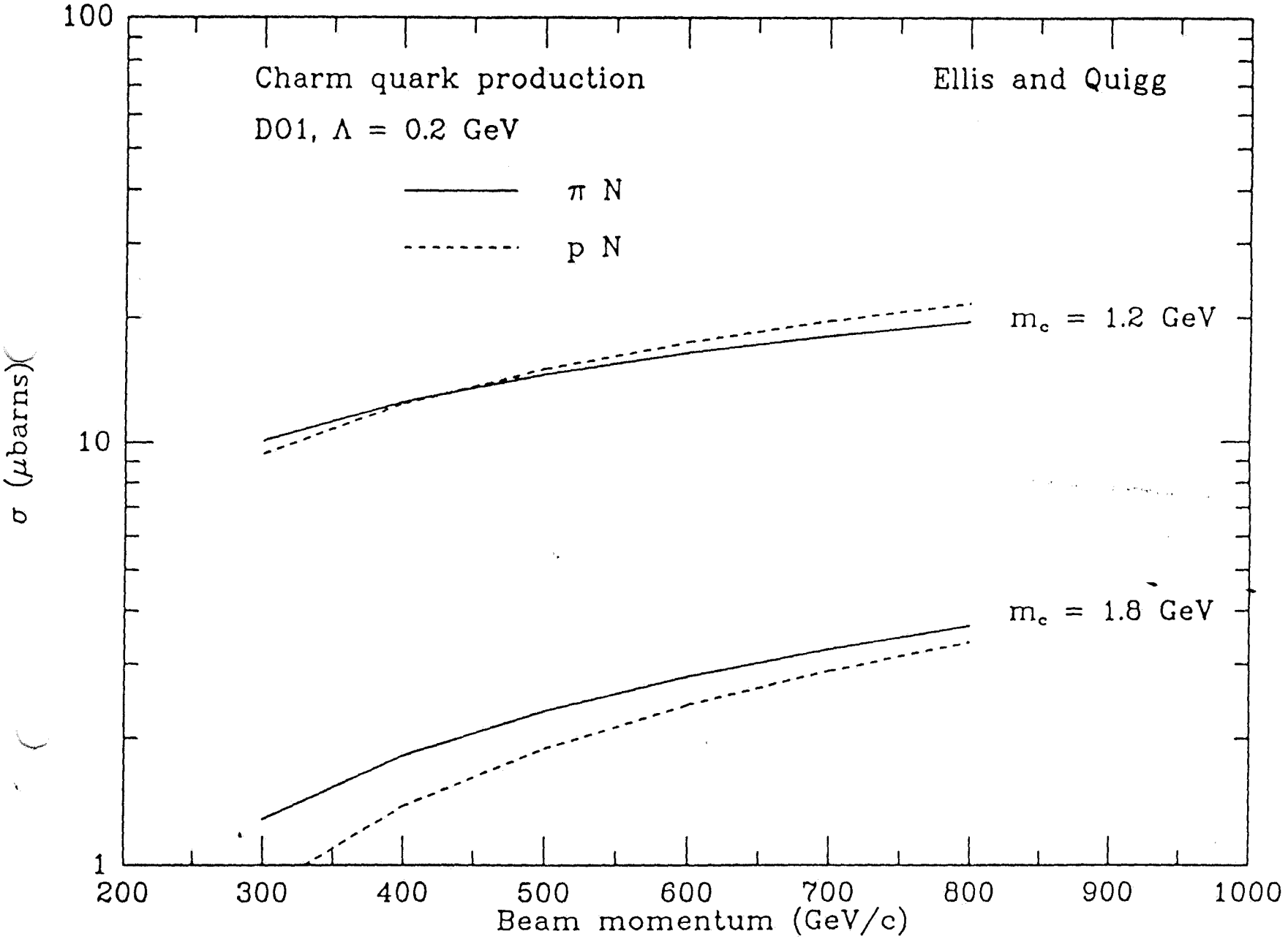
Charm quark production
Ellis and Quigg
D01, Λ = 0.2 GeV
π N
p N
m_c = 1.2 GeV
m_c = 1.8 GeV
σ (μbarns)
100
10
1
200
300
400
500
600
700
800
900
1000
Beam momentum (GeV/c)

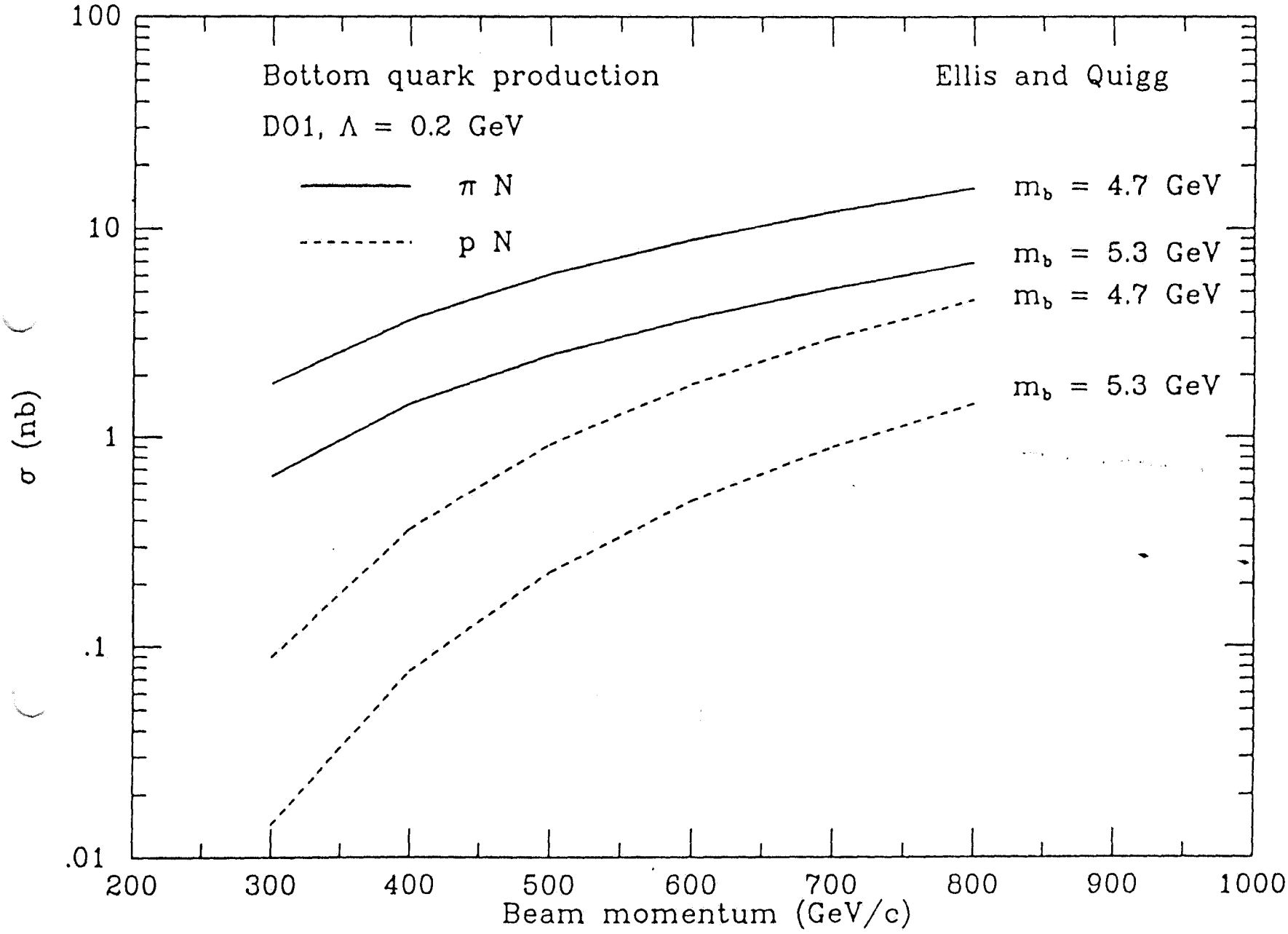
Bottom quark production
Ellis and Quigg
D01, Λ = 0.2 GeV
π N
p N
m_b = 4.7 GeV
m_b = 5.3 GeV
m_b = 4.7 GeV
m_b = 5.3 GeV
σ (nb)
100
10
1
.1
.01
200
300
400
500
600
700
800
900
1000
Beam momentum (GeV/c)

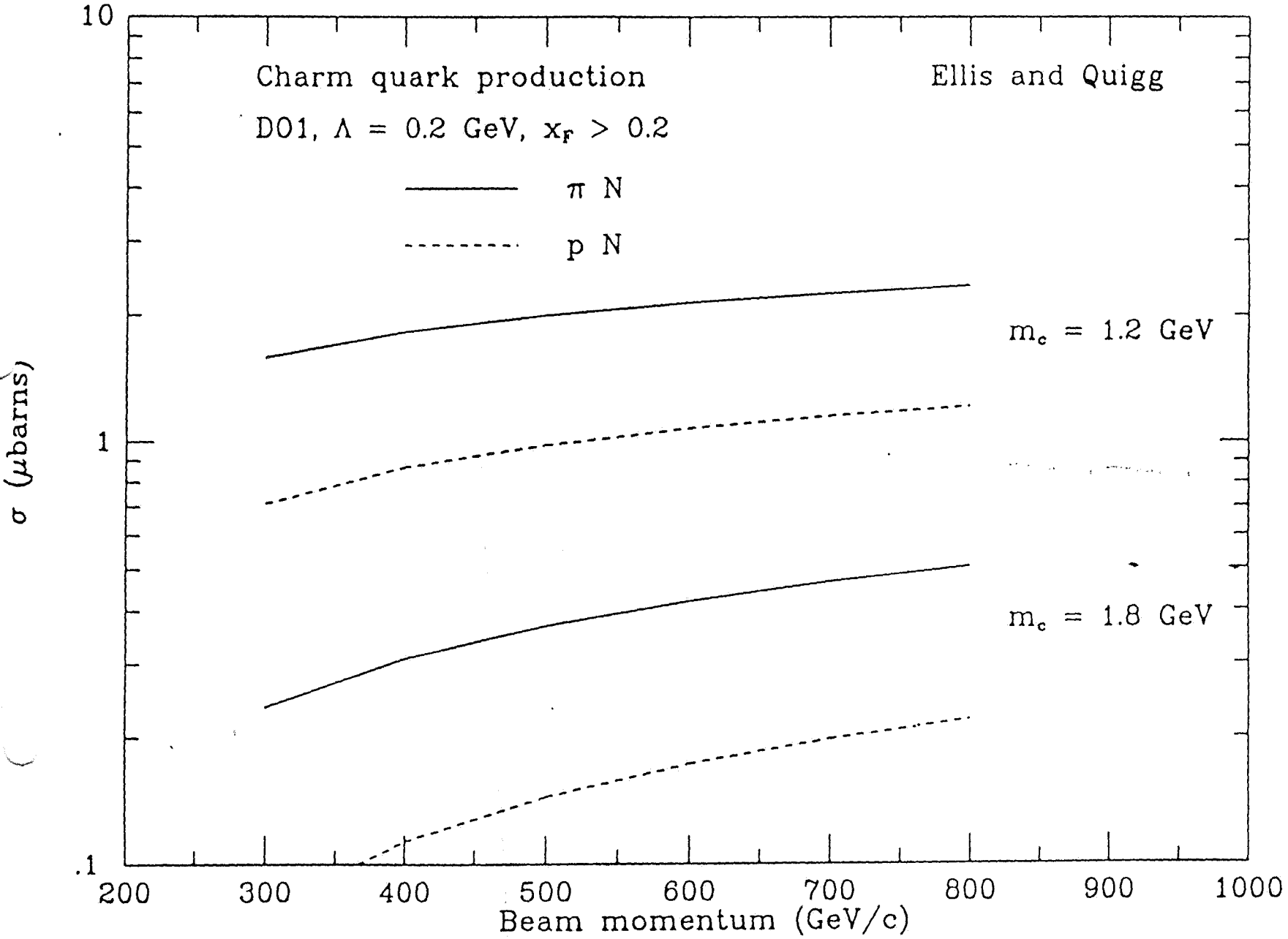
Charm quark production
Ellis and Quigg
D01, Λ = 0.2 GeV, x_F > 0.2
π N
p N
m_c = 1.2 GeV
m_c = 1.8 GeV
σ (μbarns)
10
1
.1
200
300
400
500
600
700
800
900
1000
Beam momentum (GeV/c)

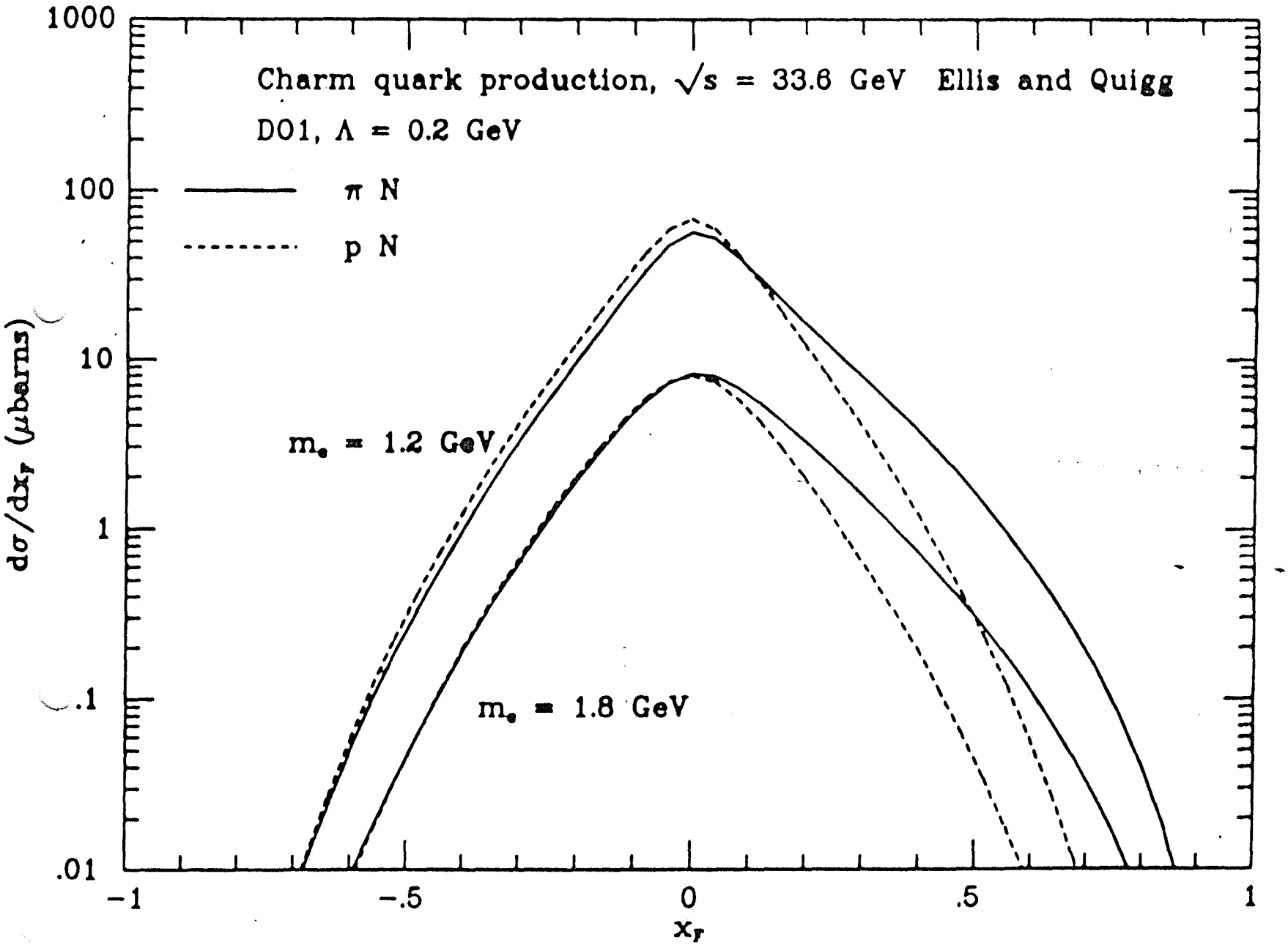
Charm quark production, √s = 33.6 GeV Ellis and Quigg
DO1, Λ = 0.2 GeV
π N
p N
m_c = 1.2 GeV
m_c = 1.8 GeV
dσ/dx_F (μbarns)
x_F
1000
100
10
1
.1
.01
−1
−.5
0
.5
1

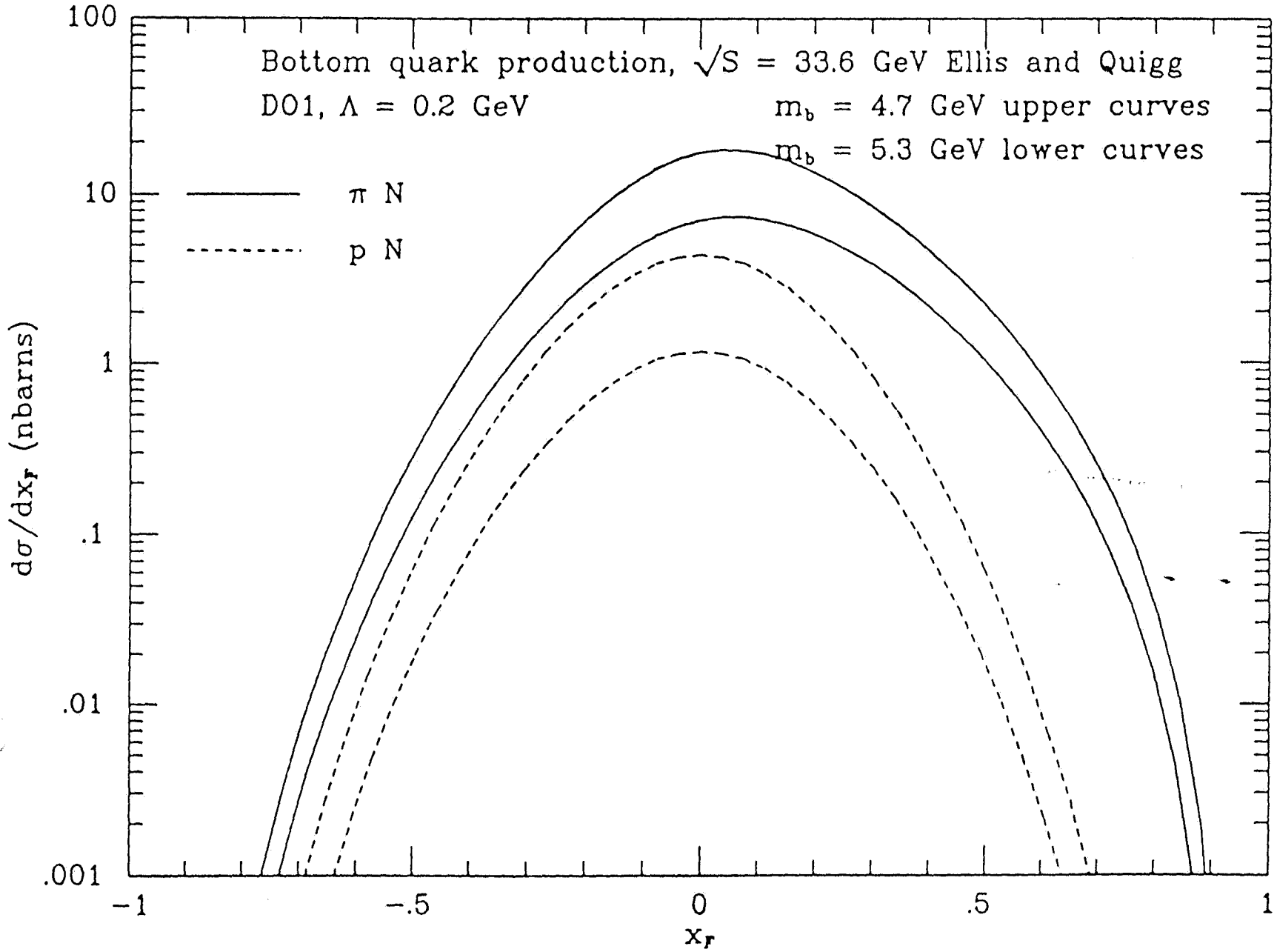
Bottom quark production, √S = 33.6 GeV Ellis and Quigg
D01, Λ = 0.2 GeV
m_b = 4.7 GeV upper curves
m_b = 5.3 GeV lower curves
π N
p N
100
10
1
.1
.01
.001
dσ/dx$_F$ (nbarns)
−1
−.5
0
.5
1
x$_F$